UNIVERSITÀ
DEGLI STUDI
DI PADOVA

Sede Amministrativa: Università degli Studi di Padova

Dipartimento dei Beni Culturali: Archeologia, Storia dell'Arte, del Cinema e della Musica

---

SCUOLA DI DOTTORATO DI RICERCA IN : Studio e Conservazione dei Beni Archeologici ed Architettonici

CICLO: 27°

Roman and late-Roman glass from north-eastern Italy: comparing raw materials and production technology of vessels and mosaic tesserae.

Direttore della Scuola : Ch.mo Prof. Giuseppe Salemi

Supervisore :Dott.ssa Alberta Silvestri

Dottorando : Sarah Maltoni

(**firma** del dottorando)

RIASSUNTO

La presente ricerca ha come obiettivo lo studio archeometrico del vetro circolante nell'Italia nordorientale a cavallo tra epoca romana e tarda antichità, con il fine di caratterizzarne le materie prime e le tecnologie di produzione. Diversamente dall'approccio generalmente utilizzato nello studio del vetro, che si focalizza su una delle due classi di materiali, l'oggettistica in vetro e le tessere musive vitree sono qui affrontate parallelamente con lo scopo di ottenere una più ampia visione sulla circolazione del vetro e delle tecnologie nell'area in esame.

L'oggettistica vitrea qui esaminata proviene dai due più importanti siti portuali nord Adriatici del periodo considerato: ossia Classe e Aquileia.

La campionatura di Classe, composta prevalentemente da indicatori e scarti di lavorazione e forme potorie datate ai secoli V-VIII d.C., deriva da un probabile atelier dell'area produttiva del porto. La campionatura di Aquileia, datata tra I e VIII secolo e rinvenuta nella domus di Tito Macro comprende invece prevalentemente vasellame da mensa e alcuni indicatori di lavorazione e pani di vetro.

La possibilità di analizzare contestualmente oggetti e indicatore di lavorazione provenienti dai due siti permette di avanzare ipotesi sul tipo di vetro lavorato, sulle fonti di approvvigionamento delle materie prime e sulle rotte commerciali.

Le tessere musive vitree provengono da tre siti: tessere sciolte provenienti dagli edifici romani rinvenuti sotto la cattedrale di Santa Maria Maggiore a Trento (II-IV sec d.C.), tessere sciolte provenienti dalla villa romana di Torre di Pordenone (I-V sec d.C.) e il mosaico *in-situ* della Domus delle bestie Ferite di Aquileia (seconda metà del IV sec d.C.).

Le tessere sono caratterizzate da un'ampia gamma cromatica comparabile tra i tre siti considerati permettendo così di fare confronti puntuali

L'analisi chimica, mineralogica, isotopica e tessiturale è stata condotta per mezzo di un articolato insieme di tecniche analitiche dotate di elevati standard di accuratezza e precisione delle misure. Per ogni tipologia di materiale qui considerato sono state privilegiate le tecniche analitiche che garantissero l'accurata ed esaustiva caratterizzazione e la massima salvaguardia dei campioni in esame.

I metodi utilizzati sono OM, SEM-EDS, XRF, EMPA, MS-ICP-MS, XRPD, FORS, EPR e Spettroscopia Micro Raman.

I due siti di Classe sono caratterizzati dalla presenza di vetri a composizione ascrivibile all'epoca tardoantica e da un elevato grado di comparabilità in termini di composizioni chimiche e segnature isotopiche, che permettono di ipotizzare per le due città in epoca tardoantica le medesime rotte commerciali provenienti da analoghe località di produzione primaria localizzare sulle coste del Mediterraneo orientale.
L'esame delle tessere musive ha invece evidenziato una certa uniformità composizionale nelle tessere dei siti di Pordenone e Trento, nei quali vetro di base, coloranti e opacizzanti sono caratteristici dell'epoca Romana mentre nel mosaico Aquileiese è stata riscontrata una maggiore varietà di composizioni chimiche e tecniche di colorazione e opacizzazione anche ascrivibili all'epoca tardoantica, indicative di una pronta ricezione delle novità tecnologiche.

ABSTRACT

The present research focuses on the archaeometric study of glasses circulating in north-eastern Italy between Roman times and Late Antiquity with the aim of clarifying raw materials and production technologies. Unlike the approach generally used in the study of glass, which focuses on one of the two classes of materials, vessels and vitreous mosaic tesserae are here addressed in parallel, in order to have a wider picture on the circulation of glass and glass-technologies in the area.
The glass vessels here examined come from the most important north-Adriatic harbours of the considered time span: Classe (Ravenna) and Aquileia (Udine).
The assemblage of Classe, mainly composed of working wastes and drinking vessels dated to the 5th-8th century, was excavated in the productive area of the harbour of Classe and is thought to derive from a glass workshop. The assemblage excavated in the *domus of Tito Macro* in Aquileia comprises mainly tableware dated to the 1st-8th century, and some working indicators including chunks.
The opportunity of analysing vessels and glassworking wastes excavated in the two cities allows speculating on the composition of locally-worked glass, the location of supply of raw materials and trade routes.
The glass tesserae here investigated come from three sites: the disrupted decoration of the Roman buildings excavated under the church of Santa Maria Maggiore in Trento (Italy) and dated to the 2nd-4th century; the disrupted decoration of the Roman villa of Torre di

Pordenone dated to the 2nd-5th century AD; and the in-situ mosaic of the *Domus delle Bestie Ferite* in Aquileia, dated to the second half of the 4th century. The tesserae show a wide chromatic range, comparable in the three sites, that allows direct comparisons.
Chemical, textural and mineralogical analyses were conducted by means of an articulated set of analytical methods aimed to obtain the highest standards of precision and accuracy. The analytical methods employed are OM, SEM-EDS, XRF, EMPA, MC-ICP-MS, XRPD, FORS, EPR, and Micro Raman Spectroscopy.
The two sites of Classe and Aquileia are characterized by the presence of glass compositions referable to the late Antiquity, with a high degree of comparability in terms of chemical composition and isotopic signatures, which allow hypothesizing that the two cities had similar trade routes from similar supply areas located along the eastern Mediterranean shores.
The examination of the mosaic tesserae highlighted a compositional uniformity in the sites of Pordenone and Trento, in which base glass, colouring agents and opacifiers are characteristic of the Roman time; differently, the mosaic of Aquileia shows a greater variety of chemical compositions and colouring/opacifying techniques, partly referable to the Late Antiquity, which indicates a prompt reception of technological innovations.

INDEX

1. AN INTRODUCTION TO ROMAN AND LATE ROMAN GLASS 1

2. ARCHAELOGICAL CONTEXT: SITES AND MATERIALS 8

2.1. AQUILEIA 8

2.1.1 AQUILEIA- DOMUS OF TITO MACRO (EX "*FONDI EX COSSAR*") 9

2.1.2 AQUILEIA- DOMUS OF THE "*BESTIE FERITE*" 11

2.2 CLASSE 13

2.3 PORDENONE- VILLA OF TORRE DI PORDENONE 15

2.4 TRENTO- SANTA MARIA MAGGIORE CATHEDRAL 16

REFERENCES 17

19

3. ANALYTICAL METHODS

3.1. OPTICAL MICROSCOPY (OM) 19

3.2. SCANNING ELECTRON MICROSCOPY WITH ENERGY DISPERSIVE SYSTEM (SEM-EDS) 19

3.3. X- RAY FLUORESCENCE (XRF) 20

3.4. ELECTRON PROBE MICRO ANALYSIS (EPMA) 20

3.5. X-RAY POWDER DIFFRACTION (XRPD) 21

3.6. MULTI COLLECTOR INDUCTIVELY COUPLED PLASMA MASS SPECTROMETRY (MC-ICP-MS) 22

3.7. MICRO-RAMAN SPECTROSCOPY 23

3.8. ELECTRON PARAMAGNETIC RESONANCE 24

3.9. FIBER OPTIC REFLECTANCE SPECTROPHOTOMETRY (FORS) 24

4. GLASS VESSELS AND WORKING WASTES 26

4.1 OPAQUE COLOURED VESSEL GLASS 26

4.1.1 TEXTURAL CHARACTERIZATION 26

4.1.2 CHEMICAL CHARACTERIZATION 33

4.1.3 DISCUSSION 35

4.1.4 CONCLUSIONS 39

4.2 TRANSPARENT GLASS 40

4.2.1 ROMAN GLASS FROM AQUILEIA 41

4.2.1.2 COLOURLESS GLASS 43
4.2.1.3 COLOURED GLASS 55
4.2.2. OUTLIERS FROM CLASSE 59
4.2.3 ROMAN GLASS – CONCLUSIONS 59
4.3 LATE-ANTIQUE GLASS FROM AQUILEIA AND CLASSE 61
4.3.1 HIMT COMPOSITION 62
4.3.2 LEVANTINE 1 COMPOSITION 71
4.3.3 SERIE 3.2 COMPOSITION 75
4.4 ISOTOPIC CHARACTERISATION FOR GLASS PROVENANCE 78
4.5 CONCLUSIONS: GLASS TRADING AND WORKING IN AQUILEIA AND CLASSE IN THE LATE ANTIQUITY 81
REFERENCES 83

5. GLASS MOSAIC TESSERAE 91
5.1 GLASSY MATRIX 92
5.1.1 BASE GLASS 94
5.1.2 COLOURLESS AND GOLD TESSERAE 103
5.1.2.1 IRON COLOURED TESSERAE 106
5.1.2.2. COBALT COLOURED 108
5.1.2.3 COPPER COLOURED 113
5.2 OPACIFYING AGENTS 122
5.2.1 CA-ANTIMONATES 123
5.2.2 PB-ANTIMONATE 132
5.2.3 PB-SN-ANTIMONATE 136
5.2.4 PB-STANNATE 140
5.2.5 COPPER AND CUPRITE 145
5.2.6 QUARTZ + BUBBLES 158
5.3 TEXTURAL FEATURES (OTHER INCLUSIONS) 161
5.4 GLASS MOSAIC TESSERAE- CONCLUSIONS 167
REFERENCES 171

178

CONCLUDING REMARKS

APPENDIX A : SAMPLES

APPENDIX B: CHEMICAL DATA OF VESSELS (CHAPTER 4)

APPENDIX C: CHEMICAL DATA OF MOSAIC TESSERAE (CHAPTER 5)

APPENDIX D: XRPD PATTERNS OF MOSAIC TESSERAE

1. AN INTRODUCTION TO ROMAN AND LATE ROMAN GLASS

Glass as a synthetic material was produced since the Bronze Age in Egypt and Mesopotamia melting a silica rich material as sand or pebbles with an alkaline flux (Tite et al. 2006). In Prehistory, glass production was based on quartz pebbles and soda-plant ash as a flux; from the 1st millennium BC, conversely, the majority of the glass was produced employing natron as flux (Shortland et al. 2006).

The name "*natron*" indicates a mixture of evaporitic minerals rich in sodium carbonate and other Na-bearing minerals (chlorides and sulphates), found mainly in the area of the salt lake of Wadi-el-Natrun (Egypt). Archaeological evidences demonstrates that *natron* was known in Egypt since the 4th millennium BC for mummification, food preservation and soap production (Shortland et al. 2006) and its use as a flux in early vitreous materials is attested (even though very rare) from the 4nd millennium BC on glazed steatite and faience. The use of *natron* as a flux for glass production can be assumed from the 1st century BC when it replaced plant-ash in the Mediterranean basin, up to the west of the Euphrates; differently, in Mesopotamia, Iraq and Central Asia, plant-ash technology does not seem to be displaced by *natron* (probably due to a lack of mineral soda source) and continued without solution of continuity (Henderson and Barkoudah 2006).

The use of *natron* continued throughout Roman and Byzantine times until the 8th-9th century AD, when its use for some reason ceased; mineral soda was therefore replaced by soda-ash in the eastern Mediterranean, and wood-ash (potash rich) in northern Europe (Whitehouse 2002; Tite et al. 2006)

The change in flux that occurred in the 1st millennium BC was also accompanied by a change in silica and lime source: soda plant ash, differently from *natron*, contains considerable quantity of lime, that works as a stabiliser of the glass. Glass produced with quartz and *natron* was deficient in lime, and was therefore extremely susceptible of weathering (Shortland et al. 2011); for this reason, a different source of lime was required, usually limestone or sea shells, either naturally present in the sand or intentionally added to the batch.

Roman and Byzantine glass was generally produced employing a coastal sand, naturally rich in lime in the form of mollusc shells, and fluxed with natron. Differently from the glass industry of Bronze Age and Iron Age, devoted to the production of small precious objects such as beads and decorated vessels in deeply coloured opaque glass, the Roman

and Byzantine glass industry aimed to supply a wide and diversified market, comprising both high status vessels, ornaments and ordinary tableware; the discovery of glassblowing in the 1st century AD was followed by an expansion in production and the naturally coloured, transparent glass become the most common type glass (Freestone 2006); the expansion of the transparent glass production was also helped by the discovery of recycling (Stern 1999). The large quantity of glass produced between the 1st century AD and the 8th-9th century AD in the Roman and Byzantine world required a large quantity of raw materials and fuel and a well-organized productive structure. According to both literary source and archaeological evidences, the Roman and Byzantine glass industry was organised in a two-step productions (Freestone 2008): the primary production, which employed large quantities of raw materials (sand, flux and fuel) to produce raw glass, and a secondary production, that employed raw glass to shape vessels. This model of production is indicated by Pliny the Elder in his *Naturalis Historia* (Freestone 2008) and supported, in the case of the Late Antique and Byzantine glassmaking, also by the recovery of primary glass furnaces in Egypt (Nenna et al. 1997; Nenna et al. 2000) and Israel (Freestone et al. 2000; Gorin-Rosen 2000; Freestone et al. 2002). Unfortunately, primary furnaces of early Roman times haven't been recovered, yet; however, the trade of raw glass is testified also by the finding of chunks of Roman composition in the "Embiez" shipwreck and in many secondary workshops of the western Mediterranean (Foy et al. 2000).

What is still uncertain about the primary Roman glassmaking is the location(s) where the primary production took place. Differently from the secondary production (i.e. vessel shaping), which could be conducted virtually in every place of the Empire, the primary production of glass required the proximity of raw materials and availability of abundant fuel. The substantial chemical homogeneity of Roman glass suggests the use of well-defined raw materials, and in particular of specific sands characterised by relatively low content of feldspars, iron and heavy minerals. Only a few segments of the Mediterranean coasts present sand that are compatible with the production of Roman glass, as testified by ancient literary sources (Pliny and Strabo) and demonstrated by recent geochemical studies (Silvestri et al. 2006a; Brems et al. 2012). In absence of a clear archaeological evidence, two different possible production models were hypothesised: a centralized model, according to which the glassmaking took place in a very few primary production

sites, located in the Eastern Mediterranean, and a dispersed model, according to which different locations of primary production were located in both the eastern and western part of the Empire.

While in the case of Late Antique and Byzantine primary production the centralized model is generally more accepted, for the early Roman production a univocal consensus still lacks and a primary production in the western Europe is seldom hypothesised on the basis of chemical and isotopic data (Wedepohl and Baumann 2000; Silvestri et al. 2006b; Ganio et al. 2012).

Roman and Late Antique glass have in common the use of a carbonatic coastal sand and *natron* as a flux, but the chemical composition of glass dated before and after the 4th century AD suggests that a major change is the sand source occurred. Roman glass of the 1st- 3rd century is characterised by a relatively homogenous composition, as evidence by the abundant archaeometric literature (Foy et al. 2003; Vichy et al. 2004; Jackson 2005; Silvestri et al. 2008; Silvestri 2008; Foster and Jackson 2010; Ganio et al. 2012; Rosenow and Rehren 2014); during the 4th century AD new glass composition start to be traded across the Mediterranean and Europe. A first one, characterised by elevated content of iron oxide, alumina, titania, magnesia and manganese, and also elevated content of sodium and relatively low lime, dubbed HIMT (Freestone 1994) is of probable Egyptian provenance, and the impure sand employed for its production is reflected in the chemical composition that is unequivocally different from the one of early Roman glass. A second composition, named Levantine 1 (Freestone et al. 2000), is characterised by elevated content of lime and sometimes potash, and lower contents of soda with respect to Roman glass; the primary production of this kind of glass was proved to be in the Palestinian coast in the 4th century AD at Jalame (Brill 1988) and in the 6th-7th century in the primary furnaces of Dor, Apollonia and Bet Eli'ezer (Freestone et al. 2000): the area is coincident with that indicated by the ancient literary sources for early Roman glassmaking and, despite the remarked differences, the overall composition of Levantine glasses is not completely inconsistent from that of Roman glass.

In addition, a third compositional group seldom identified in Late Antique vessels is the so-called Sèrie 3.2 (Foy et al. 2003), a late antique Mn-decoloured composition that is very close to the early Roman glass. Despite primary production furnaces have not been

recovered, yet, it is suggested to derive from the Palestinian coast, although in a different area with respect to Levantine1 glass.

Another technological difference between the Roman and Late Antique/Byzantine glass is related to the decolouring agent: early Roman glass was decolourised with the addition of antimony or, to a minor extent, manganese. While the manganese decoloured glass is generally considered as a "less-standardized" composition, antimony decoloured glass tend to have specific composition (Jackson 2005; Silvestri et al. 2008; Foster and Jackson 2010) that suggest the use of a specific source of sand. In addition, the large Roman colourless assemblages so far published usually report a large majority of antimony decoloured samples, while Mn-decoloured are usually less-represented (Jackson 2005); this could be for different reasons, including the fact the Mn-decolouring seems to be less effective and probably more difficult to control.

From the 4th century AD onward, differently, the deliberate addition of manganese becomes one of the distinctive traits of the new compositions: HIMT, Sèrie3.2 and Levantine1 indeed contain elevated manganese, while the use of antimony seems to cease.

The reason for this technological change is unknown, but it is probably related to the availability of antimony. A similar technological change was identified in the colouring technique: antimony was used to produce Pb-antimonate and Ca-antimonate, that were employed as pigments and opacifiers in yellow and white glass, respectively, since the Bronze Age; from the 4th century onward AD antimony- based opacifiers are replaced by tin based compounds, such as tin oxide for white and lead-stannate for yellow (Tite et al. 2008); as in the case of the Late Antique glass composition, also the new opacifying techniques seem to have been introduced in the Late Roman world from the eastern Mediterranean.

In this context, the archaeometric and geochemical characterisation of glass vessels, wastes and opaque coloured glass excavated in Italy and dated between Roman and Late Antique time can provide a unique insight into glass circulation in the western Mediterranean, shedding light on commercial trade routes, location of supply and reception of technological innovation.

The geographical area under consideration in the present work is the north-Adriatic Italy represented by five different sites with a specific focus on Aquileia; the presence of proved commercial link between north-eastern Italy and the Levantine coast raises questions

about the provenance of glass circulating in this area, that the archaeological records report as particularly rich in glass finds. In the present work, differently from what usually found in the archaeometric literature, vessels and mosaic tesserae are considered with a parallel approach, with the aim of clarifying the presence and extent of changes in raw materials and production technologies and the reception of technological innovations around the 4th century AD.

Brems, D., Degryse, P., Hasendocks, F., Gimeno, D., Silvestri, A., Vassilieva, E., Luypaers, S., and Honings, J., 2012, Western Mediterranean sand deposits as a raw material for Roman glass production, *Journal of Archaeological Science*, **39**, 2897–907.

Brill, R. H., 1988, Scientific investigations of the Jalame glass and related finds , In *Excavations at Jalame: site of a glass factory in late roman Palestine* (ed. G. Davidson Weinberg), 257–94, University of Missouri press, Columbia (MO).

Foster, H. E., and Jackson, C. M., 2010, The composition of late Romano-British colourless vessel glass: glass production and consumption, *Journal of Archaeological Science*, **37**(12), 3068–80.

Foy, D., Vichy, M., and Picon, M., 2000, Lingots de verre en Méditerranée occidentale (IIIe siècle av.J.-C.-VIIe siècle ap.J.-C.), In *Annale du 14e Congrès de l'Association International puor l'Histoire du Verre*, 51–7, Association International pour l'Histoire du Verre, Venezia- Milano.

Foy, D., Vichy, M., and Thirion-Merle, V., 2003, Caractérisation des verres de la fin de l'Antiquité en Méditerranée occidentale: l'émergence de nouveaux courants commerciaux , In *Actes du colloque de l'Association Française pour l'Archéologie du Verre* (eds. D. Foy, and M. D. Nenna), Vol. Aix-en-Pro, 41–85, Monique Mergoil, Montagnac.

Freestone, I. C., 1994, Chemical analysis of raw glass fragments., In *Excavation at Carthage, The Circular Harbour, North Side. the Site and Finds Other than Pottery. Vol II* (ed. H. R. Hurst), 290, British Academy Monographs in Archeology, Oxford University Press, Oxford.

Freestone, I. C., Gorin-Rosen, Y., and Hughes, M. J., 2000, Primary Glass from Israel and the Production of Glass in Late Antiquity and the Early Islamic Period, In *La Route du Verre. Ateliers Primaires et Secondaires du Second Millènaire av. JC au Moyen Age* (ed. M. D. Nenna), 65–83, Maison de L'orient Mediterranéen, Lyon.

Freestone, I. C., Greenwood, R., and Gorin-Rosen, Y., 2002, Byzantine and early Islamic glassmaking in the eastern Mediterranean: production and distribution of primary glass. In, In *Hyalos-Vitrum-Glass. History, technology and conservation of glass in the Hellenic world* (ed. K. G.), 167–74, Glasnet Publications, Athens.

Freestone, I. C., 2006, Glass production in Late Antiquity and the Early Islamic period: a geochemical perspective, *Geological Society, London, Special Publications*, **257**(1), 201–16.

Freestone, I. C., 2008, Pliny on Roman glassmaking, In *Archaeology, History and Science. Integrating Approaches to Ancient Materials* (eds. M. Martinon-Torres, and T. Rehren), 77–100, UCL Institute of Archaeology Publications, Oxford.

Ganio, M., Boyen, S., Fenn, T., Scott, R., Vanhoutte, S., Gimeno, D., and Degryse, P., 2012, Roman glass across the Empire: an elemental and isotopic characterization, *Journal of Analytical Atomic Spectrometry*, **27**(5), 743.

Gorin-Rosen, Y., 2000, The ancient glass industry in Israel. Summary of the finds and new discoveries. , In *La Route du Verre: Atelieres primaires et secondaires du second millinaire av. J.-C. au Moyen-Age.* (ed. M. D. Nenna), 49–64, Maison de l'Orient Méditerranéen, Lyon.

Henderson, J., and Barkoudah, Y., 2006, Plant ashes from Syria and the manufacture of ancient glass: ethnographic and scientific aspects, *Journal of Glass Studies*, **48**, 297–321.

Jackson, C. M., 2005, Making colourless glass in the Roman period, *Archaeometry*, **47**(4), 763–80.

Nenna, M. D., Vichy, M., and Picon, M., 1997, L'atelier de verrier de Lyon, du Ier siècle après J.-C., et l'origine des verres "romains" , *Revue d'Archéométrie*, **21**, 81–7.

Nenna, M. D., Picon, M., and Vichy, M., 2000, Ateliers primaires et secondaires en Ègypt à l'époque gréco-romaine, In *La Route du Verre: Atelieres primaires et secondaires du second millinaire av. J.-C. au Moyen-Age* (ed. M. D. Nenna), 97–112, Maison de l'Orient Méditerranéen, Lyon.

Rosenow, D., and Rehren, T., 2014, Herding cats - Roman to Late Antique glass groups from Bubastis, northern Egypt, *Journal of Archaeological Science*, **49**(1), 170–84.

Shortland, A. J., Schachner, L., Freestone, I. C., and Tite, M. S., 2006, Natron as a flux in the early vitreous materials industry: sources, beginnings and reasons for decline, *Journal of Archaeological Science*, **33**(4), 521–30.

Shortland, A. J., Degryse, P., Walton, M., Geer, M., Lauwers, V., and Salou, L., 2011, the Evaporitic Deposits of Lake Fazda (Wadi Natrun, Egypt) and Their Use in Roman Glass Production, *Archaeometry*, **53**(5), 916–29.

Silvestri, A., Molin, G., Salviulo, G., and Schievenin, R., 2006a, Sand for Roman glass production: an experimental and philological study on source of supply., *Archaeometry*, **48**(3), 415–32.

Silvestri, A., Molin, G., Salviulo, G., and Schievenin, R., 2006b, Sand for Roman glass production: an experimental and philological study on source of supply, *Archaeometry*, **48**(3), 415–32.

Silvestri, A., 2008, The coloured glass of Iulia Felix, *Journal of Archaeological Science*, **35**(6), 1489–501.

Silvestri, A., Molin, G., and Salviulo, G., 2008, The colourless glass of Iulia Felix, *Journal of Archaeological Science*, **35**(2), 331–41.

Stern, M., 1999, Roman glassblowing in a cultural context, *American Journal of Archaeology*, **103**(3), 441–84.

Tite, M. S., Shortland, A. J., Maniatis, Y., Kavoussanaki, D., and Harris, S., 2006, The composition of the soda-rich and mixed alkali plant ashes used in the production of glass, *Journal of Archaeological Science*, **33**(9), 1284–92.

Tite, M. S., Pradell, T., and Shortland, A. J., 2008, Discovery, production and use of tin-based opacifiers in glasses, enamels and glazes from the late iron age onwards: A reassessment, *Archaeometry*, **50**, 67–84.

Vichy, M., Thirion-Merle, V., and Foy, D., 2004, Contribution à l'étude des verres antiques décolorés à l'antimoine, *Revue d'Archéométrie*(28), 169–77.

Wedepohl, K. H., and Baumann, a., 2000, The use of marine molluskan shells for Roman glass and local raw glass production in the Eifel area (western Germany), *Die Naturwissenschaften*, **87**(3), 129–32.

Whitehouse, D., 2002, The transition from natron to plant ash in the Levant, *Journal of Glass Studies*, **44**, 193–6.

2. ARCHAELOGICAL CONTEXT: SITES AND MATERIALS

In order to investigate the circulation of glass and the reception of the technological innovations between Roman and Late Antique times in northern Adriatic Italy, five glass assemblages from four different sites were selected and analysed. In detail, the selection included two assemblages composed of vessels and glass-working wastes from Classe and Aquileia, and three assemblages composed of glass tesserae from Trento, Pordenone and Aquileia (*Fig. 2.1*). Each site is presented in the following paragraphs, together with a brief description of the analysed materials.



Fig: 2.1*: Nortern Italy. The position of the cities here considered is reported.*

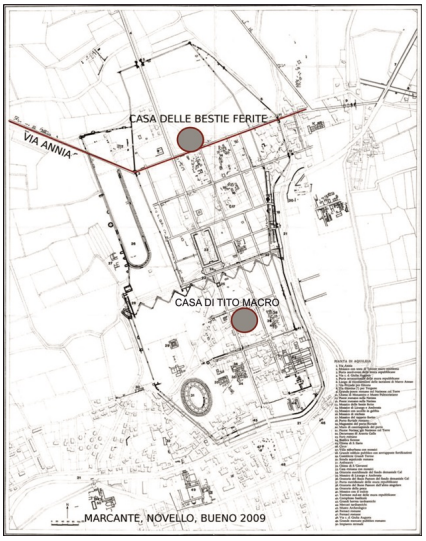

Fig.2.2*: plan of the ancient city of Aquileia. The sites of Tito Macro and Bestie Ferite are indicated*

2.1. AQUILEIA

Aquileia is one of the main archaeological sites of north-eastern Italy. It was founded as a Latin colony in 181 BC and its significance during Roman and Late Antique times is due to its strategic position: being the most northern Adriatic harbour, it was connected with the Transalpine area and the Levant by means of both maritime and terrestrial trade routes; in addition, an important road system connected Aquileia to Genoa (by *via Postumia*), Rimini (by *via Popilia*) and Padova (by *via Annia*) (Gallo et al. 2014 and references therein).

The excavations in the city and surrounding area, conducted since the second half of the 19th century, reveal the presence of abundant quantities of glass vessels; glassworking wastes and chunks are also reported (Buora et al. 2009). The abundance of glass was interpreted in the past as an indicator of glass production activity in the city (Calvi 1968), but the hypothesis has no archaeological proof and has only been supported by circumstantial evidences so far. The provenance of the glass circulating in the Aquileia area is of particular interest as Aquileia was one of the main harbours of the Mediterranean during the Roman and early Medieval times, directly linked to the eastern Mediterranean where primary glassmaking was proved at least for the Late Antiquity (Gorin-Rosen 2000; Freestone et al. 2002). In order to investigate the circulation of glass in the city, two assemblages were selected: a group of vessels and glassworking wastes excavated in the dwelling of Domus of Tito Macro dated between the 1st century BC and the 8th century AD, with a focus on the 3rd-5th century AD; and a group of glass tesserae from the mosaic of the Domus "Bestie Ferite", dated to the 4th century AD. Each assemblage and site of provenance is presented in detail. The location of the two domus is indicated in Fig. 2.2

2.1.1 AQUILEIA- DOMUS OF TITO MACRO (EX "*FONDI EX COSSAR*")

The domus of Tito Macro lays in the southern part of the city and represents the only example of "atrium *domus*" identified so far in Aquileia. The Domus was founded probably at the end of the 1st century AD and frequented until the 5th century AD.

The area was investigated for the first time in the mid-19th century; between 1920 and -1940 the excavations were carried on under the guide of Brusin; between 1959 and 1971 the area was again excavated by L. Bertacchi. Despite the long series of surveys, excavations and restorations, a good knowledge of the area was not achieved: due to the extremely concise reports produced, the absence of graphical documentation, and the lack of a critical re-examination of the archaeological data, a chronological reconstruction was not possible (Bonetto and Ghedini 2014).

From 2009 to 2014 a new systematic excavation campaign was conducted by the Department of Cultural Heritage of the University of Padova, Italy, aimed to clarify the chronology of the domus, the urbanistic arrangement and its relationship with the residential buildings (Bonetto and Ghedini 2014). As a result of the numerous ancient excavation, conducted in the absence of a systematic and organic project, the

stratigraphy of the site of Tito Macro (ex "Fondi ex-Cossar") is particularly complex and heavily manipulated; the dating of the stratigraphy is still in progress, therefore in the present archaeometric study the dating of each vessel is assumed as coincident with the dating of the type.

The recent excavations brought to light a very large quantity of archaeological materials including pottery, coins, metals and glass; the archaeological study of the materials is still in progress. Among the abundance of finds, more than 900 glass fragments were recovered and the archaeological study was conducted by Dr. A. Marcante. The glass is constituted mainly by tableware dated between the 1st century BC and the 9th century AD but also window panes, game counters, sporadic mosaic tesserae, beads and ornaments, toilet bottles, lamps and a few very important glassworking wastes (including chunks) were recovered.

78 glass fragments were selected for the archaeometric analysis among the most frequent vessels types, including all the glassworking wastes; to enhance the statistical significativity of the assemblage, for each type of vessel, all the available colours were chosen. Most of the selected types are drinking vessels and bottles, made of transparent glass naturally coloured in blue, green or yellow; colourless and intentionally-coloured glasses are also represented; a few opaque coloured glasses, including mosaic vessels, and a single pre-Roman, core-formed vessel were also selected. The assemblage also includes five glassworking wastes and two glass chunks, that are of particular interest in the present study as they could provide a unique insight into glass working and trading in the area. Selected types and their datings are reported in fig. 2.3.

A full list of the samples is given in appendix A1

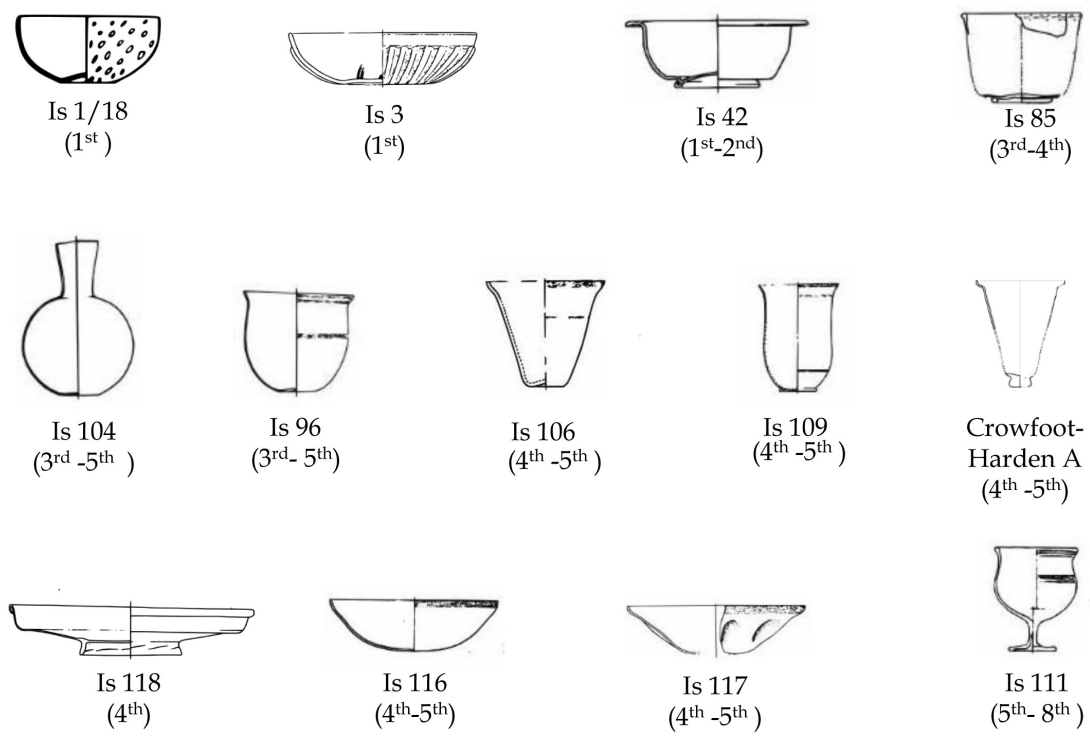

Fig.2.3*: most frequent types and dating of the archaeological form. The abbreviation "Is" indicated archaeological tyupes classified under Isings 1957. Images from: Isings, 1957 (Isings, 1957) Mandruzzanto and Marcante 2005 (isings 3,42,996, 104,106, 109,116, 117, 118) drawing by A. marcante (Isings 85, 111, Crowfoot- Harden group A). All datings are AD(Drowings from Isings, 1957.*

2.1.2 AQUILEIA- DOMUS OF THE "*BESTIE FERITE*"

The Domus of the "Bestie Ferite" (House of the Wounded Animals) derives its name from the mosaic of hunting scenes that characterises the main room.

The Domus lies in the north-eastern part of Aquileia and occupies a surface of about 800 m^2. The site was partially investigated by L. Bertacchi between 1961 and 1962; since 2007 it has been the object of a systematic archaeological campaign by the Department of Archaeology of the University of Padova. The area, apparently peripheral with respect to the forum, was located in a strategic position, limited by the via Annia (an important road that connected Aquileia to the city of Padova)and the *cardus maximum* (Bueno et al. 2012). Recent excavations revealed three main construction phases for the Domus: a first one, dated within the first half of the 1st century AD; a second one, dated to the late 2nd-early 3rd century AD; and a third one in the 4th century AD, when the Domus was completely restructured (Bueno and Centola 2014). The third constructive phase, dated to the late Antiquity, is the most relevant one to the present study: the large restructuring of the domus comprised the realization of a large and complex

figurative mosaic, object of the present study. The mosaic represents a complex figurative composition *(for a schematic reconstruction see fig 2.1*) that comprises large hunting scenes (7), wild animals (5), a personification of the seasons (6) and other decorative motifs with birds (3), fish (4) or vegetal patters (9); decorative geometric patterns frame the different figurative parts (Salvadori and Boschetti 2014). The mosaic employs a large quantity of stone tesserae, but glass and ceramic tesserae are also present. Glass tesserae, probably more expensive than ceramic ones (Salvadori and Boschetti 2014), are concentrated in the figurative areas, where a wider range of colours was required.

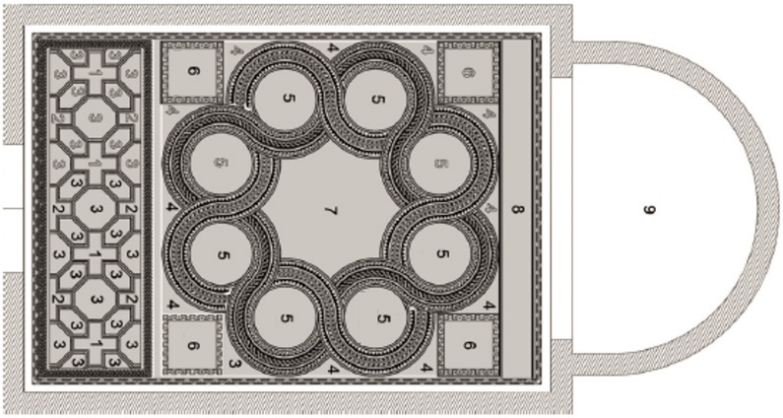

Fig. 2.4.: compositional scheme of the mosaic of the Domus delle Bestie Ferite (House of the Wounded Animals). 7: hunting scenes, 5: wild animals; 6: personification of the Seasons; 3: decorative motifs with birds; 4: fish; 9: vegetal patterns. (Drawing from Salvadori, Boschetti 20014- modified.)

The qualitative level of the technical execution is variable: low in the background, high in the figurative scenes, where also smaller tesserae were employed (Salvadori and Boschetti 2014). Higher execution quality is evident in the Spring and Summer representation, and in the hunter of the central scene. A detailed examination of the technique employed by the mosaicists evidenced differences in the realization of specific patterns (such as water, leaves, geometric motifs) and mistakes in the geometric frames (Salvadori and Boschetti 2014). On the basis of stylistic observation, Salvadori and Boschetti (2014) hypothesise that the mosaic was carried out by a group of at least five mosaicists: two different people probably worked on the high-quality figures of the Seasons and the hunting scene, while three different sets of hands carried out the less

complex parts; in addition, a number of unspecialized workers probably devoted to the execution of backgrounds shall be considered.

The mosaicists involved in the complex decoration, though, worked independently one from the other, following a general project in the absence of a centralized control. The lack of organization is evidenced in the stylistic differences and mistakes (Salvadori and Boschetti 2014).

In order to investigate the production technologies employed in the mosaic of the Domus of the "Bestie Ferite", 38 samples were selected for the archaeometric analysis. As the mosaic is still in-situ, only tesserae that were not in the mortar were chosen selecting all the available colours; in the case of orange and sealing-wax red tesserae, all *in-situ*, a micro-sampling was conducted. According to their macroscopic colour, tesserae were classified in seven chromatic macro-groups: blue, turquoise, green, yellow, red, white, and colourless. The macro-group of "white" tesserae only includes grey tesserae, as in this mosaic white tesserae are made of stone and therefore were not sampled. A detailed list of samples is reported in appendix A2

2.2 **Classe**

The area of Classe was frequented and inhabited since the Roman time but it is in the 5th century AD, when Ravenna became the new capital city of the Empire, that Classe is transformed into a city with walls, a channel system that connected the city to Ravenna and the Adriatic sea, a drainage system and a large harbour (Augenti and Cirelli 2012) (*see fig. 2.5*). The harbour area is of particular interest for the present study: at least 18 warehouses were mainly devoted to the storage of food and other goods coming from the eastern Mediterranean and north Africa (Augenti and Cirelli 2010; Cirelli 2014). The excavations conducted in 1970 by the *Soprintendenza per i Beni Archeologici dell'Emilia Romagna* and then between 2002 and 2005 by the University of Bologna evidenced the presence of productive activities in some of the warehouses: iron slabs, slags, and traces of iron forging were unearthed. In one warehouse in particular, named Building 6 (*Fig. 2.6*), a round circular kiln was identified and interpreted as a possible glass kiln; around the kiln, a large quantity of glass fragments were recovered, which had been used to fill the basement (Tontini 2006; Cirelli and Tontini 2010). The largest part of the finds is represented by glass-working wastes: chunks, moils, threads, drops, deformed

fragments and other wastes indicate the presence in the area of a glass-working activity that took place mainly in the 5th century. Another glass assemblage, comprising vessel fragments and glass-working wastes, was excavated in a small dump named US4381, dated between the end of the 5th and the beginning of the 6th century AD (Cirelli and Cannavicci 2014). This dump is particularly relevant for its location in the productive area of the harbour (*Fig.2.6*). Glass vessels are usually highly fragmented, and comprise a very large quantity of Late Antique types and undefined vessels. Such fragmentation may indicate that vessels fragments were collected as cullet for recycling, which would be in accordance with the secondary glass-working activity that took place in the area (Chinni et al. in press).

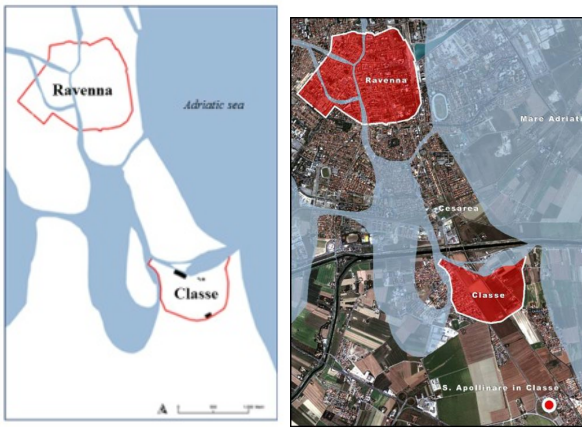

***Fig2.5**: position of the ancient city of Classe with respect to Ravenna and the Adriatic sea (left) and to the current topography of the area (right).*
(Courtesy of E. Cirelli.)

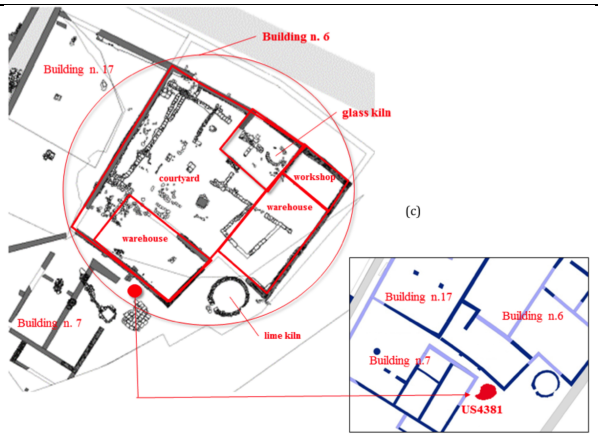

***Fig.2.6**: Reconstruction of the Building n.6 and position of the dump US4381.*
(Courtesy of E. Cirelli)

Among the over 1700 glass fragments, 78 samples were selected for the archaeometric analysis[1], favouring glassworking wastes, chunks, and selecting all types of vessels found in the site. Among the vessels, the most frequent types are beakers Isings 96, 106 and 106 late, 109 and 111, although the latter are present in the Building6 assemblage only. Most of the vessels are naturally coloured in various shades of green, blue and yellow, but some intentionally coloured blue samples were identified.

A full list of samples is given in appendix A3

[1] *Some of the samples from Building6 here included were previously analysed (Fiori and Vandini 2010; Fiori 2014) but in order to guarantee the full comparability among all the samples of the present PhD thesis, the samples were re-analysed and re-discussed.*

2.3 PORDENONE- VILLA OF TORRE DI PORDENONE

Pordenone is a small city located in the inland of north-eastern Italy (Fig.2.1) The Villa of Torre is located at Torre di Pordenone, a small village just outside the modern city, in the area between the Castle of Torre (current location of the Archaeological Museum of Western Friuli) and the Noncello river. The area was inhabited during the Roman times, although it is peripheral with respect to other important Roman centres.

The area of Torre di Pordenone was investigated for the first time between 1940 and 1952 by the Earl of Ragogna, owner of the castle, a self-tought scholar and archaeology enthusiast, and afterwards between 2008 and 2009 by the *Soprintendenza per i Beni Archeologici del Friuli Venezia Giulia*.

The excavations conducted by the Earl of Ragogna revealed the presence of mural structures interpreted as Roman baths and then as the remains of an important *villa rustica* dated to the 1st century AD. The excavations were conducted in the absence of any systematic and stratigraphic approach, and the large quantity of decorative elements such as sculpture, high-quality fresco paintings, bas-reliefs and mosaic tesserae were removed and located in the private museum of the Earl, which constitutes the first nucleus of the Archaeological Museum of Western Friuli. Unfortunately, the excavations were conducted in the absence of a systematic approach and no detailed description about the stratigraphy or provenance of the finds was produced. The large quantity of glass tesserae, mainly coloured in blue and turquoise, that were excavated in the baths, and the very concise descriptions made by the Earl and his co-workers (mainly workmen and young students) indicate the existence of mosaic geometric decorations, confirmed by the recovery of fragments of mosaic.

Due to the lack of stratigraphic information, the mosaic tesserae, mostly found in secondary sites or removed from the original decorations, are dated within the main chronological frame of the *Villa*, i.e. between the 1st century AD and the 5th century AD.

The large quantity of glass tesserae recovered testifies the abundance of musive decorations in the Domus. In order to clarify the technology of production of the glass tesserae employed, 28 samples were selected for the archaeometric analysis. Samples were selected on the basis of their macroscopic colour, and classified in seven main

chromatic macro-groups: blue, turquoise, green, yellow, red, white, and colourless. All tesserae show a very good conservation state.

A full list of samples is given in Appendix A4

2.4 Trento- Santa Maria Maggiore Cathedral

Trento is an inland city located in the extreme north of Italy (see *Fig.2.1*).

The current church of Santa Maria Maggiore was built in the 16th century, although its foundation is traced back to the paleo-Christian times. The history of the church is complex and the recent excavation campaign conducted between 2007 and 2008 by the University of Bologna revealed the complexity of its history. The modern Renaissance church was built on the remains of a paleo-Christian church dated to the 4th century AD, that was partly renovated in the Middle Age; below the Christian building, remains of Roman baths and of the *forum* dated to the 1st-4th century AD were identified (Guaitoli 2011). The excavation revealed the presence of abundant glass tesserae and mosaic fragments, employed to fill a tank of the baths, and other tesserae were identified in residual contexts. The tesserae probably derive from the decoration of the baths, carried out within the 2nd century AD and disrupted in the 4th century AD when the construction of the paleo-Christian church covered the pre-existing buildings. Another mosaic decoration (still *in-situ*) and relative to the paleo Christian church (4th century) was also excavated (Guaitoli 2011).

The tesserae considered in the present study derive from a secondary site, and were excavated from the materials filling the bath and in layers dated to the 5th-12th century; due to subsequent manipulation of the area it is probable that the tesserae found in later layers also derive from the materials excavated from the tank or from the paleo-Christian mosaic. The absence of any archaeological evidence and literary source indicating the presence of further mosaic decorations after the 4th century AD, allow dating all the tesserae found in the site between the 2nd and the 4th century AD.

32 glass tesserae representing all colours available were selected for the archaeometric analysis on the basis of their macroscopic colour; they were classified in seven main chromatic macro-groups: blue, turquoise, green, yellow, red, white, and colourless. The tesserae were in a poor conservation state and affected by

surface weathering that partially affected their macroscopic examination and the definition of colour. A full list of samples is given in appendix A.5

REFERENCES

Augenti, A., and Cirelli, E., 2010, Classe: un osservatorio privilegiato per il commercio della tarda antichità, In *LRCW 3: late Roman coarse wares, cooking wares and amphorae in the Mediterranean: archaeology and archaeometry* (eds. S. Menchelli, S. Santoro, M. Pasquinucci, and G. Guiducci), Vol. II, 605–15.

Augenti, A., and Cirelli, E., 2012, From suburb to port: the rise (and fall) of Classe as a centre of trade and redistribution. , *Rome, Portus and the Mediterranean. Archaeology Monographs of the British School at Rome*, **21**, 205–21.

Bonetto, J., and Ghedini, F., 2014, Vitruvio ad Aquileia. La casa ad atrio dei Fondi ex Cossar, In *Vitruvio e l'archeologia* (ed. P. Clini), 49–64, Marsilio, Venezia.

Bueno, M., Mantovani, V., and Novello, M., 2012, Lo scavo della casa delle Bestie Ferite, In *L'architettura privata ad Aquileia in età romana, Atti del Convegno di Studio (Padova, 21-22 Febbraio 2011)* (eds. J. Bonetto, and M. Salvadori), 77–100, Padova University Press, Padova.

Bueno, M., and Centola, V., 2014, Le domus di Aquileia e le loro evoluzioni architettonico-funzionali in età Tardoantica: i casi delle domus delle Bestie Ferite e di Tito Macro presso i Fondi Ex-Cossar., In *Costantino il Grande a 1700 anni dall'"Editto di Milano"* (ed. G. Cuscito), 317–34, Editreg, Trieste.

Buora, M., Mandruzzato, L., and Verità, M., 2009, Vecchie e nuove evidenze di officine vetrarie romane ad Aquileia, *Quaderni Friulani di Archeologia*, **XIX**.

Chinni, T., Cirelli, E., Maltoni, S., Vandini, M., Silvestri, A., and Molin, G., La diffusione del vetro nell'Adriatico centrale: studi tipologici e dati chimici da Classe, In *Economia e Territorio nell'Adriatico centrale tra tarda Antichità e alto Medioevo* (eds. E. Cirelli, E. Giorgi, and G. Lepore), Bononia University Press, Bologna.

Cirelli, E., and Tontini, S., 2010, Produzione vetraria a Classe nella tarda antichità , In *Riflessioni e trasparenze. Diagnosi e conservazione di opere e manufatti vetrosi. atti del convegno* (ed. M. Vandini), Vol. Ravenna, 125–33, Bologna.

Cirelli, E., and Cannavicci, A., 2014, A 6th century dump from Classe (Ravenna). In (). , In *Late Roman Coarse Wares, Cooking Wares and Amphorae in the Mediterranean. Archaeology and archaeometry.Proceedings of the 4th International Conference* (eds. N. Poulou-Papadimitriou, E. Nodarou, and V. Kilikoglou), Vol. Thessaloni, 963–74, Archaeopress Publishers of British Archaeological Reports, Oxford.

Cirelli, E., 2014, Typology and diffusion of Amphorae in Ravenna and Classe between the 5th and the 8th centuries AD. , In *Late Roman Coarse Wares, Cooking Wares and Amphorae in the Mediterranean. Archaeology and archaeometry. Proceedings of the 4th International Conference* (eds. N. Poulou-Papadimitriou, E. Nodarou, and V.

Kilikoglou), Vol. Thessaloni, 541–52, Archaeopress Publishers of British Archaeological Reports, Oxford.

Fiori, C., and Vandini, M., 2010, Produzione di vetro a Classe (Ravenna) nel V-VI sec d.C., *Rivista della Stazione Sperimentale del Vetro*, **5**, 15–24.

Fiori, C., 2014, Mosaic tesserae from the Basilica of San Severo and glass production in Classe, Ravenna, Italy, In *New light on old glass: recent research on Byzantine mosaics and glass* , 33–41, The British Museum, London.

Freestone, I. C., Greenwood, R., and Gorin-Rosen, Y., 2002, Byzantine and early Islamic glassmaking in the eastern Mediterranean: production and distribution of primary glass. In, In *Hyalos-Vitrum-Glass. History, technology and conservation of glass in the Hellenic world* (ed. K. G.), 167–74, Glasnet Publications, Athens.

Gallo, F., Marcante, A., Silvestri, A., and Molin, G., 2014, The glass of the "Casa delle Bestie Ferite": A first systematic archaeometric study on Late Roman vessels from Aquileia, *Journal of Archaeological Science*, **41**, 7–20.

Gorin-Rosen, Y., 2000, The ancient glass industry in Israel. Summary of the finds and new discoveries. , In *La Route du Verre: Atelieres primaires et secondaires du second millinaire av. J.-C. au Moyen-Age.* (ed. M. D. Nenna), 49–64, Maison de l'Orient Méditerranéen, Lyon.

Guaitoli, M., 2011, Il progetto di Santa Maria Maggiore (Trento). Relazione preliminare: dallo scavo alla diffusione dei dati, *FOLD&R FastiOnLine documents & research*, 1–18.

Salvadori, M., and Boschetti, C., 2014, "Lavorare stanca": la disorganizzazione di una bottega di mosaicisti in età tardoantica. Il caso del mosaico delle Bestie Ferite, In *Costantino il Grande a 1700 anni dall'"Editto di Milano"* (ed. C. G.), 335–50, Editreg, Trieste.

Tontini, S., 2006, Vetri e produzione vetraria a Classe (Ravenna) in età tardoantica e altomedievale, *Bulletin. Association pour L'Antiquité Tardive*, **15**, 45–55.

3. ANALYTICAL METHODS

3.1. OPTICAL MICROSCOPY (OM)

Optical microscopy observations were carried out under stereoscopic vision on the whole fragment with a Zeiss Stemi 2000C microscope to investigate the homogeneity of the samples, in particular for vessels and glassworking wastes.

Optical microscopy observations were also conducted under reflected light on polished sections with a Nikon Eclipse ME600 for a preliminary textural investigation of the non-homogenous samples and of mosaic tesserae.

Both microscopes are available at the Department of Geosciences, University of Padova (Italy)

3.2. SCANNING ELECTRON MICROSCOPY WITH ENERGY DISPERSIVE SYSTEM (SEM-EDS)

SEM-EDS analyses were carried out on all the mosaic tesserae considered in the present study for textural and preliminary chemical evaluation. Samples of glass tesserae were prepared in polished sections; in the case of whole tesserae, sections were obtained by cutting each *tessera* perpendicularly to the surface or, in the case of banded textures, by cutting along the most representative direction.

In the case of micro-samples of mosaic tesserae, they were entirely embedded in epoxy resin blocks.

The surface of each sample was then polished with a series of diamond pastes and colloidal silicon down to 0.02 □m grade and coated with conductive carbon film. The same polished sections were also employed for EPMA analysis.

SEM-EDS analyses were performed with ESEM FEI Quanta Inspect equipped with an Oxford energy dispersive spectrometer. The radiation source is a tungsten filament. Working conditions with low-vacuum accelerating voltage of 200 V – 30 kV; resolution of 3 nm at 30 kV; EDS working distance of 10 mmTungsten filament; Probe current: up to 2□A available at the Department of Cultural Heritage of the University of Bologna.

and with a FEI Quanta 200 FEG-ESEM instrument at the Institute of Inorganic chemistry and surfaces (IENI-CNR) Padova, Italy equipped with a Genesys energy-dispersive X-ray spectrometer, with accelerating voltage of 20-25 kV.

3.3. X- RAY FLUORESCENCE (XRF)

The bulk chemistry of vessels and glassworking wastes of suitable dimensions was determined by X-Ray Fluorescence (XRF) on a Philips PW 2400 instrument equipped with an Rh tube and WDS spectrometer available at the Department of Geosciences, University of Padova and IGG-CNR, Padova (Italy). Samples were cut with a diamond saw and the external layers were removed with a micro-drill to avoid contamination. The samples were then crushed in an agate mortar. The powders thus obtained were put in an oven at 110°C for 12 hours in order to determinate the loss on ignition (LOI). The powders were then mixed with $Li_2B_4O_7$ in a 1:10 ratio and beads were prepared.
XRF analyses allowed determining all the chemical components which characterise archaeological glass, excluding Cl, S, Sn and Sb that were checked by means of EPMA. XRF precision was better than 0.6% for major and minor elements, and about 3% for trace elements; accuracy was within 0.5 wt.% for Si, lower than 3% for other major and minor elements, and lower than 5% for traces.

Results are expressed as percent concentrations of element oxides for major and minor elements and as ppm for trace elements.

Full instrumental parameters and analytical conditions are detailed in (Silvestri et al. 2011).

3.4. ELECTRON PROBE MICRO ANALYSIS (EPMA)

EPMA analysis was employed to check the concentrations of Cl, S, Sn, and Sb in all the samples analysed by XRF, to determine the chemical bulk composition of the fragment of glass vessels and working indicators with dimensions not suitable for XRF, and the chemical composition of the glassy matrix of the mosaic tesserae. For EPMA analysis, in the case of glass vessels and glassworking indicators, small fragments were cut perpendicularly to the surface, avoiding weathered areas, with a diamond-coated saw,

and embedded in epoxy resin blocks; in the case of glass mosaic *tesserae*, a section of each *tessera* was cut perpendicularly to the surface or, in the case of banded textures, selecting the most representative direction of cut, and mounted on sections. In the case of micro-samples of mosaic tesserae, they were embedded in epoxy resin blocks, too. The surface of each sample was then polished with a series of diamond pastes down to 1 □m grade and coated with conductive carbon film.

The instrument employed is a CAMECA-CAMEBAX, equipped with four wavelength-dispersive spectrometers (WDS) and available at the Institute of Geoscience and Earth Resources (IGG-CNR, Padova-Italy). Operating conditions were 20kV and 2nA sample current for Na, Al, Si, and K, with a counting time for peak and background of 10s each, with a focalised beam of 1□m in the case of opacified tesserae and 10□m in the case of homogenous glasses.
Synthetic pure oxides were used as standards for Al, Cr, Fe, and Sn, synthetic MnTiO3 for Mn and Ti, wollastonite for Si and Ca, albite for Na, periclase for Mg, vanadinite for Cl and Pb, orthoclase for K, apatite for P, sphalerite for S and Zn, SbS_3 for Sb, and pure elements for Co, Cu, Ni. The precision of EPMA analysis was between 0.5% and 10% for major and minor elements. The accuracy was lower than 1% for SiO_2, Na_2O, and FeO, lower than 5% for minor elements, and not higher than 12% for trace elements.

An average of six analytical points in the case of homogenous glasses, and an average of 12 analytical points on non-homogenous glasses (i.e. glass *tesserae*) were carried out and mean and standard deviations were calculated.

Detection limits, calculated on the basis of the analytical conditions, are fully reported in (Silvestri et al.)

3.5. X-RAY POWDER DIFFRACTION (XRPD)

X-ray powder diffraction was employed to determine the opacifying agents in mosaic tesserae.

X-ray powder diffraction (XRPD) analyses were performed on the whole tesserae for conservative purposes. The instrument used is a PANalytical X'Pert PROdiffractometer (Bragg-Brentano geometry), equipped with a Cu X-ray tube (40 kV

and 40 mA) and X'Celerator detector, at the Department of Geoscience of the University of Padova (Italy). Scans were collected in the angular range 3-80°2□ with 0.03° virtual step size, and 100 s/step counting time.

Micro-XRPD measurements were performed to identify the opacifying phase of micro-samples of red and orange glass tesserae that were not suitable for bulk XRPD. Micro samples of 50-200 μm were removed from the sections a mounted on a capillary tube (see fig.3.1).

The instrument employed is a prototype, unique in the world, allowing very fast measurements accompanied by high sensitivity and dynamic range. It is a single-crystal diffractometer Agilent Supernova equipped with a micro-X-ray source (Mo Kα radiation) working at 50 kV and 0.8 mA with a spot size of 0.11 mm, and a Pilatus 200 K detector (Dectris).

Data were collected in micro-X-ray powder diffraction mode, due to the policrystalline nature of the samples.

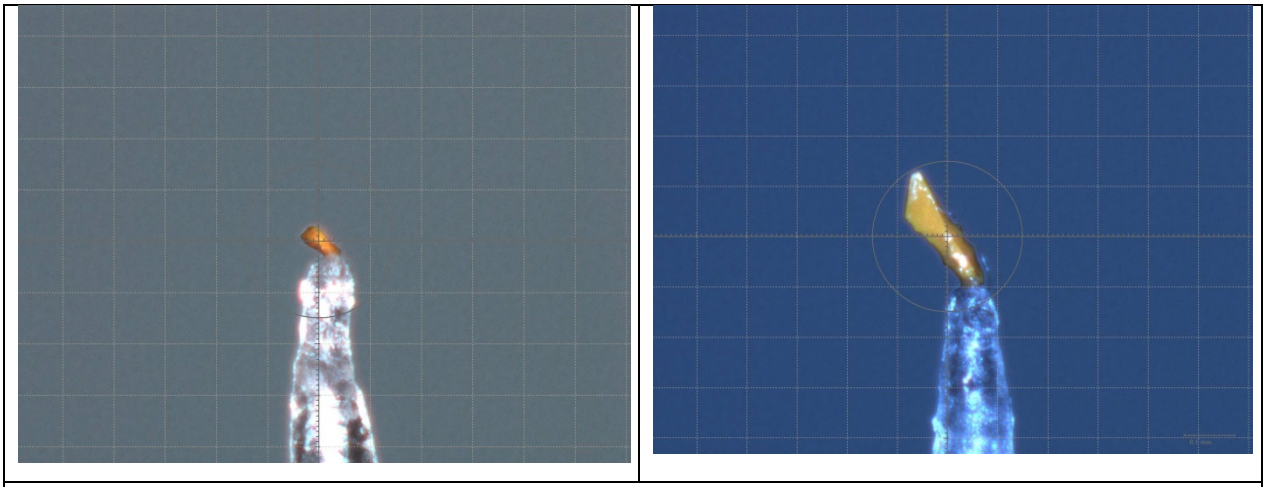

Fig. 3.1: micro sample of glass mounted on a capillary tube for micro-XRPD analysis. Grating represents 100 microns.

3.6. Multi Collector Inductively Coupled Plasma Mass Spectrometry (MC-ICP-MS)

To determine the isotopic ratios for Sr and Nd on selected samples of glass vessels and glassworking wastes, isotopic analyses were performed with Multi Collection Inductively Coupled Plasma Mass Spectrometry (MC-ICP-MS)

Fragments of about 100 mg were sampled and ground in an agate mortar.

In order to separate Sr and Nd from the glass matrix, a chromatographic separation was carried out in a class 10 clean lab at Ghent University (Belgium) following the methods reported in (Ganio et al. 2012).

After the separation process, the concentration of both Sr and Nd was checked by means of a Perkin-Elmer SCIEX Elan quadrupole-based ICP-Mass Spectrometer at Ghent University (Belgium). The isotopic ratio for Sr and Nd was then determined by Multi Collector Inductively Coupled Plasma-Mass Spectrometry (MC-ICP-MS) performed with a Thermo-Scientific Neptune instrument at Ghent University (Belgium).

The detailed procedure for Nd isolation, and the full analytical conditions for the elemental analysis and the isotopic ratio determination are reported in (Ganio et al. 2012).

3.7. MICRO-RAMAN SPECTROSCOPY

Micro-Raman spectra were performed on selected samples in order to identify specific mineralogical inclusions whose concentration was too low to be detected by XRPD.

The same sections employed for SEM and EPMA analyses were employed.

The instrument is a DXR Thermo Scientific Raman microscope, equipped with a diode-pumped solid state 532 nm laser, available at the Chemistry Department of the University of Padova (Italy). The analytical points were performed with an 50x LWD (Long Working Distance) objective, operating at a power of 8-10 mW, with a spectral resolution in the range of 2.7–4.2 cm□1 and a spatial resolution of 1.1 □m. The acquisition time adopted was 5 s for 32 scans accumulation.

The on-line RUFF database was employed for the attribution of crystalline phases (http://rruff.info).

3.8. ELECTRON PARAMAGNETIC RESONANCE

Electronic Paramagnetic Resonance spectra were performed in order to have information about the oxidation state of iron in selected samples of vessels and mosaic tesserae. Small fragments (2-3 mm) were removed from the samples and mounted on a

quartz tube of 2 mm inner/ 3 mm outer diameter, and the sample holder was inserted in the TMH resonator for the measurement.

Continuous wave X-Band EPR spectra were acquired by means of a Bruker ECS106 Electron Spin Resonance instrument, with a TMH resonator and a frequency counter Hewlett Packard 5342° available at the Chemistry Department of the University of Padova (Italy). All spectra were acquired at room temperature under the following conditions: microwave power of 20 mW, modulation amplitude 8 G, microwave frequency 9.55 GHz.

3.9. FIBER OPTIC REFLECTANCE SPECTROMETRY (FORS)

In order to obtain information on the chromophoric ion present in selected glass tesserae, reflectance spectra were acquired. To guarantee maximum reflectance, glass tesserae were flattened and polished with a series of diamond pastes up to 5 □m.

The instrument is an Ocean Optics Fiber Optic Reflectance Spectrophotometer (FORS)

The instrument, available at the Department of Chemistry of the University of Padova (Italy), consists in a light source, an integrating sphere and a spectrometer, all connected by means of optical fibres. In particular, the light source employed is a deuterium-halogen lamp (DH-2000), generating radiation between 210 and 1500 nm and connected through a quartz-core fibre optic cable (QP-600-2-SR-BX) to the top of an integrating sphere (ISP-50-8-R) with an 8 mm opening on the bottom. The spectrometer is a wavelenght-dispervive system (HR 2000+) which is connected to a quartz-core fibre optical cable (QP-600-2-SR-BX) to the integrating sphere.
To record and process the signal, the SpectraSuite software was employed.
As a reference for white standard, a disc of polished PTFE was used.
FORS spectra of the samples were acquired between 188 and 1100 nm, with 10 replicas and acquisition time of 60 seconds. Only the visible interval (between 350 and 800 nm) is displayed.

Ganio, M., Latruwe, K., Brems, D., Muchez, P., Vanhaecke, F., and Degryse, P., 2012, The Sr-Nd isolation procedure for subsequent isotopic analysis using multi-

collector ICP-mass spectrometry in the context of provenance studies on archaeological glass, *Journal of Analytical Atomic Spectrometry*, **27**(8), 1335–41.

Silvestri, A., Tonietto, S., Molin, G., and Guerriero, P., (in press) Multi-methodological study of palaeo-Christian glass mosaic tesserae of St. Maria Mater Domini (Vicenza, Italy), *European Journal of Mineralogy*.

Silvestri, A., Molin, G., and Pomero, V., 2011, The stained glass window of the southern transept of St. Anthony's Basilica (Padova, Italy): study of glasses and grisaille paint layers, *Spectrochimica Acta Part B: Atomic Spectroscopy*, **66**(1), 81–7.

4. GLASS VESSELS AND WORKING WASTES

4.1. OPAQUE GLASS

Among the samples from the Domus of Tito Macro in Aquileia, 5 samples are made of intentionally coloured and opacified glass. They are: the only pre-Roman core-formed blue vessel (AQ-FC-Alab_1, dated to 300-250 BC), two fragments of mosaic bowls, respectively an Isings 1/18 (AQ-FC-1/18_1) dated to 1st century and made with yellow, red and green glass and an Isings 3 (AQ-FC-3_3) dated to 1st century AD made with transparent blue and opaque white glass; two opaque working wastes, coloured respectively in blue and turquoise, are also included. Unlike the vessels, which can be dated on the basis of the archaeological type, working wastes cannot be dated and therefore chemical and mineralogical analysis can provide unique information about any glassworking activity that took place in Aquileia and its surrounding area in Roman-late Roman time.

Opaque coloured glasses are constituted by two main components: a glassy matrix, that may be coloured, and the opacifying agents, generally constituted by abundant small crystals; due to their complexity, these objects were analysed from a textural point of view, with a Scanning Electron Microscopy coupled with an Energy Dispersive Spectrometer (SEM-EDS) for a preliminary chemical characterisation; chemical analysis of the glassy matrix was then conducted by means of an Electronic Micro Probe (EPMA) avoiding, when possible, the opacifying crystals and other relic and newly formed phases.

4.1.1. TEXTURAL CHARACTERIZATION

The three opaque coloured vessels are composed of different glasses.

The only core-formed vessel of the assemblage **(AQ-FC-alab_1***)* is made of a blue translucent body decorated with yellow and white opaque threads applied to the external surface. Both the internal and the external surface appear corroded, in particular the internal surface presents the rough irregular surface which is typical of core formed glasses. The three colours are treated as three different samples, named AQ-FC-alab1_blue, AQ-FC-alab1_yellow and AQ-FC-alab1_white, respectively.

SEM-BSE images (Fig 4.1) of the sample clearly show the difference in the average atomic number of the decorations, brighter (i.e. high atomic number) than the translucent body (grey, i.e. low atomic number). The white and yellow threads seen in section (fig. 4.2 and

4.3) are not regular in their shape and texture. The yellow decoration shows an uneven distribution of opacifying crystals embedded in a very bright glassy matrix. Although the yellow decoration and the body are clearly distinguishable, there is no clear border between them, as can be observed in the SEM-BSE images (Fig 4.3-4.4), and this can be due to a local mixing of the yellow and blue glass. Conversely, the white decoration is more defined, characterised by a large quantity of small crystals, both isolated and aggregated in small lumps (fig 4.2-a) and identified by EDS analysis as probable Ca- antimonates (Fig.4.2-b)

The large yellow decoration of fig. (4.3-4.4) is constituted by two different layers of opacified glass, respectively white and yellow, where the white layer is in contact with the vessel body while the yellow one, that is the visible part, is applied on it. This characteristic is not visible with the naked eye, as the white layer is hidden by the yellow one and can be seen only in section, therefore this may be a mistake of the vessel maker or a change in the decoration pattern.

The textural examination of the decorations also evidenced the presence of relic phases of relatively large dimension, characterised by an irregular shape and a low atomic number, identified in the white and yellow decoration (fig 4.2, 4.4) and interpreted by SEM-EDS data as probable relics of quartz, presumably deriving from the sand employed in the primary production.

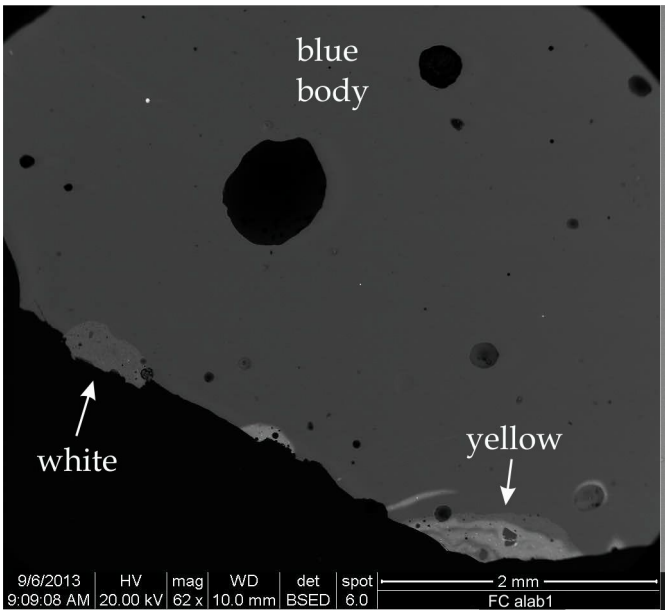

Fig4.1: *SEM BSE image of sample AQ-FC-Alab_1. The blue body and the yellow and white decorations are clearly*

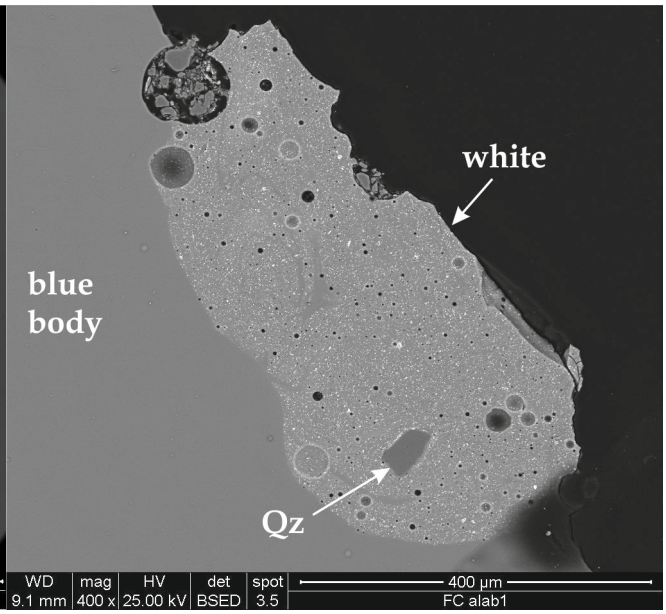

Fig. 4.2a*: SEM BSE image: detail of the white decoration. The opacifying crystals are well dispersed. Note the*

distinguished. Black circular items are gas bubbles.

presence of quartz inclusion, indicated as "Qz" and gas bubbles, in black.

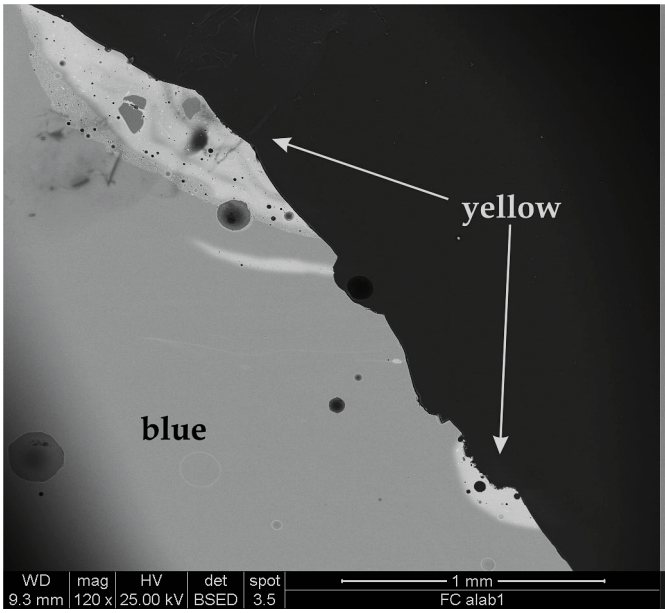

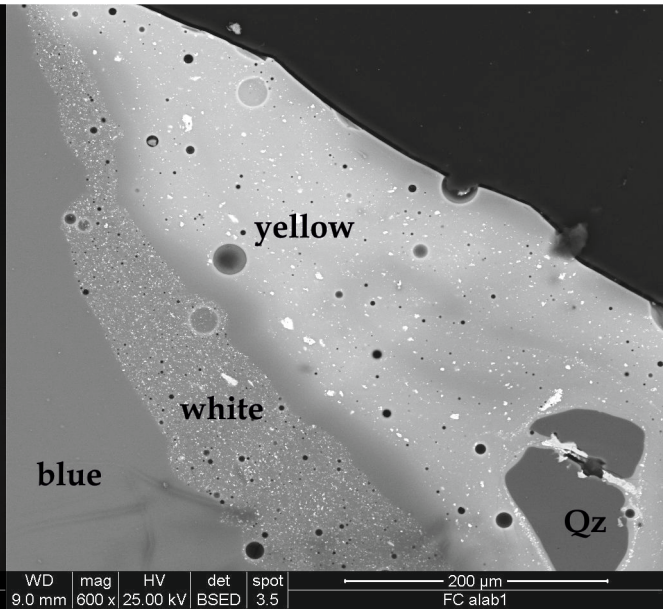

Fig 4.3: SEM-BSE image, detail of the yellow decoration. The highlighted area is enlarged in fig.4.4

Fig.4.4: SEM BSE image, detail of the yellow decoration; the overlap between white and yellow is evident; the uneven texture of the yellow decoration is highlighted by the fluidal banding, marked by different grey tones.

The blue body of the vessel is homogenous, with no opacifying agent and a few bubbles of variable dimensions, from micrometric to millimetric size (fig 4.1). Despite the general homogeneity, some interesting inclusions were identified in the blue part: a droplet of relic CuS (fig. 4.4) with a Cu:S atomic ratio close to 50:50 and, according to SEM-EDS data, interpreted as covellite, and some other inclusions Figs 4.5-6-7-8.

The high contrast SEM-BSE image of the CuS drop (fig. 4.5) indicates the presence of a segregation area of higher atomic number, which was identified by SEM-EDS as constituted mainly by Sb and Cu, together with other diagnostic elements such as nickel and arsenic (see tab); a similar association of elements, although in different ratios, was identified also in the partially dissolved, bright rounded droplets of Fig. 4.6 and in one of the inclusions of Fig 4.7 (point 5). An uncommon inclusion is presented in Fig. 4.7: a cluster of bright droplets, identified by SEM-EDS as probable iron oxides, surrounded by a low atomic number relic phase whose composition and atomic ratio, according to SEM-EDS data, are consistent with a pyroxene (point 6), and a bright, relatively large inclusion indicated as point 5, which contains cobalt associated with Sb, Ni and As (SEM-EDS data, see Fig.)

In addition, some sporadic inclusions of tin oxide, probably in the form of cassiterite (fig 4.8) were identified.

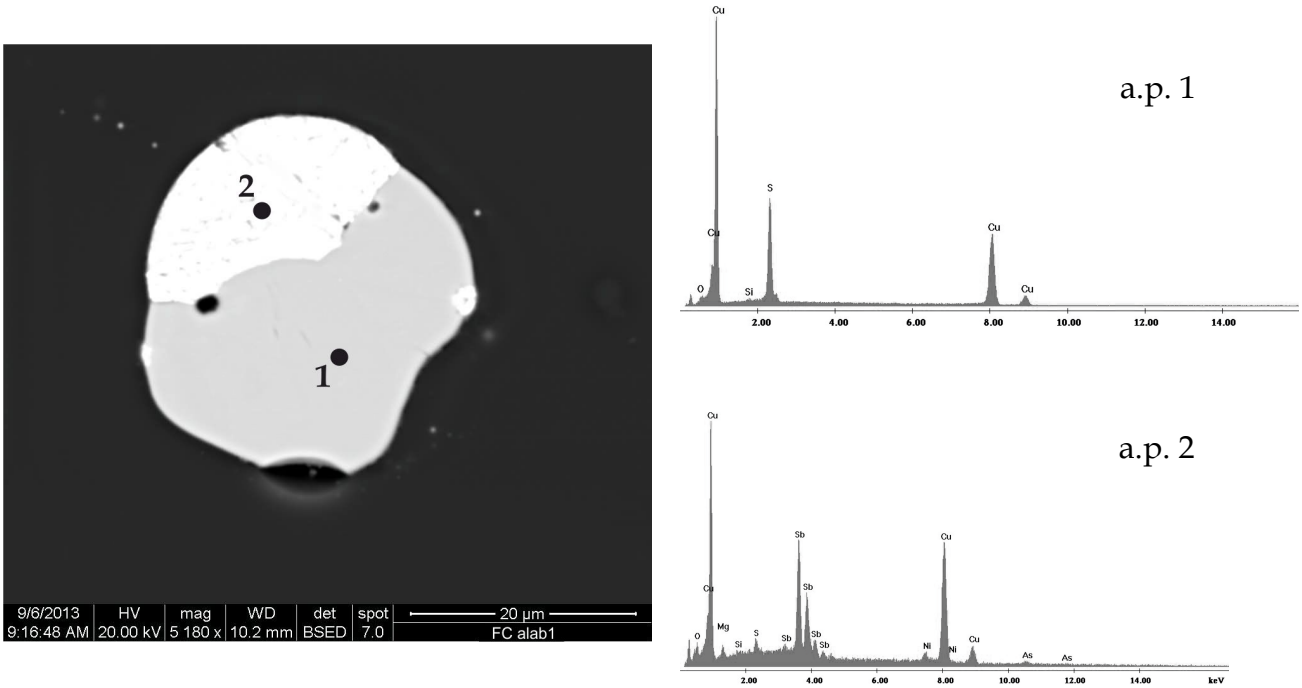

***Fig.4.5(a) left**: SEM EDS image. Of a Cu-rich inclusion. SEM-EDS spectrum of point1 and 2 are reported in **(b) right**: a.p. 1 (grey) corresponds to CuS, probably covellite; a.p. 2 corresponds to a Cu-Sb segregation, rich in Ni, As, and S.*

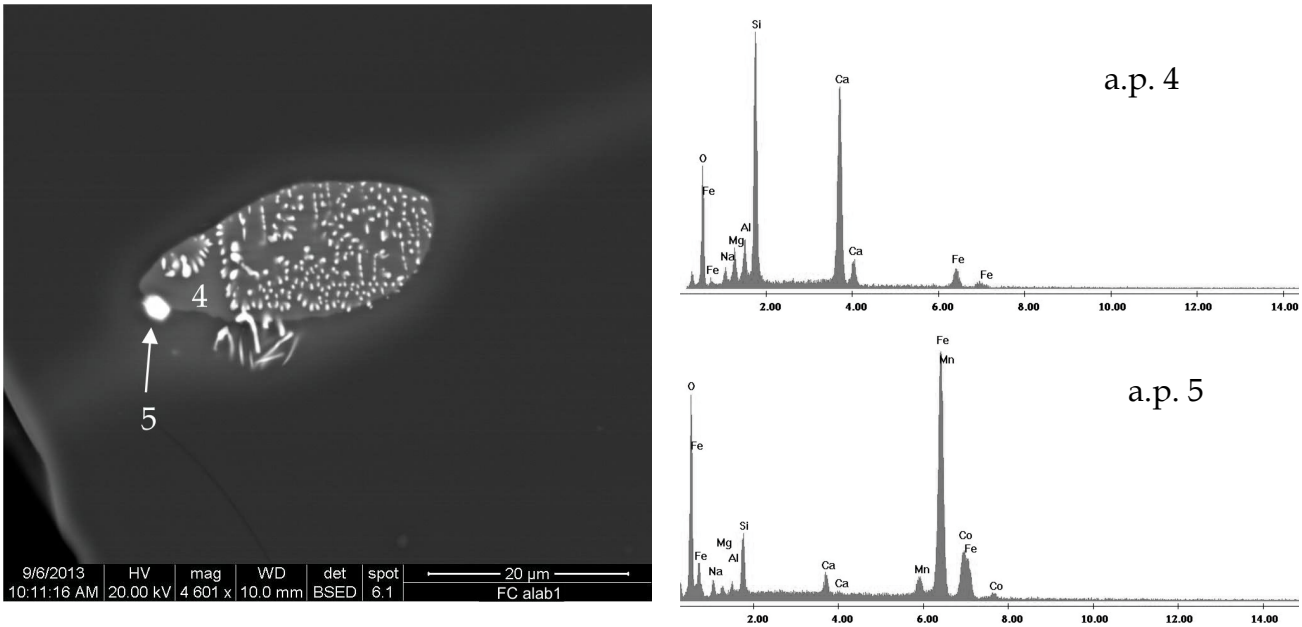

*Fig.4.7: detail of the blue body **(a) left**: SEM-BSE image of a probable pyroxene inclusion (grey, a.p.4) with iron oxides (white flakes) and an uncommon Co-rich inclusion (white a.p.5**);** the bright zone around the inclusion is enriched in iron **(b) right**: EDAX spectrum for point 4 and 5*

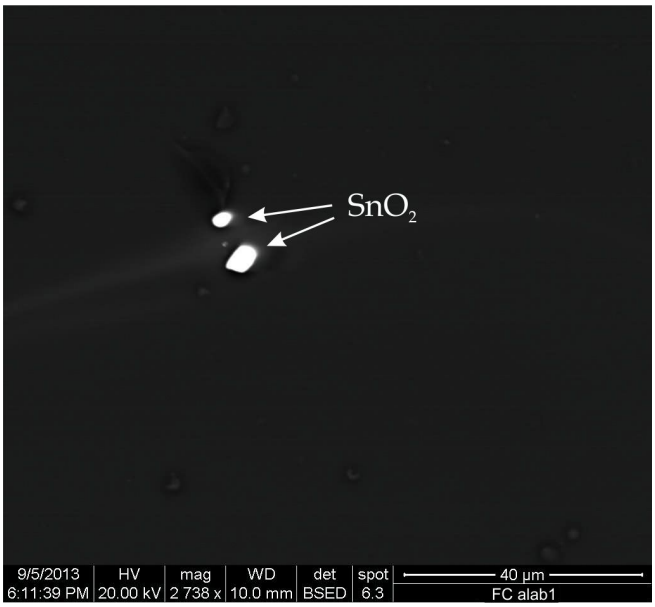

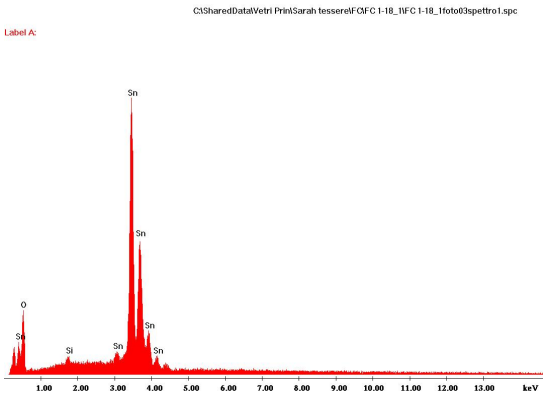

Fig.4.8: (a)left: *SEM-BSE image: cassiterite SnO_2, partly dissolved as testified by the tin-rich stripes. (b) right: EDAX spectrum*

Sample 3_3 is a mosaic cup made with translucent blue and opaque white glass.

The SEM-BSE image highlights the very homogenous texture of the blue glass (grey) and the abundance of fine, well-dispersed opacifying crystals in the white bands (fig.4.9) characterised by a higher average atomic number with respect to the blue parts. Crystal of the opacyfing agents are generally small and finely dispersed, occasionally clustered in large lumps and generally euhedral in habitus (Fig. 4.10). According to SEM-EDS data, the opacifier is probably Ca-antimonate. The very small amount of gas bubbles, the virtual absence of any relic or newly formed phase (except for the opacifier) is indicative of the high technological skills of the glassmaker.

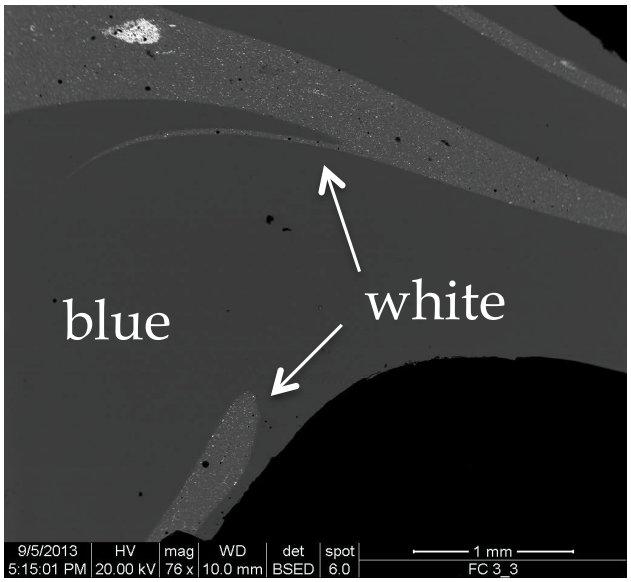

Fig. 4.9: *SEM-BSE image of sample AQ-FC-3_3. The white stripes are characterised by high atomic number (white)*

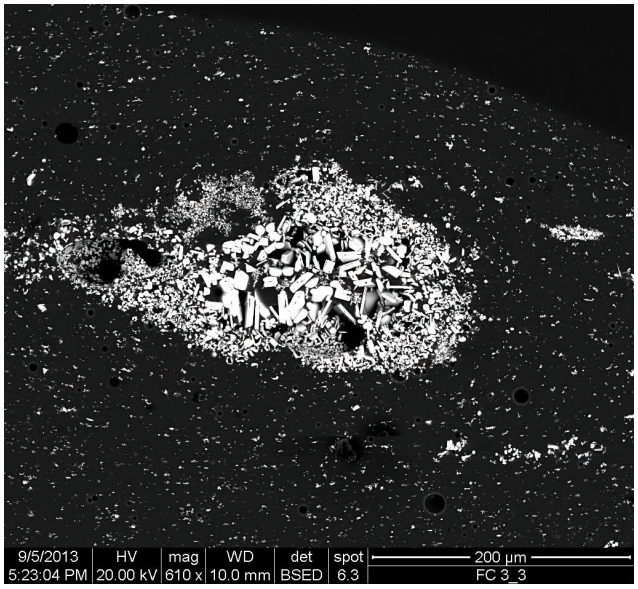

Fig. 4.10*: SEM BSE image: detail of a white area: large aggregate surrounded by abundant, small and well dispersed euhedral crystals Ca- antimonates.*

Sample 1/18_1 is a mosaic cup made with three different glasses coloured in yellow, red and green, respectively. The external surfaces are heavily weathered and only the yellow and green glasses were visible at a macroscopic observation. When the sample was prepared in polished section, the fresh cut revealed the presence of the red component.

As shown by the SEM-BSE image, the texture of this sample is quite complicated: red zones are surrounded by yellow glass that prevents contact with the green glass. The latter seems to act as a "matrix" embedding pieces of yellow and red canes deformed by vessel shaping.

The yellow glass is very bright in SEM-BSE images and is characterised by higher average atomic ratio with respect to red and green (Fig. 4.11). It is characterised by the presence of abundant crystals of small dimensions, euhedral in habitus, and very bright (i.e. high average atomic number) interpreted, according to SEM-EDS data, as probable Pb-antimonate crystals.

The red glass is apparently homogenous, when examined at low magnification, such as in Fig. 4.11. Conversely, when the red area is observed under very high magnification, a large amount of nanometric crystals, well dispersed in the glass matrix become visible. SEM-EDS data allow identifying the crystals as copper-rich phases, although discerning between metallic copper and copper oxide is not possible; no other relic phase or gas

bubble was identified in the red glass, indicating the high technological skills of the glassmaker.

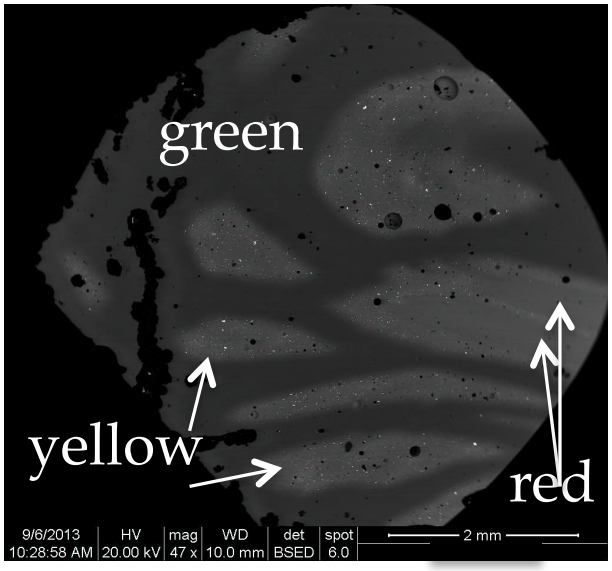

Fig 4.11: *SEM-BSE image showing the different coloured zones. Dark areas correspond to green glass, bright areas with white small inclusions correspond to yellow; red areas (medium grey) appear homogenous at low magnification*

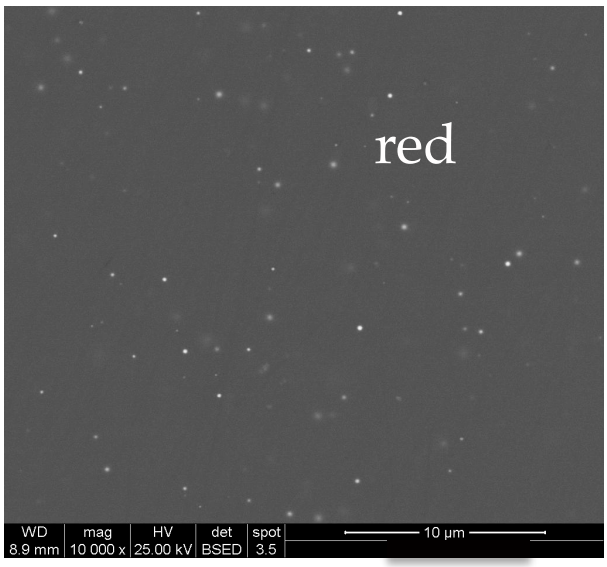

*Fig. **4.12:** SEM-BSE image: detail of the red zone. Nanometric particles suspended in the glass matrix of a Cu-rich phase (probably metallic copper) are visible.*

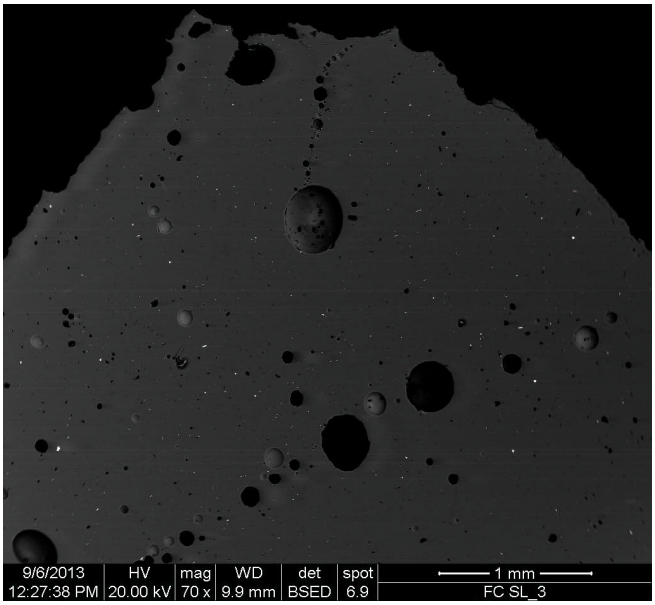

Fig.4.13 *SEM-BSE image of sample AQ-FC-SL3. Note the low density of opacifiyng crystals (bright small dots) and the numerous gas bubbles (black)*

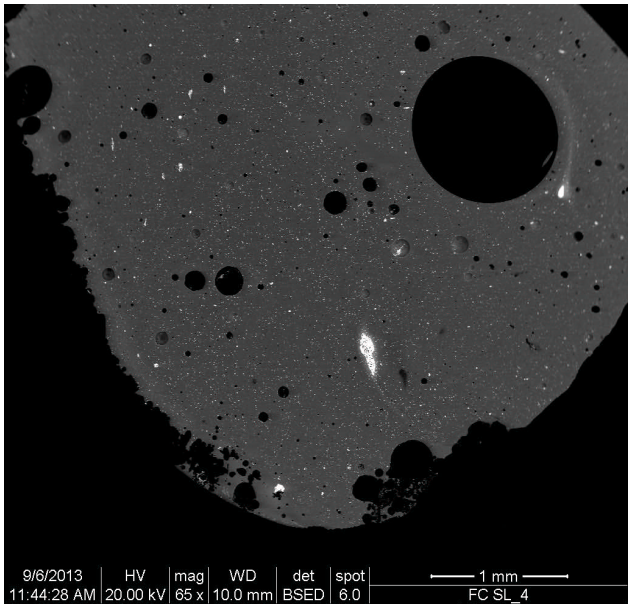

Fig.4.14 *SEM-BSE image of sample AQ FC SL4. Note the high density of opacifiyng crystals (bright small dots) and the numerous gas bubbles (black)*

The two working wastes here included (**AQ-FC-SL_3 and AQ-FC-SL_4)** are made of opaque glass, coloured respectively in blue and turquoise and both contain opacifiying agents identified with SEM-EDS analysis as presumed Ca-antimonates; as both are drops of glass, their macroscopic aspect does not allow to relate the wastes to a specific step of

glassworking, as it happens with other kind of wastes such as moils or puntil wads; some information may be therefore deduced from the textural and chemical examination.
The examination of the texture shows that the blue sample has a very small amount of opacyfiers that, when detected, are isolated Ca- antimonate crystals; a large amount of bubbles of variable dimensions is also present.
Conversely, the turquoise drop (AQ-FC_SL4) is well opacified by abundant, finely dispersed crystals, probably Ca-antimonate, that generally are euhedral and show no clear evidence of re-melting. Large inclusions of partly dissolved iron oxides are present, as highlighted in Fig. 4.14; abundant large gas bubbles are also present.

4.1.2. CHEMICAL CHARACTERIZATION

Most of the coloured and opaque samples here analysed have a complex texture, therefore defining the chemical composition of the glassy matrix of each colour is not always possible without quite a degree of uncertainty: the weathering processes may have led to the loss of alkali, and the EMPA analysis may have been affected by the absence of a clear border between different colours, the small size of the coloured areas and the presence of abundant opacifiers. For these reasons the chemical data acquired on the analysed vessels shall be considered as bulk analyses, aimed to give an overall idea of the average composition of the sample. Full chemical compositions are presented in table 4.1
The samples here included are silica-soda-lime glass; the low content of MgO and K_2O, generally below 1.50%wt (tab. 4.1) indicates that they are produced with natron as a flux, according to the Roman and Late Roman tradition. The only exception is AQ-FC-1/18_1red, which shows higher values for MgO, K_2O, P_2O5, and CaO and is probably produced with soda plant ash as a flux.

The *alabastron* AQ-FC-alab_1 is produced with three glasses, slightly different in composition. The three colours show different contents of silica and soda, as can be seen in table 4.1): in the white and yellow colour, the soda content is very low if compared to the blue vessel and to natron glass in general, being 13.67% wt in the white and 11.60%wt in the yellow, respectively; in addition the white glass has a slightly higher potash content and the yellow has a slightly lower alumina content. The three coloured glasses have high

manganese, above 1%wt, variable lead, antimony, cobalt and copper contents, while tin, arsenic and zinc are always below detection limits.
In detail, the blue body is characterised by the presence of cobalt (662 ppm), copper (969 ppm), lead (796 ppm), and antimony (Sb_2O_3=0.32wt%).
The yellow component is rich in lead (PbO ≈11wt%) and antimony (0.92wt%). Conversely, in the white component lead is present in lower concentrations (PbO 0.5wt%) and antimony is very high (Sb_2O_3=4.21wt%).

Sample AQ-FC- 3_3 is made of opaque white (AQ-FC-3_3white) and translucent blue glass (AQ-FC-3_3blue); the low levels of MgO and K_2O of both glasses indicate that natron was employed as a flux.
The blue part contains high cobalt and copper contents, both in the range of several hundred parts per million, and iron (Fe_2O_3= 0.94 wt%); antimony and lead are below detection limits. The white part is characterised by the presence of abundant antimony (Sb_2O_3= 4.41wt%), while lead, tin, zinc and arsenic are below detection limits in all samples.
Both glasses have high MnO contents, respectively 0.80wt% in the blue and 1.15wt% in the white glass. Lead, tin, arsenic, zinc are below detection limits in both glasses.

Sample 1/18_1 is made of three different glasses: a transparent, green glass (AQ-FC-1/18_1 green), an opaque red glass (AQ-FC-1_18/1 red) and an opaque yellow glass (AQ-FC-1/18_1yellow). While the green and yellow glasses show low levels of MgO and K_2O, both below 1.50wt%, consistent with a natron-based production, the red glass shows high contents of calcium oxide (9.02wt%), magnesia (2.49%wt) potash (1.53 wt%) and phosphorous oxide (1.00%wt) that, together with the relatively high soda content (14.42wt%), may indicate a soda-plant ash base glass. The red component, the only probable plant ash glass identified here, also presents high amounts of copper (CuO=3.5wt%), iron (Fe_2O_3 1.74wt%), tin (SnO=0.25wt%), zinc (734 ppm), antimony oxide (0.32wt%) and lead (PbO ≈3.5wt%)
Despite the analogy in the flux employed, the green and the yellow glasses differ in their major and minor oxides: the yellow sample has lower soda (13.74wt%), alumina (1.75wt%) and lime (5.79wt%) and negligible manganese, high lead (≈PbO 4wt%) and antimony

(Sb_2O_3 =0.87wt%). Differently, the green glass is characterised by higher contents of soda (15.50wt%), alumina (2.31wt%) and lime (7.84wt%), high iron (2.19wt%), copper (CuO≈1.5wt%), low lead (0.3wt% as PbO) and some cobalt (350 ppm), tin (0.15 wt% as SnO) and zinc (334 ppm). The opaque red and the translucent green glasses have in common high iron, copper, and lead contents, the presence of tin zinc and antimony, despite some differences in concentrations.

Samples **AQ-FC-SL_3** and **AQ-FC-SL_4** are both natron glasses showing the usual composition of Roman glass, although sample AQ-FC-SL_4, coloured in turquoise, is characterised by a high potash content (2.03 wt%).
Both samples have very high iron, respectively 1%wt in the turquoise AQ-FC-SL_4 and 1.31wt% in AQ-FC-SL_3, high antimony (above 2 wt%) and high lead contents, around two thousand ppm in both samples.
High concentrations of cobalt (953 ppm) and copper (1941 ppm) were detected in the blue AQ-FC-SL_3, while the turquoise sample AQ-FC-SL_4 contains considerable amounts of CuO (more than 12 000 ppm) and some tin (SnO= 0.06wt%). Zinc and arsenic are below detection limits in both the samples.

4.1.3 DISCUSSION

The pre-Roman core-formed alabastron (AQ-FC-alab1) is produced employing three coloured natron glasses of slightly different composition. The main chemical difference between the blue body and the decoration is in the alkali content, which is significantly lower in the latter. The thin threads decorating the vessel appear weathered, therefore the alkali content may be affected by leeching. It must be noted that natron glasses with low sodium contents are already reported in published work on northern Italian late-Iron Age finds (Arletti et al. 2011; Panighello et al. 2012), indicating that the low soda content is not unusual in early natron glasses; in addition, the high content of lead and antimony in the white and yellow glass can explain the low soda content: lead in particular can act as both flux and network former, substituting the silica and soda in the network.
The high lead and antimony levels detected in AQ-FC-Alab_1-yellow can be related to the presence of lead-antimonates, employed as colouring and opacifying agents. Similarly, the high antimony content of AQ-FC-Alab_1white is related to the presence of Ca-

antimonates, employed in the white glass as opacifiers; in the white part, lead is relatively high but its role is not clear: it may have been employed as a flux, aiding the fluidity of the melt, or to enhance the refractive index of the glass, making it more "shiny".

The blue body (AQ-FCalab_1blue) is coloured by a combination of cobalt and copper, although the colouring power of cobalt is much stronger and prevalent on that of copper: a few hundreds ppm of cobalt are indeed enough to convey a deep blue colour to a silica-soda-lime glass, while copper at comparable concentration is not as effective. The presence of copper and lead in several hundreds of ppm may be related to the source of cobalt, although a deep investigation on the source of this element is not possible in absence of trace elements data. The contemporary presence of cobalt and copper in the glassy matrix may be explained by the deliberate addition of two different minerals or more, probably to the exploitation of a Co-Cu mineral, such as trianite ($2CoO \cdot 2CuO \cdot 6H_2O$); the presence of iron-nickel-arsenic-sulphur association in some inclusions may indicate the exploitation of minerals such as skutterudite $(Co,Fe,Ni)As_3$ and cobaltite CoAsS, that can also contain considerable amounts of iron and nickel. The presence of lead in low concentration may derive from the cobalt source, as Co-bearing minerals are usually found in high temperature hydrothermal deposits, in association with other sulphides of iron and lead such as galena PbS. Antimony can also be introduced with the Co-bearing mineral, although in this case its concentration is quite high to support an unconscious addition: 0.32wt% is above the limit of 0.2 wt% generally accepted for the intentional addition (Sayre and Smith 1961; Foster and Jackson 2010) and it is more probably added as a refining agent or decolouriser.

Manganese may also be introduced with cobalt, but the high content here identified, much above 1wt% in all three glasses, does not support this hypothesis as it is difficult to think that the introduction of about 600 ppm of cobalt may have caused the unintentional introduction of about 15 000 ppm of manganese. In addition, manganese is very high in the white and yellow glass too, where cobalt was not intentionally added.

The three glasses indeed show a high content of manganese oxide, above 1%wt in each case, which is consistent with a deliberate addition of manganese, probably as decolouriser to contrast the undesired effect of iron. Such elevated contents of manganese are not common in early glasses; comparisons with published objects of comparable type, dating and production technique did not succeed. Comparable high contents of

manganese in objects of similar archaeological form were detected by (Gallo et al. 2013) in blue and white glasses from Adria (northern Adriatic Italy) dated from the 1st century AD onward. Iron age glasses of similar dating excavated in Adria and Spina (Arletti et al. 2010; Panighello et al. 2012; Gallo et al. 2014a) do not contain manganese and, to date, Iron-Age glasses with such high content of manganese are unknown.

Despite the archaeological evidence and the early dating of the finding (based on the archaeological evidence, in the absence of stratigraphic data), sample AQ-FC-alab_1 is surprisingly produced with a Mn-decoloured base glass, that is typical of the Roman time. The colouring and opacifying technique unfortunately cannot help in dating the sample, as cobalt-based colouring and antimony-based opacification were employed from the Bronze Age to the Late Antiquity.

The uncommon Mn-rich composition, which to date has no comparison in the archaeometric literature, may be indicative of a technological transition between the Iron Age and the Roman time.

Chemical data obtained from the glassy matrix of sample **AQ-FC-3_3** evidence that both the blue and the white glasses are produced with a natron base glass consistent with a Roman composition.

The high content of iron (0.94%wt) is probably linked to the colouring element (i.e. cobalt) and it was likely introduced with the colouring element (cobalt) or even through the recycling of glass cullets.

Differently, the white glass has a MnO content which is consistent with an intentional addition and its high MnO/Fe_2O_3 ratio (>2) indicates that the manganese was probably added to decolourise the glass. In the white glass a colourless base-glass was employed, and the abundant antimony added probably enabled the precipitation of Ca-antimonate; in the case of the blue glass, a common blue-green base glass was coloured with cobalt and copper.

The presence of an antimony-based opacification in a manganese-decoloured glass may give important information about the glassmaking technology: manganese was probably added to a primary batch, where a colourless glass was produced, while antimony was employed in a secondary workshop to opacify the glass. The colouring and opacification of the white glass took place in a secondary workshop.

Sample **AQ-FC-1/18_3** is produced with three different glasses: an opaque yellow natron glass, a translucent green natron glass and an opaque red glass probably fluxed with plant ash.

Concerning the colouring/decolouring elements, in the yellow glass both colouring and opacity are due to Pb-antimonate crystals, as already discussed in the previous paragraph, which explains the high contents of lead and antimony in the yellow glass matrix.

The green transparent glass is coloured mainly by the high amount of copper even though the high iron (2.19%wt) and some cobalt (350 ppm) present in the matrix probably contribute to the colour of the glass; some lead is also present, in the range of thousands of ppm and therefore it is likely it was added intentionally to enhance the brilliance or improve the fluidity of the melt.

The red glass, due to the postash content, cannot be included unequivocally in the plant ash field, although it is clearly different from natron samples

produced with a plant ash base glass is coloured and opacified by nanometric Cu-rich crystals finely dispersed in the glass matrix. The high amount of copper is consistent with this evidence.

Despite the difference in the base glass composition, the red and green glasses have in common the high copper, iron, lead, antimony tin and zinc; tin and zinc in particular may derive from the copper-bearing materials in the form of metalworking scraps of bronze, brass or similar copper alloys. The presence of antimony and lead may have different explanations as these elements play different roles in the green and red glasses: they may be introduced in the melt as refining agents to improve clearness and brilliance (in the case of green glass) but also as internal reducing elements to help the formation of the reduced copper-rich crystals (in the case of the red). The relative proportion among copper, antimony, zinc and tin is very similar in red and green glass and this technological similarity suggests that these two coloured glasses are the result of the same technological choice in term of colouring elements.

The opaque red glass, together with the so called “peacock green” or “emerald green” translucent glass were challenging and desired colours in antiquity; the production of this kind of glass in Roman times was probably reserved to specific glass workshops, this hypothesis is supported by the evidence that these colours are often produced with a plant

ash composition. The presence of plant ash glasses in Roman times is not common, but has already been observed in Roman *tesserae* and vessels (Jackson et al. 2006; Van Der Linden et al. 2009; Van der Werf et al. 2009; Nenna and Gratuze 2009; Paynter and Kearns 2011) and the primary production of this kind of glass is generally considered based in Mesopotamia, were plant ash technology was never replaced by natron. However the red glass here considered, due to the relatively low content of potash, is not unequivocally consistent with a plant ash glasses. Red glasses with an intermediate composition between natron and soda-ash are relatively common and this could be explained with the addition of carbon in the form of charcoal or vegetal ashes as internal reducing agents (Freestone 1987; Schibille et al. 2012a) to help the development of the red colour.

In the present vessel, though, the red glass may have been produced with a natron glass additioned with vegetal ash as internal reducing agent, while the green one is a natron-based glass (with a slightly higher magnesia content). This evidence suggests the hypothesis of a common origin for the green and red glass.

The two glass-working wastes AQ-FC-SL_3 and 4 are two opaque glass droplets and are debris of glass-working activity. They are both natron glasses consistent with a Roman composition: the low content of manganese indicates that probably a blue-green glass was employed as base glass.

AQ-FC-SL3 is coloured by cobalt in combination with copper, while the turquoise AQ-FC-SL_4 is coloured by the very abundant copper. Little amounts of tin can be related to the introduction of copper trough metalworking scraps. Lead is present in both samples in comparable concentrations, probably added to enhance the brilliance or the fluidity of the melt; antimony is related to the Ca-antimonate opacification identified in both samples.

The amount of opacifiers is very different in the two glass-working wastes: very abundant in the turquoise sample, but scarce in the blue one, the latter having different possible interpretations none of which is proved.

The two wastes may derive from the production of opaque coloured glass, starting from a colourless/naturally coloured base glass; they may also derive from the re-melting of mosaic tesserae. Unfortunately, in lack of stratigraphic data such activities cannot be located in a precise chronological range.

4.1.4 CONCLUSIONS

The opaque-coloured glasses here analysed are all made with natron glass (with the exception of the red glass), consistent with a Roman composition.

Opacification is obtained with antimony compounds (Ca-antimonate in the white, opaque blue and opaque turquoise samples, lead-antimonate in the yellow samples); cobalt is responsible for the colour of the blue samples, while copper is responsible for the colour of the turquoise and green glass when present in its oxidised form, and of the red colour when present in the form of reduced copper-rich phases. Glass-working wastes here included are consistent with a Roman glass composition but the glassworking activity cannot be related to a specific chronological moment.

The only pre-Roman sample included, dated on the basis of the archaeological evidence, is very close in its chemical composition to the Roman samples, and it is probably a product of the transition between the Iron Age and the Roman time.

4.2. TRANSPARENT GLASS

The largest part of the vessels and working wastes here analysed is made of transparent glass, some are deliberately coloured or decoloured: all the 72 glass samples from Classe and 72 out of the 78 samples from Aquileia-Domus of Tito Macro were chemically analysed by means of XRF and EPMA, their full chemical composition is given in Table (4.2).

All the samples here considered are silica-soda-lime glasses; potash and magnesia are both generally below 1.50%wt (fig 4.14), indicating the use of natron as a flux, and according to the Roman and Late Roman technology (Lilyquist and Brill 1993; Shortland et al. 2006).

On the basis of their chemical composition the samples are divided in two main macro-groups: the first referable to early Roman composition and the second referable to the late Antiquity.

In the assemblage from Aquileia-Domus of Tito Macro 57% of the samples fall in the Roman group, while the remaining 43% have Late Antique compositions (fig. 4.15); differently, in the assemblage from Classe only 2 samples, considered outliers, are in some way consistent with a Roman composition while the remaining 70 samples belong to the Late Antique macro-group.

The difference between the two assemblages is consistent with the dating of the sites and types, which range from Roman to early Medieval times in the case of the Domus of Tito Macro in Aquileia, and are limited to late Antiquity in the case of Classe.

On the basis of the chemical composition, each macro-group can be further divided in homogenous compositional groups that will be discussed in detail further on. In particular, within the Roman composition two main groups are identified: colourless glasses, produced with the addition of decolouring agents (manganese and antimony) and coloured glasses, with the unintentional or deliberate presence of colouring agents; within the Late Antique composition, three main Late-Antique groups are identified, referable to published compositional groups: HIMT, Levantine1, Série 3.2.

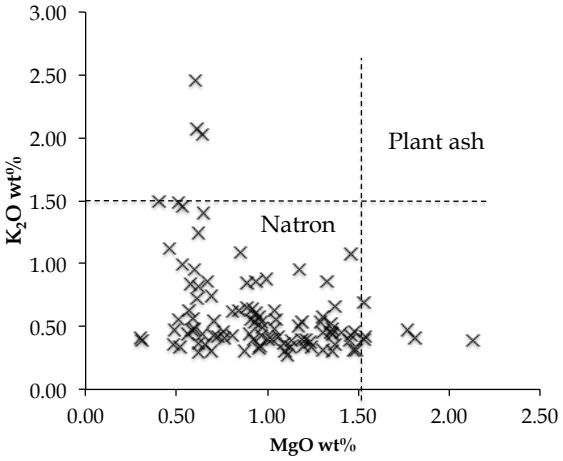

Fig. 4.14: biplot diagram K2O/MgO. Compositional limits of natron and plant ash glasses are reported in broken lines

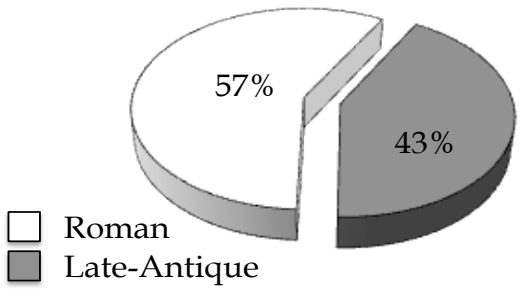

Fig 4.15: relative distribution pattern between Roman and Late Antique composition in the Tito Macro assemblage

4.2.1. ROMAN GLASS FROM AQUILEIA

The composition of the Early Roman glass has been surprisingly homogenous over hundreds of years, and it is a consequence of the strict control on the raw materials and the perpetuation of traditional production techniques (Sayre and Smith 1961). Examining the published data it is evident that Roman glasses generally fall within certain compositional ranges for their major oxides (SiO_2 ≅ 65-71%wt; Na_2O ≅ 15-18%wt, CaO ≅ 6-7%wt, Al_2O_3 ≅ 2.00-2.60%, Fe_2O_3 ≅ 0.30-0.90%wt) as testified by the abundant

archaeometric literature (Foster and Jackson, 2010, 2009; Silvestri, 2008; Silvestri et al., 2008 *and references therein)*. Most of Roman glasses are blue-green or *aqua* (Price and Cottam 1998), without the intentional addition of colouring or decolouring elements; on the other hand, both deeply coloured and clear colourless glasses were popular and particularly fashionable in certain historical times: Clear colourless glass was particularly fashionable during the late 1st-3rd century AD (Price and Cottam 1998) while deeply coloured glasses (black, purple, blue, red, emerald green, amber) were particularly fashionable in proto-historic times and in the early Roman times. Obtaining a truly colourless glass was not easy in preindustrial times: it required pure (i.e. low iron) sand and a strong control on the firing conditions; nevertheless a slight tinge was almost impossible to avoid, therefore antimony or manganese could be added to the batch to contrast the undesired colour of the natural-occurring iron.

Large Roman assemblages analysed and published in the past years report the presence of coloured glass (both naturally or intentionally coloured) and intentionally decoloured glasses, with either manganese or antimony or a combination of the two (Jackson 2005; Silvestri et al. 2008). The intentional addition of colouring or decolouring agents is therefore one of the most important technological choices of early glassmaking and for such reason in the present work, as in many other published works, it is considered as a marker.

Among the glass findings of the domus of Tito Macro, 30 samples characterised by high silica (≅67-72wt%), soda (≅15-19wt%) lime (≅6-9wt%) and iron (≅0.3-0.6wt%), medium-low alumina (≅1.75-2.50 wt%) and very low titania (generally below 0.20wt%) with variable amounts of manganese and/or antimony can be referred to early Roman glass composition. Archaeological types here included are mainly bowls Ising 3, 42, 42 Limbourg, 85 of which dated to the 1st-3rd century, but also some later types, dated between the 4th and the 8th century AD, such as bottles Ising 104, beakers Isings 106 and 109, bowls Isings 117 and goblets Isings 111.

On the basis of the chemical composition, two main compositional groups may be distinguished: "FC colourless", comprising samples with a variable amount of decolourisers (antimony and manganese) and "FC coloured", comprising the naturally coloured and intentionally coloured samples. Each compositional group is further divided on the basis of the colouring/decolouring elements present.

The average composition and standard deviation of each group and subgroup are reported in table B).

4.2.1.2. COLOURLESS GLASS

This group comprises 22 samples, all characterised by the presence of decolouring elements. On the basis of the decolouriser employed they are subdivided into three groups that will be discussed into detail: FC colourless1 (antimony decoloured); FC colourless2 (manganese decoloured) and FC colourless3 (antimony+manganese decoloured). The relative differences are highlighted in fig 4.16.

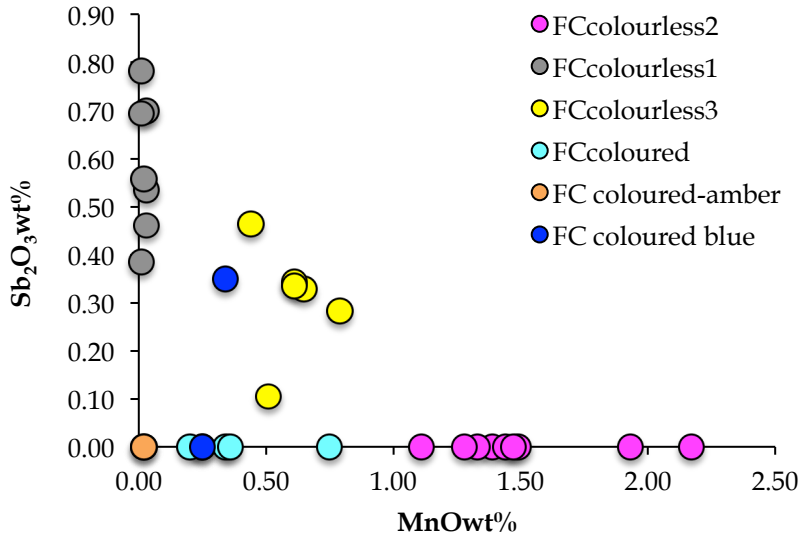

***Fig. 4.16**: binary plot antimony vs. manganese of the Roman samples of Tito Macro. Intentionally coloured samples are indicated as blue and amber, respectively, while the blue-green colour indicates naturally coloured glasses*

FC colourless1 (antimony decoloured)

This group includes 7 samples: a single working waste (thread) and six drinking vessels of the types Isings 85 (n=3), Isings 117 (n=1) and Isings 109 (n=2).

While the cups Isings 85 are dated to the 3rd century, the beaker Isings 109 and the bowls Isings 117 are dated to the 4th-5th century and their presence in this compositional group will be discussed in detail further on. In the absence of stratigraphic data and archaeological type, no hypothesis of dating can be given for the working residue.

The main characteristic of this group is the presence of antimony in high concentration (0.67±0.13%wt) and the absence of manganese; other characteristics are the high silica (71.08±2.01%wt) and soda (17.84±1.03%wt), low calcium oxide (5.86±1.15%wt) and relatively low (although variable) alumina (2.18±0.39%wt) (tab.4.3)

To a closer observation, samples of FC colourless1 may be split into two sub-groups, one characterised by higher silica (71.75±1.99%wt) and lower alumina (1.83±0.88%wt) (tab.4.3), including the working waste, two Ising 85 and a bowl Ising 117, and a second one with slightly lower silica (69.43±1.26) and higher alumina (2.50±0.10%wt) (tab 4.3) that comprises a cup Isings 85, a bowl Isings 117 and a beaker Isings 109.

Discussion

Samples of group FC colourless1 have antimony as decolouriser, Sb_2O_3 being always above the limit of the deliberate addition of 0.2wt% (Sayre and Smith 1961).

The chronological limits of the Sb decolouring technique are not perfectly defined, although it is generally accepted to be the main decolouring technique between the 1st and the 3rd century AD. From the end of the 3rd century onwards, an increase in the content of manganese is observed (Jackson 2005) and from the 4th century onwards the most common decolouriser is manganese, as testified by the Late Antique compositions that will be discussed in the following paragraphs; Late Roman assemblages, dated to the 3rd-4th century AD showing antimony decoloured glasses with limited extent of recycling are known in the literature (Foster and Jackson 2010) from Britain.

Isings 85 cups here included are dated to the 3rd century and this is consistent with the dating of the Sb-technology. On the other hand, the presence of types dated to the 4th-5th produced with antimony colourless glass may be explained as a product of re-melting of older glass in later times but other explanations will be discussed.

The difference in the alumina content identified within the FC colourless1 group is of particular interest as it can be related to the sand employed in the primary production: the high-alumina subgroup is slightly richer in calcium, iron, magnesium and titanium with respect to the low-alumina one and seems to be produced with impure sand, while the low alumina samples present a composition that is indicative of a purer sand.

According to this evidence, the current assemblage seems to include Sb-decoloured glasses produced exploiting two different sand sources: a pure sand (high silica, low iron, low alumina, low lime), and a more impure one, as the one generally used to produce the common blue-green glass.

Samples of the "antimony colourless" composition are frequently recorded in the archaeometric literature (Sayre and Smith 1961; Jackson 2005; Baxter et al. 2005; Paynter

2006; Silvestri et al. 2008; Huisman et al. 2009; Foster and Jackson 2010; Rosenow and Rehren 2014). The Sb-based decolourization of glass, characteristic of the 1st-3rd century AD is more efficient than the one based on manganese; in addition, while helping gas bubbles escape from the melt, antimony also worked as a refining agent and aided the transparency and clearness of the final object. These could be some of the reasons of the choice of Sb-glass for high-status glass vessels, such as *diatreta*, cameo-cut and other cut-decorated vessels ((Jackson 2005; Foster and Jackson 2010) and references therein). Nevertheless, Sb-decoloured glass was not reserved only for the production of very high status objects, as demonstrated by the large assemblages published in the past, which report the presence of abundant non-decorated tableware made with Sb-colourless glass composition. Among the Sb-decoloured samples from the domus of Tito Macro indeed no high-status, decorated vessel is included.

Examining the published data from Britain (Jacson 2005; Foster and Jackson 2010), Italy (Silvestri et al. 2008) and Egypt (Rosenow and Rehren 2014), it is clear that the largest part of the Sb-decoloured samples show a low-alumina content, generally below 2.20%wt and in most cases between 1.50% and 2.00% wt, suggesting that a pure sand, rich in silica and poor in feldspars and accessory minerals, was exploited for their production. Only a few British and Egyptian samples (Foster and Jackson 2010; Rosenow and Rehren 2014) contain high alumina levels (between 2.20 and 2.50%wt), similarly to the three "high-alumina" samples from Tito Macro (see fig. 4.17 a-b)

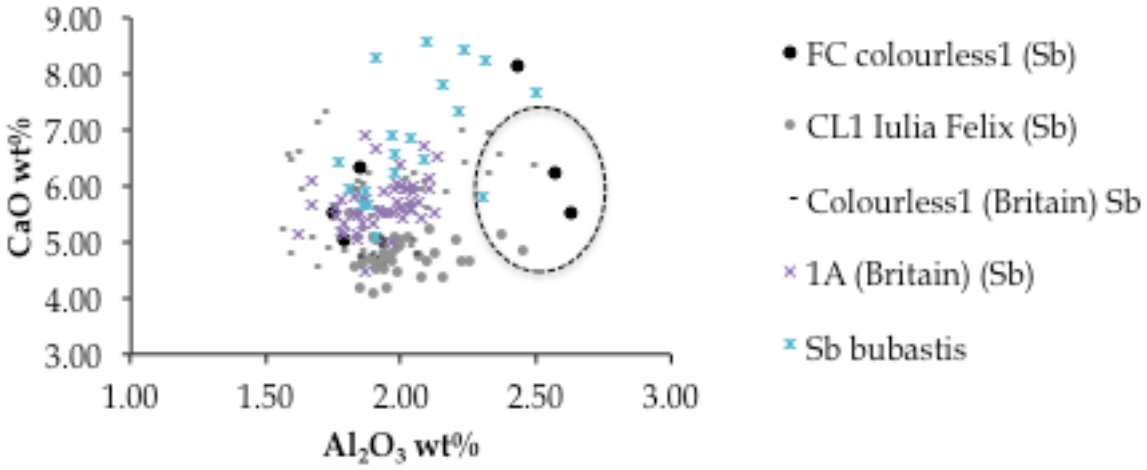

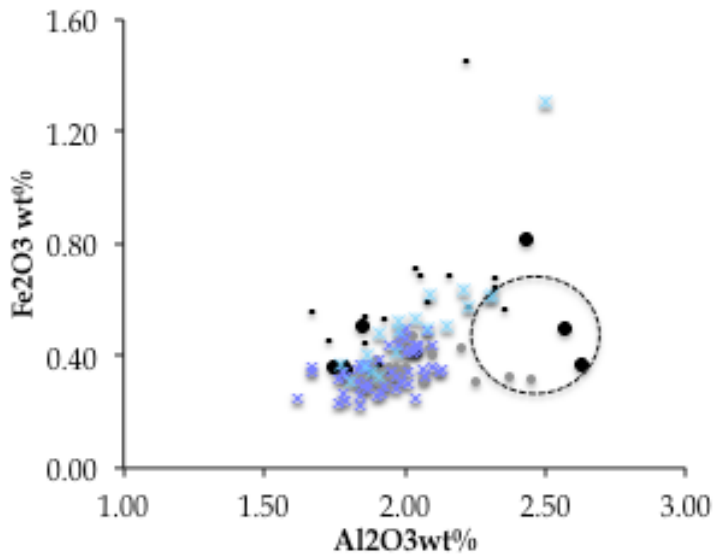

Fig. 4.17-a *(above) and* ***–b*** *(left): biplot diagrams. FCcolourless1 samples are plotted with reference groups CL1 (Silvestri 2009) Colourless 1 (Foster&Jackson 2009), 1a (Jackson 2005 and Sb-decoloured (Rosenow&Rehren 2014). Broken lines indicate the usual compositional range for blue-green glasses.*

Conversely, the three low alumina samples here analysed fit perfectly with most of the published Sb-decoloured glasses.

Yet, if we consider the major oxides and neglect Mn and Sb, the average composition of the high-alumina subgroup resembles more the one of the blue-green Roman glasses rather than that of the Sb-colourless.

Biplot diagram Al_2O_3/Fe_2O_3 reinforces this evidence: the largest part of the published samples fall below 2.25%wt alumina and 0.60 iron oxide but a few of them, including the three high alumina samples of Tito Macro fall in the compositional field of the blue-green glasses (Fig 4.17b)

On the basis of the chemical evidence of samples from York, Leicester and Manchester, (Jackson 2005)hypothesised that Sb was associated with pure sand, while Mn was added to decolourise the more impure sand usually employed for the blue-green glass.

The present assemblage seems to contradict partly such hypothesis: in the four low alumina samples Sb is associated with a quite pure sand, while in the three high alumina samples antimony was probably added to a blue-green glass batch.

The possibility that such uncommon composition could derive from recycling different glasses must be considered, even though it is hard to support: assuming that glass cullets were selectively collected on the basis of their macroscopic colour, regardless of their chemical composition, and considering that colourless glasses in the Roman time could be

produced either by adding manganese and antimony or by employing an extremely pure sand, the recycling of colourless glasses would have caused at least the dilution of antimony, and possibly the introduction of other elements such as manganese. The virtual absence of manganese tends to exclude the possibility that these glasses were produced by mixing together different glasses.

One possible explanation is the presence of a different location of primary production that employed impure sand, naturally poor in manganese. In this case antimony must have been added in the first stage of the glass production (the so-called primary production)

Another, not proved, possibility regards the addition of antimony to blue-green raw glass naturally low in manganese. In this case, the addition of antimony could also be a product of a secondary stage of production, but no evidence supports it.

The generally homogenous composition of antimony decoloured glass, and the recovery of antimony decoloured raw glass chunks in the Les Embiez shipwreck (Vichy et al. 2004), supports the hypothesis that antimony was added at the initial stage of glass production (i.e. primary production) rather than in secondary workshop.

The picture is complicated by the chronology of antimony technology, that does not coincide perfectly with the dating of the types, dated between the 3rd and the 5th century AD. In such cases, considering the possibility of recycling is necessary, even though in the current group there are no clear evidences of this practice: in the case of recycling, the unconscious introduction of manganese is expected and it seems unlikely that Sb-colourless glass has been recycled exclusively with other Sb-glasses for centuries. The possibility that Sb colourless glass recycled in later times preserved its "pure" composition without contamination is difficult to support. It is more likely for the chronological range of the antimony decolouring technology to be approximate: Sb-decoloured glass did not disappear suddenly from the market and it is reasonable to think that Sb-decoloured, Mn-decoloured and late Antique compositions coexisted in Aquileia in the 4th-5th century AD.

Concerning the glassworking evidence, a single waste was detected in group FC colourless1 but no dating can be given to this sample on the basis of the archaeological study; it testifies the presence in the area of some kind of secondary working of Sb-

colourless glass, but it is not possible to define whether it derives from an occasional or a systematical activity, nor to collocate this activity in a time scale.

FC colourless 2

Manganese decoloured

This group comprises 9 samples of vessels of the types Ising 85 (n=4, dated to the 3rd century), Isings 42 Limbourg (n=1, dated to the 1st century), beaker Isings 109 (n=1, dated to the 4th-5th century), bottle Isings 104 (n=1, dated to the 3rd-4th c. AD) and goblet Isings 111 (n=2, dated to the 5th-8th century).

Samples of FC colourless2 are characterised by the very high manganese (1.51±0.33wt%) content in the absence of antimony; other common characteristics are low soda (15.40±0.44wt%) and high calcium (CaO=8.07±0.47wt%), relatively high alumina (2.68±0.20wt%) and lower potash (0.56±0.12wt%), magnesia (0.53±0.09wt%), iron oxide (0.42±0.07wt%), titania (0.07±0.01wt%). Despite the extremely high content of manganese, none of these samples is purple, as the Mn acts as decolouriser.

Discussion

Manganese has been used as decolouriser for glasses in the Roman time, between the 1st and the 3rd century, and in the Late Antiquity, between the 4th and the 9th century AD, to decolourise the undesired tinge given by iron.

In the scientific literature the limit between the content of the Mn naturally occurring in the sand, and that intentionally added as a decolourant, is debated. Some scholars consider intentional the addition of very low levels of manganese, 0.1-0.2%wt according to Wedepohl (Wedepohl et al. 2011) and 0.2%wt (Sayre and Smith 1961), but later studies demonstrate that contents of MnO=0.40%wt in the sand (as in the case of the river Volturno (Brill 1999)) turns into 0.30% in the glass. Considering this evidence, Jackson raised the level for the intentional addition to 0.5%; furthermore, Silvestri evidenced that to be efficient as a decolouriser, apart from the absolute content, manganese must be at least two times the iron content (Silvestri et al. 2008). In his recent work on Western Mediterranean sand deposits for Roman glassmaking (Brems et al. 2012), Brems reconsiders the limits: taking into account sand deposits that, according to his study, are suitable for Roman glassmaking, the limit of Mn that can be introduced in the glass from

the sand is as low as 0.1%wt. On the other hand, the average iron content of Roman blue-green glass is relatively high and the quantity of manganese required for decolouring must be at least twice the iron content, therefore the limit of the intentional and deliberate addition of manganese seems more likely to be 1%wt; according to Brems, manganese content between 0.1 and 1% wt must be considered as an effect of recycling.

The samples of FC colourless2 have very high manganese (MnO= 1.51%wt) and a very high MnO/Fe_2O_3 ratio (above 3 in all the samples) and are fully consistent with the intentional deliberate addition of manganese.

Most of the previous works analysing Roman vessel glass from Great Britain, Egypt, Italy, and France (Nenna et al. 1997; Jackson 2005; Foster and Jackson 2010; Rosenow and Rehren 2014) evidenced that Mn-decoloured glasses are very close in composition to the more common blue-green glasses: Jackson's group 2b(Jackson 2005), Foster's group 2a (Foster and Jackson 2010), Nenna's Group 3 (Foy et al. 2003)are an example of this.

Although manganese decoloured glasses are quite common and relatively homogenous in published Roman assemblages, the samples included in FC colourless2 have a peculiar composition, with low sodium, high calcium and relatively high alumina levels (see tab. 4.2, 4.3).

Plotting Calcium content *versus* alumina content of Mn-decoloured glasses from Britain, Egypt and Italy with the present assemblage (fig. 4.18-a) leads to splitting samples in two groups: one made of British samples, with low alumina and lime and similar to the blue green glasses, whose compositional range is indicated by a dotted line, and a second one with samples from this work cluster and samples from Britain, Egypt and Italy.

The evaluation of a single diagram can be misleading. According to figure 4.18, samples of FCcolourless2 may seem to have a similar composition to the largest part of the manganese decoloured samples previously published, but they do not: samples from Tito Macro have low soda content, which is quite uncommon for manganese decoloured glasses. The low-sodium, high-calcium composition of this group may indicate the exploitation of a different sand source and a probably a different sand/natron ratio. When soda content is plotted *versus* lime (fig.4.18-b) such difference becomes clearer: FCcolourless2 clusters with the Italian samples of Iulia Felix (CL/2 (Silvestri et al. 2008) and part of the Egyptian samples from Bubastis (Rosenow and Rehren 2014), while British samples cluster separately. A direct comparison of chemical data highlights that Iulia Felix

CL/2 and FCcolourless2 samples are very close in composition. This evidence is of particular interest, as the *Iulia Felix* was a cargo ship transporting 140kg of glass cullet, that wrecked off the shore of Grado (a few kilometres from Aquileia) in the first half of the 3rd century AD. It is interesting to note that in the 3rd century this specific Mn-glass was traded along the Adriatic coast in the form of cullet. Lime and alumina are indicative of the sand employed in the primary production, while soda and manganese are indicative of the technological choice, i.e. the quantity of natron and manganese employed; the similarity between the two assemblages of Tito macro and Iulia Felix regards all the major and minor elements, including the high manganese content: it is thus possible to establish a link between the primary production of these two samples groups.

Concerning the lime and alumina content, Mn-decoloured samples with high lime and alumina can be identified in the British assemblages of Foster&Jackson 2009 (Group 2b); whereas they are scarce in the British assemblage of Jackson (2005) and abundant in the Egyptian assemblage of Bubastis (Rosenow 2004).

Concerning the lime and alumina content, Mn-decoloured samples with high lime and alumina can be identified in the British assemblages of Foster&Jackson 2009 (Group 2b),

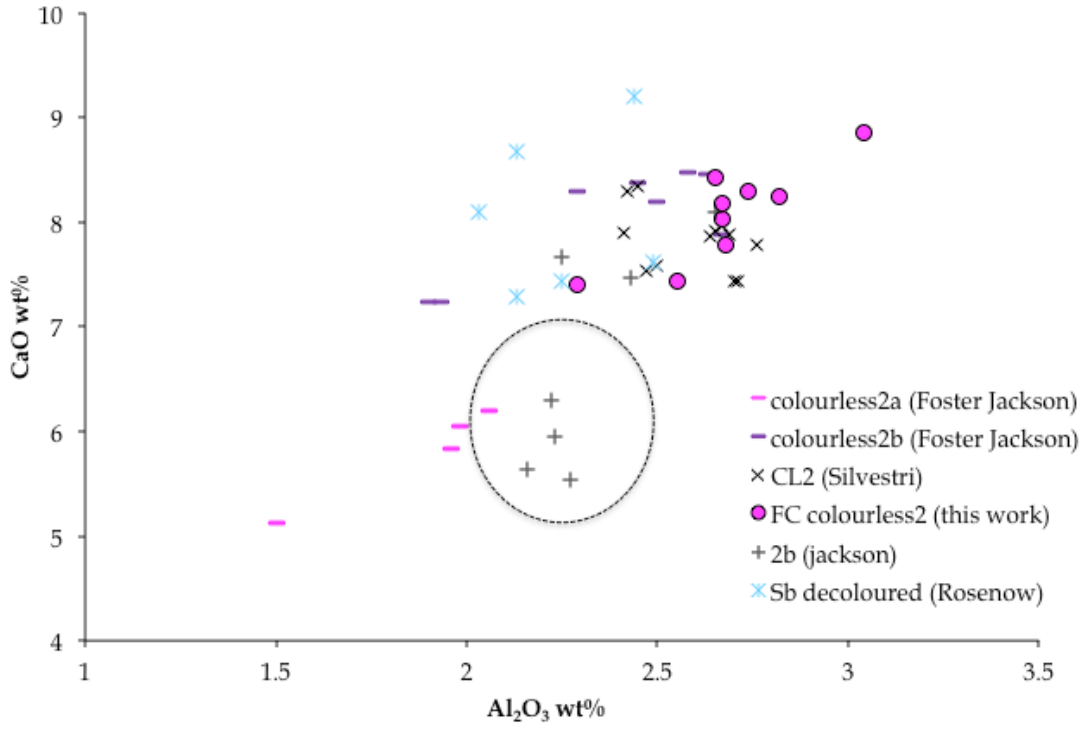

***Fig. 4.18**: binary diagram lime vs alumina. The broken line indicates the usual compositional range of blue-green Roman glasses.*

sporadicly in the British assemblage of Jackson (2005) and most of the Mn-decoloured samples from the Egyptian assemblage of Bubastis (Rosenow 2014). The examination of alumina, soda and manganese shows important compositional differences: the British samples have higher soda content, indicating a different natron/sand ratio, while the Egyptian samples, closer in composition, have lower alumina; in addition, the manganese content is generally lower. Comparisons on the basis of silica/soda ratio cannot be done: the British assemblages of Foster&Jackson (2009) and Jackson (2005) were analysed by ICP-MS, which does not measure silica; recasting would be based on the wrong assumption that the difference between the total and 100 is due to silica, which is formally incorrect.

A general consideration may be done taking into account the hypothetical compositional field for silica and soda of the British assemblages after recasting (Fig. 4.18 c, grey area): the general tendency to higher soda content in the British assemblages is highlighted, while the silica range is relatively wide and comparable in all the assemblages.

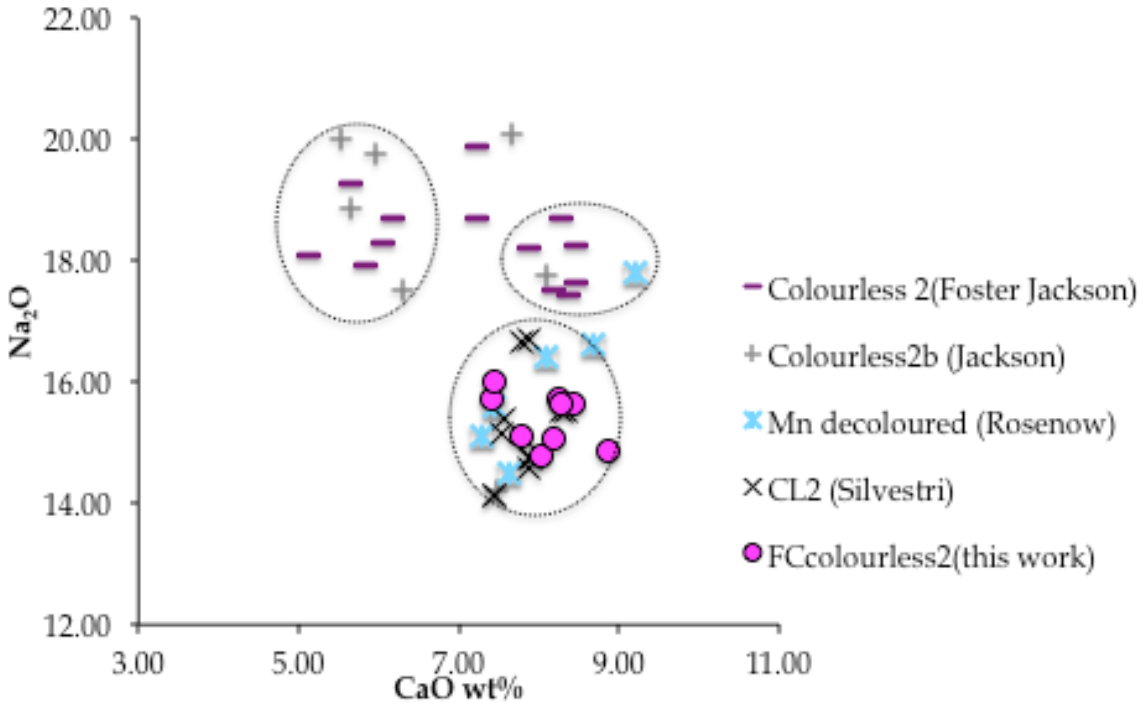

Fig. 4.18b *(below): biplot diagram soda vs lime. The dotted line highlights the three main compositions identified in Mn-decoloured Roma samples. Samples from Tito Macro.*

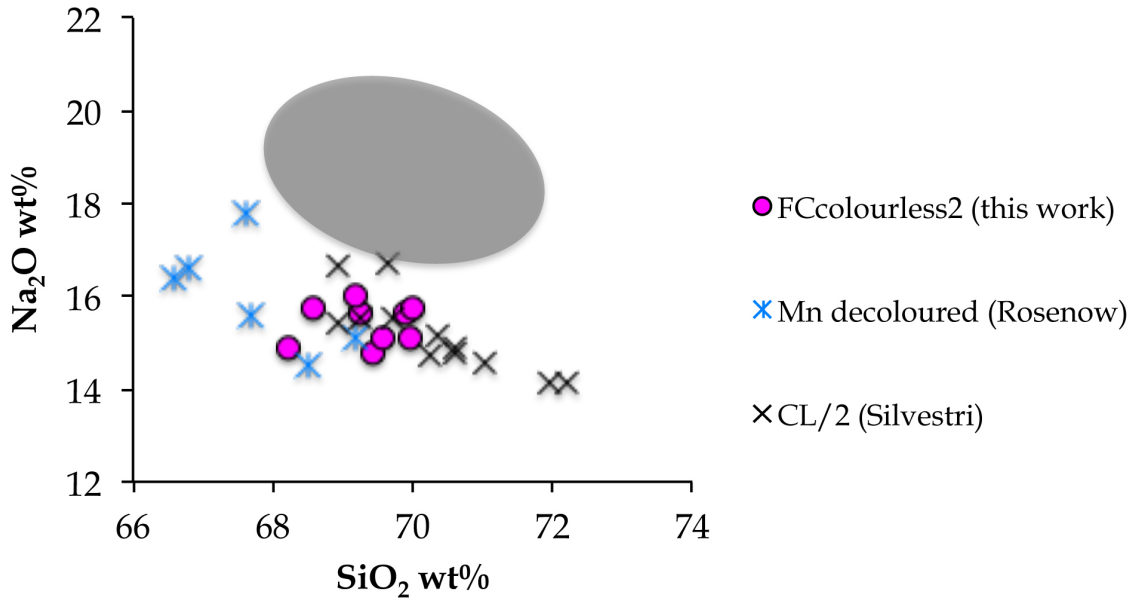

Fig. 4.18-c: binary diagram Soda vs. silica; the grey area indicates the hypothetical compositional field of the British assemblages Colourless 2b (Jackson) and Colourless 2 (Foster&Jackson), after recasting of silica.

It seems that Mn decoloured samples were produced employing two different sands (one with low lime and low alumina, one with high lime and high alumina) and two different sand/natron ratios (high soda and low soda) that generate at least three possible combinations:

1- high lime-high alumina- high soda (British samples)
2- high lime-high alumina-low soda (Iulia Felix, Tito Macro)
3- low lime- low alumina- high soda (British samples)

The samples from Bubastis show an intermediate composition: high lime-low alumina-low soda that could indicate a different primary production, but also recycling. The small number of samples, and their internal compositional variability do not allow pushing interpretation much further.

Samples from FC colourless 2 are dated to a wide chronological range, that once again is not fully consistent with the chronology of the manganese decoloured Roman glass: goblet Isings 111 is dated to the Early Middle-Age (5th-8th century AD) and its presence in the current assemblage may be explained as a product of re-melting of earlier glass, as may also be the case of bottle Ising 104 and beaker Isings 109.

What seems surprising is that, as in the case of antimony decoloured glass, Roman glass arrived almost unmodified to the Late Antiquity and early medieval time, preserving the "purity" of its chemical composition.

It has already been said that the collection of cullet for recycling was most likely conducted on the basis of the apparent colour, therefore Sb decoloured and Mn decoloured glasses were reasonably melted together. The presence of late objects with early composition and virtually no signs of recycling is not easy to explain. It is possible, although hard to prove, that large quantities of early Roman raw chunks were still available in the 4th-5th century AD, in Aquileia (when considering the vessels as locally shaped) or in the place of origin of the objects (when considering the objects as imported). Another possibility is that this peculiar high lime, high manganese, low soda composition derives from a specific primary production that continued its activity throughout the 4th-5th century AD.

What is evident is that in the current assemblage as in the Iulia Felix samples, manganese was added to a specific glass composition that differs from the common blue-green glass composition and is closer at some points (lime, alumina, soda, manganese content) to the Levantine1 production that started to circulate in the eastern Mediterranean in the 4th century AD and invaded the glass market in the 6th-7th century AD.

FC colourless 3: antimony+ manganese decoloured.

Group FC colourless 3 comprises 6 samples of vessels: bowl Isings 42 and 42Limbourg (dated to the 1st-2nd century AD, n=2), cup Isings 85 (dated to the 3rd century AD, n=3), bottle Isings 104 (3rd-5th century AD) beaker Isings 106(dated to the 4th-5th century AD, n=1) and goblet Isings 111 (dated to the 5th-8th century AD, n=1).

The main characteristic of this group is the presence of both Mn (MnO=0.60±0.12wt%) and Sb (0.31±0.12%wt) (Fig. 4.16). Apart from the decolouring elements, these samples fall within the compositional ranges of the common blue-green glass (fig 4.19): high SiO_2 (69.94±0.51wt%), Na_2O (17.33±0.54 wt%), CaO(6.75±0.31wt%), Al_2O_3 (2.26±0.11wt%), Fe_2O_3 (0.49±0.05%wt) and very low titania (0.08±0.01wt%); trace elements are also very low, with the exception of Sr (406±22 ppm) and Ba (225±33 ppm) that are related to the sand of origin.

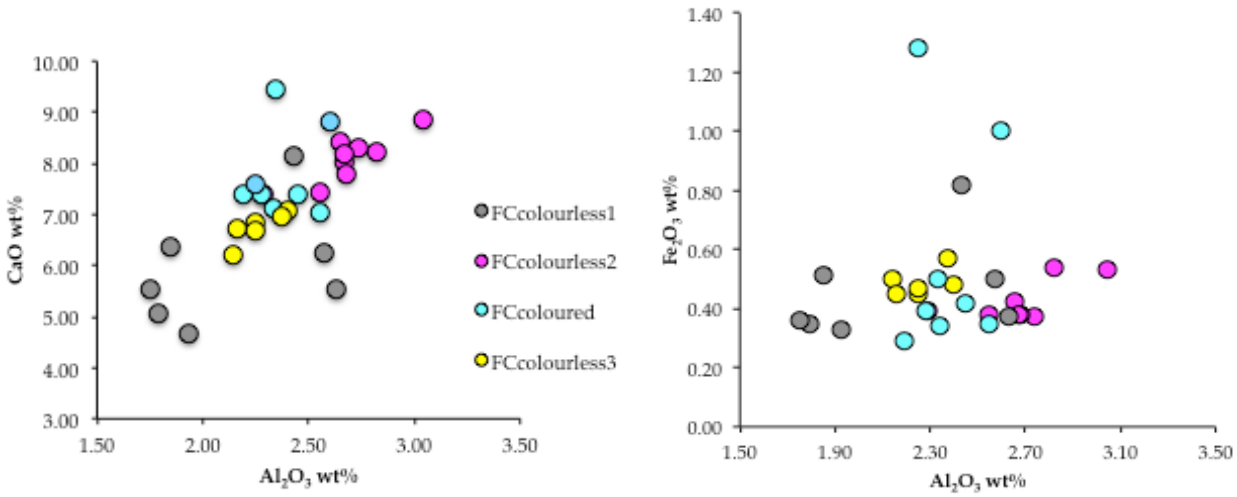

Fig.4.19 *a(left):biplot diagram lime vs. alumina; b(right): biplot diagram of iron vs. alumina: samples of FCcolourless3, with mixed antimony+manganese decolouriser cluster together the naturally coloured blue-green glasses.*

There were different ways to obtain a colourless glass in Roman times: exploiting extremely pure sand with very low iron would result in a colourless glass; as an alternative, a decolouriser (Sb and Mn) could be added to the glass; another probably common and easy way to obtain colourless glass was recycling colourless glass.

Cullets were collected according to their colour: it is therefore reasonable to assume that manganese-decoloured, antimony decoloured and naturally colourless glasses were melted together. The resulting glasses are colourless (or nearly colourless) and characterised by the presence of both decolourisers in comparable amounts and very low trace elements.

The presence of mixed Sb+Mn glasses is frequent in large Roman assemblages (Jackson 2005; Silvestri et al. 2008; Foster and Jackson 2010). Jackson (2005) interpreted them as an intermediate decolouring technique, although the hypothesis of recycling is not rejected. Later studies (Silvestri et al. 2008; Foster and Jackson 2010) interpreted those glasses as recycled, due to the fact that the presence of both decolourisers was not necessary and probably unconscious. Antimony decolouring was efficient and did not require the addition of manganese; on the contrary, manganese decolouring is efficient only when the manganese/iron ratio is very high, as already explained. The mixed Sb+Mn samples usually have manganese in low concentration if compared to iron; therefore the addition of low quantities of manganese would have almost no benefit. Even if the introduction of

decolourisers was not conscious, the selection was made with the aim of obtaining a colourless glass, and for this reason those – probably recycled – samples are here included in the colourless glasses.

4.2.1.3. COLOURED GLASS

In the Roman sample group from the Domus of Tito Macro, 8 samples belong to the coloured category: four are intentionally coloured and four naturally coloured or blue-green samples.

Intentionally coloured glasses- results

Four Roman samples are intentional coloured: two are deep blue and two yellow-amber. Two fragments, one for each colour, are Ising 1/18, and two fragments, one for each colour, belong to the Isings 3 type. Both types are dated to the 1st century AD.

The four intentionally coloured samples are not homogenous in their chemical composition, as evidenced by the high standard deviation in their content of silica (68.33 ±1.1.5%wt), soda (17.71±1%wt) and lime (8.31±0.98 wt%), while their content of alumina(2.40 0.18wt%), titania (0.06±0.01wt%) magnesia (0.50±0.05 wt%) and potash (0.62±0.07wt%) is lower and more homogenous.

The blue samples have high Fe_2O_3 (above 1%wt in both samples), cobalt and copper in few hundreds of ppm and low manganese (0.30±0.06wt%); one of them also contains Sb (0.35%wt) and zinc (204 ppm).

The two yellow-amber samples differ especially in their silica and lime content (see table 4.4); common features are the very low iron content (≈ 0.30%wt) and the negligible content of both antimony and manganese.

Naturally-coloured samples, results

Four samples of the FC coloured group are naturally coloured, as their colour is not manipulated by adding colouring/decolouring agents. Naturally coloured samples are bowls Ising 3 (dated to the 1st century, n=1) and Isings 42 (dated to the 1st century, n=2) and beaker Isings 109 (dated to the 4th-5th century, n=1)

They are homogenous in composition with high silica (70.79±1.40wt%) medium sodium (16.05±0.92wt%), relatively high lime (7.23±0.19 wt%) and low alumina, iron, magnesia potash. They are also characterised by low manganese (0.41 ±0.24wt%) and no antimony.

Coloured samples, discussion

The coloured samples here analysed and included in FC coloured are generally homogenous in composition (see tab 4.2-4-3).

Excluding the blue samples, where the introduction of a colouring element modifies the trace element content, the samples of this group are characterised by very low trace elements (Pb, Sb, Sn, Co and Cu), indicating a low level of recycling. In the group a single fragment of a late type is present (beaker Is.109), probably a product of recycling.

Concerning the colouring and decolouring elements, in the naturally coloured samples the only chromophoric ion is iron, while cobalt and copper are present in only a few ppm and have no effect; the content of manganese is too low to be considered as intentionally added (i.e. below 1%wt in all samples) and it is rather introduced with sand or recycling.

The deep blue samples owe their colour to cobalt and copper, both present in a few hundreds of ppm associated with iron, the latter being higher in the blue samples with respect to all the other coloured glasses; the association between cobalt, copper and iron is very common in intentional blue samples and can be related to the cobalt-bearing mineral.

One of the blue samples also contains manganese and antimony in equal proportions, as already found in the Sb+Mn colourless samples; it is therefore probable that this glass is recycled.

The two amber-yellow glasses have a specific composition: despite the intense yellow colour they are incredibly pure in composition, with a very low iron content, absence of a decolouring agent and, apart from Sr and Ba, deriving from the sand employed in the primary production very low trace elements. The main chemical difference between the two yellow samples is in the high CaO content of sample AQ-FC-1/18_2 that is very high for Roman glass. The two samples have a chemical composition that is fully consistent with the use of a very pure sand with very low iron content. The intense amber colour, in the absence of any other colouring agent, is due to the presence of the Fe^{3+} and (Fe^{3+}-S^{2-}) complex (Jackson et al. 2006), probably formed under reducing conditions in the furnace or in the melt. The presence of the sulphur-iron complex in the amber samples here investigated was verified by Electronic Paramagnetic Resonance (EPR): the Fe^{3+} signal is visible in both samples, characterised by a "shoulder" at 500G and a "narrow peak" at 1600G (red arrows), a "large peak" between 3000 and 4000 G (green arrow); a very weak

peak around 1000 Gauss corresponding to the axial signal of Fe^{3+}-S^{2-} complex (orange arrow). In addition, weak signals of Mn^{2+} (purple arrows).

Nenna and co-authors (Nenna et al. 1997) suggest the possibility that the reducing conditions required to develop the iron-sulphur complex were probably obtained by adding carbon to the melt, as an internal reducing agent.

Comparisons with the yellow amber glasses reported in the literature are complicated by the scarcity of published data. Some amber glasses of comparable dating were published from Adria (northern Adriatic Italy, reported by (Gallo et al. 2013)) and other particularly relevant ones as excavated in a secondary workshop of the mid-1st century AD from Lyon (Nenna et al. 1997).

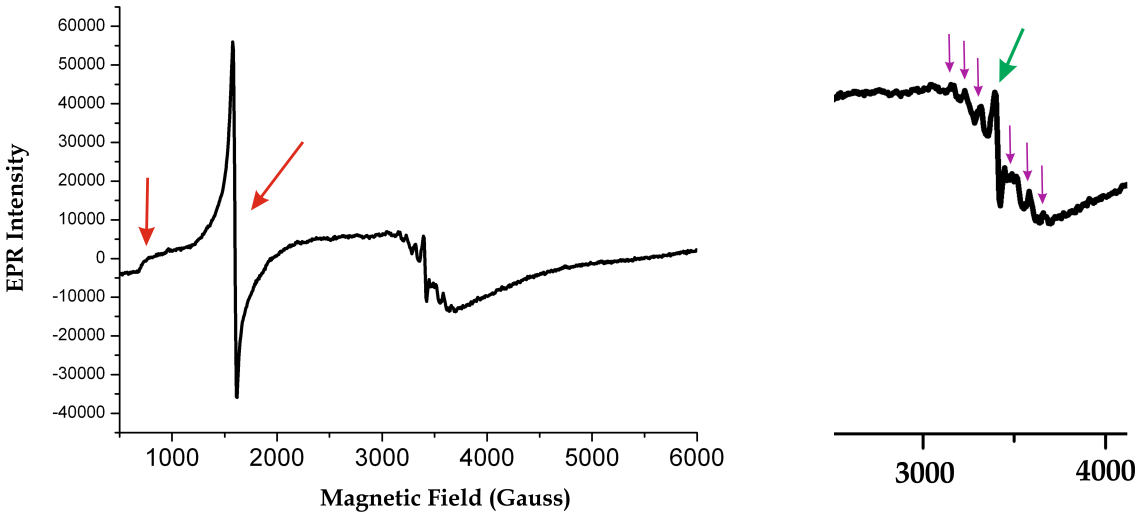

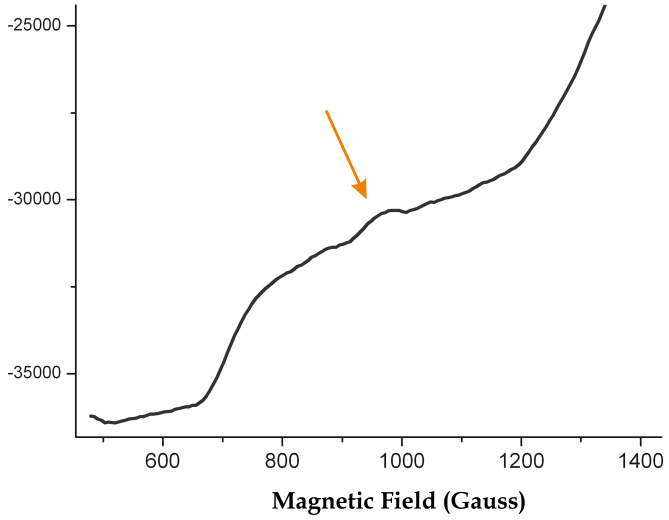

Fig.4.20 *EPR Spectrum of the amber samples.* ***(a)*** *Red arrow highlights the* Fe^{3+} *signal, the green arrow highlights a weak signal of Cu 2+ while the purple arrows highlights a weak signal of* Mn^{2+}*;* ***(c)*** *the orange arrow highlights the axial signal of* Fe^{3+}-S^{2-} *complex. (purple arrows).*

The (scarce) published samples are characterised by high soda, high lime, low potash, magnesia and titania, low iron, negligible manganese and antimony, evidencing the general homogeneity of the sand employed in the primary production. When comparing the two amber glasses here analysed with those from Adria and Lyon some differences in the major oxides emerge: the samples from Lyon have in general lower silica with respect to the Adria and Tito Macro samples, although this evidence may be affected by the low total of the analysis, that the authors related to the presence of organic matter in the batch; apart from this evidence, the main difference among the samples is the very high lime content of sample FC-1/18_2 However, comparisons with an unpublishe dataset of amber glasses from Frejus (France) highlighted the existence of several amber samples characherised by elevated lime content, above 9%wt as CaO (C.M. Jackson, pers.comm)

Amber glasses are the product of high technological skills and strict control on the raw materials and furnace conditions. Chemical data suggest that the glass employed in the two samples from Aquileia may have slightly different origins, to date, we do not know if amber glass was traded as finished objects or glass chunks; unfortunately the work of Nenna and co-authors (1997) reports the presence of raw chunks of coloured glass, but does not explicate if the amber glass is present in the form of chunks or vessels. Considering the highly selected raw materials and the degree of technological skills required to obtain the colour, we can suppose that the amber colour was a product of the primary production, rather than a colour imparted in a secondary workshop.

The considerable amount of calcium of some of the samples suggests the presence of more than one primary production for amber glass; however this hypothesis remains at the moment only a speculation to be confirmed with further studies on amber glass.

4.2.2. OUTLIERS FROM CLASSE

In the assemblage from **Classe** two samples, both excavated in Building 6, show a chemical composition probably referable to Roman times: samples D32 and D35, a cup Uboldi 1986 and a probable palm cup or lamp fragment, respectively. The two samples are different, as D35 contains manganese and antimony as decolourisers, while D32 contains only antimony. Due to the dating of the site (fully Late Antique) they are here considered two outliers.

4.2.3 ROMAN GLASS – CONCLUSIONS

The Roman assemblage of Tito Macro comprises both coloured and colourless glasses, with a large predominance of colourless samples (22 samples out of 30). Roman glass findings excavated in Tito Macro are in general consistent with published data of Roman glasses, from both an archaeological and a compositional point of view.

The three main categories of colourless glasses are here represented: the antimony decoloured, the manganese decoloured, and the mixed Sb+ Mn decoloured.

For what concerns the coloured samples, they are scarce, and only four samples are intentionally coloured, respectively in blue and amber. With respect to other early Roman assemblages, a scarcity of intentionally coloured glass is evident: the deep coloured ones are only blue and amber, and no purple, black or green sample is recorded.

Naturally coloured glasses are also scarce (4 samples), when considering that blue-green glass was the largest part of Roman production (Price and Cottam 1998).

On the other hand, all the samples included in FCcoloured are identifiable as Roman types mainly dated at the 1st-2nd century AD, with the only exception of a beaker Ising 109, dated to the 4th-5th century.

Conversely, the colourless glass is employed mostly in types dated to the 3rd-5th century and in some cases even later.

Antimony decoloured glass, usually considered as the early Roman decolouriser, is here employed in vessels dated from the 3rd century onwards; in parallel, the manganese-decoloured samples are in most cases dated to the Late Antiquity.
The hypothesis of recycling is one of the possible interpretations, but it does not explain how these well-defined compositions were not "polluted" by different compositions.
The largest part of the samples included in the Roman composition is indeed constituted by late types: only 10 samples out of 30 are indeed dated to the 1st-2nd century, 8 are dated to the 3rd century and 11 are dated to the 4th-8th centuries. The surprising evidence is that samples with very different dating present the same peculiar composition.

How may this evidence be explained? It is possible that in the 4th-5th century large assemblages of early glass of certain decoloured composition, in the form of chunks or also large vessel assemblages, were still available and, for some unknown reason, were re-melted without mixing with other kind of glass; this could have preserved the chemical composition. More probably, the primary production of antimony-decoloured and manganese-decoloured glass slowly gave way to the new composition of the Late Antiquity, and a period of overlap shall be considered reasonable.

It is evident that in the 4th-5th century, Roman decoloured glass was still employed in Aquileia in vessels and bottles in parallel with the Late Antique composition, which will be discussed later on.
A strict comparison was made between the manganese decoloured of FCcolourless2 and those analysed from the Iulia Felix shipwreck, confirming that the peculiar composition was in circulation in the mid-3rd century and was traded in the form of cullet.
For what concerns the decolouring technology, the current assemblage seems to contradict the hypothesis according to which antimony was employed on pure, low-alumina sands, while manganese was combined with the more common sand. In the present study antimony seems to be employed on both pure, low-alumina sands, and common sand; while manganese is employed only in association with a specific high-lime sand.
Further information will be given by isotopic analysis for provenance study, which will be discussed later.

4.3 LATE-ANTIQUE GLASS FROM AQUILEIA AND CLASSE

Results

42 samples of the Tito Macro assemblage and 70 samples of Classe are compositionally different from the early Roman glass, mainly for their content of lime, alumina, iron oxide, titania, potash and trace elements that are indicative of changes in silica sources.

In both assemblages three main homogenous groups were defined on the basis of the chemical composition, as shown in the CaO/Al_2O_3 diagram (fig.4.21): the first composition corresponds to group FC/1 (Aquileia) and CL/1 (Classe) and is represented by green squares; the second composition corresponds to FC/2 (Aquileia) and CL/2 (Classe) and is indicated by orange triangles; the third composition corresponds to groups FC/3 and CL/3 (violet diamonds). Each compositional group will be discussed in detail.

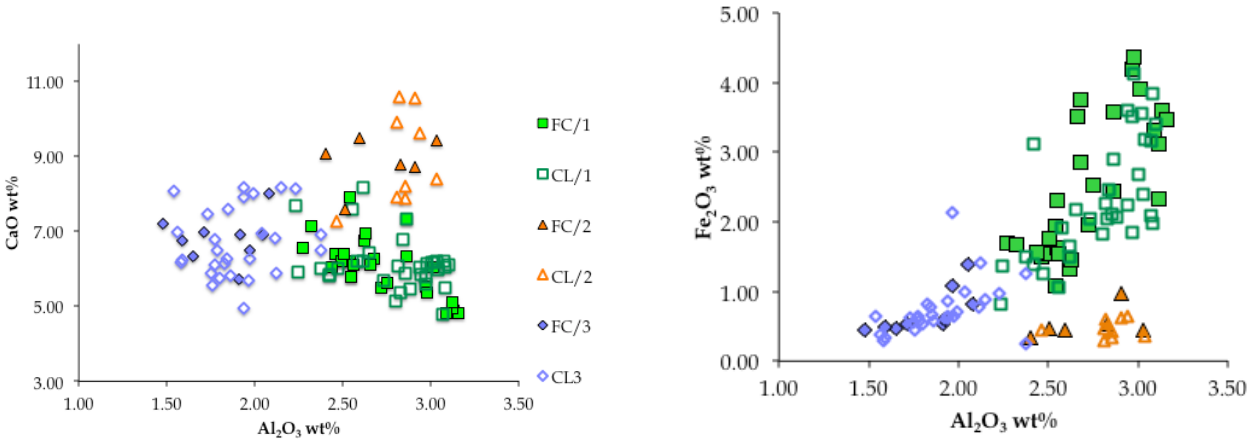

Fig.4.21: *(a) left: biplot diagram lime vs. alumina; (b) right: iron vs. alumina diagram. FC indicates Aquileia-Tito Macro sample, CL indicates Classe samples while colour indicate different compositions.*

4.3.1 HIMT composition

Results

The first composition, that corresponds to group **FC/1** (Aquileia, domus of Tito Macro) and **CL/1** (Classe) is characterised by high contents of sodium, iron, alumina, manganese, magnesia, titania and trace elements such as zirconium and barium. (tab 4.2-4.3)

Group FC/1 comprises 29 samples and 27 objects, 26 of which are vessels fragments and 1 is a raw glass chunk. Vessels are all dated from the 4th century onwards and comprise the following types: bowls Isings 96 (n=3) and 117 (n=5), beakers Isings 106 (n=11), bottles Isings 104 (n=4), plate Isings 118 (n=1), lamp Crowfoot Harden-A (n=1) and goblet Isings 111 (n= 3) dated to the 5th-8th century AD.

All samples are non-decorated, and most of them are naturally coloured in green and yellow. Only a few samples present an intentional deep colour: the raw glass chunk (AQ-FC-PV2) and two vessels (AQ-FC-104_5 and AQ-FC-111_8) are deep blue; two cups of the type Isings 96 (AQ-FC-96_1 and AQ-FC-96_2) are produced with a naturally coloured glass and decorated with blue drops; in the present study both the vessel body and the decorations were analysed and treated as different samples, the decorations are indicated with the names "AQ-FC-96_1blue" and "AQ-FC-96_2 blue" respectively. For these reasons the number of the analysed samples (29) do not correspond to the number of the analysed vessels (27).

From a chemical point of view, FC/1 is characterised by relatively low silica (65.40±1.35 wt%) and calcium (CaO=6.05±0.78wt%), very high soda (18.21±1.24wt%), iron oxide (Fe_2O_3=2.49±1.00wt%) and manganese (MnO=1.71±0.62wt%), high alumina (2.72 ±0.26wt%), magnesia (1.16±0.18wt%) and titania (0.50±0.18wt%); concerning the trace elements, elevated values are reported for Sr, Zr, Ba, Cr, V and Ni. (see tab 4.2-4.3)

On the basis of the iron content, group FC/1 can be subdivided into two subgroups: FC/1a (7 samples, of the type Isings 104, 106, 117 and 118) with a surprisingly high iron content (Fe_2O_3=3.73±0.51) and FC/1b (22 samples of the types Ising 96, 104, 106, 111, 117, 118 and Crowfoot Harden-A, including the raw chunk) with a more usual composition (Fe_2O_3=1.85±0 when excluding the deep blue samples). The five intentionally coloured blue samples are included in the "lower-iron" subgroup FC/1b for their content of alumina, magnesia and titania, while iron oxide cannot be considered as a discriminating factor: the intentional addition of colouring elements (mainly cobalt) may have influenced the iron content, therefore those samples are treated separately.

Group CL/1 comprises 33 samples, 13 of which are working wastes, including 3 raw chunks; the remaining 20 objects are vessel fragments, whose more represented types are bowls Isings 96, beakers Isings 106 and 109, goblet 111; other late types here represented are fully listed in table 4.4 and (tabella dei campioni); it is worth underlining that CL/1, as the assemblage from Classe in general, comprises some fragments of unknown type and a large variety of working wastes and indicators.

Most of the samples are naturally coloured in green and yellow-brownish colours apart from 3 vessels (respectively a beaker Ising 107, a bottle Isings 92 and a bottle Foy 2000) that are intentionally coloured in blue.

CL/1 is characterised by relatively low silica (65.29±1.47wt%) and calcium (CaO=6.13±0.71wt%), very high soda (18.23±1.36wt%), iron oxide (Fe_2O_3=2.34±0.86 wt%), manganese (MnO=1.75±0.64wt%) and high alumina (2.79 ±0.26wt%), magnesia (1.28±0.29wt%) and titania (0.48±0.16wt%); trace elements are, when available, quite high for Sr, Zr , Ba, Cr , V and Ni (table 4.4-4.5)

On the basis of the iron content, group CL/1 can be subdivided into three subgroups: CL/1a composed of 10 samples (3 beakers Ising 96 and 7 working wastes comprehensive of 2 raw chunks), with a very high Fe_2O_3 content (3.38±0.51 wt%), CL1/b, composed of 15 samples (16 vessels of various types and 5 working wastes including 1 raw glass chunk), with slightly lower iron (Fe_2O_3=2.74±0.24wt% excluding from the average the two deep blue samples) and CL1c, composed of two samples both from US 4381 (1 vessel and 1 working waste), with lower iron (Fe_2O_3= 0.93±0. 17 wt%). This last group also shows lower titanium (TiO_2=0.14wt% in both cases) and alumina (Al_2O_3= 2.39± 0.23 wt%) and higher calcium (CaO=7.64± 0.07 wt%) than CL/1a and CL/1b (tab.4.5).

The two blue samples, both included in group CL1/b, are coloured by a combination of cobalt and copper in the concentration of thousands of ppm and are also characterised by a very low content of manganese with respect to all other samples of CL/1.

HIMT discussion

Group FC/1 and CL/1, appear to be very close in composition; yet, from an archaeological point of view, there are a number of differences, due to the different activities that took place in the sites: CL/1, deriving from a productive area, comprises abundant wastes and working indicators, including some glass chunks; among the vessels, frequent types in common between the two sites are Isings 96, 106 and 111.

Samples included in FC/1 and CL/1 have high contents of iron, alumina, magnesia, manganese, titania and trace elements (Ba, Zr, Ni, V, Cr) that allow to hypothesise that they were produced with an impure sand, rich in heavy, non-quartzous or accessory minerals such as biotite, pyroxenes, iron oxides and hydroxides, zircons and garnets and they are consistent with the so called HIMT glass, using the acronym created by Freestone

(Freestone 1994) to indicate glasses with high iron, manganese and titanium, probably produced in Egypt, that started to circulate in Europe and the Mediterranean after the 4th century.

HIMT samples are well documented in the scientific literature (Mirti et al. 1993; Freestone 1994; Foy et al. 2003; Freestone et al. 2005; Foster and Jackson 2009; Rosenow and Rehren 2014; Gallo et al. 2014b).

Together with the uncertainty on its production region, the composition of HIMT glass has not been properly defined yet(Foster and Jackson 2009). In the archaeometric literature, HIMT glasses are often split in "weak" and "strong" HIMT, depending of the content of iron, titanium and manganese (see HIMT 1 and HIMT 2 (Foster and Jackson 2009); groups 1 and 2 (Foy et al. 2003); WH and H (Rosenow and Rehren 2014); HIMT1 and 2 (Conte et al. 2014)). The glasses included in groups CL/1 and FC/1 are more similar to the "strong" groups and are, in most cases, even "stronger", with very high iron (Fe_2O_3 ≥3.50 wt%). Examining the chemical composition of group FC/1 and CL/1 clearly shows that the iron content is very high if compared to other datasets reported in the literature (Figs. 4.22-a,b). FC/1a and CL/1a comprise the "extremely strong" samples, while FC/1b and CL/1b comprise the "strong" samples; CL/1c, that includes two samples only, comprises weak HIMT glasses and has no corresponding group in Aquileia.

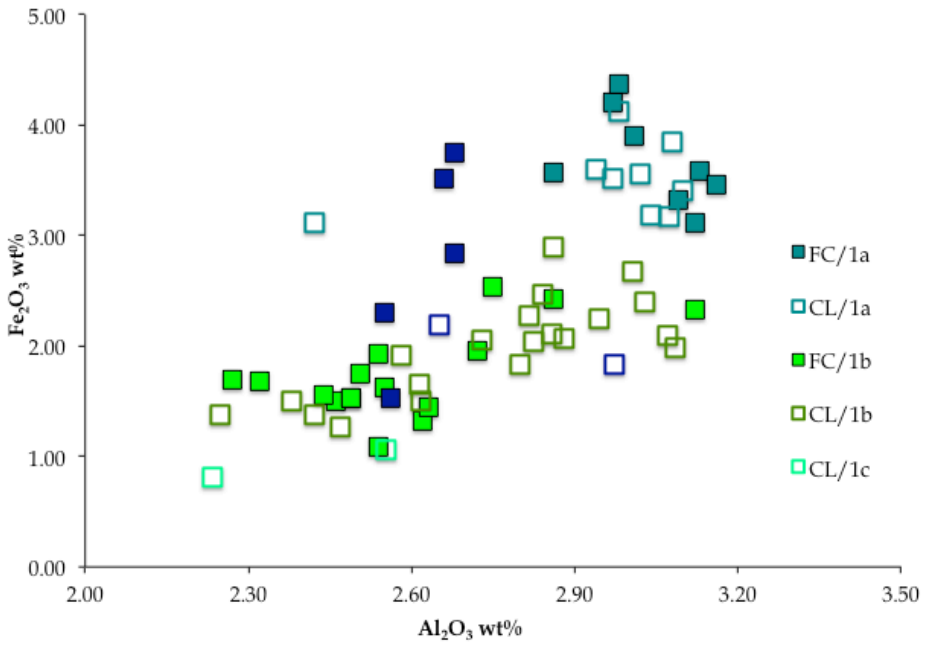

Fig 4.22-a *(left): iron vs. alumina. Tito Macro sample in filled symbols, Classe samples in empty symbols; the blue colour indicates samples intentionally coloured in blue. Note the presence of a slight positive trend among the two elements.*

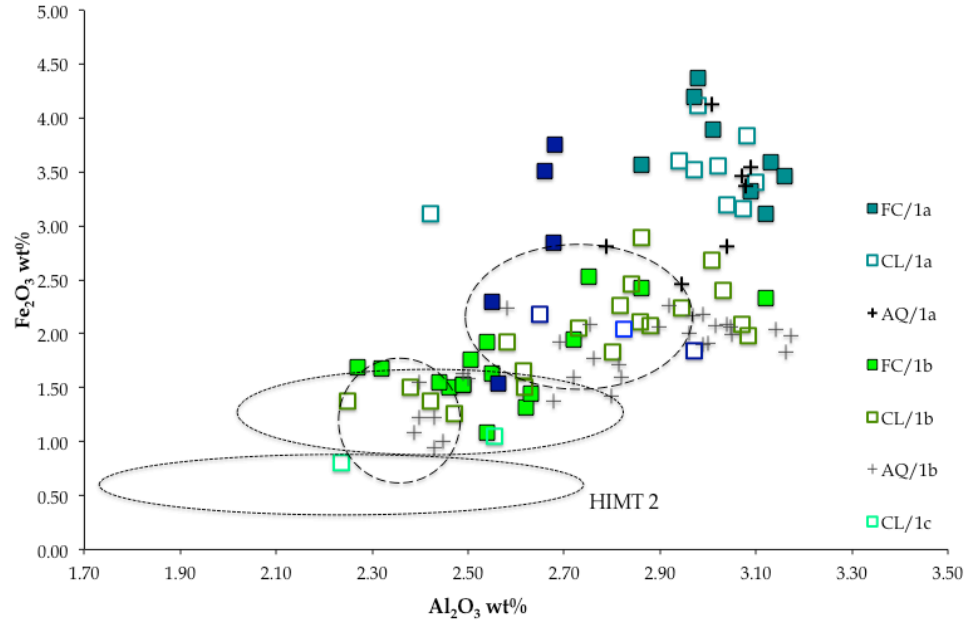

Fig 4.22-b *(left). Samples of Tito Macro and Classe are compared with the Bestie Ferite samples (Gallo 2014) and to reference compositional groups: HIMT1-2 (Foster&Jackson) in dotted line; Group1-2 (Foy 2003) in broken line.*

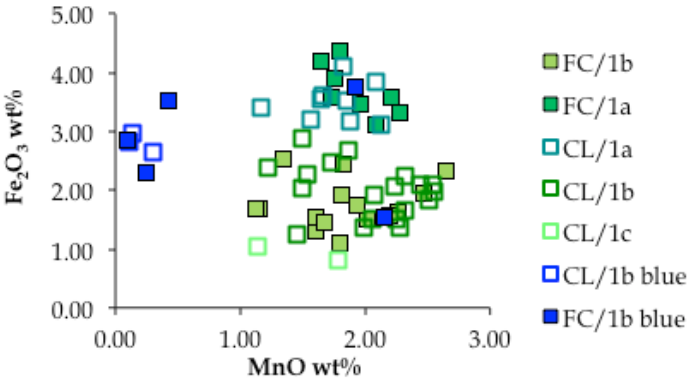

Fig. 4.23 *iron vs. manganese. No clear correlation is present, although a general positive trend can be noted in groups of samples. Note that the majority of the blue samples contain negligible MnO*

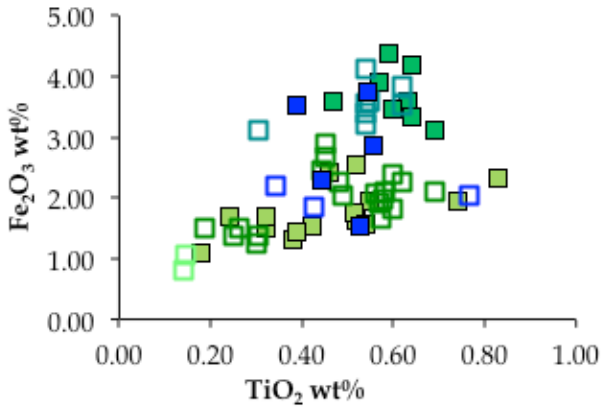

Fig 4.24*: iron vs. titanium: a general positive trend can be noted, although a clear correlation lacks.*

HIMT glasses with very high contents of iron are sometimes detected in large HIMT assemblages as sporadic cases; a whole HIMT assemblage with similar characteristics was detected only in the previously studied Late Antique samples from the Domus delle Bestie Ferite in Aquileia (Gallo et al. 2014b), where a similar subdivision between "very strong HIMT" (AQ1a) and "strong HIMT" (AQ1b) was identified. HIMT from Aquileia and Classe seems therefore to have a peculiar, very strong composition, which can be assimilated to the "strong" one of Group1 of Foy and co-workers. This is also consistent with the dating of the site and the objects, as Group1 starts to be massively traded along

the Mediterranean shores from the beginning of the 5th century and its circulation seems to stop at the beginning of the 6th century AD.

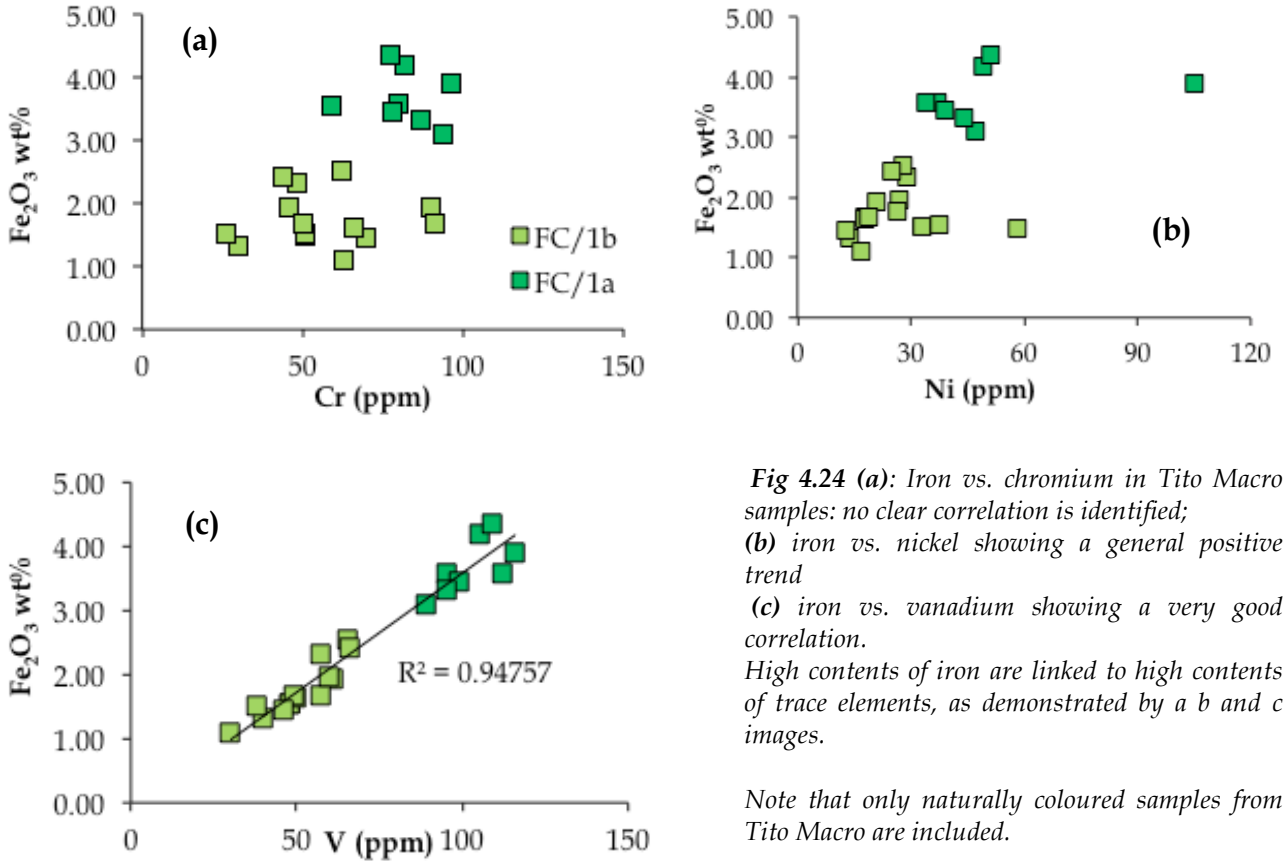

***Fig 4.24 (a)**: Iron vs. chromium in Tito Macro samples: no clear correlation is identified;*
***(b)** iron vs. nickel showing a general positive trend*
***(c)** iron vs. vanadium showing a very good correlation.*
High contents of iron are linked to high contents of trace elements, as demonstrated by a b and c images.

Note that only naturally coloured samples from Tito Macro are included.

Comparing the present samples with those reported in the literature, the high iron content is not the only difference identified: some studies (Freestone et al. 2005) restrict the definition of HIMT to glass samples that show a positive correlation between iron and alumina, titania and manganese and such positive correlations are identified in some assemblages (Foster and Jackson 2009; Gallo et al. 2014b). In the present study, such diagnostic correlations lack, and only some general positive trends can be identified (Fig 4.23-24a,b,c).

The lack of such diagnostic correlations may be due to the varied mineralogical composition of the sands employed in the primary production of HIMT glasses in different moments and, possibly, in slightly different locations, or it can also be interpreted

as the result of inter-mixing raw HIMT glass chunks and/or HIMT cullet of different origins.

Minor and trace elements can provide further useful information to discriminate the quality of the sands employed in the primary production and to evaluate the level of recycling. We have already underlined that samples included in FC/1 and CL1 have, where measured, high contents of Ba, Zr, V, Cr, Ni, deriving from the heavy and mafic minerals naturally contained in the sand of origin. To evaluate the extent of recycling, contents of Co, Cu, Pb, Sn, Zn and Sb could be particularly useful; it is generally assumed that low contents of these elements (in the 1-100 ppm range) originated from heavy mineral constituents in the sand (Wedepohl and Baumann 2000), whereas their presence in the 100- 1000 ppm range may be explained by the recycling of earlier glass and the addition of intentionally coloured glass cullet during melting. HIMT samples coming from Aquileia show very low levels of the above-mentioned elements, while samples from Classe show generally low, but not negligible, levels of the above-mentioned elements when detectable, suggesting very limited (if any) recycling in the glass from Aquileia and a slightly higher degree of recycling in the materials from Classe. Obviously, intentionally coloured glasses are excluded from this evaluation, as the mentioned element (Co, Co, Sb, Zn and Pb) may be intentionally introduced in the batch with the colouring elements. In this context, one sample from Classe (D1) has an ambiguous trace elements pattern: the high levels of copper and lead oxides could be related to the intentional addition of colouring elements, but also to a high degree of recycling; this point cannot be solved as the object presents a deep green colour, typical of HIMT glasses; the chromophoric elements could derive both from intentional and unintentional additions.

It is worth underlining that both in group CL/1a and CL/1b there are raw chunks, working wastes and objects, demonstrating that this "very strong" HIMT glasses was traded, and locally worked. In particular, subgroup CL1/a comprises only chunks, working wastes and Ising 96 cups; one of the hypothesis is that the atelier of Classe shaped Isings 96 vessels; of course the large variety of different types identified in the site tends to support the hypothesis that most of the vessels fragments were cullets (or also failures), collected for recycling.

Blue samples

5 samples of group FC/1b (respectively the raw glass chunk, one bottle Isings 104, one goblet Isings 111 and the decorative blue drops of the Isings 96 cups) and 2 vessel fragments of CL1/b (a beaker Isings 107 and a bottle Isings 92) are intentionally coloured in deep blue. The blue colour is due to the presence of chromoforic ions dispersed in the glass matrix, mainly cobalt and copper, both in the order of thousands of ppm; iron is also probably contributing to the colouration of the samples, and it is probably introduced partly with the sand of origin and partly with the colouring elements.

Comparing the chemical composition of the intentionally blue samples included in FC/1 and CL/1, a first major difference emerges: while in the blue decorations (AQ-FC-96_1 blue and AQ FC-96_2blue) manganese is present, as expected, in very high concentrations, the 3 other samples from Domus of Tito Macro and the 2 vessels from Classe have very low manganese if compared to the other HIMT glasses reported in the literature.

The blue drops decorating the Isings96 cups (here named AQ-FC-96_1blue and AQ-FC-96_2blue) are fully consistent with HIMT composition, with high manganese.

AQ-FC-96_1blue is coloured by a combination of cobalt and copper; its very high iron and lead content are also probably related to the colouring agent.

Differently, AQ-FC-96_2blue is coloured by copper in very high concentration, antimony is also present in high concentration while cobalt and lead are below detection limits.

These blue decorations were produced by adding colouring elements to HIMT base glass.

Comparing the blue decorations with the composition of the respective body vessel we can see that, despite the apparent difference in the silica content, the vessels bodies and their decorations are very close in their compositions and that the existing differences are mainly due to the colouring agents. It is possible to hypothesise that each cup and the corresponding blue decoration were made starting from the same base glass of HIMT composition; in the case of AQ FC 96_1, the blue glass was made by adding cobalt, probably iron and lead and some tin was also introduced with the colouring, while in AQ FC 96_2 the blue part was made by adding copper and some antimony.

In the case of these two Isings 96 cups, we can conclude that the blue glass employed in the decoration was produced by adding colorants to the same HIMT base glass employed in the vessel, which indicates that the addition of colorant took place in a secondary workshop.

The same evidence was detected in Isings 96 from Altino (northeastern Italy) (Silvestri et al. 2007) and seems therefore to represent a routine procedure in the production of Isings 96 cups, at least in the north Adriatic area.

High manganese content is one of the distinctive traits of HIMT, and it is usually ≈1%wt; on the other hand, manganese in HIMT is deliberately added, its presence is this glass having two main explanations: to contrast the deep green-brown colour of the glass due to the high iron and, according to freestone, to prevent sulphur oxidation, that would turn the glass black (Freestone et al. 2005). Its presence in the glass is a deliberate choice of the glassmakers. In three samples of Tito Macro, and in three of Classe, all coloured in blue, manganese is virtually absent, or very low.

Pseudo-HIMT glasses with negligible manganese (i.e.: MnO = 0.05%wt) have already been identified in the assemblage from Dichin (Bulgaria), dated to the 5th-6th century (Rehren and Cholacova 2010) and dubbed HIT (High Iron and Titanium); three probable HIT glasses intentionally coloured in blue (as those object of the present study) were also detected in the assemblage of Butrint (Albania) dated to the 5th-6th century (Conte et al. 2014) and two where included in the assemblage of the North Sinai, dated to the 4th-5th century (samples 77 and 85 of table 1, in (Freestone et al. 2002)). Comparing the low-manganese HIMT (or HIT) samples under investigation with those reported in the literature, it is evident that the samples considered are not so homogenous in composition: glasses from Dichin are naturally coloured and MnO = 0.05wt%; the blue samples from Butrint, Classe, North Sinai and Aquileia are intentionally blue, and the content of Mn varies from negligible to 0.49wt%; such levels can hardly be introduced in the glass with the sand, as already noted when discussing the early Roman glasses of this work; on the other hand, this concentration is too low to consider an intentional addition and could derive from the recycling of cullet and, to a minor extent, from the cobalt ore exploited to colour the glass.

Intentionally coloured blue glasses probably did not require the addition of a decolouriser to modify the tint, and this could be one of the reasons for the absence of manganese in these three blue samples. It is worth noting that the six low manganese glasses here analysed and the three reported by Conte from Butrint are all intentionally blue and, it should be underlined, a raw chunk is also included in the present assemblage. The blue

chunk of probable HIT composition suggests that coloured glass was traded as a raw material; furthermore, assuming that HIT blue glass and HIMT glass were both produced at the same primary production location (that is suggested by the chemical composition), the addition of manganese and the addition of colouring elements must have taken place at the same stage of primary production, and were alternative to each other. Adding cobalt to an HIMT glass with manganese is possible but, in the economy of a primary furnace, would not be worthwhile, as decolouring is superfluous when producing a blue glass.

Although generally low, manganese is present in some of the blue HIT samples here considered, in a concentration that is more probably introduced with recycling. The origin of manganese in HIT blue glasses may be related to the primary production that probably took place at the same location of HIMT glasses: adding cullet to the batch of a primary production was a common practice that helped decreasing the melting temperature; in the case of HIT blue production, assuming that HIT blue glass and HIMT were produced at the same primary workshops, it is possible that HIMT cullet was added to the batch, introducing some manganese.

Due to the small number of samples, and the paucity of published data, these hypotheses cannot be proved. The evidence is that blue glass was traded and, reasonably, worked in Aquileia; the peculiarity of the HIT composition and the presence of a raw chunk allows the formulation of hypotheses about the existence of a local secondary workshop aimed at the shaping of objects and, although the import of finished vessels cannot be discarded, it is possible that the bottle Isings 104 and the goblet Is 111 were locally produced with raw HIT blue glass.

HIT samples are, to date, very rare: the 3 samples from Bulgaria are naturally coloured, while the 3 from Albania, the three from the domus of Tito Macro and the two from Classe are deep blue.

Further studies will be necessary to define the chronology, compositional limits, locations of production and use of this peculiar late composition.

4.3.2 LEVANTINE1 COMPOSITION

The second composition, corresponding to groups **FC/2** (Aquileia-domus of Tito Macro assemblage) and **CL/2** (Classe assemblage) is characterised by high silica, very high lime content, high potash and low soda.

Group **FC/2 (n=6)** comprises 6 vessel fragments of the types Isings 106, 109, 109b/111 (n=2), 116 and 96; no raw glass chunk of working waste is here included. The group is characterised by a silica content of 67.44±1.65%wt, relatively low soda (16.76±1.15%wt) and iron (0.53±0.22wt%), high calcium (8.85±0.69wt%) alumina (2.71±0.25wt%), potash (1.07±0.4wt%) and manganese (1.06±0.74wt%).

On the basis of the manganese content, glasses of FC/2 are further grouped into FC/2a with negligible manganese (0.18±0.22wt%), and FC/2b, with high manganese (1.51±0.35wt%). The low manganese subgroup includes only two samples of the types Isings 109b/111 and 116 (see tables 4.2-4.3).

Group **CL2 (n=10)** is composed of 5 wastes and 5 vessel fragments; two of the vessel fragments are not identified, the remaining three belong respectively to type 106 (n=2) and lamp Israeli 2007 (n=1). Among the working indicators, a pontil wad and two shearings *(T04 and T10*) are included but no raw glass is present.

This group is characterized by high levels of CaO (8.82±2.54wt%), alumina (2.84±0.80 wt%) and potash (1.82 ±0.60%wt) and lower contents of Fe_2O_3 (0.46±0.16), TiO_2 (0.08±0.03wt%) and variable MnO (0.41±0.40%wt) (see table 4.4-4.5)

On the basis of the manganese content, CL/2 samples can be grouped in CL/2a with negligible Mn (0.03±0.0wt%, n=5) and CL2b with higher manganese (1.51±0.35wt%,n=5). Vessels and indicators are present in both subgroups (fig 4.4-4.5).

Levantine1 Discussion

Group FC/2 and CL/2 represent the less numerous groups of each assemblage, with only 6 and 10 samples respectively. The vessel fragments (when identified) belong to a limited number of late antique types: Isings 96, 106, 109, 109b/111, 116; most of these types are represented by a single sample, and only one type (Isings 106) is common to the two assemblages.

Working wastes of this composition are present in the Classe assemblage only, and no raw chunk is identified.

Chemical data, substantially comparable for the two groups, indicate the exploitation of a sand source rich in carbonates and K-bearing minerals, such as K-feldspars, but relatively poor in accessory minerals, which is reflected in the low content of iron, magnesium titanium, zirconium. This composition can be correlated to that dubbed Levantine1 by Freestone and well documented in the literature. Levantine1 glasses were identified in many different sites in all the Mediterranean and Europe (Jalame, (Brill 1988), Apollonia and Dor (Freestone et al., 2000); France, Tunisia and Egypt (Foy et al. 2003); Jordan (Schibille et al. 2008); Great Britain (Foster and Jackson 2009); Italy (Gallo et al. 2014b)) demonstrating that Levantine1 glass was traded in the Mediterranean between the end of the 4th and 7th century AD. Primary production centres for Levantine1 raw glass were excavated at Jalame (Brill 1988), Dor (Freestone et al. 2000) and Apollonia-Arsuf (Freestone et al. 2008), all in the Syro-Palestinian area.

Comparing the samples of FC/2 with those of CL/2, a first difference emerges: samples from Tito Macro have on average lower silica (67.44wt%) and higher soda (16.76%wt) with respect to those from Classe, where silica is higher and soda is lower (68.79wt% and 15.77 wt% respectively).

Examining data reported in the literature for Levantine1 glasses, we can see that samples of Levantine composition are usually characterised by low soda (≈15%) and high silica (≈70%), lime (≈9%) and alumina (≈3%); whereas samples from Tito Macro have a "weaker" composition with slightly higher soda and lower silica that was already reported by Foy (Foy et al. 2003) in Group 3.1 and from Freestone et al. (Freestone et al. 2000) in the primary furnace of Dor, dated to the 6th-7th century.

CL/2 on the contrary fits more closely with a large part of published data such as those of Jalame (Brill 1988) and Petra (Schibille et al. 2012b).

Another compositional characteristic that differentiates Levantine glasses of Tito Macro and Classe from the previously published samples is the elevated potash content: respectively 1.07±0.43wt% and 1.32±0.60wt% on average, with peaks of more than 1% in most cases and a few low potash samples. This compositional characteristic can be indicative of the sand employed for the primary production, peculiarly rich in K-feldspars, and it was identified in the Levantine samples (group AQ/2) of Gallo et al. from Aquileia (2014), and in part of the samples excavated at the primary furnace of Dor (Freestone et al. 2000).

Once again a compositional similarity is highlighted between the two Aquileian sites and between Aquileia and Classe, underlining an interesting trend in the trade and consumption of glass in the northern Adriatic area that will be discussed in the conclusions.

Considering the manganese content, groups FC/2 and CL/2 were further divided into two sub-groups, one characterised by very low manganese (0.18wt% in FC/2a and 0.03w%t in CL/2a) and one characterised by high manganese (1.51±0.35wt% FC/2b and 0.78±0.16 in CL/2b) Figs 4.25-a. The samples from Classe cover a wider range of manganese content, and the average content is lower, probably indicating a more extensive recycling practice.

A similar subdivision into "no-manganese" and "with manganese" Levantine glass was already observed by Brill (Brill 1988) in his work on the 4th century AD primary furnace of Jalame; later, a similar trend was noted by Foster&Jackson in the British assemblage (Foster and Jackson 2009) and Gallo et al. (Gallo et al. 2014b) in the Bestie Ferite assemblage from Aquileia. Manganese, as already discussed in the previous sections, is to be considered intentional when present in elevated concentration but the limit between the manganese naturally occurring in the sand and that introduced with recycling is, as already said, debated; Brill, discussing Levantine glasses from Jalame, states that MnO<0.4%wt is to be considered a natural impurity of the sand but recent work by Brems on Roman glass attributes to recycling MnO contents between 0.1 and 1%. The samples from FC/2b have high manganese, always above 1%, which is with no doubt an intentional addition, while FC/2a are only two, one of which has an intermediate value (MnO=0.33%wt) that could be consistent with the hypothesis of recycling. A very similar trend was highlighted in the assemblage Bestie Ferite from Aquileia, as shown in figure 4.25.b, where the two Aquileian Levantine assemblages are compared.

Differently, among the Levantine samples from Classe, the "no-manganese" subgroup (CL/2b) is constituted by 5 samples with negligible manganese, and the "with manganese" subgroup (CL/2a) comprises 5 samples with a relatively high concentration (MnO= 0.78±00.16). Manganese content of CL/2b is high even though below the limit of 1% and could also be considered as introduced by recycling (Fig 4.25-a).

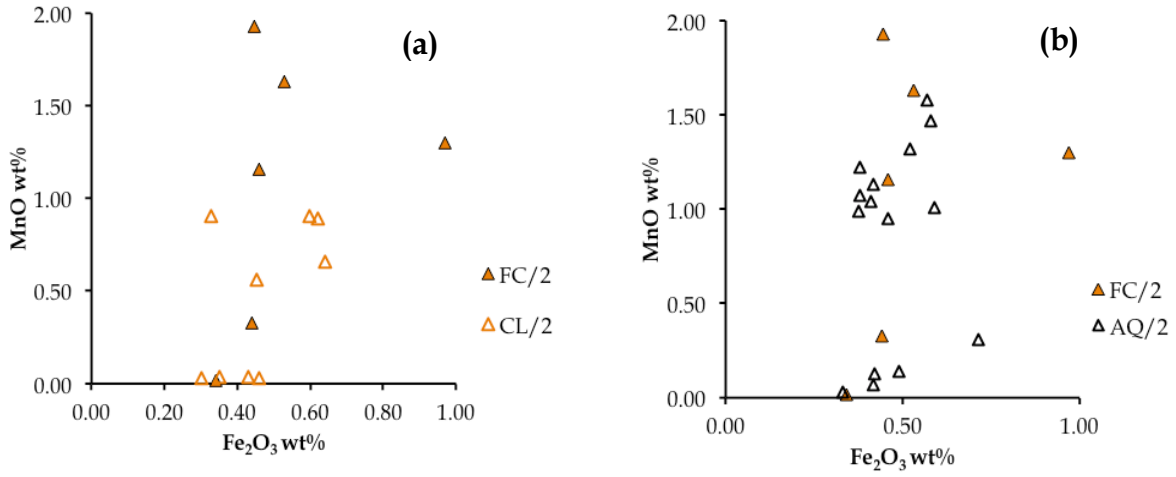

Fig 4.25 (a): *Manganese vs. iron in CL/2 and FC/2: FC/2 samples clearly split, while CL/2 samples show a wide range of compositions and a lower average content.* **Fig 4.25 (b):** *FC/2 compared with samples of AQ/2 group of Gallo and co-authors (Gallo et al. 2014) evidencing the same distribution pattern.*

When considering the practice of recycling, the possibility that glass cullets were melted with raw materials in primary furnaces shall be taken into account; therefore the presence of low but not negligible contents of manganese in these glasses, that have a clear Levantine1 composition, could derive also from recycling at the stage of primary production rather than from an extensive recycling of random cullet in secondary workshops, that could result in the modification of the general composition.

Recycled vessels?

Two samples of the Levantine groups have an uncertain interpretation: AQ-FC 109_1 from the Domus of Tito Macro appears to be slightly different from the others for its high soda and very high manganese content that put it in an intermediate composition between Levantine1 and Roman Mn-decoloured; its average composition is closer to the FC/2 group, and therefore it is included here even though it could be a product of recycling.

A similar unclear composition was determined in the unidentified cup D33 from Classe: its average composition is between Roman blue-green and Levantine1. Samples of similar borderline composition are seldom identified in Levantine assemblages; in the absence of a consistent early Roman samples group from Classe and considering the Late Antique dating of site, it is included in CL/2, although with an uncertain attribution.

4.3.3 SÉRIE 3.2-RESULTS

The third composition, corresponding to groups **FC/3** and **CL/3,** respectively, is well represented in both assemblages, and it is characterised by high silica, high soda and very low alumina.

Group FC/3 (n=9) includes a raw glass chunk, a working indicator and 7 fragments of drinking vessels of the late antique types Isings 116, 117, 109b/111 and the Early Medieval Isings 111. This group is characterised by high soda (19.37±00.37wt%) and very low alumina (1.82±0.22wt%), generally high manganese, and low potash, titania and trace elements (Tab 4.2-4.3.) All the samples are naturally coloured in shades of pale blue.

Group CL3 (n=25) includes 14 working wastes and 11 vessel fragments; among the working wastes there are 3 raw glass chunks, one moil, three pontil wads and a large quantity of generic wastes. Vessel fragments are mainly drinking vessels of the types Isings 106, 109 and 111; some fragments are of uncertain or unidentified attribution. One of the vessels is deeply coloured in blue, while all the others are naturally coloured, mostly in various shades of pale blue. This group is characterised by high soda (18.92±1.11%wt), very low alumina (1.90±0.22wt%), variable iron (0.68±0.26 %wt excluding the intentionally blue sample) and low magnesia, potash, titania and – when available – trace elements.

Sample D7 (Beaker Isings 109), intentionally coloured in blue, is differentiated by the high content of cobalt, copper and lead, in concentration of thousands of ppm, and a very low? iron content (Fe_2O_3 2.14%wt).

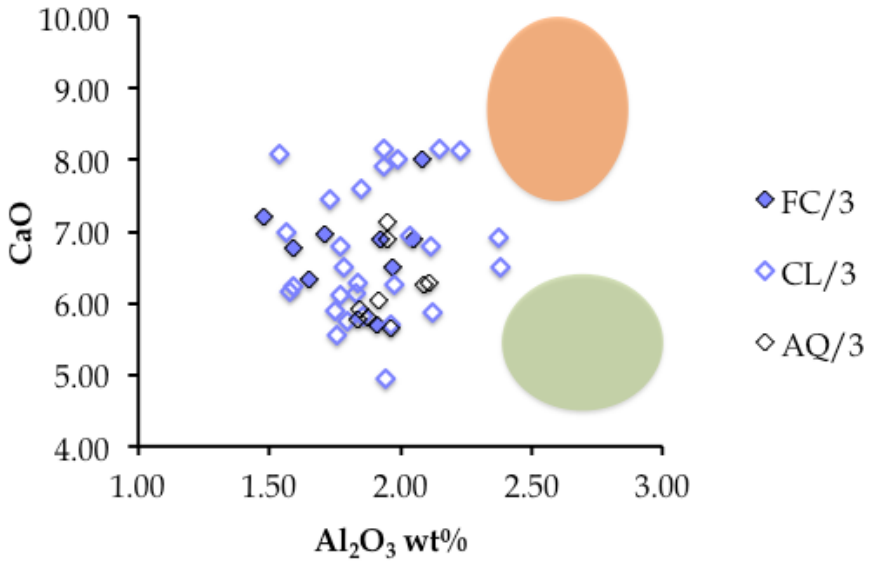

Fig 4.26: *FC/3 and CL/3 samples in a diagram, lime vs. alumina compared with samples AQ/3 (Gallo2014), CL/3 and FC/3 samples compared with the reference group Sèrie 3.2 of Foy and co-authors (2003) in broken line; usual compositional fields for HIMT and Levantine 1 are reported respectively in green*

Sèrie 3.2-discussion

The chemical composition identified in groups FC/3 and CL/3, mainly characterised by the very low alumina, high soda, relatively high iron and manganese, low potash, magnesia and titania and trace elements, is indicative of the exploitation of a particular sand, relatively rich in iron but poor in Al-bearing minerals and other accessory minerals. This composition can be related to Série 3.2 composition, first identified by Foy and co-authors (Foy et al. 2003) among glass findings excavated in France, Tunisia, Libya, Lebanon and Egypt and recently identified by Gallo et al. (Gallo et al. 2014b) in the late antique assemblage of Domus delle Bestie Ferite in Aquileia.

The comparison of the analysed samples with those reported by Foy and Gallo shows that the samples from Tito Macro and Classe are well included in the compositional ranges of the reference groups (fig 4.26).

This composition is dated by Foy and co-workers between the end of the 5th century and the beginning of the 6th century AD and, even though sand deposits and primary working sites have not been identified yet, they are hypothesised to be on the Levantine coast (Foy et al. 2003). The chronological limits of Série 3.2 group are consistent with the dating of the site of Classe, and the archaeological types considered dated to the 4th-5th or 5th-8th century AD.

All samples show very low trace elements, indicating the exploitation of a sand poor in mafic minerals; in addition, the very low content of Cu, Co, Pb, Sb and Sn indicate the low extent of recycling, at least with glasses of different composition. The single deep blue sample of Classe is characterised by a high content of cobalt, copper and lead, that is related to intentional colouring rather than recycling; the elevated iron content is also due to the added colouring elements.

The presence of working wastes and raw chunks in both sites indicates that both in Classe and Aquileia this composition was traded and worked.

Due to the productive vocation of the site, the evidence is very strong in Classe: among the working wastes, puntil wads, moils and shearings testify that this glass was blown;

regarding the vessels types, Isings 111 are present in both assemblages and it is not to exclude that, at least in the case of Classe, they were shaped in the workshop.

One sample included in FC/3 presents some antimony, unlike all the other Série 3.2 samples. This is surprising, as the antimony decolouring technique is typical of the early Roman glassmaking and it is generally limited to the 3rd-early 4th century AD; in addition, antimony decoloured glasses generally have Sb_2O_3 around 0.80%wt, much higher than the 0.35 of these samples. The contemporary presence of antimony and manganese can be considered as a sign of recycling, as already said when discussing the Roman glass.
Despite the different dating, Sb decoloured and Sèrie 3.2 are quite similar in the composition of their major oxide, in particular silica, soda, lime, and alumina; the main compositional difference is in the decolouring element, that is Sb in the Roman and Mn in the late composition. The presence of manganese, the low antimony and the late dating of the type do not allow including it in Roman compositional groups without consequences. As a probable product of late recycling and intermixing of Sèrie 3.2 and Sb decoloured glass, it is thus included in FC/3 with reservations.

4.4 ISOTOPIC CHARACTERISATION FOR GLASS PROVENANCE

Shedding light on the provenance of glass is a great challenge that tantalises glass scientists and archaeologists. To trace the raw materials employed in primary production, important information can be obtained by the isotopic composition of the glass combined with the chemical data.
In the case of natron glass, the Sr and Nd isotopes turned out to be valuable tools for the study of provenance as they derive in glass respectively from the carbonatic and the heavy, non-quartzous fraction of the sand (Degryse et al. 2009).

In the present work we analysed a selection of the late-antique samples from Classe and Aquileia and a selection of the antimony-decoloured glasses from Tito Macro. Nd is introduced in the glass with the heavy fraction of the sand and, having virtually no possibility of enrichment or pollution from other sources, it is a valuable tool to trace the sediment of origin in a glass. The Mediterranean coastal sediments have an East-to-West gradient in neodymium signature that varies from the very negative values of the Western

Sahara and Southern Spain (-13 ,-12 as □Nd) to the less negative value of the Middle Eastern coast (-3, -6 as □Nd) (Brems et al. 2013b). In a silica-soda-lime glass, Sr is introduced mainly with the carbonatic fraction of sand and, to a minor extent, from silicates. In the case of coastal sand, the carbonatic fraction is constituted predominantly by mollusc shells and only to a minor extent by limestone. Mollusc shells are constituted in large part by Ca-carbonate in the form of aragonite, that can host a large quantity of Sr in substitution of Ca^{2+} ions, therefore a glass produced with a coastal sand rich in mollusc shells is expected to have a high Sr content, around 300-600 ppm; on the contrary, a glass produced with limestone, constituted by calcite has a low Sr content, around 100-150ppm (Brems et al. 2013a). As mollusc shells are in equilibrium with the oceanic seawater, their isotopic signature is expected to be close to that of the water. Strontium is not fractioned by heat treatment, is not influenced by the addition of natron and therefore glass produced with Holocene sand, where Sr derives from the carbonates of the shells, is expected to have a Sr isotopic ratio near the value of modern oceanic water, that is equal to 0.7092 expressed as $^{87}Sr/^{86}Sr$.

The samples were selected on the basis of their chemical composition, the size of the fragment and, when possible, privileging working residues.
Intentionally coloured blue samples were excluded from the isotopic analysis, as the addition of colouring element, cobalt in particular, may interfere severely with the isotopic signature of Nd in particular.

Full analytical results are given in table 4.6).

Group	Sample ID	Sr (ppm)	87Sr/86Sr	2□	143Nd/144Nd	2□	□Nd
FC/1	106-5	368	0.70823	0.00008	0.512388	0.000046	-4.88
FC/1	106-9	463	0.70868	0.00006	0.512396	0.000064	-4.73
	109b/111-1	442	0.70905	0.00006	0.512370	0.000061	-5.22
	109b/111-3	471	0.70891	0.00006	0.512430	0.000051	-4.06
	109-2	411	0.70904	0.00007	0.512406	0.000050	-4.52
	109-3	457	0.70903	0.00009	0.512381	0.000052	-5.01
	109-5	550	0.70905	0.00006	0.512386	0.000047	-4.92
	111-2	379	0.70896	0.00006	0.512390	0.000076	-4.83
	111-4	697	0.70887	0.00006	0.512367	0.000051	-5.29

	111-7	478	0.70895	0.00006	0.512370	0.000065	-5.22
	116-1	448	0.70909	0.00005	0.512444	0.000043	-3.77
	116-2	488	0.70912	0.00006	0.512383	0.000055	-4.97
	117-2	398	0.70821	0.00006	0.512398	0.000058	-4.67
	117-3	406	0.70860	0.00007	0.512374	0.000062	-5.14
	117-6	345	0.70914	0.00007	0.512377	0.000069	-5.09
	117-7	449	0.70898	0.00009	0.512402	0.000074	-4.61
	118-1	537	0.70890	0.00008	0.512395	0.000065	-4.74
	118-2	382	0.70825	0.00006	0.512403	0.000055	-4.59
	85-1	587	0.70917	0.00008	0.512385	0.000067	-4.93
	85-6	340	0.70908	0.00008	0.512394	0.000053	-4.76
	96-3	405	0.70904	0.00006	0.512418	0.000052	-4.29
antimony	sl1	502	0.70911	0.00006	0.512381	0.000058	-5.02
FC/3	sl2	396	0.70902	0.00007	0.512395	0.000055	-4.75
CL/3	a3	438	0.70897	0.00007	0.512393	0.000058	-4.79
CL/2	c4	504	0.70903	0.00006	0.512438	0.000058	-3.91
CL/3	d16	419	0.70916	0.00007	0.512396	0.000054	-4.73
CL/3	d23	366	0.70884	0.00007	0.512387	0.000051	-4.90
CL/1	d24	380	0.70841	0.00007	0.512425	0.000053	-4.15
CL/3	d25	410	0.70892	0.00006	0.512401	0.000053	-4.62
CL/1	d29	536	0.70861	0.00007	0.512399	0.000049	-4.67
CL/3	d36	381	0.70897	0.00006	0.512407	0.000041	-4.51
CL/1	d5	413	0.70849	0.00007	0.512380	0.000064	-5.02
CL/1	fd	443	0.70829	0.00007	0.512409	0.000053	-4.48
CL/3	pv	420	0.70871	0.00007	0.512404	0.000054	-4.57
CL/3	pv1	514	0.70907	0.00007	0.512393	0.000059	-4.78
CL/3	pva	584	0.70909	0.00006	0.512373	0.000053	-5.17
CL/1	pvs	451	0.70840	0.00005	0.512362	0.000048	-5.38
CL/1	tb	505	0.70845	0.00007	0.512382	0.000057	-4.99

Tab. 4.6: *isotopic data of Classe ad Tito Macro samples. The absolute content of Sr expressed in ppm is included*

All the analysed samples show an □Nd value between -5.5 and -3.5, consistent with the eastern Mediterranean area; it is interesting to note that FC/2 and CL/2 samples, corresponding to Levantine 1 composition, have a distinct, although close, Nd signature when compared to the Sèrie 3.2 composition (FC/3 and CL/3). HIMT (FC/1 and CL/1),

Série 3.2 (FC/3 and CL/3) and antimony decoloured (FC colourless1) show a slightly more negative signature for Nd, comprised between -5.5 and -4, while Levantine 1 compositions (FC/2 and CL/2) are comprised between -4 and -3.5. Examining the Sr absolute content, it is evident that all the analysed samples, regardless of their chemical composition, are rich in Sr, with an average content around 400-500 ppm and are therefore reasonably produced with a coastal sand rich in mollusc shells. Despite this evidence, the Sr isotopic ratio ranges between 0.7092 and 0.7081. In particular, the Roman samples of group FCcolourless1, the late antique samples of group FC/2 and CL/2 (Levantine1 composition), FC/3 and CL3 (Série 3.2 composition) have a Sr isotopic ratio close to that of modern oceanic water and typical of Holocene beach sands, while FC/1 and CL/1 (HIMT composition) tend towards lower values.

Comparing the isotopic data of the Late-Antique samples here analysed with those reported in the literature is not easy, as large assemblages so far analysed regard mostly early Roman glasses (Degryse and Schneider 2008; Ganio et al. 2012a; Ganio et al. 2012c); the few data available on Late Antique glasses from Sagalassos (Turkey)(Degryse et al. 2008; Degryse et al. 2010), Bet Eli'Ezer (Freestone et al. 2003) Cartaghe, North Sinai, Apollonia, and London - Billingsgate Bath House (Freestone et al. in press) are generally characterised by □Nd values between -6 and -5, while in the present assemblage all samples are comprised between -5.5 and -3.5; the same trend was highlighted in the Bestie Ferite assemblage (Gallo et al. *forthcoming*) and was hypothesised to be indicative of the exploitation of a different coast segment (Gallo, personal communication). Particular care is necessary, as the remarked difference and the tendency towards less negative values could be a consequence of the new protocol of Nd isolation, recently published (Ganio et al. 2012b), which has been applied in the present study and in the one of the Bestie Ferite. Despite the slight difference in Nd signature, the samples here analysed are still fully consistent with a Middle-Eastern provenance.

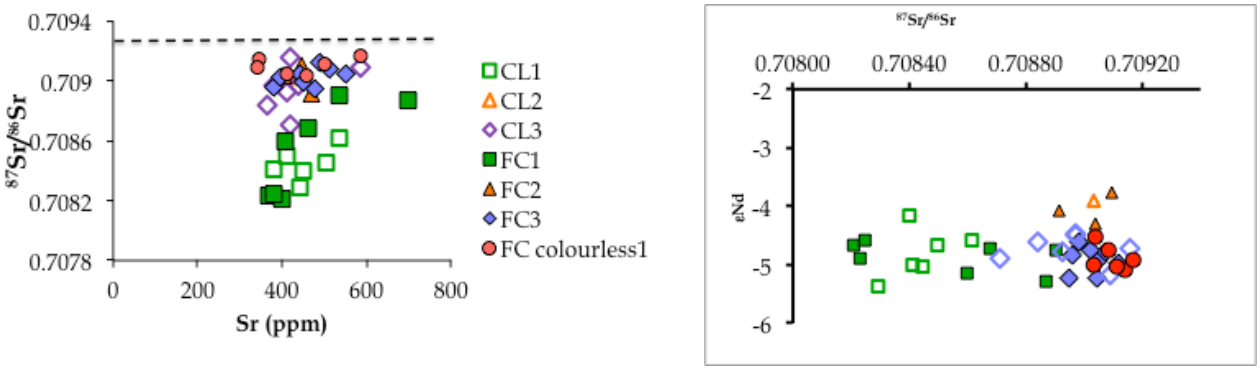

Fig. 4.27 (a) left *Sr isotopic ratio vs. Sr absolute content. Broken line indicates the Sr isotopic ratio of modern seawater.* ***(b) right*** *Sr isotopic ratio vs. Nd*

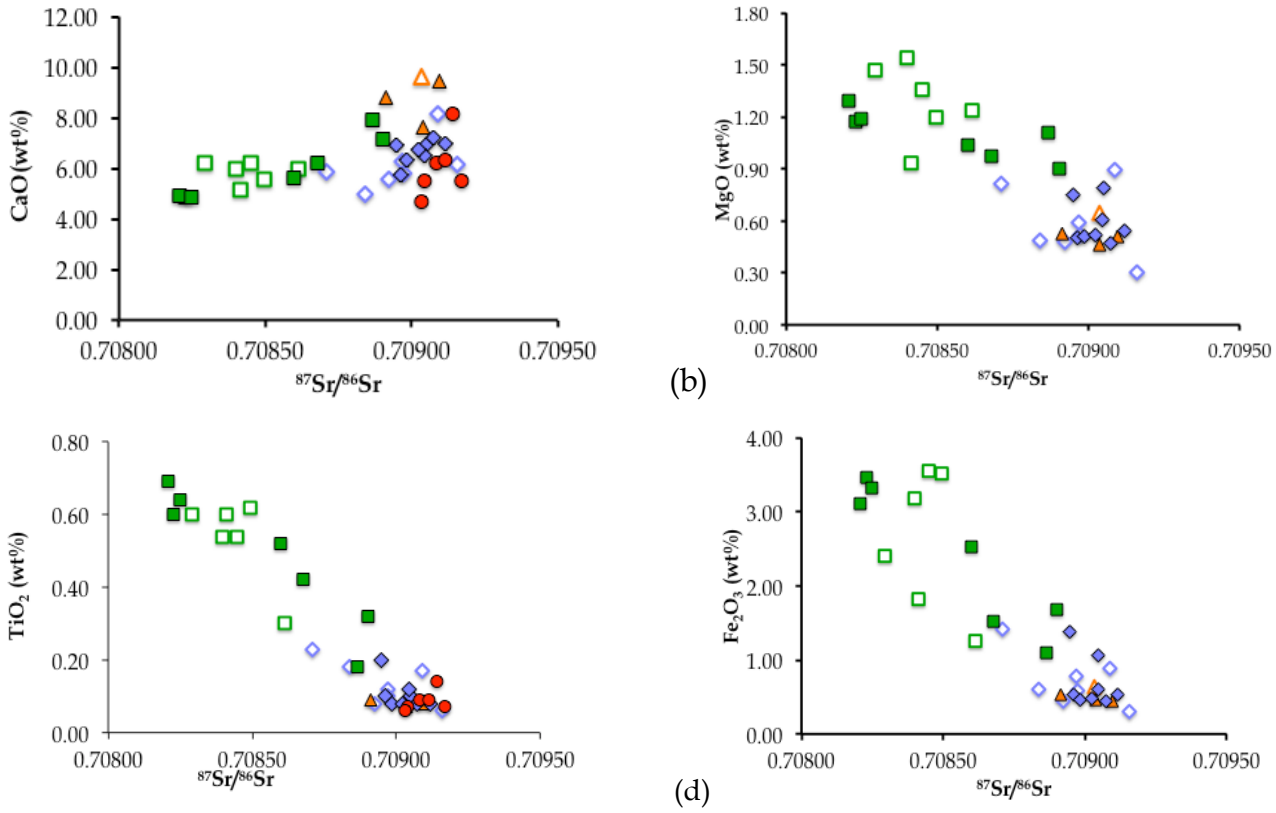

Fig. 4.28 (a) above, left: Sr isotopic ratio plotted vs. CaO absolute content. HIMT (green symbols), Série 3.2 (violet symbols) and antimony-decoloured (red symbols) show similar content of calcium and very different values for Sr isotopic ratio. ***(b) (c) (d)****: magnesia, titania and iron oxide content plotted vs. St isotopic ratio show a negative correlation, indicating that samples with high contents of iron, titanium and magnesium also show a lower isotopic ratio for Sr.*

It is noteworthy that Sèrie 3.2 glass (groups FC/3 and CL3) differs from Levantine 1 (FC/2 and CL/2) in Nd signature and cluster with Roman samples of group FC colourless1 (antimony decoloured). It is not possible to relate a specific signature to a precise area of provenance, and only an East/West distinction is possible, but the highlighted difference

supports the hypothesis of Foy and co-authors, according to which the Série 3.2 glass may derive from the Syro-Palestinian coast, but from a different area with respect to Levantine1 glass. It is also interesting to note that samples of group FC colourless1, the antimony decoloured samples, have an isotopic signature for □Nd that is very close to that of the Série 3.2.

The strontium isotopic signature is fully consistent with a coastal sand of the Palestinian coast for groups of Levantine 1 (FC/2 and CL/2), Série 3.2 (FC/3 and CL/3) and antimony decoloured (FCcolourless1) while in HIMT glass of groups FC/1 and CL/1 there is a tendency to lower values. Such low values, around 0.7080, are typical of geologically aged limestone, but all the analysed samples have a high Sr content that demonstrates the use of aragonitic mollusc shells as lime-bearing source. Therefore in FC/1 and CL/1 glasses (HIMT composition), other Sr-bearing minerals, besides carbonates, influenced the Sr signature.

In order to clarify the origin of Sr in the glass, binary plots? of the Sr ratio towards the absolute content of lime, magnesia, iron oxide and titania are particularly useful.

The binary plot of the CaO content versus $^{87}Sr/^{86}Sr$ diagram (fig 4.28-a) shows a very weak positive trend between the two elements. HIMT glasses of groups FC/1 and CL/1 with Sèrie 3.2 glasses of groups FC/3 and CL/3 have comparable calcium contents, but different isotopic ratios; assuming that the lime content is almost entirely referable to shells in all samples, such evidence indicates a difference in the Sr-bearing mineral between the HIMT samples and the others.

The negative correlation between $^{87}Sr/^{86}Sr$ and, respectively, MgO, Fe_2O_3 and TiO2, indicates that to a higher content of the above-mentioned elements corresponds a lower Sr isotopic ratio, (*Fig 4.28 b, c, d*) suggesting that the same mineral introducing magnesium, iron and titanium is also responsible for the introduction of strontium.

Although strontium is present in various silicatic minerals, phases that contain iron, titanium, magnesium and strontium at the same time are restricted to inosilicates such as pyroxenes and amphiboles. Freestone and co-workers in their in-press work report that when progressing up the Eastern Mediterranean coast, from the mouth of the Nile towards Syria, there is a general decline in the heavy mineral content of the beach sand,

mainly pyroxenes and amphiboles (hornblende in particular) (Freestone et al, in press); this supports the hypothesis of an Egyptian provenance of the samples of FC/1 and CL/1.

Sèrie 3.2 and antimony decoloured glass have a quite similar isotopic signature, that reflects the similarity in the base composition: the two groups differ almost uniquely for the decolouriser employed: Sb in the Roman composition, Mn in the Late Antique one; the high degree of chemical similarity is also reflected in a very close isotopic composition and indicates not only the probable continuity in raw materials for glassmaking, but also that manganese additions, at least in this case, have a negligible influence in the Sr and Nd isotopic ratios.

4.5 Conclusions: glass trading and working in Aquileia and Classe in the Late Antiquity

Despite the difference in the activity of the two sites, the Late-Antique glass assemblages of Aquileia and Classe share several features, which can be useful to clarify glass circulation in the north-Adriatic area.

All the vessel fragments included in the Late-Antique compositional groups belong to late antique types dated to the 4th-8th century AD with a large predominance of 4th-5th century types.

Both assemblages report abundant HIMT and Série 3.2 glasses, while Levantine1 glass is less represented in both sites. Raw glass chunks are present in both sites and limited to HIMT and Série 3.2, demonstrating that this two compositions were traded as raw glass and worked in local secondary ateliers. Levantine1 chunks lack in both sites, and only a few evidences of working activity were detected in Classe.

HIMT from Classe and Aquileia show a specific composition, particularly rich in iron, which is rare in the archaeometric literature and previously reported only in the assemblage of "Bestie Ferite" in Aquileia. The presence in Classe of the same HIMT composition proves that this specific "very strong" HIMT glass was traded in the Adriatic area in the 5th-6th century. Furthermore, some blue samples of probable HIT composition, including a chunk, were identified in both sites, evidencing once again that the two cities were supplied by the same trade routes.

The reasons for the different ratio among HIMT, Série 3.2 and Levantine1 in Tito Macro and Classe could be related to a series of factors: cost can be one of the reasons, as

probably Levantine1 glass was more expensive than the high-sodium groups (Série 3.2 and HIMT); technological factors can also affect the choice of certain compositions especially in a workshop, thus viscosity and working ranges could be primary elements for the vessel-maker; chronology could also play an important role, Levantine 1 glass started to be produced in the 4th century in Palestine, but the largest part of the production and exportation seems to be dated to the 6th-7th century; HIMT starts in 4th century and the small composition Sèrie 3.2 and HIT seem to be typical of the 5th century. Classe is mainly dated to the 5th-6th century, it is therefore possible that the assemblages under investigation were mainly formed around the 5th century, before the glass market was "invaded" by Levantine 1. The remarked abundance of Levantine 1 glasses in the Bestie Ferite assemblage (Aquileia) with respect to the assemblages here considered may also be related to a slight difference in dating or other unknown factors.

In the evaluation of possible connections between chemical composition and archaeological type, some interesting trends were highlighted: as already suggested by Gallo in the Bestie Ferite assemblage, bottles Isings 104, (present in the Aquileian assemblage only) are produced predominantly with HIMT glass (except 2 cases of Roman glass of Tito Macro); in both sites cups Isings 96 are not produced with Série 3.2 glass; goblets Isings 111 are present in groups of Roman glass, HIMT and Série 3.2 glass, but not in Levantine 1, differently from what evidenced in the Bestie Ferite assemblage; beakers Is. 106 on the contrary are present in all the compositions in the three sites. In addition, some specific forms such as lamp Crowfoot-Harden A and dish Isings 118 are produced with HIMT glass only, but the small number of samples does not allow drawing general conclusions.

Aquileia and Classe, both Late-Antique harbours of northeastern Italy, were supplied by the same trade routes and show similar patterns of glass consumption and working. Probably thanks to their strategic position and their importance in the Late Antiquity, the two cities promptly received the new glass compositions introduced in the Mediterranean in the 4th-5th century AD and confirm their role of "outpost" in the western Mediterranean trades.

Arletti, R., Maiorano, C., Ferrari, D., Vezzalini, G., and Quartieri, S., 2010, The first archaeometric data on polychrome Iron Age glass from sites located in northern Italy, *Journal of Archaeological Science*, **37**(4), 703–12.

Arletti, R., Rivi, L., Ferrari, D., and Vezzalini, G., 2011, The Mediterranean Group II: analyses of vessels from Etruscan contexts in northern Italy, *Journal of Archaeological Science*, **38**(9), 2094–100.

Baxter, M. J., Cool, H. E. M., and Jackson, C. M., 2005, Further studies in compositional variabilities of colourlessRomano-British vessel glass, *Archaeometry*, **47**(1), 47–68.

Brems, D., Degryse, P., Hasendocks, F., Gimeno, D., Silvestri, A., Vassilieva, E., Luypaers, S., and Honings, J., 2012, Western Mediterranean sand deposits as a raw material for Roman glass production, *Journal of Archaeological Science*, **39**, 2897–907.

Brems, D., Ganio, M., Latruwe, K., Balcaen, L., Carremans, M., Gimeno, D., Silvestri, A., Vanhaecke, F., Muchez, P., and Degryse, P., 2013a, Isotopes on the beach, part 1: Strontium isotope ratios as a provenance indicator for lime raw materials used in Roman glass-making, *Archaeometry*, **55**, 214–34.

Brems, D., Ganio, M., Latruwe, K., Balcaen, L., Carremans, M., Gimeno, D., Silvestri, A., Vanhaecke, F., Muchez, P., and Degryse, P., 2013b, Isotopes on the beach, part 2: Neodymium isotopic analysis for the provenancing of roman glass-making , *Archaeometry*, **55**, 449–64.

Brill, R. H., 1988, Scientific investigations of the Jalame glass and related finds , In *Excavations at Jalame: site of a glass factory in late roman Palestine* (ed. G. Davidson Weinberg), 257–94, University of Missouri press, Columbia (MO).

Brill, R. H., 1999, *Chemical analyses of Early Glasses*, Corning Museum of Glass, Corning, NY.

Conte, S., Chinni, T., Arletti, R., and Vandini, M., 2014, Butrint (Albania) between eastern and western Mediterranean glass production: EMPA and LA-ICP-MS of late antique and early medieval finds, *Journal of Archaeological Science*, **49**(1), 6–20.

Degryse, P., and Schneider, J., 2008, Pliny the Elder and Sr-Nd isotopes: tracing the provenance of raw materials for Roman glass production, *Journal of Archaeological Science*, **35**(7), 1993–2000.

Degryse, P., Schneider, J., Lauwers, V., and Brems, D., 2008, Sr-Nd isotopic analysis of glass from Sagalassos (SW Turkey), *Journal of Cultural Heritage*, **9**, e47–9.

Degryse, P., Henderson, J., and Hodgins, G., 2009, Isotopes in vitreous materials, a state-of-the-art and perspectives, In *Isotopes in vitreous materials* (eds. P. Degryse, J. Henderson, and G. Hodgins), 15–30, Leuven University Press, Leuven.

Degryse, P., Shortland, A. J., De Muynck, D., Van Heghe, L., Scott, R., Neyt, B., and Vanhaeckec, F., 2010, Considerations on the provenance determination of plant ash glasses using strontium isotopes, *Journal of Archaeological Science*, **37**(12), 3129–35.

Foster, H. E., and Jackson, C. M., 2009, The composition of "naturally coloured" late Roman vessel glass from Britain and the implications for models of glass production and supply, *Journal of Archaeological Science*, **36**(2), 189–204.

Foster, H. E., and Jackson, C. M., 2010, The composition of late Romano-British colourless vessel glass: glass production and consumption, *Journal of Archaeological Science*, **37**(12), 3068–80.

Foy, D., Vichy, M., and Thirion-Merle, V., 2003, Caractérisation des verres de la fin de l'Antiquité en Méditerranée occidentale: l'émergence de nouveaux courants commerciaux , In *Actes du colloque de l'Association Française pour l'Archéologie du Verre* (eds. D. Foy, and M. D. Nenna), Vol. Aix-en-Pro, 41–85, Monique Mergoil, Montagnac.

Freestone, I. C., 1987, Composition and microstructure of copper opaque red glass, In *Early vitreous material. British Museum Occasional Paper, 56* (eds. M. Bimson, and I. C. Freestone), 173–91, British Museum, London.

Freestone, I. C., 1994, Chemical analysis of raw glass fragments., In *Excavation at Carthage, The Circular Harbour, North Side. the Site and Finds Other than Pottery. Vol II* (ed. H. R. Hurst), 290, British Academy Monographs in Archeology, Oxford University Press, Oxford.

Freestone, I. C., Gorin-Rosen, Y., and Hughes, M. J., 2000, Primary Glass from Israel and the Production of Glass in Late Antiquity and the Early Islamic Period, In *La Route du Verre. Ateliers Primaires et Secondaires du Second Millènaire av. JC au Moyen Age* (ed. M. D. Nenna), 65–83, Maison de L'orient Mediterranéen, Lyon.

Freestone, I. C., Greenwood, R., and Gorin-Rosen, Y., 2002, Byzantine and early Islamic glassmaking in the eastern Mediterranean: production and distribution of primary glass. In, In *Hyalos-Vitrum-Glass. History, technology and conservation of glass in the Hellenic world* (ed. K. G.), 167–74, Glasnet Publications, Athens.

Freestone, I. C., Leslie, K. A., Thirlwall, M., and Gorin-Rosen, Y., 2003, Strontium Isotopes in the Investigation of Early Glass Production: Byzantine and Early Islamic Glass from the Near East*, *Archaeometry*, **45**(1), 19–32.

Freestone, I. C., Wolf, S., and Thirlwall, M., 2005, The production of HIMT glass: elemental and isotopic evidence, *Annales du*, **16**, 153–7.

Freestone, I. C., Jackson-Tal, R. E., and Tal, O., 2008, Raw Glass and the Production of Glass Vessels at Late Byzantine Apollonia-Arsuf, Israel, *Journal of Glass Studies*, **50**, 67 – +.

Gallo, F., Silvestri, A., and Molin, G., 2013, Glass from the Archaeological Museum of Adria (North-East Italy): new insights into Early Roman production technologies, *Journal of Archaeological Science*, **40**(6), 2589–605.

Gallo, F., Silvestri, A., Molin, G., Marcante, A., and Guerriero, P., 2014a, Iron Age vessels from the Archaeological Museum of Adria (North-Eastern Italy): a textural, chemical

and mineralogical study, In *Proceedings of the 39th International Symposium on Archaeometry* (eds. R. B. Scott, D. Braekmans, M. Carremans, and P. Degryse), 198–207.

Gallo, F., Marcante, A., Silvestri, A., and Molin, G., 2014b, The glass of the "Casa delle Bestie Ferite": A first systematic archaeometric study on Late Roman vessels from Aquileia, *Journal of Archaeological Science*, **41**, 7–20.

Ganio, M., Boyen, S., Fenn, T., Scott, R., Vanhoutte, S., Gimeno, D., and Degryse, P., 2012a, Roman glass across the Empire: an elemental and isotopic characterization, *Journal of Analytical Atomic Spectrometry*, **27**(5), 743.

Ganio, M., Latruwe, K., Brems, D., Muchez, P., Vanhaecke, F., and Degryse, P., 2012b, The Sr-Nd isolation procedure for subsequent isotopic analysis using multi-collector ICP-mass spectrometry in the context of provenance studies on archaeological glass, *Journal of Analytical Atomic Spectrometry*, **27**(8), 1335–41.

Ganio, M., Boyen, S., Brems, D., Scott, R., Foy, D., Latruwe, K., Molin, G., Silvestri, A., Vanhaeckec, F., and Degrysea, P., 2012c, Trade routes across the Mediterranean: A Sr/Nd isotopic investigation on Roman colourless glass, *Glass Technology: European Journal of Glass Science and Technology Part A*, **53**(5), 217–24.

Huisman, D. J., Groot, T. D., Pols, S., Van Os, B. J. H., and Degryse, P., 2009, Compositional Variation in Roman Colourless Glass Objects From the Bocholtz Burial (the Netherlands), *Archaeometry*, **51**(3), 413–39.

Jackson, C. M., 2005, Making colourless glass in the Roman period, *Archaeometry*, **47**(4), 763–80.

Jackson, C. M., Price, J., and Lemke, C., 2006, Glass production in the 1st century AD: insight into glass technology, In *Annales du 17e Congrés de l'Association International pour l'Histoire du Verre* (eds. K. Janssens, P. Degryse, P. Cosyns, S. Caen, and L. Van't Dack), Vol. Anvers, 150–5.

Jacson, C. M., 2005, Making colourless glass in the Roman period, *Archaeometry*, **47**(4), 763–80.

Lilyquist, C., and Brill, R. H., 1993, *Studies in Early Egyptian Glass*, Metropolitan Museum of Art, New York.

Van Der Linden, V., Cosyns, P., Schalm, O., Cagno, S., Nys, K., Janssens, K., Nowak, A., Wagner, B., and Bulska, E., 2009, DEEPLY COLOURED AND BLACK GLASS IN THE NORTHERN PROVINCES OF THE ROMAN EMPIRE: DIFFERENCES AND SIMILARITIES IN CHEMICAL COMPOSITION BEFORE AND AFTER ad 150*, *Archaeometry*, **51**(5), 822–44.

Mirti, P., Casoli, a., and Appolonia, L., 1993, Scientific analysis of Roman glass from Augusta Praetoria, *Archaeometry*, **35**, 225–40.

Nenna, M. D., Vichy, M., and Picon, M., 1997, L'atelier de verrier de Lyon, du Ier siècle après J.-C., et l'origine des verres "romains" , *Revue d'Archéométrie*, **21**, 81–7.

Nenna, M. D., and Gratuze, B., 2009, Etude diachronique des compositions de verres employès dans le vases mosaique: rèsultats prèliminaires , In *Annales du 17e Congès de l'Association Internationale pour l'Histoire du Verre*, Anvers.

Panighello, S., Orsega, E. F., van Elteren, J. T., and Šelih, V. S., 2012, Analysis of polychrome Iron Age glass vessels from Mediterranean I, II and III groups by LA-ICP-MS, *Journal of Archaeological Science*, **39**(9), 2945–55.

Paynter, S., 2006, Analyses of colourless Roman glass from Binchester, County Durham, *Journal of Archaeological Science*, **33**(8), 1037–57.

Paynter, S., and Kearns, T., 2011, West Clacton Reservoir, Great Bentley, Essex: analysis of glass tesserae, http://research.english-heritage.org.uk/report/?14996.st , *Research Department Report Series*.

Price, J., and Cottam, S., 1998, *Romano-British glass vessels: a handbook*, Practical handbooks in archaeology ;no. 14, Council for British Archaeology, Walmgate, York.

Rehren, T., and Cholacova, A., 2010, The early Byzantine HIMT glass from Dichin, nothern Bulgaria, *Interdisciplinary Studies*, 81–96.

Rosenow, D., and Rehren, T., 2014, Herding cats - Roman to Late Antique glass groups from Bubastis, northern Egypt, *Journal of Archaeological Science*, **49**(1), 170–84.

Sayre, E. V, and Smith, R. W., 1961, Compositional categories of ancient glass, *Science*, **133**(3467), 1824–6.

Schibille, N., Marii, F., and Rehren, T., 2008, Characterization and Provenance of Late Antique Window Glass From the Petra Church in Jordan*, *Archaeometry*, **50**(4), 627–42.

Schibille, N., Degryse, P., Corremans, M., and Specht, C. G., 2012a, Chemical characterisation of glass mosaic tesserae from sixth-century Sagalassos (south-west Turkey): Chronology and production techniques, *Journal of Archaeological Science*, **39**(5), 1480–92.

Schibille, N., Degryse, P., O'Hea, M., Izmer, A., Vanhaecke, F., and McKenzie J, 2012b, Late Roman glass from the Great Temple at Petraand Kirbhet Et-Tannur, Jordany: technology and provenance, *Archaeometry*, **54**, 997–1022.

Shortland, A. J., Schachner, L., Freestone, I. C., and Tite, M. S., 2006, Natron as a flux in the early vitreous materials industry: sources, beginnings and reasons for decline, *Journal of Archaeological Science*, **33**(4), 521–30.

Silvestri, A., Busana, M., Larese, A., Olmeda, G., Serra, C., Pesavento Mattioli, S., and Molin, G., 2007, Indagini archeometriche sui vetri dal territorio di Altino, In *Atti delle*

XII Giornate Nazionali di Studio dell'AIHV, Comitato nazionale italiano, "l vetro nel Medioevo tra Bisanzio, l'Islam e l'Europa (VI-XIII secolo)," 143–54, AIHV, Venezia.

Silvestri, A., 2008, The coloured glass of Iulia Felix, *Journal of Archaeological Science*, **35**(6), 1489–501.

Silvestri, A., Molin, G., and Salviulo, G., 2008, The colourless glass of Iulia Felix, *Journal of Archaeological Science*, **35**(2), 331–41.

Vichy, M., Thirion-Merle, V., and Foy, D., 2004, Contribution à l'étude des verres antiques décolorés à l'antimoine, *Revue d'Archéométrie*(28), 169–77.

Wedepohl, K. H., and Baumann, a., 2000, The use of marine molluskan shells for Roman glass and local raw glass production in the Eifel area (western Germany), *Die Naturwissenschaften*, **87**(3), 129–32.

Wedepohl, K. H., Simon, K., and Kronz, A., 2011, Data on 61 Chemical Elements for the Characterization of Three Major Glass Compositions in Late Antiquity and the Middle Ages, *Archaeometry*, **53**(1), 81–102.

Van der Werf, I., Mangone, A., Giannossa, L. C., Traini, A., Laviano, R., Coralini, A., and Sabbatini, L., 2009, Archaeometric investigation of Roman tesserae from Herculaneum (Italy) by the combined use of complementary micro-destructive analytical techniques, *Journal of Archaeological Science*, **36**(12), 2625–34.

Israeli Y., Chapter 7. The glass vessels, in J. Patrich (eds), *Archaeological Excavations at Caesarea Maritima Areas CC, KK and NN, Final Reports. Volume 1: The Objects*, Israel Exploration Society, Jerusalm 2008.

5. GLASS MOSAIC TESSERAE

Glass mosaic *tesserae* are complex artefacts whose intense colours and characteristic shining effects were produced by adding some colouring and decolouring elements, pigments or other mineral phases and variable quantity of lead to a base glass. It is generally assumed that colouring and opacifying agents were added in secondary workshops, but in some cases it is also possible that colouring elements, lead and other components were added to primary batches or at least at the primary production stage or that some specific colours were produced in specific primary production sites.

Some base glass composition and colouring/opacifying technique are also indicative of certain geographical regions and/or historical periods, therefore a detailed textural, chemical and mineralogical study of a large assemblage of Roman and Late Roman mosaic tesserae can shed light on the glassmaking technologies, technological level, availability of knowledge and materials, circulation of innovations. In the present study north-eastern Italy is investigated selecting three Roman and late Roman asemblages excavated from the coastal harbour of Aquileia and the inland cities of Pordenone Trento.

In particular, the sites involved in the study are the *in-situ* mosaic of the domus of Bestie Ferite in Aquileia (here named "BF"), dated to the second half of the 4th century AD, and two disrupted decorations derived from the villa of Torre in Pordenone (here named "PN") dated to the 2nd-5th century AD and from the Roman baths below Santa Maria Maggiore cathedral (Trento here named "TN", dated to 2nd-4th century AD,) respectively.

All available colours were sampled from each site. On the basis of their macroscopic appearance, samples were divided into seven colour macro-groups: blue, turquoise, green, yellow, red, white and colourless; each macro-group is further grouped into various chromatic groups, which are identified by ad abbreviation (full details are given in table 5.1) following the colourimetric subdivision already applied to the glass tesserae of the St. Prosdocimus mosaics in Padova (Silvestri et al. 2011).

The majority of the tesserae are opaque, but some transparent and translucent samples are also included: colourless and "gold" tesserae are defined as transparent, while deeply coloured tesserae with no opacifier are defined as translucent. Among the gold tesserae in addition there is one sample (PN AG1) that, due to the presence of a black/grey layer between the *tessera* and the *cartellina,* was wrongly interpreted as a silver *tessera*. Successive analysis revealed the absence of any metallic foil and the tesserae probably

represents a failure, but due to the presence of a *cartellina* it is still considered in the group of the "gold" tesserae.

Two samples(PN M3 and TN VOL1) represents a very complex case: they are olive green translucent tesserae with opaque red stripes and are therefore classified as "olive/red and are considered as a colour group belonging to the macro colour group of "red". The labels of the "olive/red" tesserae are coincident with those of other chromatic groups, i.e. brown (M) and olive green (VOL) because a first macroscopic examination they appeared dark brown and olive green, respectively.

Due to the complexity of the materials, which imply different production technologies, the glassy matrix and inclusions identified in the *tesserae* were analysed separately.

Chemical analysis of the matrix was conducted by EPMA, avoiding inclusions and opacifiers in order to obtain information on the base glass and colouring/decolouring elements; in addition the presence of cobalt in azure samples in which this element was below detection limits of EPMA was checked by Fiber Optic Reflectance Spectrometry (FORS); the oxidation state of iron in selected translucent dark green samples samples was checked by Electronic Paramagnetic Resonance (EPR).

The investigation of micro-texture, opacifiers and mineralogical inclusions was conducted by Scanning Electron Microscopy (SEM) coupled with Enargive Dispersive Spectrometer (EDS). X-Ray Powder Diffraction (XRPD) and in specific cases micro-XRPD and micro-raman Spettroscopy were employed to determinate the mineralogical phase involved in the opacification of the tesserae.

In the case of banded tesserae, different bands were analysed separately and are treated as different samples.

Colour	Chromatic group	label	BF	PN	TN
Blue	Blue opaque	BO, B	1	1	1
	Blue translucent	B	none	none	1
	Azure	AZ	5	2	2
Turquoise	Dark blue translucent	BS	1	1	1
	Turquoise	TU+ Tu TR	2	3	3

	Aquamarine	AQ	2	1	1
	Pale blue	CE	2	1	1
	Pale green	V CH	3	1	1
Green	Dark green	VS	1	1	1
	Dark green translucent	VS- V TR	1	2	1
	Green	VP	4	1	2
	Olive green	V OL	none	none	1
	Yellow green	VG	1	1	2
Yellow	Yellow	GSO	4	2	2
	Light amber	NC	none	1	none
Red	Orange	AV	1	2	1
	Red	R	1	none	none
	Brown	M	4	2	3
	Olive/red striped	PN M3 and TNVOL	none	1	1
	Dark amber	NS	none	none	1
White	White	BI OP	none	1	1
	Grey	GR	1	1	2
Colourless	Clear colourless	TR INC	3	none	1
	Gold	AU or AG	1	3	1

Table 5.1: chromatic groups, colour, labels and number of samples from each site

5.1 GLASSY MATRIX

5.1.1 BASE GLASS

- **Introduction**

Glass was produced since the Protohistoric times employing a silica source (quarz pebbles or quartz sand) a carbonatic fraction (limestone or seashells) and a flux (plant ash or mineral soda). Until the mid-first millennium BC, glass was produced using quartz sand or pebbles fluxed with ash of coastal plants, generally identified with Salicornia or Salsola Kalii, as a source of alkali and lime. In the mid-1st millennium BC plant ash was replaced by natron, the main flux employed in the Mediterranean and European glassmaking until the 9th-10th century AD (Sayre and Smith 1961). Although most of the glass production occurring between the mid-first millennium BC and the 9th century AD employed carbonatic coastal sand and natron as a flux, the production of soda ash never interrupted in the inner regions of the Middle East and Mesopotamia (Brill 1999; Freestone 2006). According to some authors (Lilyquist and Brill 1993) the compositional field of plant ash glass is characterized by relatively high levels of magnesia and potash (both above 2.5wt% as MgO and K_2O) and high levels of phosphorous and lime, the last one being introduced in the batch also with the flux. On the contrary, the compositional field of natron is limited to glasses with MgO and K_2O contents below 1.50wt%.

Comparisons of the chemical composition of glassy matrices with those published in the literature is not easy, as most of the mosaic tesserae analysed are dated to the Byzantine time or later (Arletti, Fiori, & Vandini, 2010; Ruffini, Fiori, & Vandini, 1999; Schibille, Degryse, Corremans, & Specht, 2012; Silvestri, Tonietto, Molin, & Guerriero, 2012; Silvestri, Tonietto, & Molin, 2011; Silvestri, Tonietto, Molin, & Guerriero, 2014; Verita & Vallotto, 2003; Verità & Vallotto, 1998; Vezzalini, Fiori, & Vandini, 2011); analytical studies of Roman glass tesserae were glassy matrices are analysed separately from the opacifiers are not available and only a few paper investigate the base glass composition of tesserae (Silvestri et al. 2011; Schibille et al. 2012; Silvestri et al. 2014a). Comparison of the glassy matrices with the reference compositional groups of vessels glass for Roma and Late Antique were made.

- **Results**

The majority of the samples here considered are characterised by a high soda content, generally comprised between 15 and 20 wt%, calcium generally comprised between 5 and 8wt%, low potash, magnesia (both below 1.50wt%) and phosphorus (generally below 0.20wt%); in addition, the samples here analysed contain lead in very variable concentrations, from negligible to very high (PbO> 30wt%). (Fig 5.2a-b). Three *tessereae* (the orange TN-AV1, and the brown BF-M3 and PN-M2) have both magnesia and potash above 1.50wt% and relatively elevated content of phosphorus and lime (Fig.5.1a).

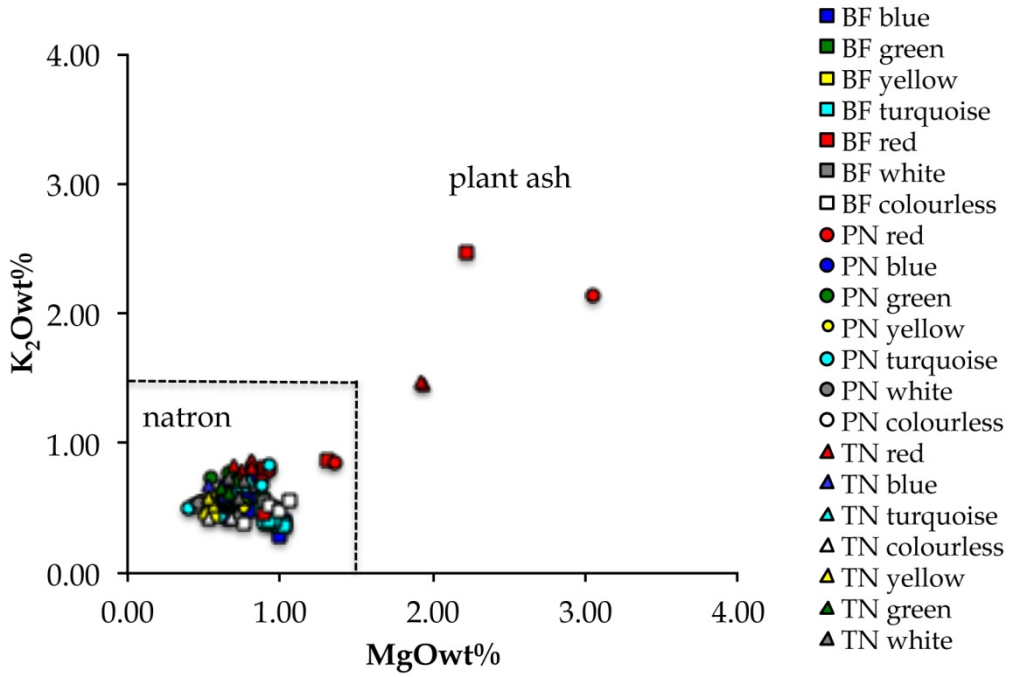

Fig. 5.1a: *diagram K_2O/MgO; broken line indicates the compositional fields of natron and plant ash. Samples are grouped in seven macro-group of colours: turquoise, blue, green, yellow, red, white and colourless. The majority of the samples fall in the field of natron glass, with the only exception of few red tesserae.*

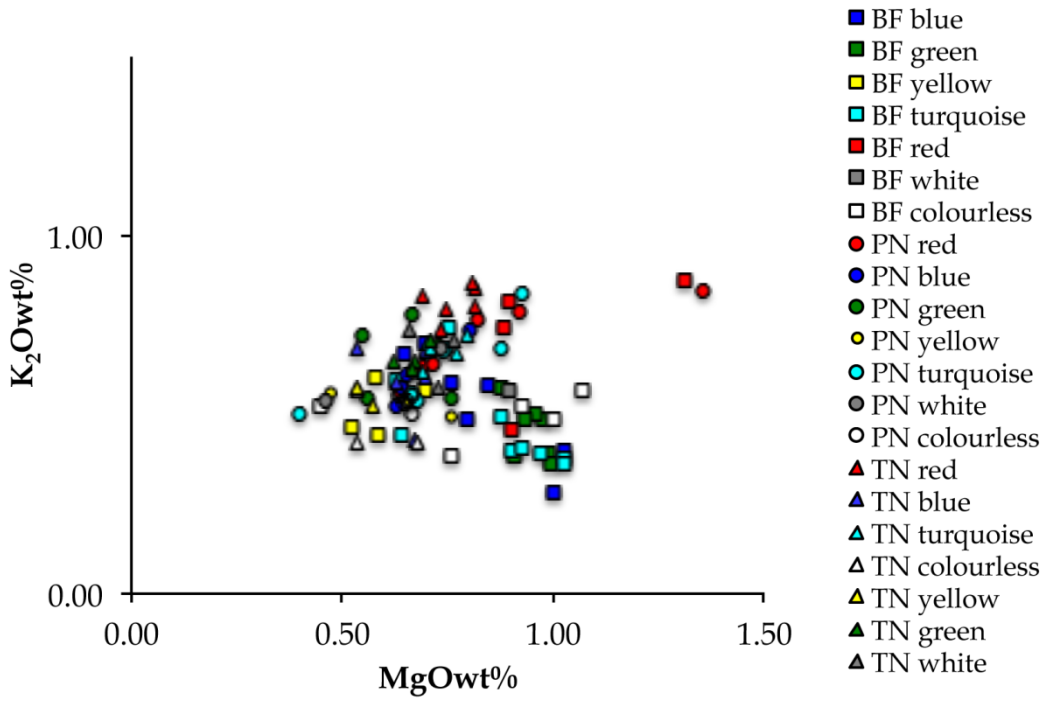

***Fig. 5.1b**: diagram K_2O/MgO limited to the natron compositional field. Samples are grouped in seven macro-group of colours: turquoise, blue, green, yellow, red, white and colourless. Note the presence of two red tesserae separated from the main group.*

Apart from some red *tesserae*, which show a general high content of MgO and K_2O (Fig. 5.1b), no clear trend between potash-magnesia content and colour is identified. An interesting trend is though evidenced when samples are distinguished on the basis of the site of provenance, instead of their colour, as shown in figures 5.2a-b.

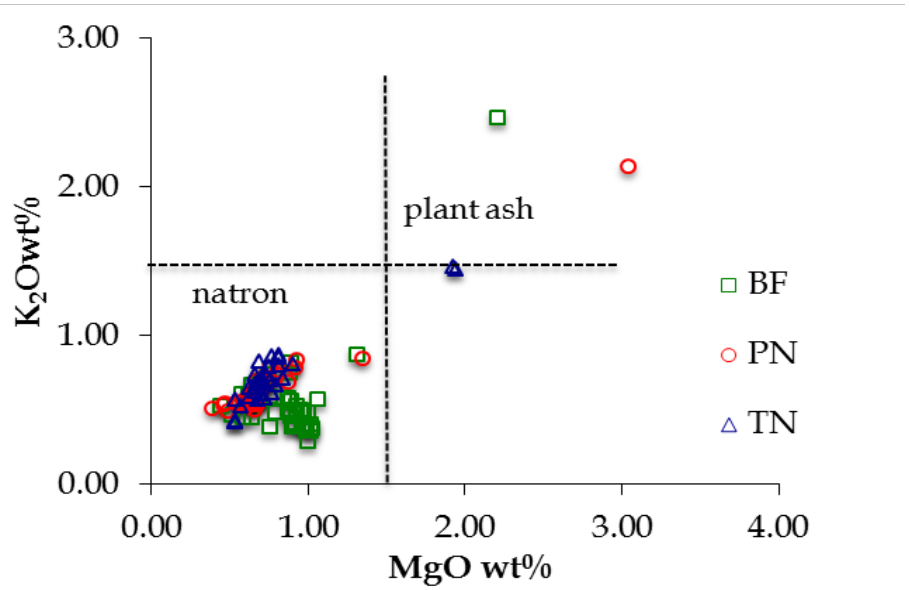

***Fig. 5.2a**: binary plot K_2O/MgO; samples are distinguished by shape and colour on the basis of the site of provenance only; green blue and red symbols indicate Aquileia trento and Pordenone samples, respectively.*

Indicating with different colours the different sites of provenance (Fig. 5.2a-b) it becomes clearer that samples from Pordenone (here indicated in red circles) and Trento (blue triangles) cluster together and show a positive trend between magnesia and potash; conversely, only a small part of Aquileia samples (green squares) cluster with Trento and Pordenone tesserae: a large group of Aquileia samples create a cluster characterised by higher magnesia and lower potash, with no correlation between them.

Those samples are the aquamarine BF AQ1,2; the pale blue BF CE2, the pale green BF VCH1,2,3; the dark blue translucent BF BS1; the azure BF AZ1,2,3 the grey BF GR1, the dark green BF VS1,2 the green BF VP1,2,3,4; the yellow green BF VG1 and the gold BF AU1. The same evidenced is also preserved in the reduced composition.

The chemical composition of the base glass of the t*esserae* was classified following the method proposed by Fiori and co-authors (Fiori et al. 2004) for Byzantine mosaic *tesserae*.

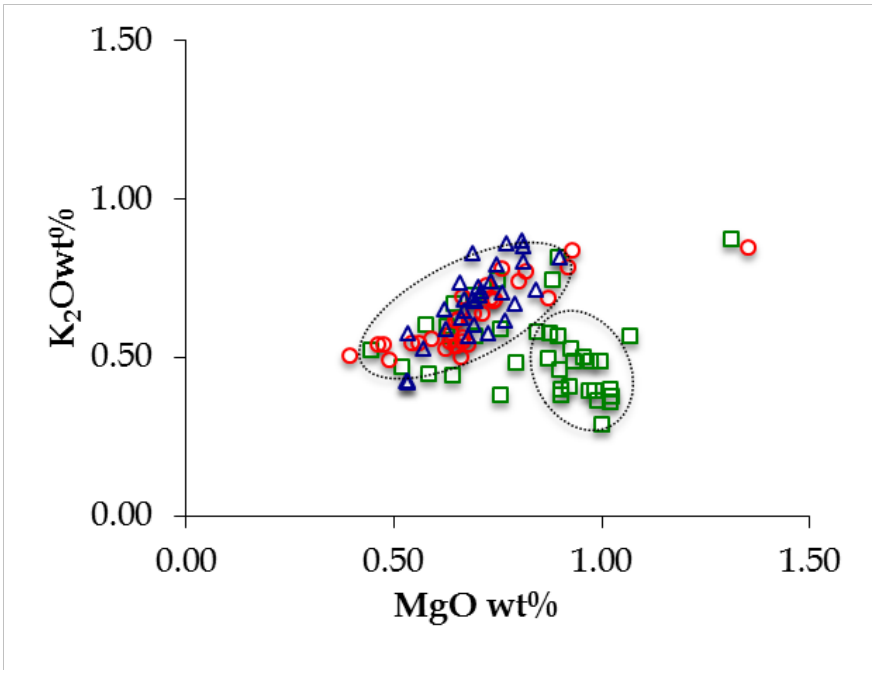

***Fig. 5.2b**: binary plot K_2O/MgO limited to the natron compositional field. Dotted lines indicates the distribution of the samples in two main groups, one comprising almost all the Trento and Pordenone samples and part of the Aquileia samples, and one comprising Aquileia samples only.*

The proposed method is based on the ratio between lead oxide and the sum of the three major oxides (SiO_2+Na_2O+CaO). Glass is then classified as lead-glass if its PbO/(SiO_2+Na_2O+CaO) ratio is over 0.1, silica-soda-lead glass if it is between 0.1 and 0.01, silica-soda-lime if it is smaller than 0.01. (tab 5.3 and 5.4)

Colour	Chromatic group	Abbr.	Lead glass	Silica-soda-lead	Silica-soda-lime
Blue	Blue opaque	BO, B	none	none	3
	Blue translucent	B	none	none	1
	Azure	AZ	none	none	8
Turquoise	Dark blue translucent	BS	none	none	3
	Turquoise	TU	none	1	7
	Aquamarine	AQ	none	none	4
	Pale blue	CE	none	none	4
	Pale green	V CH	none	none	5
Green	Dark green	VS	none	3	1
	Dark green translucent	V TR, TN VS1	none	2	1
	Green	VP	2	5	none
	Olive green	V OL	1	none	none
	Yellow green	VG	none	1	1
Yellow	Yellow	GSO	1+1*	5	1*
	Light amber	NC	none	1	none
Red	Orange	AV	3	1	none
	Red	R	none	1	none
	Brown	M	none	6	3
	Olive/red	PN M3 and TN	1	none	1

		VOL1			
	Dark amber	NS	none	1	none
White	White	BI OP	none	1	1
	Grey	GR	none	none	4
Colourless	Clear colourless	TR INC	none	none	4
	Gold	AU or AG	none	none	4+ cart

Tab 54: classification of the base glass related to the colour of the tesserae. The number of samples is also reported.

** indicates two different bands of the same tesserae. "+cart" indicates the cartellina of gold tesserae.*

Most of the samples here analysed (more than 66%) can be classified as silica-soda-lime glass, only 8% are lead glasses and the remaining 26% is made of silica-lead glass. Considering each assemblage on its own, despite different internal distribution this trend is confirmed: all the three assemblages present glass tesserae referable to each of the three category, with a great majority of silica-soda-lime glass and only a very few samples of lead glass.

Comparisons between the chromatic groups and compositional categories (Tab.5.4) evidence that lead glass is employed for certain colours: the majority of the orange (AV), one of the two olive/red, a single yellow band of samples PN GSO2 (GSO) and green (VP). Silica-soda-lead glass comprise various chromatic groups: Green (VP), dark green (VS, V TR), yellow-green (VG), yellow (GSO), light amber (NC), a single orange (AV), brown (M), the single red (R), the single dark amber (NS), one of the turquoise (TU) and one of the two white (BI OP). Silica-soda-lime glass comprises all the dark blue (BS), all the blue (B and BO), azure (AZ), almost all the turquoise (TU), aquamarine (AQ), pale blue (CE), pale green (VCH), some of the brown (M), one white (BI OP), grey (GR), and all the colourless (TR INC) and gold (AU and AG) and the semi-opaque part of PN GSO2.

In order to put in relation the composition of the glassy matrix of the *tesserae* with those of transparent vessel glass, a reduced composition was calculated subtracting all the intentionally added elements (i.e.: Mn, Co, Cu, Sn, Sb, Zn and Pb) from the total and then recasting; iron and titanium are introduced in Roman and Late Antique glass as an

impurity of the sand in the form of heavy, non-quartz minerals; in the case of specific colours requiring strong reducing conditions (i.e. brown, orange and red), iron oxide may have been intentionally added as internal reducing agents (Freestone et al. 2003) and this may influence the evaluation of the base glass. To minimize the discrepancy between the percentage of iron and titanium naturally occurring in the sand and that intentionally added, in the case of red, orange and brown *tesserae*, maximum values of 0.12 wt% TiO_2 and 1.40 wt% Fe_2O_3 were considered assumed as the upper limit of the non-intentional addition for Roman and late Roman glass. In the case of iron and titanium exceeding respectively 1.40wt% and 0.12wt% (percentage of the oxide as Fe_2O_3 and TiO2), they were set at those values following the method proposed by Silvestri (Silvestri et al. 2014a).

A detailed examination of the samples in both their original and reduced formula evidences that the majority of the *tesserae* here considered have a silica content of 65-70wt%, soda around 15-20 wt %, lime 5-8 wt%, alumina around 2-2.6 wt% and titania generally below 0.15wt%. A more careful examination of the reduced formula evidences that tesserae from Aquileia show a general higher content of soda, magnesia and titania with respect to the assemblages from Trento and Pordenone (Tab.5.2-5.4) although a clear distinction cannot be done.

Clear colourless *tesserae* and in some cases translucent (i.e. deeply coloured but not opacified) *tesserae* and can be examined in their full chemical composition, as it tends to be very close or coincident with that of the base glass (Tab 5.2). The clear colourless and gold tesserae will be discussed separately in the next paragraphs, while the base glass composition of the few translucent tesserae is here presented: the translucent blue TN B1, is characterised by the presence of both manganese and antimony as decolouring agents, the turquoise translucent BF TUTR1 is characterised by elevated manganese (1.05wt%) and no detectable antimony; the two dark green translucent tesserae from Pordenone PN VTR1-2 have elevated lead content and their chemical composition is therefore not fully interpretable in the original composition, but they show relatively high manganese (although below 1%wt) and antimony (above 0.2wt%).

- **Discussion**

Examining the chemical composition both in its original (Tab 5.2) and in its reduced (Tab. 5.4) versions, the largest part of the tesserae here analysed is confirmed to be made with natron glass, having both MgO and K_2O below 1.50%

The orange samples TN-AV1 in its reduced formula falls in the plant ash composition field, while two sample (BF-AV1 and PN-AV1) that in their original composition appeared at the limit of the compositional range for natron glass (see fig. 5.1-b; 5.2-b), in the reduced formula appear to be intermediate between plant ash glasses (see fig5.1-5.2).

The use of vegetal ashes or charcoal as internal reducing agents in the production of red glass (see next paragraphs) may result in a variation of the chemical composition of the base glass toward plant ash and may also explain the intermediated composition between natron and plant ash glass evidenced in orange glasses PN AV1 and BFAV1. The two orange samples (BF-AV1 and PN-AV1) however show an uncommon composition and do not correspond to natron or plant ash glasses: when examined in their original composition, their potash and magnesia content allow to include them in natron glasses, while when examined in their reduced composition, they fall in the gap between natron and plant ash; BF AV1 and PN AV1 samples contain a very high lead content and low silica and when the "reduced" composition is considered (see tab. 5.5), lime and alumina become incredibly high so that, when compared to vessels glass composition of Roman and Byzantine times, these two samples appear have no direct comparisons.

It is possible to consider the possibility that these orange tesserae were produced starting from a specific primary batch where lead acts as network former and flux, rather than adding colouring elements to a base natron or plant ash glass.

Label	*SiO2*	*Na2O*	*CaO*	*Al2O3*	*K2O*	*Fe2O3*	*MgO*	*TiO2*	*P2O5*	*SO3*	*Cl*
BF AV1	37.27	7.14	7.30	3.87	0.87	2.73	1.31	0.37	0.35	0.16	0.38
*BF AV1 **	*60.84*	*11.65*	*11.82*	*6.32*	*1.41*	*4.42*	*2.14*	*0.61*	*0.58*	*0.26*	*0.62*
PN AV1	41.67	10.03	6.29	2.65	0.85	1.99	1.35	0.24	0.43	0.33	0.74
*PN AV1 **	*63.24*	*15.23*	*9.45*	*4.02*	*1.27*	*2.99*	*2.05*	*0.35*	*0.66*	*0.49*	*1.12*

Tab.5.5: original and reduced (marked with a star) composition of orange high-lead samples from Aquileia (BF AV1) and Pordenone (PN AV1). Intentionally added elements, such as MnO, SnO2, PbO, Sb2O3, ZnO and CuO are not reported.

Differently, the high lead sample PN AV2 in its reduced composition is consistent with a natron glass, therefore it is possible to hypothesised that it was produced with a natron glass additioned with lead and colouring/reducing agents.

On the basis of the chemical composition, the majority of tesserae are produced with silica-soda-lime glasses, a small part is represented by silica-soda-lead glasses and only a few samples are lead glasses. The use of different base glasses seems to be related with the colour of the tesserae: orange tesserae are all produced with lead-glass and silica-soda lead glass, suggesting that high lead content represents an essential condition for developing the orange colour. Similarly, yellow and green tesserae are produced with silica-soda-lead glass and lead glass, and not with silica soda-lime glass (with the exception of the semiopaque band of sample PN GSO2), suggesting that some lead is necessary to develop these colours. Brown glass on the contrary is produced with silica-soda-lead and silica soda lime glass but not with lead glass, indicating that the role of lead is not necessary in the development of the brown colour. Blue and turquoise tesserae are produced with silica-soda-lime glass, as colourless ones with only one exception of a turquoise tesserae.

Comparison of the analysed samples with reference group reported in the literature for both Roman and Late Antique vessels glass were made, but clear indications were obtained only in the case of transparent and translucent tesserae: the transparent tesserae are described in the next paragraph, while the translucent tesserae are here discussed: TN B1 is consistent with a Roman glass and, due to the contemporary presence of manganese and antimony can be considered as a recycled glass, similarly to the FC colourless3 discussed in Chapter4; The turquoise BF TUTR1, being characterised by elevated manganese in absence of detectable antimony, can be considered as produced with a manganese decoloured glass of Roman composition; the two translucent dark green tesserae PN VTR1,2 show both decolourisers and are probably recycled glasses.
The majority of the samples examined in their reduced composition are consistent with a Roman composition; some samples from Aquileia, as already evidence in the previous section, have a tendency to a different magnesia/potash ratio with respect to the majority of the tesserae and the evidence is maintained when the reduced composition is considered. Those samples have also a tendency to elevated soda, and variable alumina. It is possible that these glasses derive from the mixing of glass of different composition, referable to the Roman times and possibly to the Late Antiquity: the elevated content of sodium, the tendency to slightly higher titanium and the elevated magnesium might be a sign of the presence of some HIMT glass in the batch, although a clear and univocal

indication lacks; the very variable alumina content is difficult to relate to the influence of a single compositional group and other elements (iron and antimony) cannot be considered as they could be severely influenced by the addition of colouring and opacifying agents. The analytical evidences suggests that those samples are produced with the mixing of different compositions and that they differ from the majority of the samples here included. Being samples coloured and eventually opaficified with different elements, it is possible to exclude that the variation in the magnesia/potash content is influenced by the addition of a specific element or colouring/opacyfing technique.

5.1.2 COLOURLESS AND GOLD TESSERAE

- **intro**

In the present assemblages, four gold tesserae with cartellina (PN AU1,2; TN Au1; BF AU1) and four colourless tesserae (BF TRINC1,2,3 and TN TRINC1) were identified; in addition, one sample from Pordenone, named PN AG1, was wrongly interpreted as a silver tessera but it is a clear colourless tesserae with its cartellina and no metal foil and it is also here described

Colourless glass in mosaic tesserae is employed only for the production of "gold" or "silver" tesserae. These particular tesserae are produced by the application of a very thin gold or silver foil on a colourless *tesserae*. The metal foil is then covered by a thin layer of colourless glass, called "cartellina". Gold tesserae thus present a "sandwich" structure: the metal leaf is enclosed between the tesserae and cartellina (Fig 5.35-5.36)

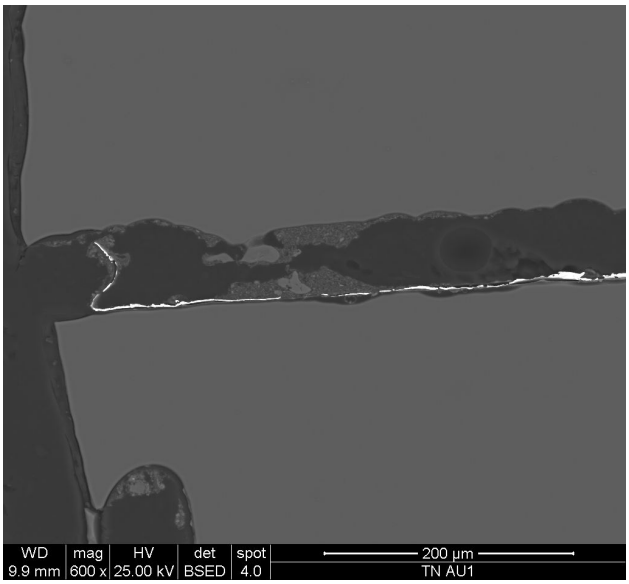

Fig5.35.: a gold tessera: the gold leaf is particularly thin

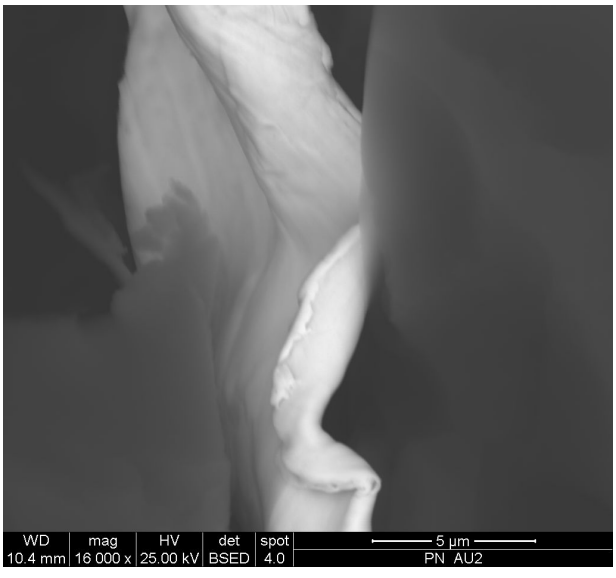

Fig.:5.36 a particular a gold foil in a "gold" tesserae from

and bright, while the glassy matrix is homogenous and characterised by a low average atomic number (grey).

pordenone, note the nanometric thickness of the metallic foil (bright layer) between cartellina (left, grey) and tesserae (right, grey)

Clear colourless tesserae recovered in tesserae assemblages probably represent gold- or silver tesserae that loose their *cartellina* and metal foil.

"Gold" tesserae are very common in Byzantine and Medieval mosaics and are known in Roman mosaic since the 1st century AD (Neri and Verità 2013). Literary sources for the ancient world do not explain what was the origin of the gold of tesserae, and the first indication is dated to the 14th century, when Cennino Cennini indicates that current coins were beated to obtain a gold leaves (Neri and Verità 2013) therefore we can hypothesise that the gold employed in Roman tesserae may come from the precious metal circulating in that period in the form of jewellery or coins. Golden coins circulating in the Roman world were constituted by almost pure gold, with low content of silver and no detectable copper, while in the coeval jewellery gold-silver copper alloys were commonly used. The alloys of Roman golden coins contained different quantities of silver, varying from less than 1% to 15%

-almost pure gold (less than 1%Ag) was mostly employed from 63 AD and then from to 253 AD

-gold-silver alloys with silver content of 1-15% were employed between 254 and 275 AD and in the 4th century AD (Neri and Verità 2013). The good match between gold foils employed in glass tesserae and coeval coins is demonstrated in a recent work by Neri (Neri and Verità 2013) analysing glass tesserae from Italy dated between the 1st and the 9th century AD.

Glass composition of gold tesserae is usually comparable with that of the coeval vessel glass (Silvestri et al. 2011; Neri and Verità 2013) and the glass composition of *tesserae* tend to correspond to that of the *cartellina*, with rare exceptions (Verità 2006).

- **Results**

The three gold samples and their *cartellina* from Pordenone (PN AU1,2 and AG1) are extremely close in composition and are characterised by a relatively high SiO2 ≈69 wt%) Al2O3≈2.25wt%, CaO≈8wt%, Fe2O3 ≈0.40wt%, no antimony and very high manganese oxide (≈1.81 with a MnO/Fe_2O_3 ratio of more than 4)

The metal leaf of PN AU1 and is constituted by pure gold.

The colourless and translucent samples from Aquileia show a very high internal variability: BF-Trinc 2 and BF-AU1/AU1_cart are very close in composition and they may derive from the same base glass, characterised by high soda (near 68wt%), low alumina (near 2wt%) lime (near 7wt%) relatively high iron (near 0.70%wt) and the contemporary presence of Mn and Sb, although not in comparable proportion. The gold leaf of sample BF AU1 is constituted by pure gold.

BF-TRINC1 conversely is a high-silica (72.42 wt%), low soda (15.73) glass with no decolouring element and low iron (0.35wt%).

Trento assemblage comprises two clear colourless tesserae (a gold *tessera* with its *cartellina* named respectively TN-AU1 and AU1cart, and clear colourless *tessera* TN-TRINC1). Chemical analysis evidenced that the two samples from Trento differ one from the other for their composition: TN AU1 and AU1cart have no intentional decolouring element and are charecterised by high SiO2≈72, Al2O3≈2.40wt%, CaO≈8wt% and low iron, with Fe2O3≈0.30wt%; differently, TN TRINC1 is characterised by high antimony (0.56wt% as Sb_2O_3) and relatively low alumina (2.10wt%), CaO= 7.20wt%, Fe2O3 =0.56 wt%; SiO2 68.04wt% and no manganese. The gold foil of TN AU1 is constituted by a gold:silver allow of approximately 95:5.

- **Discussion**

All the colourless tesserae analysed (five "gold" tesserae and four clear colourless) are silica-soda-lime in composition; in addition, the glass composition of the tesserae corresponds to that of the cartellina, indicating that the production of the tesserae and the application of gold leaf and *cartellina* took place in a single workshop and in a short period of time, so that the same base glass was employed.the composition of glassy matricesof all the present tesserae is comparable with compositional groups typical of the Roman period. In particular the three *tesserae* from Pordenone, characterised by elevated content of manganese, are consistent with a manganese decoloured Roman composition (Foster and Jackson 2010); the high manganese content (four times the iron content) indicates that it was intentionally added as a decolouriser. The very close composition of these three samples suggests that they derive from the same cake cake. The uncommon structure of sample PN AG1, which present *tesserae* and *cartellina* but no metal leaf, can be interpreted as a failed gold tessera, probably derived from the rim of the cake or an area where the

application of the gold foil failed. The gold foil of PN AU1,2 are constituted by pure gold, which is consistent with the employ of Roman golden coins as possible source.

Trento *tessera* TN AU1, showing low iron and no intentional decolouring element, is produced with a particularly pure base composition, naturally colourless. Its gold foil is made of a gold-silver alloy that indicates the probable exploitation of coins produced in the third quarter of the 3rd century or the second half of the 4th century AD (Neri and Verità 2013) therefore the production of this tessera in the 3rd century AD can be hypothesised.

Colourless TN-TRINC1 is characterised by high antimony and low alumina, no manganese and can be therefore considered a Sb-decoloured Roman glass, similar to those reported in Chapter 4 as FCcolourless1.

Samples from Aquileia show a very high internal variability: BF-Trinc 2 and BF-AU1 are very close in composition and they may derive from the same base glass, characterised by high soda, low alumina and the contemporary presence of Mn and Sb, although not in comparable proportion, indicating the recycling of glass(Silvestri et al. 2008; Foster and Jackson 2010); BF-TRINC1 conversely is a high-silica, low soda glass with no decolouring element and produced with a very pure sand, consistent with an early Roman production(Jackson 2005). BF TRINC3 resembles a manganese decoloured Roman glass. The gold foil of BF AU1 is made of pure gold, that is consistent with the use on an early Roman or a 4th century golden coin (Conventi et al. 2012); the chemical composition of the tesserae indicates that the sample is derived from recycling: the sample is a part of the "high magnesia- low potash" samples from Aquileia, that are distinguished from the large groups of the "Roman samples" for their magnesia and potash content and for their tendency to elevated soda; in addition, the contemporary presence of manganese and antimony supports the hypothesis of recycling (Silvestri et al. 2008; Foster and Jackson 2010) and it is possible that BF-AU1 was produced in the 4th century mixing different Roman and late glasses and employing a pure-gold coin.

Colourless and "gold" tesserae from Aquileia assemblage testify the use in the 4th century of different base glass of Roman and "mixed" composition, evidencing the presence of different suppliers for the glass t*esserae* of the mosaic.

5.1.3 IRON COLOURED TESSERAE

- **Introduction**

Iron is present is introduced in glass as an impurity, naturally occurring in sand. Roman glass usually is characterised by a low content of iron, between 0.30wt% and 0.70wt%, while later composition such as HIMT are characterised by elevated content of iron, even above 4%wt as those reported in the present study (Chapter 4- group AQ1a). In addition, iron can be introduced in a glass with colouring agents, as in the case of Cobalt (Gratuze et al. 1992), or it can be introduced as a reducing agent (Freestone et al. 2003) in the case of copper red glasses.

When iron is present in its oxidized state (Fe^{3+}) the glass is coloured in yellow-brownish tinge, when it is present its reduced state (Fe^{2+}) the glass results blue; usually iron in ancient glasses is present in both oxidation states, and this generates the bluish-greenish tinge that is typical of Roman glass (Foster and Jackson 2009).

Manganese in glass can act as a colouriser, in the case of purple glass, or as a decolouriser; Intentional and deliberate addition of manganese as decolouriser can be considered above 1%wt as MnO (Brems et al. 2012) and, to be effective in decolouring iron, its content must be at least double of that of iron (Silvestri et al. 2008); concentrations below 1%wt can be considered as introduced with recycling.

In the present assemblage, no manganese-coloured sample is detected.

- **Results**

Iron is present in all the samples with a wide range of concentrations, from 0.30wt% to more than 4wt%; high values of iron are detected in particular in the red, orange and brown tesserae, in some of the dark green and olive green but the largest part of the samples here included contains relatively low iron, below 1.30wt%.

Iron is the only chromoforic ion detected in the two translucent dark green (PN-V TR1 and 2) and in the yellow green from Aquileia (BF VG1) and Pordenone (PN VG1).

In PN VTR1, 2 cobalt and copper are both below detection limits while iron is high if compared to the other green samples, being respectively 1.92 and 3.06 wt%; similarly two yellow-green samples from Pordenone (PN VG1) and from Aquileia (BF VG1) contain negligible copper, no cobalt and high iron, respectively 0.93 and 1.92 wt% as Fe_2O_3.

The translucent tesserae PN-VTR1 and PN-VTR2 are particularly interesting because in absence of any other colouring ion/pigment or opacifying agent their colour is entirely due to iron that in this case generates a beautiful peacock green, usually due to copper in plant ash glasses. The presence of Fe^{3+} in these two (PN VTR 1,2) was checked with Electronic Paramagnetic Resonance (EPR) (fig.5.3) Fe^{3+} signal is represented by a small shoulder at 500G and a narrow line at 1600G (red arrows) and the while the broad line between 3000 and 4000 G (purple broken line) is related to the presence of Mn^{2+}: the strong signal of manganese, present in very high concentration, is reflects in the transformation of the sextet of small lines into a broad line (purple broken line). No signal of Cu^{2+} was identified, confirmed.

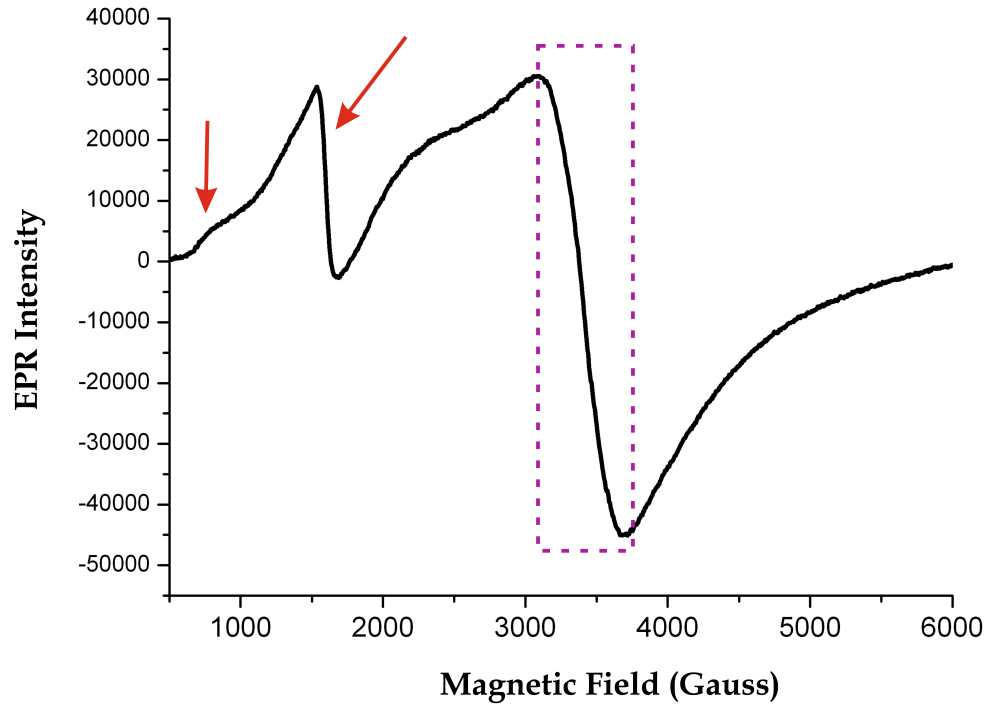

Fig.5.3: EPR spectrum of sample PN VTR1, equivalent to that of PN VTR2: red arrows indicate the line referable to Fe^{3+}, while the broken purple line delimitate the broad line corresponding to Mn^{2+}.no signal of Cu^{2+} is present.

5.1.2.2. COBALT COLOURED

- **Intro**

Cobalt has been used for colouring glass since the Bronze Age (Nicholson et al. 1997; Tite 2003) and is has been continuously employed throughout the Roman, Byzantine and medieval times (Gratuze et al. 1992; Henderson 2000; Tite 2003).

Cobalt-coloured tesserae are frequently recorded in Roman, late Roman and Byzantine mosaics (Arletti et al. 2010; Gliozzo et al. 2012; Schibille et al. 2012; Silvestri et al. 2014b)
Its colouring power is quite strong if compared to all the other chromoforic ions employed in Antiquity (iron, copper and manganese): a few hundreds ppm can impart an intense blue colour to the glass (Bamford 1977). The origin of cobalt employed in glassmaking was extensively studied in the past decades (Gratuze et al. 1992; Shortland et al. 2006; Shortland et al. 2007).
The most common cobalt-bearing minerals are trianite ($2CoO•2CuO•6H_2O$), skutterudite $(Co,Fe,Ni)As_3$ and cobaltite CoAsS, can also contain considerable amounts of copper, iron and nickel; in addition, Co-bearing minerals are usually found in high temperature hydrothermal deposits, in associations with other sulphides of iron, zinc, antimony and lead and they can therefore introduce these elements in the glass.

- **Results**

Cobalt is present above the detection limits of EPMA in 10 on 13 blue (B and BO) and pale blue (AZ) samples from the three site. In samples BF AZ1, AZ5 and TN AZ1 the presence of cobalt, expected on the basis of their macroscopic colour but not detectable in EPMA was checked and confirmed with Optic-Fibre Reflectance Spectrometry (FORS) (see fig.: 5.4) In detail, it was found in the samples of the chromatic groups "azure" (AZ BF1-2,3,4,5 PN AZ1-2; TN AZ1-2) and "blue" (BF B1; PN BO1, TN B1, TN BO1).

Fig. 5.4: reflectance spectrum of azure sample BF AZ2.

Most of the samples are intentionally opacified, with the only exception of a blue translucent (TN-B1) and an azure (PN AZ2) sample that is semi-opaque with tin stripes where opacifiers are more concentrated.

Examining the chemical composition of the *tesserae,* we can see that the "azure" (AZ) samples contain low levels of cobalt, generally between 0.03 and 0.09wt%, while "blue" (B and BO) samples contain higher values, between 0.08 and 0.17 wt%; an exception is constituted by sample PN AZ2, which contains elevated cobalt (0.19wt%). Colour saturation is also related to other factors that will be discussed in the next paragraphs.

Co-coloured samples generally contain also copper oxide in variable ranges, generally from 0.04wt to 0.15wt %, while in sample BF AZ2 it is slightly higher (0.38wt% as CuO).

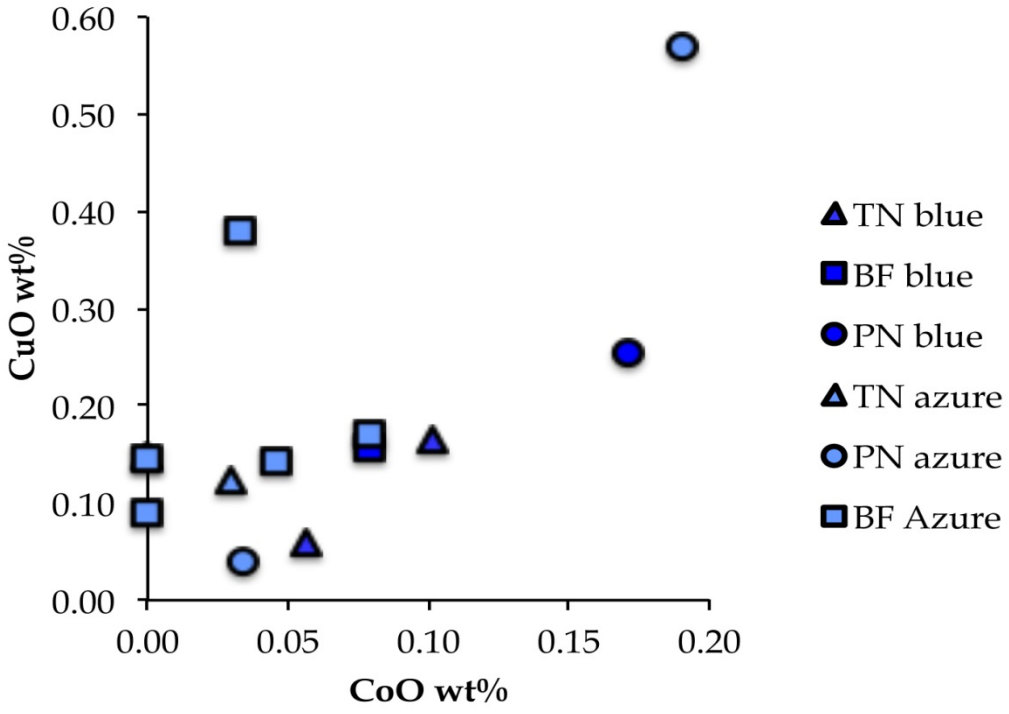

Fig. 5.6: Binary diagram copper versus cobalt in the azure and blue tesserae; only a slight positive trend between the two elements is present in some samples.

Zinc and tin are always below detection limits, apart from one sample (TN BO1) where SnO is equal to the detection limit. Lead when present is in low concentration (below 0.3wt% as PbO in almost all the sample here included) and it is below detection limits in two azure tesserae from Pordenone (PN AZ1 and 2) and in two blue tesserae from Trento (TN B1 and TN BO1). Antimony is generally present in high concentration, above 0.70wt%

in all the samples with a maximum of 6.39wt% in the translucent blue t*esserae* TN B1 antimony is below detection limits. Iron oxide shows a wide range of concentrations and is generally not correlated to the cobalt content (Fig 5.3) although a positive trend among some samples can be evidenced

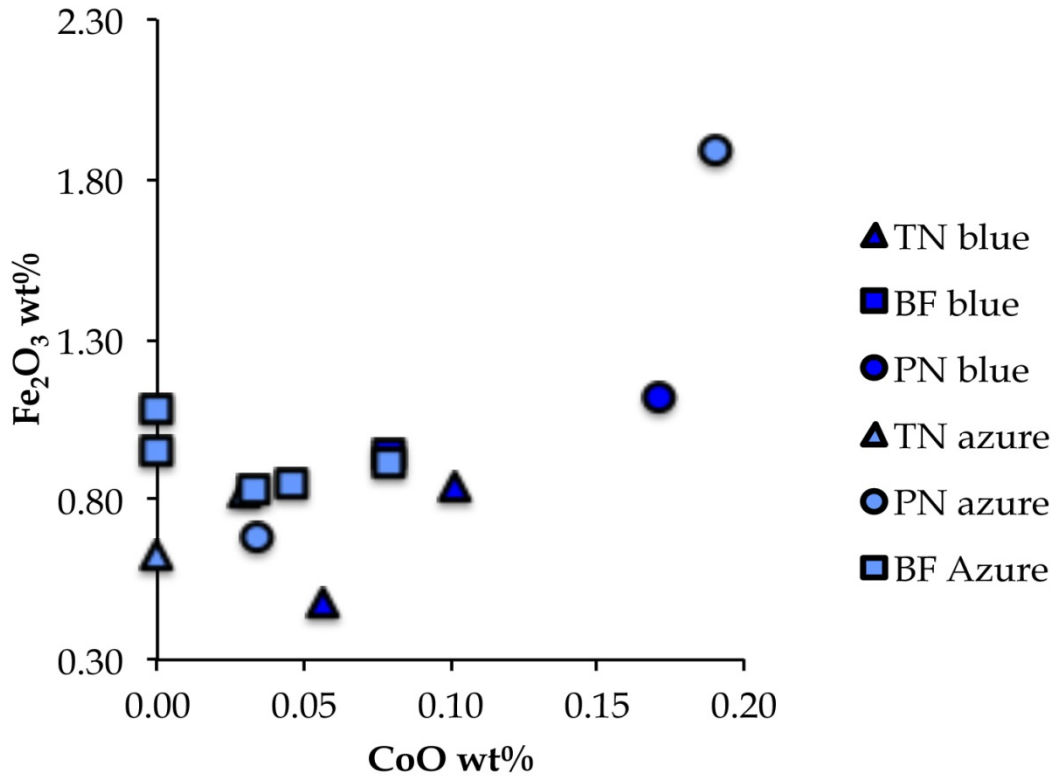

Fig 5.5. : binary diagram iron versus cobalt of the azure and blue Co-coloured tesserae. Only some tesserae show a positive trend among the two elements.

- **Discussion**

Cobalt is responsible for the blue colour of blue (BO-B) and azure (AZ) tesserae BF AZ12,3,4,5; PN AZ1,2; AZ2, TNB1, TN AZ1,2; BF B1, PN BO1. Cobalt-coloured glass here considered show relatively high iron that in some cases seems to be correlated with cobalt, although a good correlation lacks fig (5.3); copper was also detected in all the samples in variable content but the low colouring power of this element suggests that cobalt is the main responsible for the colour. On the contrary, the relatively high copper contents of the azure samples PN-AZ1 and BF-AZ2 suggest the possibility of an intentional addition or,

more probably, recycling of different glasses: given the elevated colouring power of cobalt, copper was unnecessary and therefore economically not worthwhile.

In the azure samples here investigated copper and cobalt are not correlated, suggesting the possibility that they derive from different sources. Differently, in the four blue samples TN

B1, TN BO1, PN BO1 and BF B1, cobalt and copper are positively correlated with R^2=0.89, suggesting that they derive from the cobalt-bearing mineral (FIG.5.48).

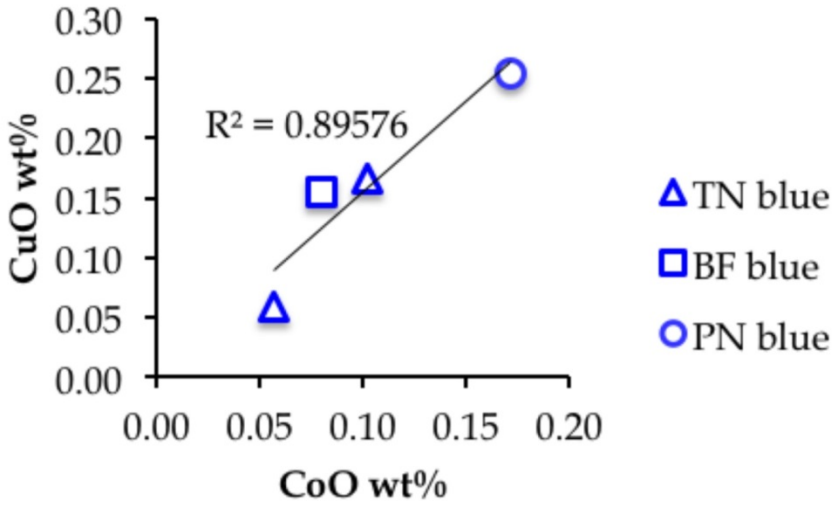

Fig. 5.48 *: binary plot CuO/CoO of the blue samples (chromatic groups B and BO). Not the positive correlation between the two elements, indicating a probable common origin of the two elements.*

The contemporary presence of cobalt and copper in the glassy matrix of blue glass is very common, and may be explained by the exploitation of a Co-Cu mineral, such as trianite ($2CoO•2CuO•6H_2O$) but unfortunately, further hypothesis about the Co-bearing mineral- or mineralogical association- cannot be formulated: trace elements data are not available and the presence of lead and antimony in the present assemblage may be related to the opacification process rather than to the cobalt ore; most of the tesserae have Ca-antimonates as opacifiers in variable quantity, and lead is often employed to help the formation of opacyfing crystals; manganese may also be introduced with the cobalt mineral and may provide information about the cobalt ore, but when considering Roman and Byzantine glass showing elevate content of this element, manganese cannot be taken in consideration, as it was widely employed as decolouriser of glass (Jacson 2005) and might have been introduce in the glass in different way including recycling.

Despite the remarked difficulties in interpreting the cobalt coloured samples, some information about the production technology of the glass can be desumed: the two azure

samples from Pordenone (PNAZ1 opaque and PN AZ2 partly opacified with Ca-antimonate) do not contain detectable lead, indicating that these two samples were produced with a different technological choice from the samples from Aquileia and Trento.

5.1.2.3 COPPER COLOURED

The majority of the tesserae here included due their colour to copper ions (turquoise) or copper compounds (red). Due to the different physical phenomena involved in the formation of colour, and the different technologies required for their production, the two cases are trated separately

Turquoise copper coloured

- **Intro**

Copper was employed to colour glass and glazes since Bronze Age (Tite 2003) and was detected in beads, vessels and mosaic tesserae from Bronze Age to the Middle Age in both opaque and translucent glass (Arletti, Maiorano, Ferrari, Vezzalini, & Quartieri, 2010; Gliozzo et al., 2012; Ruffini, Fiori, & Vandini, 1999a; Silvestri, Tonietto, D'Acapito, et al., 2012 and references therein).

The final colour of the Cu-coloured glass is influenced by the absolute content of copper, the oxidation state of the ions and the presence, quantity, dimension and distribution of opacifying crystals. The colouring power of copper is lower with respect to that of cobalt (Mirti et al. 2002): several thousands of ppm are required to colour the glass, while in the case of cobalt, few hundreds are sufficient.

Copper in the form of ions can be present in a glass in two oxidation states: Cu^{2+}, turquoise, and Cu^{1+}, colourless, (Bamford 1977) therefore the colour of the glass is not only a direct consequence of the absolute content of copper: oxidation state, that changes with the firing conditions, may also modify the final colour.

Copper employed in glass colouring can derive from different sources: copper ore such as chalcocite or covellite were probably employed, but also bronze, brass and metalworking scraps have been often suggested. The use of metalworking scraps as possible copper sources would cause the unintentional introduction of tin and/or zinc (Freestone and Stapleton 2003), therefore when copper-tin alloys such as bronze are employed as copper source, a direct correlation between the two element and an approximate ratio SnO:CuO of 1:10 are expected.

- **Results**

Copper, in absence of detectable cobalt, is detected in a large number of tesserae (n=41) of the chromatic groups Turquoise (TU and TU TR), Aquamarine (AQ), Pale Blue (CE), Pale green (VCH), Green (VP), Deep Green (VS), Yellow-Green (VG), and Dark Blue (BS) Olive green (V OL); Copper content in the tesserae here included is very variable, ranging from a minimum of 0.42 wt% to a maximum of 5.07 wt%. Examining the green and turquoise copper-coloured tesserae**,** a general trend is evidenced: paler tinges such as pale green and pale blue tend to lower values of copper, while darker tinges as Turquoise, Aquamarine, Dark Blue, Green and Dark Green tend to have higher values, above 1wt% as CuO.
Pale green tesserae (VCH) have low CuO content, generally comprised between 0.40wt% and 0.80wt%, with the exception of TN VCH1, which colour is more intense that the others and the copper content is indeed higher and equals 2.84%wt, its colour, very pale on the external surface, tends to turquoise on the fresh cut. Pale blue (CE) tesserae have variable content of copper oxide that is comprised between 0.86 and 2.70wt%. Turquoise (TU) and aquamarine (AQ) have comparable elevated copper content, but in turquoise samples, that show a very intense colour, copper is above 1.5wt% and in some cases it reaches 4%wt. The only exception is represented by the only translucent turquoise tessera BF-TU TR1 from Aquileia, where copper content is very low (1%wt).

Green samples (VP) dark green samples (VS) and olive green (TN VOL2) have elevated content of copper, generally comprised between 1.40%wt and 3wt%; the translucent BF VS1 and the green PN VP1have lower content of copper, respectively 0.90 and 1wt%.

The translucent tesserae BF VS1 is dark green but, in absence of opacifiers, the green colour is probably also due to the presence of elevated iron (1.42wt%). Yellow-green samples (VG) from Trento are characterised by the presence of CuO (respectively 0.59 and 0.89wt%) and very high iron, around 1.50wt%.

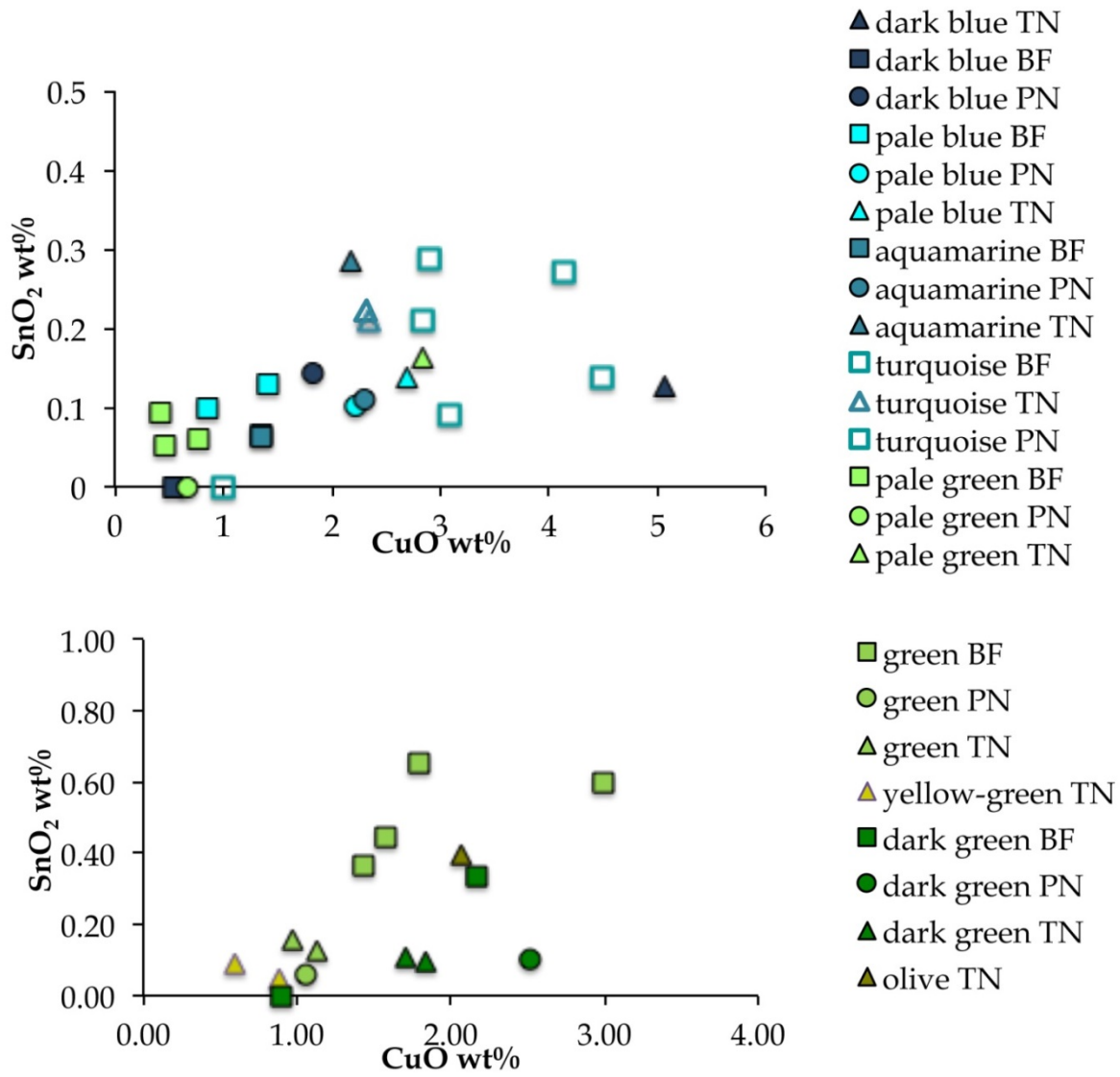

Fig. 5. 7 *binary diagram CuO /SnO2 of copper coloured samples, organised on the base of their apparent colour* ***(a)*** *above: turquoise, dark blue, pale blue, aquamarine* ***(b)*** *below: green, dark green, pale green, olive green.*

The three dark blue, translucent tesserae (BF-BS1, PN BS1 and TN BS1) are coloured by copper in variable amount: in BF-BS1 CuO equals 0.55wt%, in PN-BS1 is 1.67wt% and in TN-BS1 is 5.07wt%. In the deep blue tesserae, the variable quantity of copper is proportional to the intensity of the colour.

Tin is present in almost all the samples in concentration between 0.06 and 0.29wt% as SnO_2; only in a few tesserae, tin oxide is below detection limits: a pale green (PN-V CH1), a translucent turquoise (BF-TU TR1), a translucent dark blue (BF BS1) and a dark green (BF-VS1) (fog 5.7 a-b); conversely, in five tesserae from the Bestie Ferite assemblage tin is present in higher concentration (fig 5.7-b): they are respectively three green tesserae (BF-VP1,2 and 3) and a dark green one (BF-VS2) where SnO_2 ranges between 0.33 and 0.65wt%

(Tab 5.2). Tin is generally positively linked to copper, although a good linear correlation is absent (Fig. 5.7 a-b).

Zinc is generally below detection limits, with a few exceptions: three turquoise samples (BF TU1, PN TU1 and PN TU2) and a dark green (BF VS1) where zinc ranges from 0.06 to 0.33wt%. No sample from Trento contains zinc in the glassy matrix. (table 5.2)

Lead is generally present in variable concentration that ranges from the minimum detectable of 0.08 wt% to a maximum of 8.81wt%. In some tesserae PbO is below detection limits: they are the pale green BF-V CH2 and PN-VCH-1, the translucent turquoise BF TUTR1, the translucent dark blue (BF BS1) and the dark green BF VS1 and TN VS1 (Tab.5.2). A part from the above exceptions, a general trend is evidenced in the content of lead with respect to colour: dark blue, pale blue, turquoise, pale green, aquamarine show lower levels of lead generally below 0.5 wt%, while deep green and green have higher content of lead oxide, generally above 3 wt% (Fig.5.8).

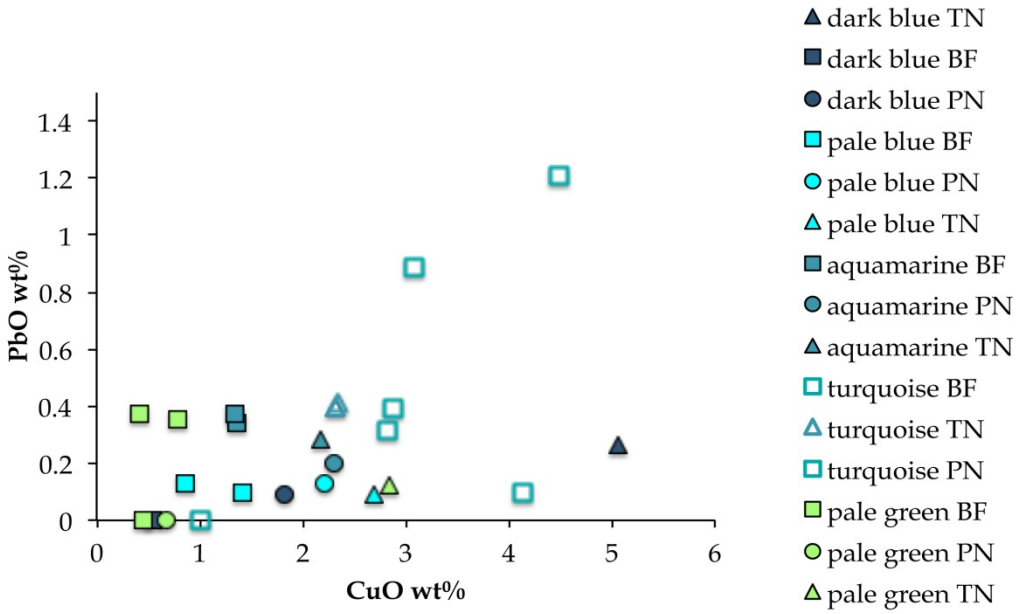

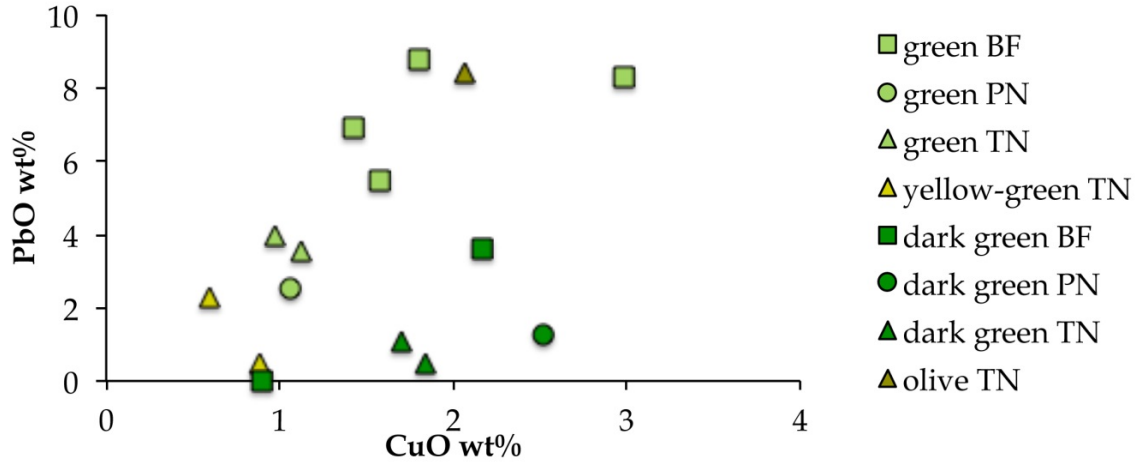

Fig.5.8*: binary plot PbO/CuO of the copper coloured tesserae: (a) above: turquoise (b): below: green*

Lead is positively correlated only in some samples of the green and yellow-green colour, that are coloured by copper and opacified by lead compounds (lead-stannate and lead antimonate)

Antimony is very variable, generally from a minimum of 0.06 wt% to a maximum of 6.39 wt% although in some samples of the Bestie Ferite (pale green BF VCH1 and 2, pale blue BF-CE2 and the translucent turquoise BF-TUTR1, dark green BF VS1,2; aquamarine BF AQ1,2; green BF VP1,4) it is below detection limits.

- **Discussion**

Copper is responsible for the colour of the glassy matrix of the dark blue translucent tesserae (BS), turquoise (TU and TU TR), aquamarine (AQ), pale blue (CE), pale green (VCH), green (VP), dark green (VS) and olive TN VOL2. Olive/red tesserae (TN VOL1 and PN M3) contain copper in the form of ions in the green part, and copper-rich particles in the red bands and are discussed in the copper-red section; yellow green from Trento (VG) are coloured by copper in association with iron.

On the basis of their copper content and the presence, abundance and quality of opacifiers it is possible to state that dark blue translucent (BS), aquamarine (AQ), turquoise (TU), pale blue (CE) and pale green (VCH) tesserae represent different shade of turquoise, their differences being mainly due to the copper content and the eventual presence of opacifiers as Ca-antimonates or quartz and bubbles.

The colour of green (VP), dark green (VS) and yellow-green (VG) tesserae is also strongly influenced by the presence, quantity and distribution of yellow pigments.

The addition of opacifying crystals aids opacity and modifies the colour: in the case of white opacifiers (Ca-antimonates or quartz and bubbles) into a paler shade of turquoise, in the case of yellow opacifiers (lead, tin and/antimony oxides) into a bright green hue. Exception are translucent tesserae BF-VS1 and yellow-green samples from Trento (TN VG1-2) which are coloured by high content of copper and probably also iron: in absence of yellow pigments, if copper was the only chromophoric ion present the glass would result turquoise; it is therefore possible that the high iron content has an active colouring effect, introducing a slight yellow ting (typical of Fe^{3+} ions) or more probably a green tinge (in the case of the co-presence of Fe^{2+} and Fe^{3+}).

Ca-antimonates are very effective opacifiers, and they white colour of the pigment strongly affects the hue of the glass, while quartz and bubbles are less effective as their refractive index is closer to that of glass, and also their "whitening" power is less strong. Therefore, comparable quantities of copper can develop different shades of turquoise in a glass that is opacified with Ca-antimonates or with quartz and bubbles; in addition, when a translucent glass is coloured, a low quantity of copper can impart an intense turquoise colour, and this explains the low copper content of dark blue translucent BF BS1 that is comparable or even lower to that of pale green tesserae BF VCH1,2,3.

Copper-coloured tesserae generally present some tin, but elevated contents are identified in green samples opacified with tin-based compounds such as lead stannate (BF VP1-2-3-4 and BF VS2). In three copper coloured tesserae (BF-BS1, PN-VCH1, BF-TU TR1, BF-VS1) tin results below detection limits. Zinc is present is very few tesserae: BF TU1, BF VS1 (translucent) and PN TU2-3, which also contain elevated copper and tin; an exception is represented by the deep green translucent BF-VS1 that contain relatively low copper and relatively high zinc but no tin.

When evaluating the tin content and the copper/tin ratio of opaque glass, the presence of opacifing phases must be taken into account: the eventual precipitation of lead-antimony-tin oxides may have caused a significant depletion of tin in the glassy matrix resulting in a bigger Cu/Sn ratio, as in the Trento green and dark green samples; similarly, the addition of high quantity of tin and lead (or tin-lead compound) as in samples BF-VP1,2,3,4 and BF-

VS2, may have introduced more tin in the melt, decreasing the Cu/Sn ratio, therefore the source of copper employed in green and deep green samples opacified by tin compounds cannot be speculated.

Excluding the green glasses opacified by lead stannate, in all the other copper-coloured tesserae, tin and zinc may have been introduced with the copper-bearing compound, such hypothesis being reinforced by the presence of a positive trend between CuO and SnO content evidenced in fig.5.4.

Examining the origin of the copper employed, the tesserae here investigated clearly constitute a heterogeneous assemblage, and only a few of them (the pale blue BF CE1-2, the pale green BF VCH2-3, the turquoise TN TU1-3 and PN TU1, the aquamarine TN AQ1) show a copper/tin ratio, comprised between 9 and 13 that is in some way consistent with bronze addition; in all the other samples copper/tin ratio is too big, indicating that different sources of copper and tin were employed.

Zinc is present in detectable concentration only in a few tesserae characterised by elevated copper and tin (BF TU1, PN TU2-3) as already evidenced in the Roman assemblage of Ascoli Satriano (Gliozzo et al. 2012) and it is also probably derived from the copper-bearing material in the form of metalworking scraps. Only one tesserae (BF VS1) contains zinc in absence of detectable tin, and shows a Zn/Cu ratio below 0.4 indicating that brass was used as a copper-bearing mineral (Freestone et al. 2003).

The most reliable evidence of copper-bearing material is given by the sporadic relics of chalcocite evidenced yellow-green (TN VG2), dark green (BF VS2), pale green (BF VCH1,2) and pale blue (BF CE2); it is also to underline that the combination of more different copper-bearing materials and the mixing of different glasses cannot be excluded: as in the case of the pale green tesserae BF VCH1,2, chalcocite relics were identified and a copper/tin ratio close to that of bronze is also present, indicating that two or more different copper-rich materials were employed.

In the case of opaque tesserae coloured by copper, lead and antimony can be related with the opacyfing technique, as they were employed to produce the opacifying agents (in the case of antimony) or to help the formation of opacifying crystals (in the case of lad). Lead in addition was frequently employed in mosaic tesserae to enhance the refractive index of

the glass improving the brilliance and the "shiny" effect of the tessera. The absence of antimony in the glassy matrix of pale green BF VCH1,2 and BF-CE2 is explained by the absence of antimony based opacifiers in these tesserae, that are opacified with quartz and bubbles. The translucent tesserae BF-BS1, BF-TUTR1, BF-VS1 do not contain detectable lead and antimony, differently samples TN BS1 and PN BS1 show the presence of detectable lead and antimony, that ca suggest the use of an antimony decoloured base glass.

Opaque-red copper coloured

- **Intro**

Colouring agent in the case of red, orange and brown glass is copper that, in suitable conditions (i.e. under reducing atmosphere) precipitates in the form of cuprite or metallic copper crystals. Red and brown tesserae therefore are coloured by the presence of copper rich phases dispersed that act as pigments and opacifiers.

Such reducing conditions, necessary for the formation of copper or cuprite do not derive only from the firing atmosphere: to maximise the glass-colouring process, some other elements could be added as internal reducing agents: carbon, iron, tin, antimony and lead (Freestone 1987; SHUGAR 2000; Freestone and Stapleton 2003) in the glassy matrices are probably introduced and act as internal reducing agents to aid the development of copper-rich crystals, explaining the elevated tenors of the above elements in red glasses.

- **Results**

Copper-coloured red tesserae belong to the chromatic categories of Orange (AV), Brown/Brickred (M), sealing wax red (R) and olive/red (TNVOL1 and PNM3)

Copper in the glassy matrix of these samples is very variable, from 0.42 wt% to 14.14 wt% (table 5.2). On the basis of the copper content, tesserae here considered split in two groups: a high copper group, with CuO>5wt% and comprising all the orange samples (BF AV1, TN AV1, PN AV1 and PN AV2) and low copper group (BF M1, 2, 3 and 4; TN M1,2, 3; PN M1 and2, BF R1) which comprises al the red and brown tesserae (fig. 5.5)

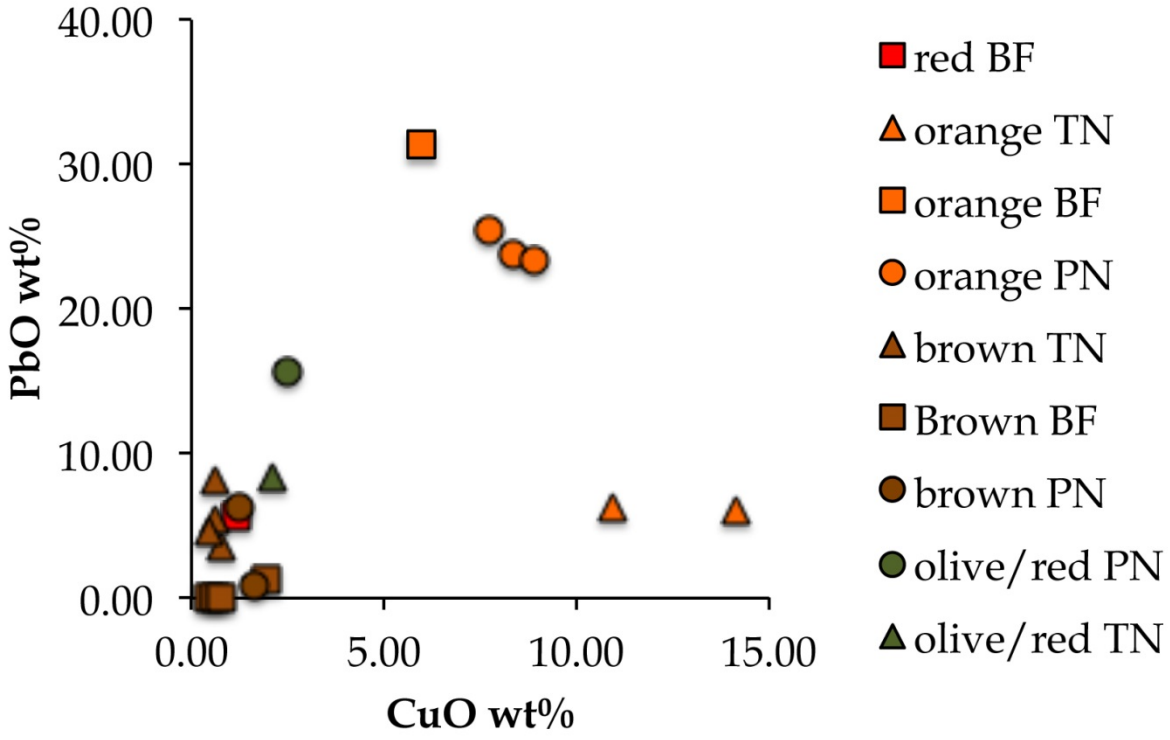

***Fig.5.8** : binary plot PbO/CuO of the copper coloured tesserae of the RED macrogroup. Olive/red striped tesserae here included are banded in copper-based red.*

In the copper-based red tesserae **tin** is generally present: its content is below 0.35wt% in the low-copper brown and red tesserae, while it is very high, around 1wt% in the high-copper orange glasses. Only in three samples from the Bestie Ferite assemblage tin is below detection limits: they are the brown BF M1,2, 4.

Zinc on the contrary is present in all the brown tesserae from Bestie Ferite and Pordenone, and almost all the orange tesserae; it is below detection limits in the three brown samples from Trento (TN M1,2 and 3) and in the only sealing wax red from Bestie Ferite (BF R1); all the orange samples contain zinc apart one from Pordenone (PN AV1).

Lead content is also very variable: very high in the orange samples from Bestie Ferite and Pordenone (PbO>20wt%), relatively high in the orange from Trento (≈6%wt) and in most of the brown and the red, and near or below detection limits in the brown tesserae from Bestie Ferite (BF M1, 2 and 4) (fig 5.8)

Antimony is present in all the samples in high concentration, generally comprised between 0.5 and 1.2wt% as Sb_2O_3 apart from three brown samples from Bestie Ferite mosaic (BF M1, 2 and 4).

Iron is also generally high, above 1wt% in every case and in some brown tesserae from Trento and Bestie Ferite it overcomes 4 wt%.

- **Discussion**

Copper in the reduced forms of cuprite or metallic copper is responsible for the colour of orange, red and brown tesserae and the copper pigments will be discussed in the next paragraphs; in the present section the glassy matrices of the copper-red tesserae are discussed. The olive-green/red striped (TN VOL1 and PN M3 tesserae and the single dark amber TN NS1 are here included.

Copper-coloured and opacified tesserae here considered are the orange samples BF AV1, TN AV1 and PN AV1,2; the single sealing wax red BF-R1; the brown BFM1,2,3, PN M1,2, , and TN M1,2,3, the olive green/red striped TN VOL1 and PN M3 and the dark amber TN NS1

As observed by other author (Freestone and Stapleton 2003), copper-red samples can be classified on the basis of their copper and lead content in two main categories: low copper low lead, up to 4%CuO and 10%PbO, and high copper high lead, with 5-12%wt CuO and 20-40% PbO.

Glass tesserae here analysed can be also grouped in high copper-high lead, which comprises all the orange tesserae (PN AV1-2, BFAV1) and low copper low lead, which comprises all the remaining red and brown tesserae. TN AV1 in on the corder, as its copper content is incredibly high (14%wt), and its lead content surprisingly low (8wt%) but it is here included in the high copper-high lead group.

Silvestri and co-authors (Silvestri et al. 2014b) porposed provide a further subdivision for Byzantine copper-red tesserae in five categories; following the same method, three sub-groups were identified:

1) High copper-very high lead: comprises the orange samples PN AV1, PN AV1, PN AV2, characterised by elevated copper, (CuO 7.74±1.28wt%) and very high lead (PbO=26.02±3.64%wt), tin (SnO=1.08±0.19), zinc (ZnO=0.16±0.03), iron and antimony in variable concentration, with only exception of sample PN AV1 where zinc is not detected.

2) Low copper-low lead: comprises red and brown tesserae BF-R1, TN-M1, TN-M2, BF-M3, TN NS1, characterised by low copper (below 2%wt), medium lead comprised between 2 and 6wt% as PbO, high although variable iron oxide (3.03 ± 1.01wt%) ti (=.19±0.08), antimony (0.64 ±0.22wt%) and no zinc.

3) Low copper-negligible lead: comprises brown tesserae BF-M1, BF-M2, BF-M4, PN M2 and olive green/striped TN VOL1, characterised by low copper (variable and below 2%) and very low lead, below1%wt; we can subdivide this groups into two further subgroups on the basis of their content of zinc, tin, iron and antimony: samples from Aquileia (BF M1,2,4) have very high iron, very low copper, some zinc, no tin, antimony and lead, while the other two tesserae have lower iron, some zinc, tin and antimony and some lead.

Four tesserae cannot be grouped according to the above method:

TN-AV1, BF M3, PN M1 and the olive green PN M3 and TN NS1 have variable copper and lead contents that do not fit in the above groups.

Elevated contents of tin (SnO 1wt%) are detected in orange samples, while in the other tesserae is generally below 0.4wt%.

Zinc is generally low, below 0.20wt% and it is absent in the Trento tesserae with the only exception of the orange sample TN AV1; The same evidence in Trento copper coloured tesserae was identified in the blu/turquoise copper based glass, indicating a different technological choice in the copper-bearing compound employed in Trento with respect to Aquileia and Pordenone.

The three natron-based brown samples from Aquileia (BF M1,2 and 4) show a specific chemical composition for their glassy matrix, characterised by high iron, zinc, no tin, no antimony, negligible lead.

5.2 OPACIFYING AGENTS

The majority of the samples here included are opacified by means of opacifying agents, generally phases that concur to both the colour and opacity of the glass. The presence of opacyfyng crystals was detected by Scanning Electron Microscopy (SEM coupled with an

EDS spectrometer for semi-quantitative analysis; XRPD diffraction was performed on the whole tesserae and, in some specific cases Raman Spectroscopy was also performed.

5.2.1 CA-ANTIMONATES

- **Introduction**

Ca-antimonates are well documented in the literature as glass opacifiers since the Bronze Age Egypt and its use continued during the Roman time until the 4th century AD (Turner and Rooksby 1959). During the Roman times antimony indeed was used as decolouriser for transparent glasses and, in the form of Ca-antimonates and Pb-antimonate, as opacifier. The use of antimony, that characterised the pre-Roman and early Roman times, decreases in the 4th century AD, when it was gradually replaced by manganese for decolouring, and by tin and phosphorus compounds in opacification. The provenance of the antimony used in glassmaking was investigated in the past and although the use of metallurgical by-product as source of antimony was hypothesised (Mass et al. 1998), in the case of Ca-antimonate, the use of stibnite or roasted stibnite is supported by experimental work (Lahlil et al. 2009; Lahlil et al. 2010) and analytical evidences (Silvestri et al. 2012a). Ca-antimonates as opacifiers in glass were produced following two methods: an *in-situ* crystallization, produced adding antimony to the batch and allowing the formation of Ca-antimonate crystals; an *ex-situ* crystallization, preparing an antimony compound and then adding it to the batch. Both procedures are accepted for Roman and Late Roman times.

Ca-antimonates in glass occurred in two stoichiometries: a rombic phase $Ca_2Sb_2O_7$ and a hexagonal phase $CaSb_2O_6$. Often the two stoichiometry co-exist, but the prevailing presence of phase or the other may indicate different conditions of firing: according to Lahlill and co-authors (Lahlil et al. 2010) the presence of both phases and hexagonal Ca-antimonate as prevailing mineralogical phase allow to hypothesize a temperature of firing close to 1100°C for one-two days: hexagonal Ca-antimonate crystallizes at 927°C at the expenses of the orthorhombic form and becomes the prevailing phase at 1094°C; the orthorhombic phase though is favoured by prolonged firing (two or more days) while hexagonal phase is favoured by elevated temperatures and relatively short firing times.

- Result

A large number of t*esserae* are opaficied by Ca-antimonates. The opacifying agents are present as abundant crystals of small dimension (5-10 **µ**m), euhedral habitus and high average atomic number, finely dispersed in the glass matrix and occasionally clustered in lumps. This kind of opacifier was detected in the majority of the tesserae of the chromatic groups opaque blue (BO), azure (AZ), turquoise (TU), aquamarine (AQ), pale blue (CE) with the exception of BF CE2, pale green (V CH), grey (GR) and white (Bi OP) from all the three sites for a total amount of 26 tesserae. Exception are some tesserae from Aquileia : all the aquamarine (BF AQ1,2) pale green (BFVCH1,2,3) azure (BF AZ1,2,3) a pale blue (BF CE1) that show a different opacifier (i.e.: quartz and bubbles) and are described elsewhere.

Despite the different opacifying technique identified (quartz+ bubbles) however samples BF AZ1,2,3 and BF VCH3 contain also some inclusions of Ca-antimonates but their low density do not allow to consider them as opacifiers.

Isolated crystals of Ca-antimonates often show hexagonal or rhombic symmetry, as shown in fig (5.9,a,b,c,d) and both symmetries are usually found in all the sample.

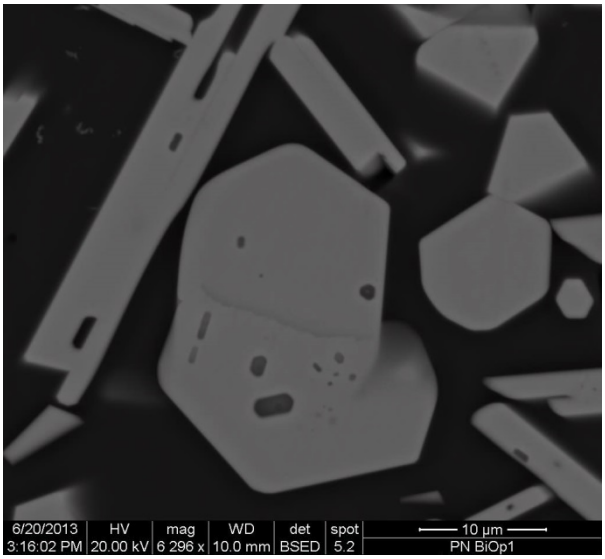

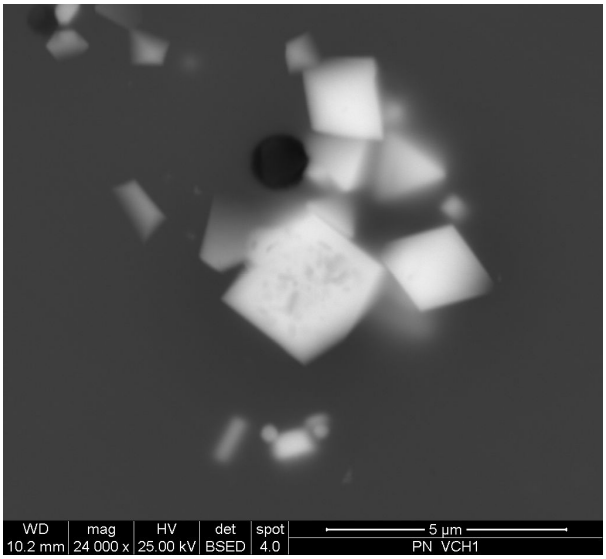

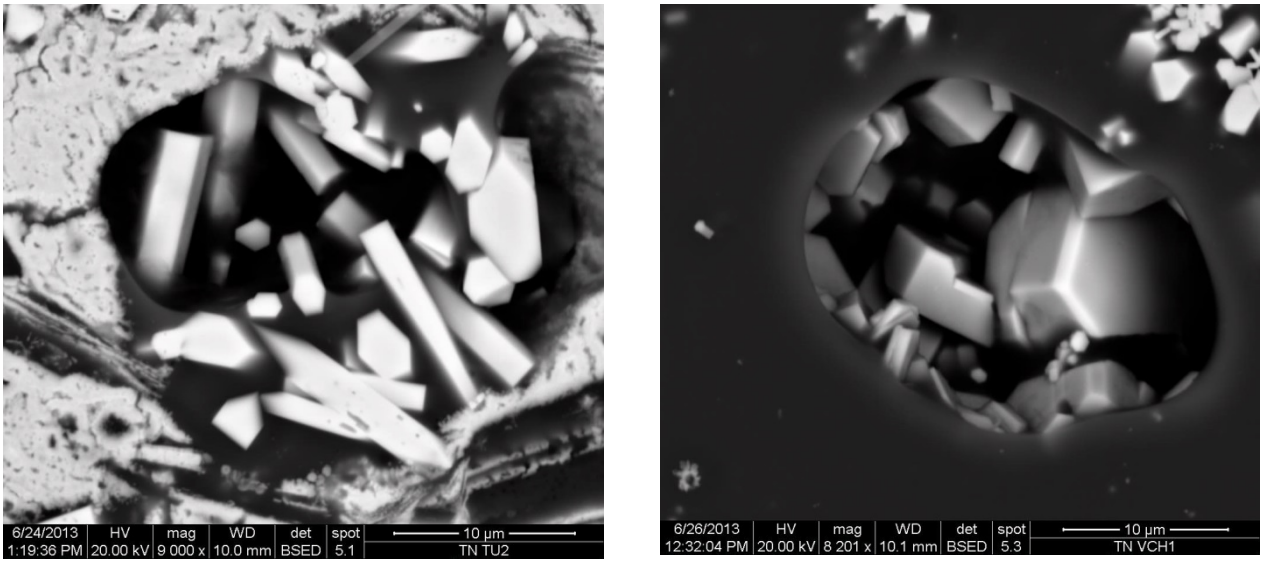

***Fig.5.9**: SEM-BSE image of Ca-antimonate crystals in **(a)** an opaque white tessera from Pordenone; **(b)** a pale green tessera from Pordenone **(c)** a turquoise from Trento and **(d)** pale green from Trento. Crystal show both hexagonal (a,c,d) and rhombic (b) symmetry.*

XRPD was performed on all the samples of suitable dimensions, but due to the low quantity of crystals, small dimension of the tesserae, uneven surface of the sample and high quantity of amorphous signal, only some sample show diffraction patterns that can be related to a crystalline phases. Full results are given in tab 5.5

	SiO_2		Ca antimonate	
sample	**quartz**	**cristobalite**	**$CaSb_2O_6$**	**$Ca_2Sb_2O_7$**
BF AZ5		X	X	?
BF CE1			X	?
BF GR1			X	X
BF TU1			X	X
PN AZ1			NO	X
PN BI OP1			X	NO
PN BO1			X	?
PN CE1			X	X
PN GR1			X	X
PN TU1			X	X
PN TU3			X	X
TN AZ2			X	NO
TN TU1			X	NO
TN VCH1			X	X

Tab 5.5.: XRPD results of samples that showed some diffraction pattern. Question marks indicates uncertain attributions: due to the presence of a single peak, although reasonable the presence of the maerked phase is not certain.

Among the Ca-antimonate opacified tesserae, samples PN BiOP1, TN AZ2 and TN TU1 evidenced only the hexagonal Ca-antimonate (general formula $CaSb_2O_6$), sample PN AZ2 evidenced only the orthorhombic Ca-antimonate ($Ca_2Sb_2O_7$) and all the others samples show the coexistence of both the hexagonal and orthorhombic forms. The absence of one of the two stoichiometries may be also related to the "detection limits" of the instrument.

In the other samples here considered (PN AZ2, BF AZ2,3,4, TN GR1,2, TN TU1,2,3, TN AQ1, TN CE1, TN BI OP1) Ca-antimonate in different concentrations was checked by means of SEM-EDS data.

The texture of Ca-antimonate opacified is variable: generally high density and homogenous distribution of small crystals characterise the samples (Fig 5.11)

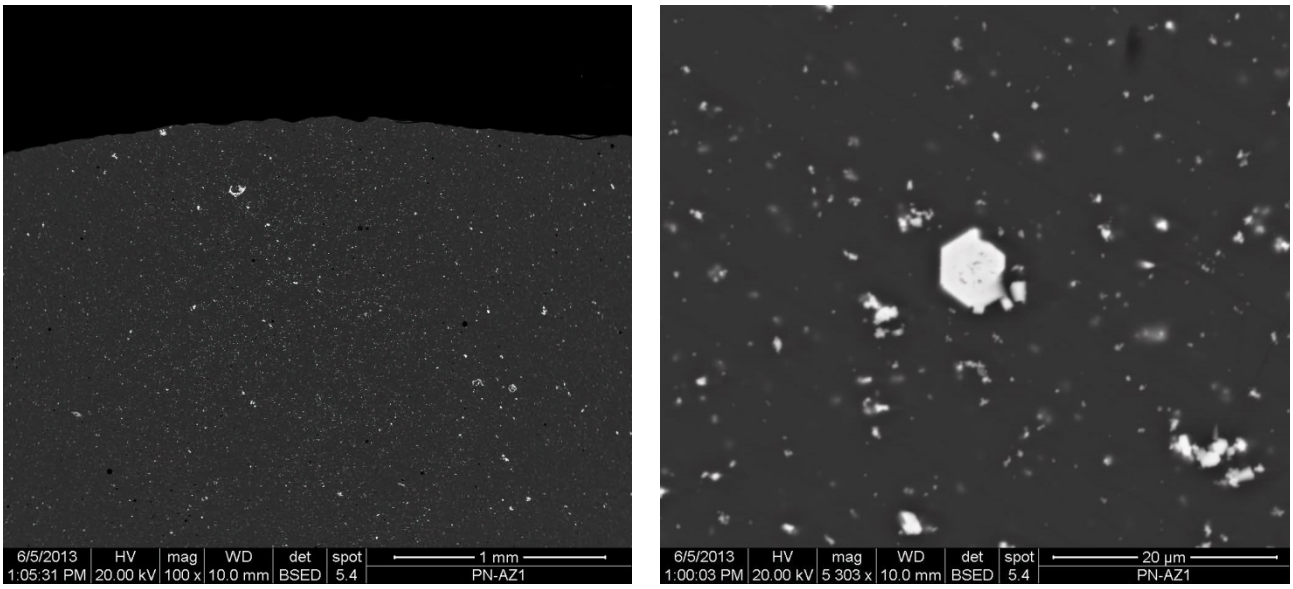

Fig. 5.11 a-b: SEM-BSE images of an azure tessera from Pordenone. Note: the homogenous distribution in virtual absence of gas bubbles (a) and the small dimension of the crystals and their euhedral habitus (b).

Some tesserae however present a zoned texture, characterised by the uneven distribution of the opacifing crystals as in the case of TN BO1, TN AZ2, TN BIOP1, TN GR1, BF GR1, BF GR2, PN AZ2 PN TU1 and PN GR1 (see *Fig. 5.12-5.13*)

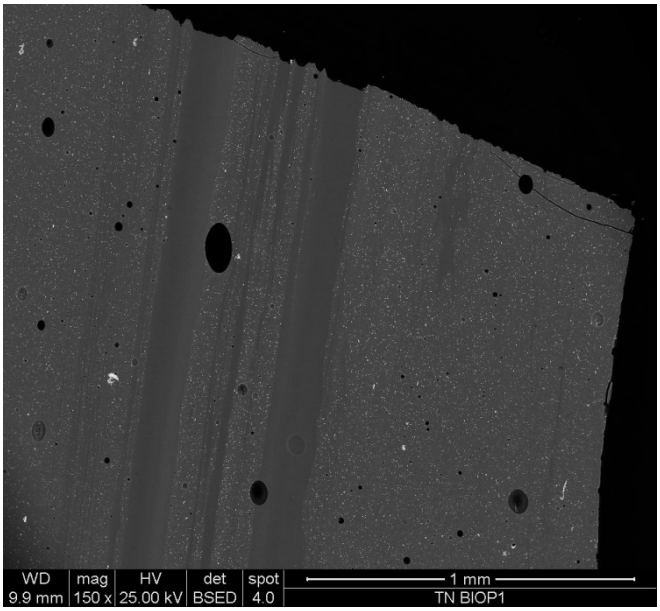

Fig. 5.12: *SEM-BSE image of an opaque white tessera from Trento: Ca-antimonate (small bright dots) are distributed not homogenously and some transparent bands are present (grey stripes). Gas bubbles are black.*

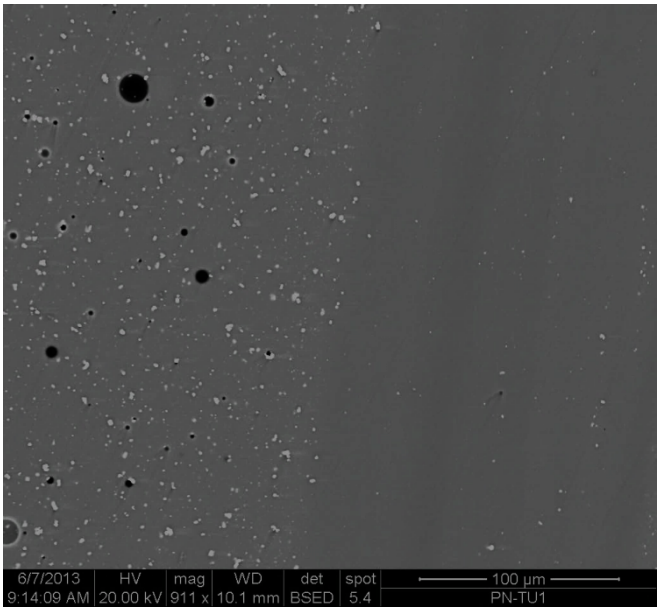

Fig 5.13 *SEM-BSE image of a turquoise sample from Pordenone. The opacified area is characterised by the presence of abundant bright crystals (left) and the transparent band (right, grey) is more homogenous*

In most of the samples, particular inclusions of large dimension, with anedral habitus of Ca-antimonate were identified (see fig.5-14 a-b-c-d), generally associated with newly formed crystals. SEM-EDS data evidence that these inclusion are mainly constituted by calcium and antimony oxides, although silica, soda and other elements of the surrounding glassy matrix are detected, and this explains the low average atomic number (medium grey) evidenced in SEM BSE picture with respect to the newly formed crystals (white).

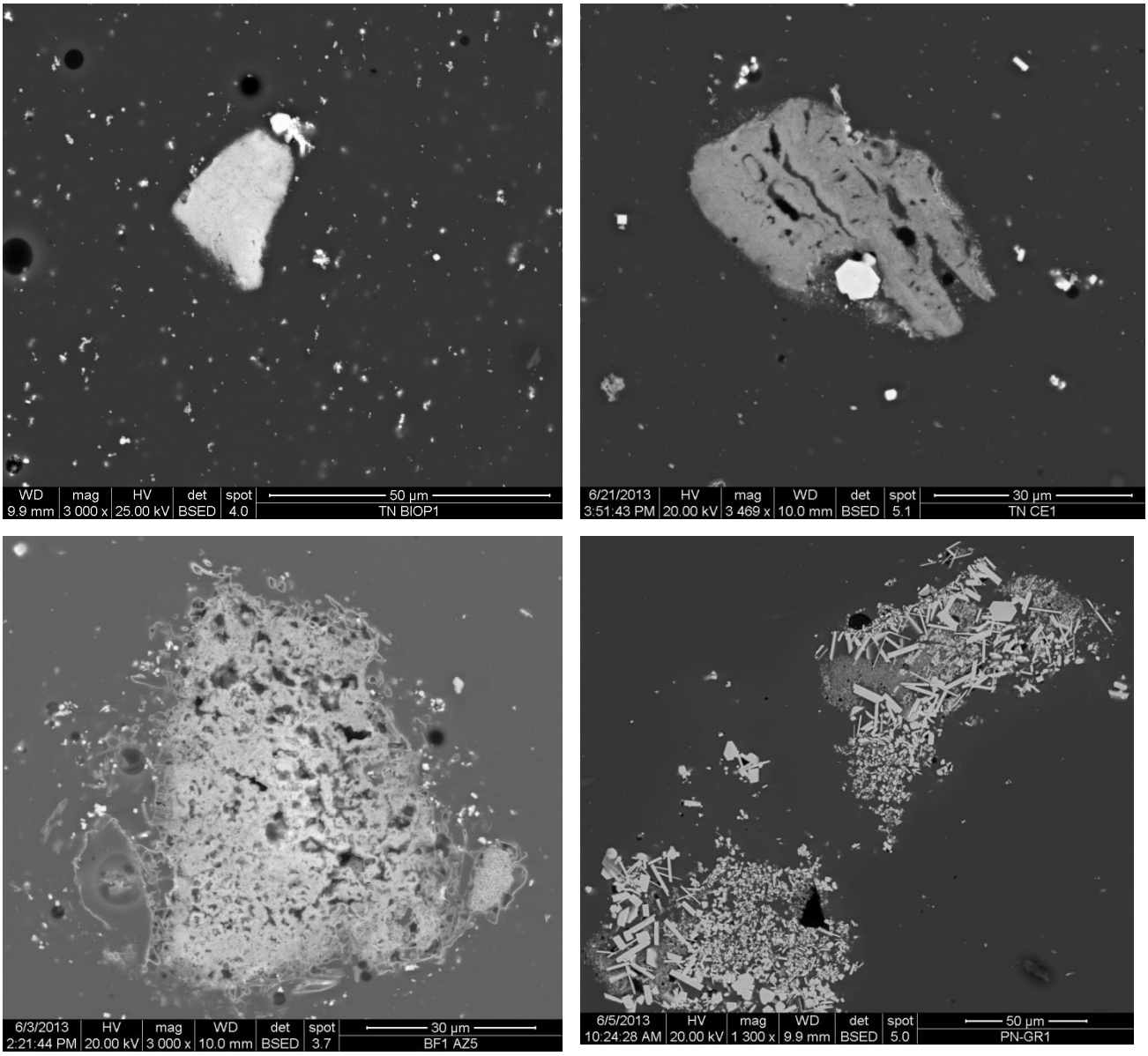

Fig. 5.15 SEM-BSE image sof relic, partly dissolved Ca-antimonate (medium grey) associated with newly formed euhedral crystalof Ca-antimonates (brighter) in ***(a)*** *white from Trento* ***(b)*** *pale blue from Trento;* ***(c)*** *azure from Aquileia* ***(d)*** *grey from Pordenone*

Such sporadic inclusions are detected in samples BF AZ4,5, BF CE1, TN BIOP1,TN CE1,TN BO1, TN GR1, PN TU1, PN CE1 and PN GR1 despite the tesserae show with newly-formed euhedral crystals. Similar inclusions are common and probably represent relics of Ca-antimonates, partly dissolved and re-crystallised.

Differently, in one tesserae from the Bestie Ferite assemblage, some relic inclusion of an antimony-rich phase were identified by SEM-EDS as apparently antimony oxide (Fig. 5.15a-b). Inclusions of this kind are relatively common in BF TU1 and represent relics from of the antimony-bearing material, probably roasted stibnite Sb_2O_3.

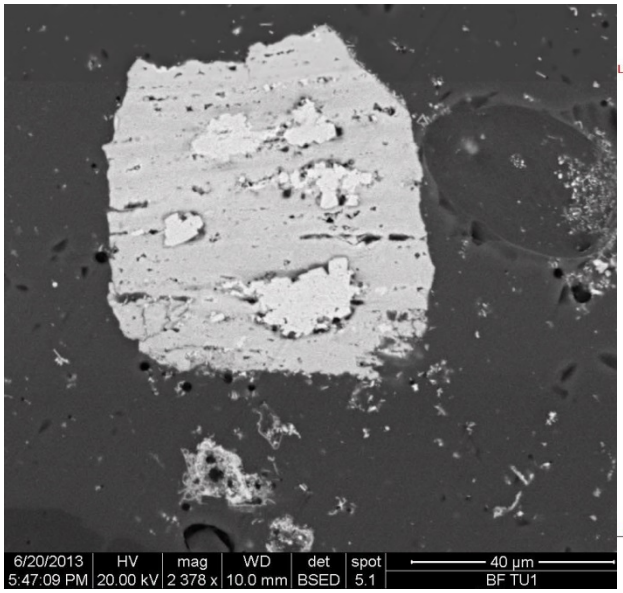

Fig 5.16 a.: SEM-BSE image of a turquoise tesserae from Aquileia: the large irregular inclusion is a relic of the Sb mineral

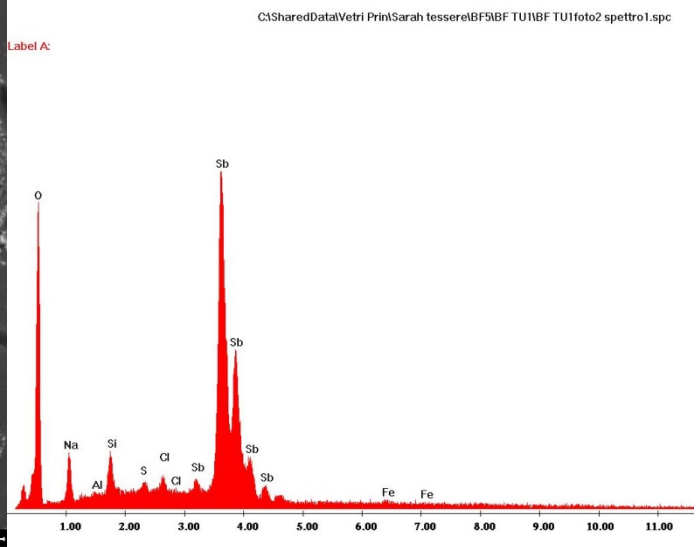

5.16 bSEM-EDS spectrum of the inclusion .point 1. Note the absence of calcium and the presence of mainly antimony and oxygen, but also sodium, silicium chlorine and sulphur probably derived from the glassy matrix

- **Discussion**

Ca-antimonates were identified as the main opacifying agents in the chromatic groups of blue, azure, turquoise, pale blue, aquamarine, pale green, grey and white, with the exception of some tesserae from Aquileia.

The presence of the two stoichiometry with a general prevalence of the hexagonal phase indicates that in most of the cases the glass was produced with a prolonged firing (1-2 days) with temperatures around 1100°C; samples PN BIOP1 and TN AZ1, TN TU1 probably were produced by a shorter firing time as the hexagonal phase is termodinamically favoured, while the rhombic phase is kinetically favoured.

Euhedral morphology and small dimensions of the opacifying phases detected in the tesserae here included seems to suggest that the crystals mainly precipitated *in-situ* from a silica-soda-lime melt where antimony was added. Distinguishing between *in-situ* and *ex-situ* crystallization however is not easy:

in many of the tesserae sporadic relic inclusions of Ca-antimonate were also detected, indicating that Ca-antimonates crystallised *ex-situ* and was subsequently added to the melt; some tesserae (TN BO1, TN AZ2 TN BIOP1, TN GR1, BF GR1, BF GR2, PN AZ2 and PN GR1) also present a uneven distribution of opacifying crystals. Some scholars suggest that in the case of in-situ crystallisation of Ca-antimonates, a depletion of calcium is expected in the glassy matrices (Shortland 2002b), while in the case of *ex-situ* crystallization, a direct proportion between calcium and antimony demonstrates that the two elements were added together as a part of the same compound. In the present assemblage however, no clear trend is evidenced and chemical data sometimes conflicts with textural examination: low-calcium tesserae present relics of Ca-antimonates, and a tendency to a positive trend between calcium and antimony lacks (see fig.); in addition, samples containing relics of Ca-antimonates do not show positive correlations between antimony and calcium.

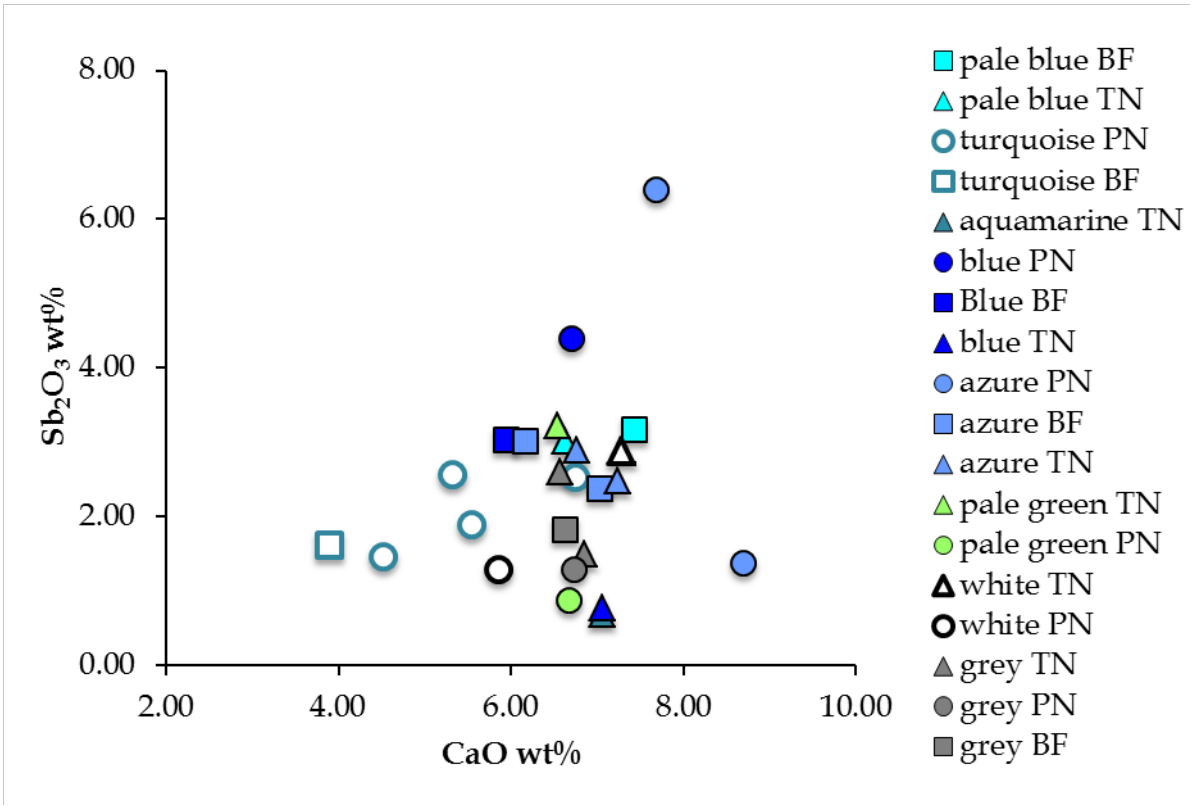

Fig.: binary plot Sb2O3/CaO of the tesserae opacified with Ca-antimonates. The absence of a neat linear correlation is evident

These evidences seem to be contrasting, but the samples here investigated clearly constitute a heterogeneous assemblage for dating, provenance and technology of

production; it is also possible that glass tesserae are a product of re-melting or the mixing of different glasses, therefore such evaluations do not give any satisfying result.

A very important textural evidence is represented by the case of BF TU1, were abundant relic of an antimony oxide were detected in association with newly formed Ca-antimonate, allowing to make inference about the source of antimony employed, in this case probably roasted stibnite Sb2O3 was probably employed as an antimony source.

The azure and pale green sample from Aquileia (BF AZ2,3,4; BF VCH3) opacified with quartz and bubbles, present also Ca-antimonates inclusions which density is too low to be effective as opacifiers; these samples are probably a product of recycling of different glasses.

5.2.2 PB-ANTIMONATE

- **Intro**

Lead-antimonate was widely used as glass opacifier from the beginning of glass production in Egypt and Mesopotania and in the Roman world until the 4th century AD, when it was replaced by tin-based opacifiers (Lahlil et al. 2011).

The mineralogical phase usually employed as yellow pigment in early glassmaking is a cubic phase with a pyrochlore structure of formula $Pb_2Sb_2O_7$ and known with the name of bindheimite. Bindheimite as a natural mineral [$Pb_2Sb_2O_6$ (O,OH)] is very rare, mostly present in weathering crusts; the only exploitable deposit of natural bindheimite in the territory of the Roman Empire is in Tunisia but no literary source neither archaeological evidence supports the trade of this mineral and its use as a pigment (Mass et al. 1998). Bindheimite employed as a colourant and opacifier in ancient glass is conversely constituted by a synthetic phase of formula $Pb_2Sb_2O_7$ produced by the combination of lead and antimony under oxidizing conditions. The origin of the lead and antimony employed in Roman glass colouring is debated and two possible sources of lead and antimony were hypothesised: lead and antimony-bearing minerals, such as stibnite and galena, or metallurgical by- products, as antimonial litarge resulting from the cupellation of silver (Mass et al. 1998; Mass et al. 2002; Shortland 2002b). The systematic use of silver extraction by-products as antimony source would explain in part the decrease of antimony use in the

4th century, as a consequence of the great decrease of silver mining in the same period, but a clear consensus on one or the other possibility does not exist yet.

The production of lead-antimonate opacified glass was extensively studied in the past decades (Mass et al. 1998; Shortland 2002a; Mass et al. 2002; Lahlil et al. 2011; Molina et al. 2014) and it is commonly accepted that the lead-antimony compound was synthesised *ex-situ* and then added to the molten glass: the evidence of uneven distribution of crystals, fluidal bands and unhomogenous chemical composition of the glassy matrices seem to support this hypothesis. The *ex-situ* synthesis of Pb-antimonates can be obtained by two main technological processes: producing a lead-antimony-silica frit, called *anime* in the later Venetian glassmaking, or calcinating lead oxide and antimony oxide(Molina et al. 2014). Previous studies (Mass et al. 1998; Molina et al. 2014) evidenced that Roman glass opacified with lead antimonate show a general higher content of silica and lower content of soda in their reduced composition with respect to the other coloured glasses and an enrichment in silica around the opacifying agents (Molina et al. 2014) and this would indicated that *anime* was employed to produce the yellow

- **Results**

Yellow samples BF-GSO1,2 ,3 from Aquileia, yellow PN-GSO1, yellow-green PN VG1, green PN-VP1 and dark green PN-VS1 from Pordenone and deep green TN VS2 from Trento are opacified with Pb-antimonate in the form of binheimite.

The opacifying phase is present in the form of abundant small crystals (1-2 **μ**m) with very high atomic number and uneven distribution in the glassy matrix that appears zoned (fig 5.17) with bands of higher atomic number; crystals are seldom clustered in lumps or "chains" (fig.5.18). SEM-EDS data acquired on the single crystals evidence the presence of Pb and Sb, together with variable although low iron (Fig.5.18b); silica and sodium, often detected by SEM-EDS analysis probably derive from the glassy matrix, but the presence of silica in the crystals is also possible.

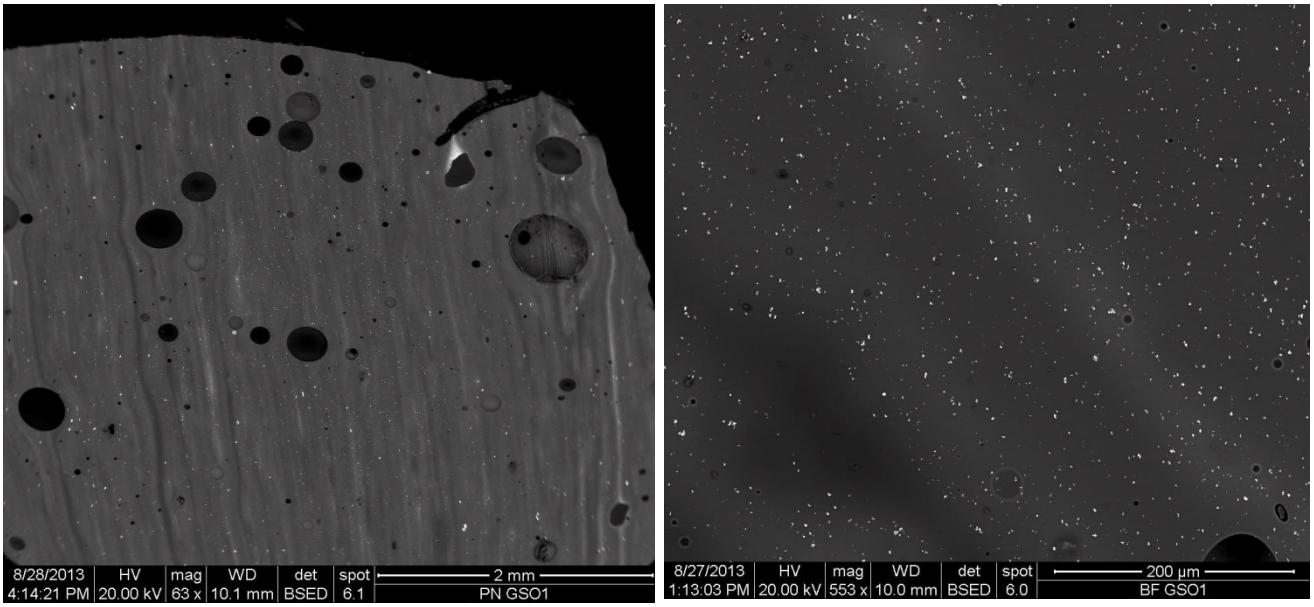

Fig. 5.17: *SEM-BSE image of yellow samples* ***(a)*** *left from Pordenone and* ***(b)*** *right: from Aquileia. The striated texture is due to thhe fifference in average atomic number of the glassy matrix (is higher in brighter areas and smaller in grey areas) and to the disomogenous distribution of opacifing crystals (bright dot)*

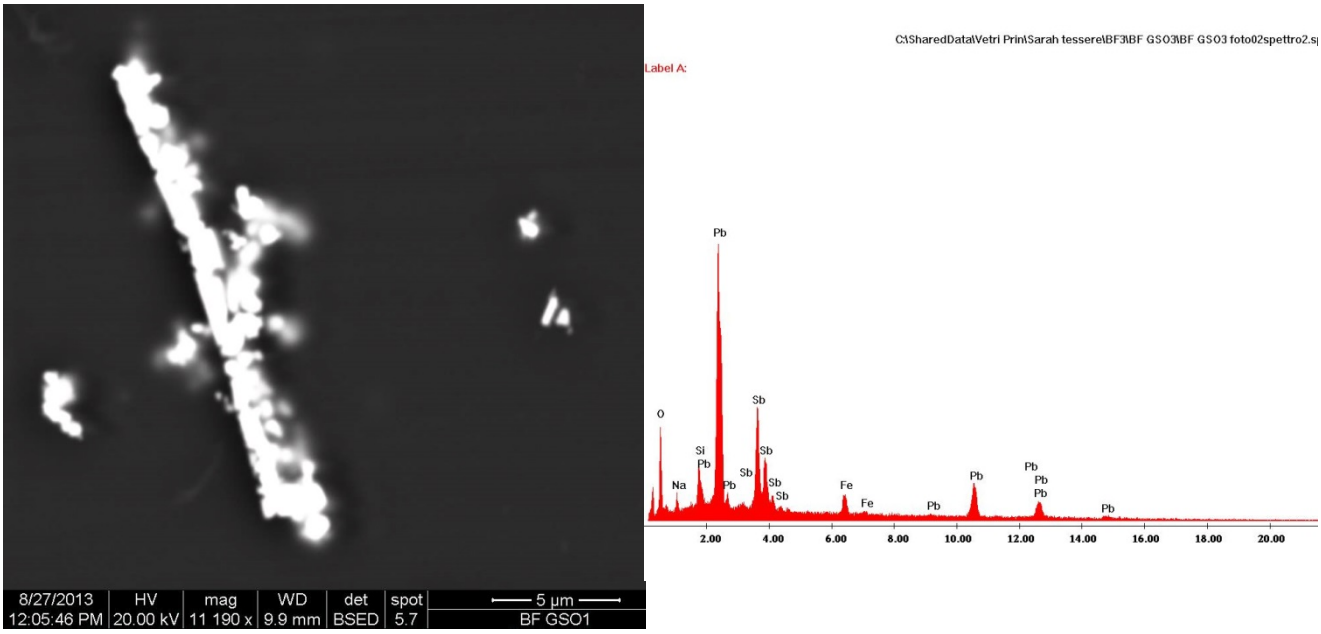

Fig.5.18 : *SEM-BSE image of lead antimonate crystals and SEM-EDS spectrum*

XRPD performed on the whole tessera confirmed the presence of Pb-antimonates in the form of anhydrous bindheimite ($Pb_2Sb_2O_{7)}$ in samples BF GSO1 and 3, TN VP1, TN VS2, PN GSO1, PN VG1 and PN VP1 while sample BF GSO2 due to the small dimension of the sample did not give any diffraction pattern. (see table)

sample	Binheimite	Pb-Sb-Sn oxide
BF GSO1	x	
BF GSO3	x	
PN GSO1	x	
PN VP1	x	
PN VG1	X	
TN VS2	x	

Table bla *XRPD results of the samples opacified with bindheimite*

- **Discussion**

In the present assemblage the yellow and green samples opacyfied with bindheimite do not show a significative difference in their silica content with respect to other colours. In addition, the systematic enrichment in silica around the opacifying particles, evidenced by Molina (Molina et al. 2014) was not observed in the here analysed samples. Silica is seldom (but not regularly) present in EDS data acquired on the singles inclusion and, due to very small dimension of the crystals, it is possible that it derive from the surrounding matrix, therefore is not possible to establish without a certain degree of uncertainty whether the opacyfing agent was produced with a lead-antimony-silica frit or a lead- antimony calx. The use of antimonial litharge is not completely sustainable in the current assmblages: Mass (Mass et al. 1998) indicates that a PbO/Sb_2O_3 ratio between 6 and 14 may be related to the exploitation of antimonal litharge as that of the Rio Tinto mine (Spain), but in the present assemblage only PN VP1, PN GSO1 and BF GSO1 satisfy this condition. Recent works on Roman yellow glass (Molina et al. 2014) support the hypothesis of the "anime" method for Roman glassmaking, observing that it enhance the stability of the particles: lead-antimonate is stable in the silica-soda melt below 1000°C, when Ca-antimonate (white) starts to be produced at expenses of Pb-antimonate; the *anime* method however was proved to enhance the stability of the Pb-antimonate and it is reasonable that it was used by ramn ; unfortunately a clear and univocal indication in the present assemblages lack and the available data do not allow to make inferences on the method employed and the possible sources.

The very low concentration of antimony detected in the glassy matrix, does not support the hypothesis of *in-situ* crystallization that would require an excess of antimony.

Textural and chemical evidence suggest that a lead-antimony compound was added to a colourless (or copper-coloured in the case of green) glass, and quickly stirred. This caused the uneven distribution of the crystals, their partial dissolution and in some cases re-crystallization, developing also the striated appearance of the glassy matrix.

The occasional occurrence of iron in the lead-antimonate crystals here investigated has already been detected in Roman and Byzantine yellow glasses (Lahlil et al. 2008; Silvestri et al. 2012a; Molina et al. 2014) but its origin is also not clear: it has been suggested that it could be a consequence of pollution from iron tools employed in silver cupellation (when considering the use of antimonal litharge) or other metallurgical treatments, from the iron ores employed as a flux in smelting; Molina also suggests it may derive from a deliberate addition to the *anime* (Molina et al. 2014), or it could also be a contaminant from the lead ore: when considering the use of lead and antimony sulphides such as galena and stibnite, they often occur in association with iron sulphides.

5.2.3 Pb-Sn-antimonate

- **Intro e state of the art**

Among the antimony-based opacifiers, a lead-tin-antimony oxide has already been reported as a pigment in 16th-17th century ceramic (Ferrer et al. 2012) and oil painting (Sandalinas and Ruiz-Moreno 2004; Sandalinas et al. 2006; Hradil et al. 2007) and seldom in glass (Wypyski and Becker 2005; Lahlil et al. 2011; Verità et al. 2013; Molina et al. 2014), usually classified as lead-antimonate. Such compound is different from bindheimite in particular for the presence of elevated contents of tin, that can be also comparable to that of antimony.

The origin of the lead and antimony employed in Roman glass colouring is debated and it was already discussed in the previous paragraphs. In the case of lead-tin antimonates however the elevated content of tin is not easily explainable and ways of tin- introduction are hypothesised: the use of tin-rich metallurgical scraps as source of lead, intentional addition of little amounts of tin or contamination. In the archaeometric literature Pb-Sn-antimonates are usually included in the group of Pb-antimonate, and the technological process for their production are considered the same: a lead-antimony calx or a lead-antimony-silica anime were added to a molten glass and quickly stirred in order to avoid phase transformation of Pb-antimonates (or Pb-Sn-antimonates) into Ca-antimonates. The

main unsolved question is related to the presence of tin in such compounds, that is not fully understood(Lahlil et al. 2011; Molina et al. 2014).

- **Results**

Yellow samples TN-GSO1-2, green TN-VP1,2 from Trento, and yellow sample from Pordenone PN-GSO2 are characterised by the presence of lead-tin-antimony oxides. Sample PN-GSO2 is semi-opaque yellow tesserae with bands of glass with higher average atomic number and higher concentration of opacifiers (fig. 5.23,) while the other sample are made of opaque glass (fig. 5.25-5.26).

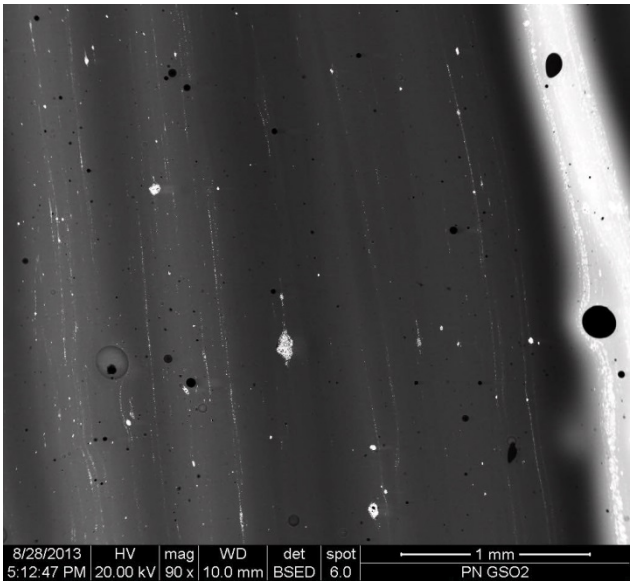

Fig.5.23 : SEM BSE image of the yellow sample PN GSO2 from Pordenone. Note the banded glassy matrix: bright areas correspond to the opaque stripes. .

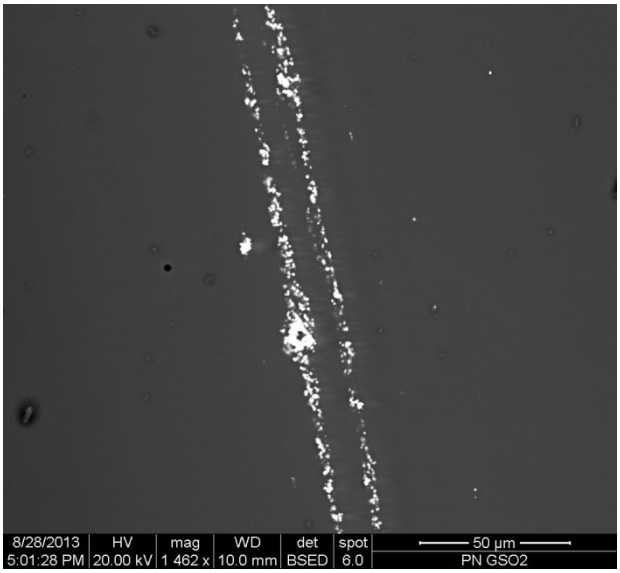

Fig.5.24 SEM-BSE image Detail of the opacifiers: note the sporadic presence of inclusions in the grey glassy matrix corresponding to the semi-opaque glass

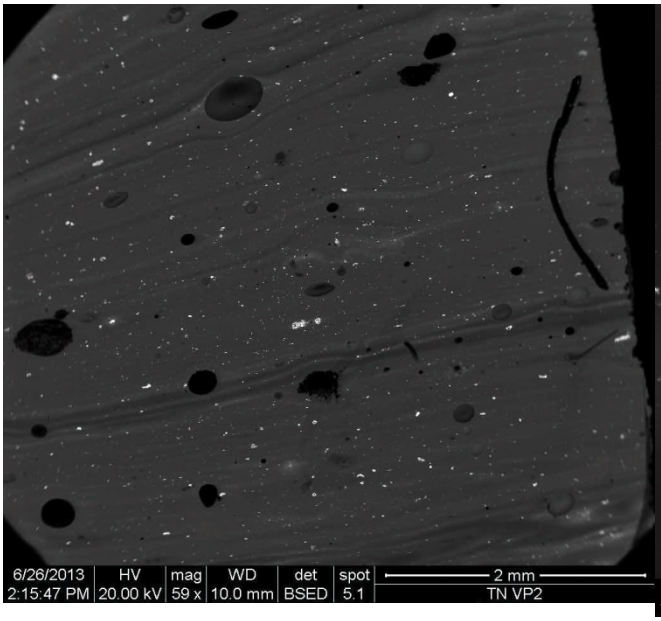

Fig.5.25 : SEM BSE image of a green sample from Trento. Note the banded glassy matrix and the very high atomic number of the opacifiers. Some grey stri

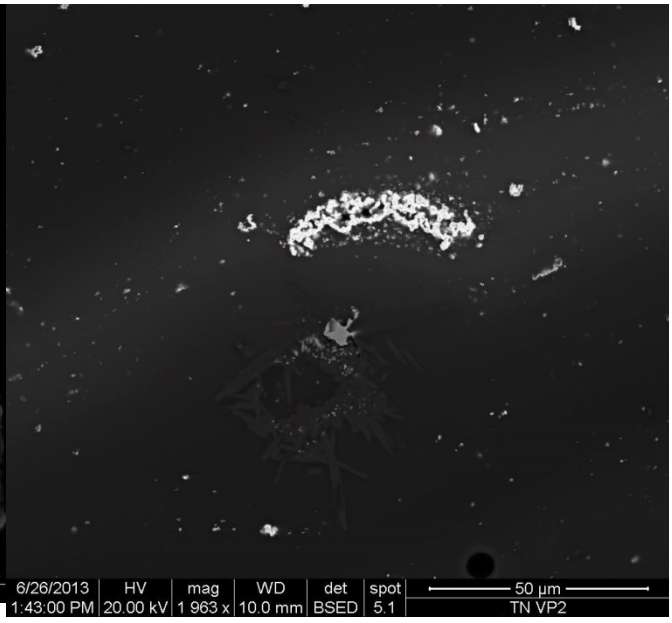

Fig. 5.26: SEM.BSE image of a green sample from Trento. Whiter areas of the glassy matrix are characterised by higher atomic number; bright dots are Pb-Sn-SB oxides crystals, isolated and aggergater in a large lumo; grey euhedral crystals are probale wollastonite.

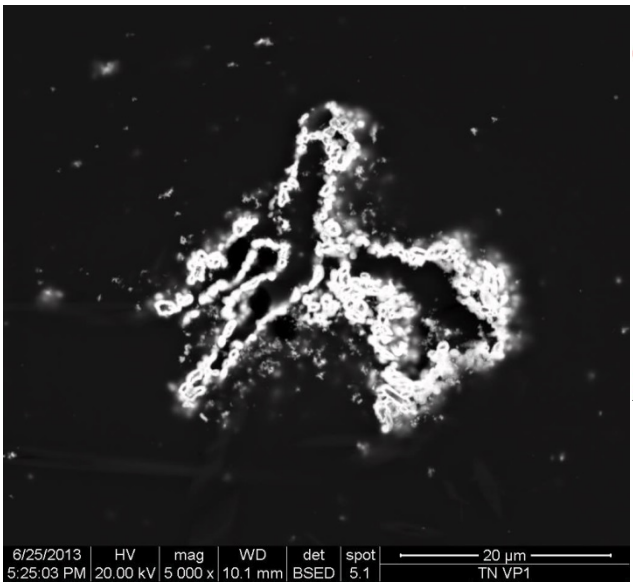

Fig.5.27 SEM-BSE image of the opacifiers, clustered in a rosary-shaped lump.

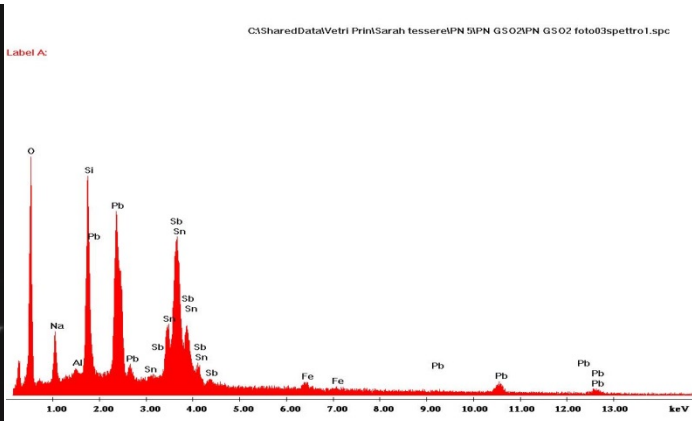

Fig: 5.28: SEM EDS spectrum of the lead-tin antimonate oxides. Notethe presence of iron; silica and soda probably derive from the glassy matrix

As in the case of Pb-stannate, XRPD diffraction performed on the whole tesserae was proved to be inefficient in distinguishing among Pb-antimonate, Pb-stannate and Pb-Sn-antimonate. Mineralogical analysis conducted on the bulk tesserae though evidenced a diffraction pattern that do not fit perfectly with that of bindheimite, and which is more

consistent with cubic pyrochlores of general formula $Pb_2MSbO_{6.5}$ where M= Sn, Hf, Zr , Hf (Cascales et al. 1986) (tab 5.7).

sample	Binheimite	Pb-Sb-Sn oxide
TN GSO1		*x*
TN GSO2		x
TN VP1		*x*
TN VP2		x

Table5.7: XRPD results for samples opacified with Pb-Sn antimonates.

- **Discussion**

Snthetic pyrochlores of lead antimony and tin constitute a complete series of solid substitutions and discerning among the different stoichiometries by means of bulk XRPD was proved to be inefficient. A different degree of substitution may indeed cause significant variation of cell parameters and, as in the case of lead-stannate that will be discussed in the next paragraph, micro-XRD would probably more worthwhile in defining the mineralogical phase.

SEM-EDS data evidenced the presence of antimony and tin in the opacifying crystals, with tin in lower concentration with respect to antimony. The presence of tin in lead-antimonate crystals of Roman yellow glass (up to 17% SnO_2 according to Lahlil) may have different origins not entirely explained: tin may have been introduces by scrap lead contaminated with soft solders, or by contamination with different metallurgical processes; it may also have been deliberately introduced in the colouring mixture or anime with the aim of stabilizing it (Molina et al. 2014). The possibility of contamination cannot be disregarded but does not seems fully reasonable when tin and antimony are present in almost equal proportions; a deliberate additions, or the employ of a tin-rich material seem more reasonable.

The very low presence of tin in the glassy matrix can be related to its lower solubility in glass with respect to of antimony and lead. The low content of both tin and antimony oxide detected in the glassy matrices and the uneven distribution of crystals supports the hypothesis of the addition of a ready compound to the molten glass rather than the in-situ crystallization, although some crystals can be re-crystallized from the melt.

As already underlined by Molina (2014), more studies are required to clarify the provenance and role of tin in some lead-antimony compounds, in particular to relate this evidence to specific chronological or geographical frame. Its presence, it is here to underline, was identified in samples from Trento and in one tesserae from Pordenone, and not in Aquileia.

PB-STANNATE

- **Intro**

Apart from some British and French glass beads dated the 2nd to the 1st century AD in tin-based opacifiers were employed in Europe and Mediterranean basin from the 4th century AD onward in the form of cassiterite (white) or lead stannate (yellow) (Tite et al. 2008). The earliest commonly accepted example of tin-based opacification is present in the in the Thomas Panel and the Kencherai panels, probably produced in Egypt and dated to the late 4th century AD, where flesh-coloured and yellow s*ectilia* are coloured and opacified with tin-based compounds. However a recent work (Verità et al. 2013) on yellow *sectilia* of the Gorga collection in Rome dated to the 2nd century AD evidenced the presence of tin-based opacifiers in some of the slabs; the early dating of the slabs is surprising and represents the earliest example of tin-based yellow in the Roman world but being an exception, does not change the general considerations about the diffusion of lead stannate.

According to some authors (Tite et al. 2008 *and references therein)*, the use of tin-based opacifiers was probably introduced in the eastern Mediterranean from India, where yellow and green tin-based glasses have been produced and exported in Egypt from the 1st century AD. The documented trade between India, Egypt and the Roman Empire may explain the introduction of this technology in the Mediterranean basin, even if the reasons of the technological change are still not clear. The switch to tin-based technology was probably caused by a breakdown in the supply of antimony; being tin readily and easily available, as involved in the production of metals and alloys, the wide employ of leaded bronze and soft solders could have paved the path for the use of lead-tin yellow compounds as glass opacifier.

The study of ancient glassmaking recipes (see: Tite et al 2008 and references therein) analysis of archaeological finds (Heck et al. 2003) and experimental replicas (Rooksby 1964; Tite et al. 2008) suggest that lead stannate was produced by a two-step process: the

preparation of an *anime*, constitute by lead oxide, tin oxide and silica, and the addition of the *anime* to a molten glass. Different recipes of post-medieval glassmaking report that the *anime* also required a two-steps production: a first stage, where lead and tin were calcinated to form a lead-tin "calx", and then a second step where the "calx" was mixed to silica with an excess of lead and then re-melted. The anime so prepared was then grounded and added to the molten glass in a very quick procedure. Previous studies on ancient glass indeed report the presence of a cubic lead-tin compound with a pyrochlore structure interpreted as pure $PbSnO_3$, employed as colouriser and opacifier in yellow and green ancient glasses (Rooksby 1964; Heck and Hoffmann 2000; Heck et al. 2003; Tite et al. 2008). The production and use of such compound continued during the Renaissance until the 18th-19th century in Venetian glassmaking as glass and painting pigment.

- **Results**

Samples BF-GSO4, BF-VP1,2,3,4 yellow-green BF-VG1 and dark green BF-VS2, all from Aquileia, are characterised by the presence of Pb-stannate as opacifiers. This opacifier is unevenly distributed in the glassy matrix that appears zoned (fig.:5.19-5-20) crystals having small dimensions and anhedral habitus are seldom clustered in lumps (Fig. 5.21). SEM-EDS data acquired on the single crystals (Fig. 5.22) highlights the presence of Pb and Sn, together with some silicium, sodium, iron and seldom antimony. Antimony, when present, varies from one analytical point to the other within the same sample but it is generally below 3wt% while silica is generally around 6-7wt%.

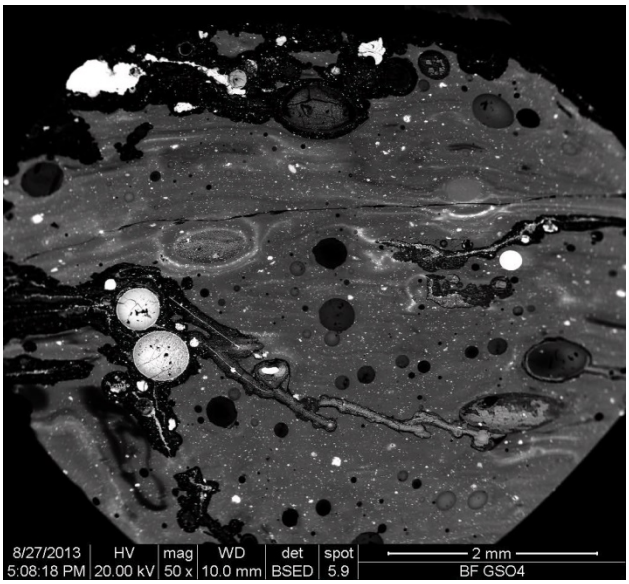

Fig 5.19 : *SEM-BSE image of a yellow tesserae from*

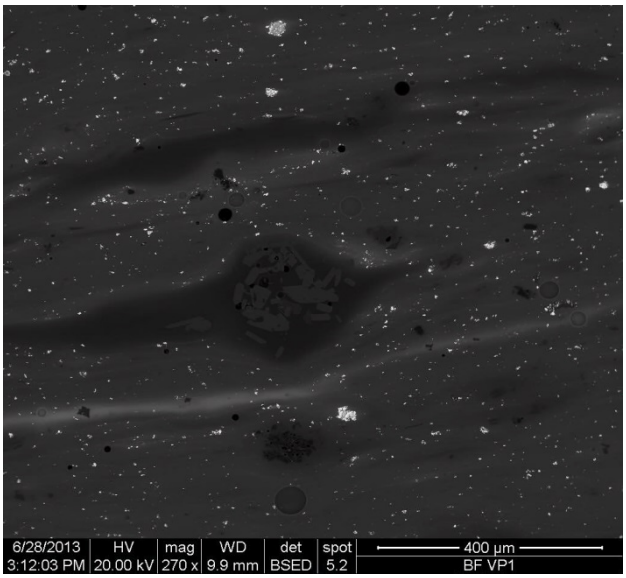

Fig*. 5.20:SEM EDS image of a green tessera from*

Aquileia. Note the zoned texture characterised by fluidal band. Large very bright circular inclusions are Pb-rich inclusions formed in cavity and fractures of the tesserae.

Aquileia. Note the unhomogenous glassy matrix and the high atomic number of opacifiers. The grey crystals in the centre are a probable Ca-phosphate.

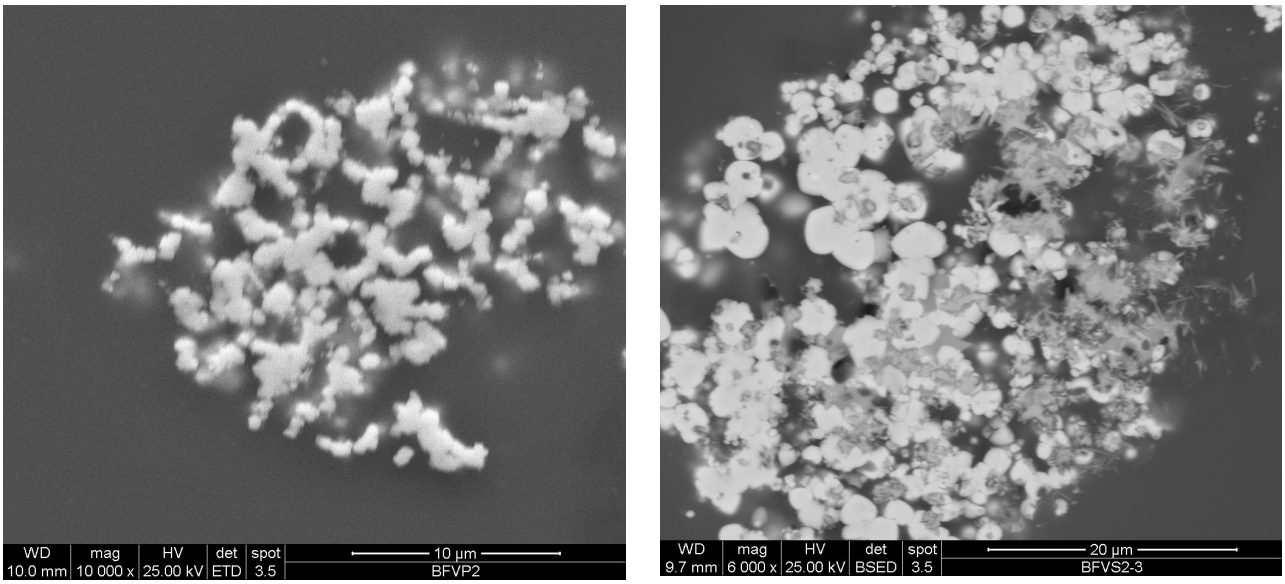

Fig. 5.21 : *high-magnification image of Pb-Sn compounds* ***(a) left****: in a green tesserae and* ***(b)*** *right: in a dark-green tessera from Aquileia. Note the small dimension and the sub-rounded habitus of the crystals.*

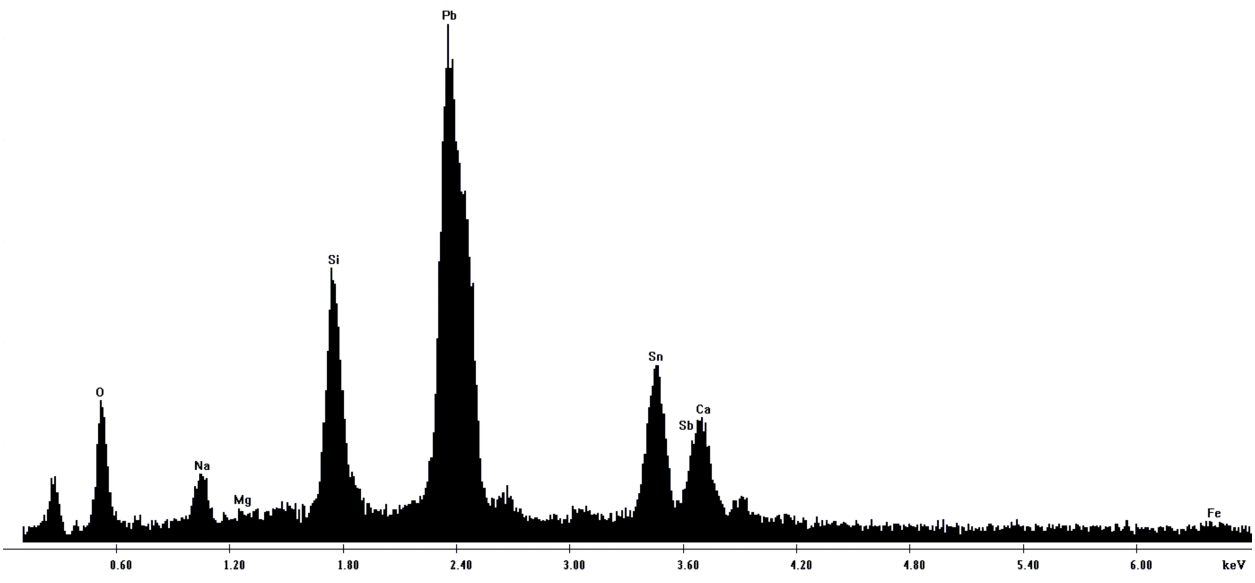

Fig 5.22 . *SEM-EDS spectrum of the lead-tin compounds of fig. (left)*

Quantitative chemical analysis of the inclusions of samples BF VP1,2,3 and BF VS2were performed with Electron Micro Probe, evidencing the presence of comparable concentration of tin lead and silica, and very low quantity of antimony and iron (see tab

5.7), confirming SEM-EDS analysis and the interpretation of the opacyfing agent as lead-stannate rather than lead-antimonate.

X-ray diffraction performed on these samples gave contrasting results, indicating a cubic mineral with a pyrochlore structure, general formula $A_2B_2O_{6.5}$, indicating a Pb-antimonate or a lead-tin antimony compound as the more probable mineralogical phase present.

sample	Binheimite	Pb-Sb-Sn oxide ?
BF VG1	-	*x*
BF VS2	-	*x*
BF GSO4	-	*x*
BF VP1	-	*x*
BF VP2	-	*x*
BF VP3	-	*x*
BF VP4	-	*x*

Tab.5.7: XRPD results of the samples giving diffraction patterns. Note that the samples from Bestie Ferite evidenced in grey amd italicsised are opacified with lead stannate interpreted by bulk XRPD as lead-tin-antimony compounds.

Finally, it is also to underline that sample BF-GSO4, the only yellow sample from Aquileia opacified with lead-stannate oxide is macroscopically different from the other: BF-GSO1, 2 and 3 show a warmer hue of yellow, while BF-GSO4 is lemon-yellow.

- **Discussion**

Lead-stannate was identified in the green (BF-VP1,2,3,4) dark green (BF VS1) yellow (BF-GSO4) and yellow green (BF-VG1) from Aquileia. The identification of these phases was proved to be difficult, as in the case of lead-tin antimonate: XRPD performed on the whole fragment gives contrasting results, suggest various possible lead-antimonate or lead-tin-antimony compounds. Phases here investigate seem to be similar to the group of cubic pyrochlores of general formula $Pb_2MSbO_{6.5}$. The reason for the partially inconsistency of XRPD with the EDS data is related to the structural similarity between lead-antimonate, lead-stannate amd lead-tin antimonate, and probably micro-XRD performed on isolated crystals or small clusters would be more reliable in determining the mineralogical phase.

The clear evidence though is that the prevalent opacifying phase detected in these samples is a cubic phase with a pyrochlore structure (sometimes indicated in painting-related

literature as lead-tin yellow tipe II) and not the orthorhombic Pb_2SnO_4, (the so called lead-tin yellow tipe I).

The opacifying crystals are unevenly distributed and suggest the addition of a lead-tin compound, rather than the in- situ crystallization. The dynamic of crystallisation and phase transformation that occur in lead-tin-silica mixture indeed are not compatible with the *in-situ* crystallization of this compound for which an ex-situ synthesis is hypothesised. Prolonged firing would indeed end in the crystallization of cassiterite (white) at the expenses of the yellow cubic $PbSnO_3$; temperature of such phase transitions vary depending on a large variety of factors, but it is generally below 900°C and in certain cases as low as 650°C . To avoid the transformation into cassiterite, a very quick process was necessary and the excess of lead helped to melt the glass at lower temperature, allowing the quick stirring of the glass and thus avoiding the formation of cassiterite. The quick mixing explains the uneven distribution of crystals in the glassy matrix.

The presence of silica in the frit, that appears to be necessary in the production of this compound, may be at the origin of the silica present in the phase structure. Such possibility is investigated in the case of painting pigments (Clark et al. 1995) where the general formula $PbSnO_3$ is better expressed as $Pb\ (Sn_{1-x}\ Si_xO)_3$. Resolving the presence of silica in the case of glass opacifiers is a big challenge, as the contribution of the glassy matrices cannot be excluded, but repeated measurements with EPMA and SEM-EDS analysis seem to support the presence of silica in the structure, together with sporadic some antimony. The presence of such substitutions may be at the basis of the ambiguous XRPD pattern: ionic substitution of silica and antimony lead to cell deformations that probably generate a misinterpretation.

The presence of tin-based opacifiers in the Aquileia mosaic, dated to the mid-4th century AD may represent a prompt reception of a new technology coming from East; these tesserae are slightly different from the main group of Roman glass for their elevated sodium, magnesium, low potash contents; as already noted for the azure, aquamarine and pale green tesserae from this site, they could have be produced mixing different glasses of Roman and late composition and this would be consistent with the late opacification technique.

It is important to note that in the same mosaic antimony and tin-based compounds are employed, indicating the presence of different glass suppliers or the coexistence of "old" and "new" tesserae.

5.2.5 COPPER AND CUPRITE

- **Intro**

Opaque red glass is known to have been made from the 17th century BC onward (Barber et al. 2003) in the near East and it has been continuously employed in beads, bracelets, enamels, *pseudo*-gemstones, vessels and mosaic *tesserae* in Roman and Byzantine time. Red, brown and orange tesserae in particular are reported in glass tesserae assemblages of Roman times (Wypyski and Becker 2005; Gliozzo et al. 2008; Gliozzo et al. 2012).

The production of copper red glass requires particularly conditions that are closer to metallurgical process then to usual glassmaking. Under oxidizing conditions copper dispersed in the glassy matrix in the form ions is present as Cu^{2+} which, as already discussed in the previous paragraphs, colours the glass turquoise. Differently, when the firing conditions are reducing, Cu^{2+} is reduced to its less soluble form Cu^{1+}. Due to low solubility of Cu^{1+} in glass, during cooling crystals of cuprite or copper precipitate from the melt. Crystals of cuprite generally produce yellow-orange or bright red colours, while metallic copper crystals generate red, brick-red and brown colours (Cable and Smedley 1992). Sometimes the two phases can co-exist in the same glass. The development of one or the other phase and the generation of colour are strongly influenced by many factors, including the presence and concentration of lead, copper, and the presence other elements, the temperatures and time of firing and, of course the redox condition.

Cuprite, in the form of small cubic crystals or large dendrites, is usually found in high lead-high copper glasses (Freestone 1987; Brill and Cahill 1988; Cable and Smedley 1992; Barber et al. 2003; Freestone and Stapleton 2003; Bayley 2005; Gliozzo et al. 2008; Silvestri et al. 2014a) suggesting that elevated copper is necessary for the nucleation of cuprite and elevated lead probably helps the formation of crystals.
Copper crystals on the contrary are usually detected in low-copper, low-lead glasses (Freestone 1987; Freestone and Stapleton 2003; Barber et al. 2003; Peake and Freestone 2012; Silvestri et al. 2014a)

Reducing furnaces were typical of metallurgical processes also in antiquity, but the balance among temperature, time, redox condition and chemical compositions necessary to produce red glass required a very high technological skill. How such reducing conditions were achieve, maintained and controlled in preindustrial times is not completely known, although some ancient glass recipe books give some indications (Oppenheim 1970) and many replica attempt were made in past decades (Ahmed and Ashour 1981; Guido et al. 1984; Cable and Smedley 1992; Welham et al. 1998). The modern experimental replicas conducted under controlled conditions report failures, development of undesired colour (mainly green and black), precipitation of large copper prills, segregation of the glass in layers of different colours and a general difficulty in working with this material, evidencing the challenge of this particular kind of glass.

The production of undesired colours is mainly due to a lack of control in the oxidising conditions: even when working under controlled condition, a reducing atmosphere in the furnace does not necessarily develop a locally reducing condition in inside the melt, where some areas of oxidized glass can remain; an excess of reduction on the contrary end in the development of tenorite (CuO, black) and large metallic prills.

To improve the local reduction without exasperating the condition of the furnace chamber, internal reducing agents were added directly to the batch: the more common –and known- reducing agents are lead, tin, antimony and iron. As in the case of turquoise/blue/green copper coloured, the sources of copper employed could be copper minerals (such as chalcocite or covellite), metalworking scraps (roasted copper, bronze, brass and others alloys); metalworking scraps and metallurgical by-products were reasonably employed as sources of both copper and internal reducing agents but distinguishing between different source is not easy in absence of relics.

- **Results**

Sample belonging to the chromatic groups red (R), orange (AV) and brown (M), are coloured and opacified by copper-rich phases dispersed in the glassy matrix.

In SEM-BSE images, crystals appear as abundant inclusion of very high atomic number, nanometric dimension of rounded- elongated or cubic habitus. Similar inclusion were identified, although in lower quantity, also in some samples of the chromatic group olive/red (TN V OL1 and PN M3) and in the single dark amber sample from Trento (TN

NS1). In order to investigate the mineralogical phase involved in the formation of the different colours, X-Ray Powder Diffraction (XRPD) was performed on the whole *tesserae* of the copper-opacified tesserae; in the case of millimetric fragments embedded in epoxy resin (BF AV1 and BF R1), that were not suitable for X-ray Powder Diffraction, micro-fragments (50-200 μm) were sampled and analysed using a single-crystal diffractometer equipped with a micro X-ray source; data were collected using a micro X-ray powder diffraction method, due to the polycrystalline nature of the samples. The same methodology was applied to the banded tesserae (TV AV1 and PN AV1), where the single coloured bands were sampled and analysed separately. Mineralogical analysis performed by XRPD and micro-XRPD evidenced that orange tesserae (AV), including both the homogenous and the banded ones are characterised by the presence of cuprite, while brown (M) and red (R) tesserae are characterised by metallic copper crystals (See tab. 5.8)

sample	**method**	**Cuprite**	**Copper**
PN M1	*XRPD*	-	-
PN M2	*XRPD*	-	-
PN M3	*XRPD*	-	-
TN M1	*XRPD*	-	x
TN M2	*XRPD*	-	x
TN M3	*XRPD*	-	x
TN AV1red	□-*XRPD*	x	-
TN AV1 orange	□-*XRPD*	x	-
PN AV1	*XRPD*	x	-
PN AV2 red	□-*XRPD*	x	-
PN AV2 orange	□-*XRPD*	x	-
BF R1	□-*XRPD*	-	x
BF AV1	□-*XRPD*	x	-
TN NS1	*XRPD*	-	-
TN V OL2	*XRPD*	-	-

Tab.5.8 XRPD analysis of the copper-coloured red brown and orange tesserae.

Although analysed with XRPD, some brown (PN M1-M2-) olive red (PN M3 and TN VOL1) and the dark amber (TN NS1) tesserae did not give any diffraction pattern probably due to the very small dimension of the crystals (tab.5.8) and the presence of metallic copper is deduced by means of other information. Differently from cuprite-rich glasses (As TN AV1, BF AV1, PN AV1 and PN AV2), the opacifying phases of the brown tesserae from Pordenone and Trento did not give any Raman effect that could suggest the presence of cuprite therefor the combination of SEM-EDS data, the absence of Raman effect, the chemical similarity with other brown tesserae and the dark colour, it was supposed that they are opacified with copper.

Cuprite was identified in orange tesserae PN AV1,2, TN AV1 and BF AV1. The orange samples (PN AV2 and BF AV1) are texturally very homogenous and show the presence of abundant inclusions of micrometric crystals of cuprite (see fig.5.31:)

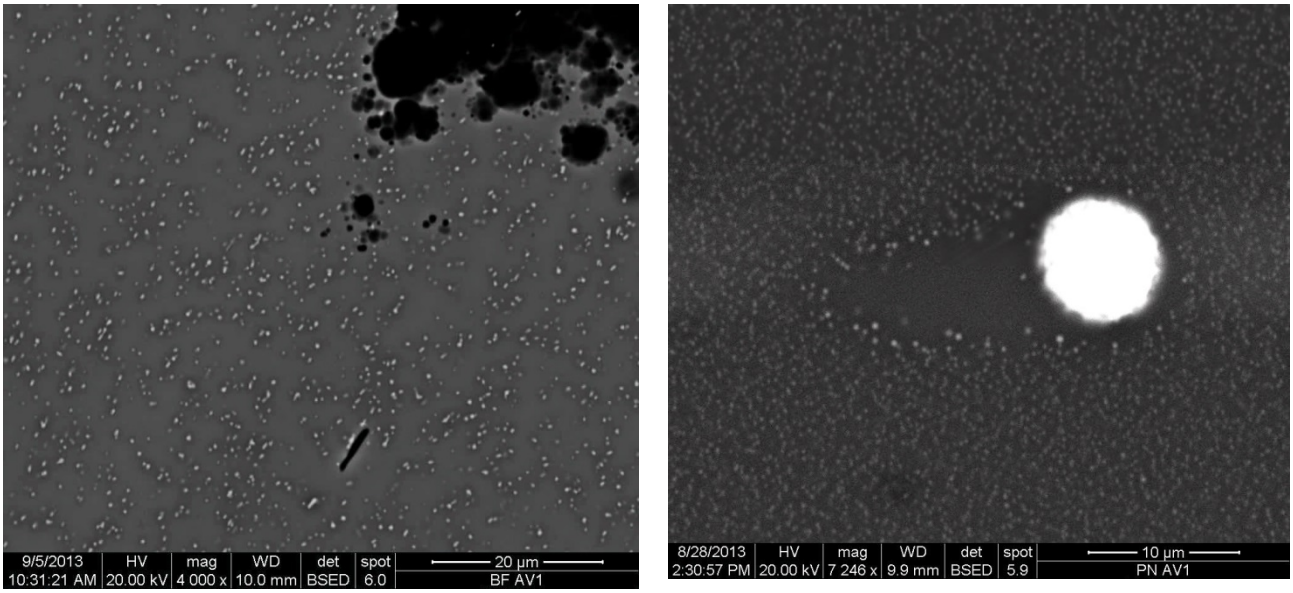

Fig. 5.31 : *SEM-BSE image of the orange homogenous samples from* ***(a)*** *left Bestie Ferite and* ***(b)*** *right Pordenone. Note the higher concentration of crystals (bright small dots) in the Pordenone sample with respect to the Aquileia one. The bright drop is metallic copper.*

The two orange tesserae (PN AV1 and TN AV1) are characterised by the presence of cuprite in both the orange and the red bands; despite this similarity, the two tesserae have different textures: orange/red banded sample TN AV1 appears to be constituted by a homogenous glass matrix, (grey in SEM-BSE image of fig.5.28) where very abundant

bright (i.e. very high atomic number) crystals are embedded; in red areas crystals appear larger and less dense, while in orange bands they appear smaller and more dense (fig 5.28a), between the bands, thin strips of apparently transparent glass are visible.

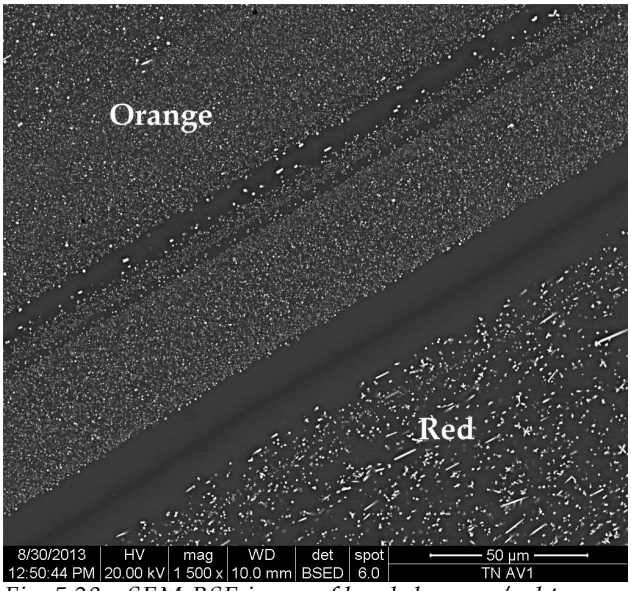

Fig 5.28a: SEM-BSE image of banded orange/red tesserae from Trento In the trento samples thin stripes of apparently transparent glass are visible between the bands.*;*

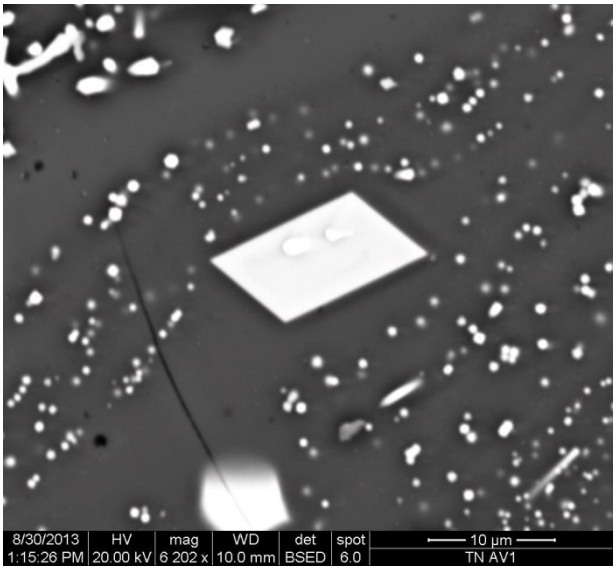

Fig 5.28b: SEM-BSE imag: detaile of orange band. Note the banded texture and the presence of apparently clear glass. Bright flakes represent cuprite crystals, the large euhedral crystal in the centre is probable malayaite, while the bright dots at the center of it ar probably cassiterite (SEM-EDS data).

Differently, the red/orange banded sample PN AV2 when observed at SEM-BSE image (Fig 5.29-) shows heterogenous glassy matrix, characterised by different average atomic number where small crystals and occasionally incipient dendrites are embedded (Fig 5.30); establishing a neat correspondence among crystal size or shape, atomic number of the glassy matrix and macroscopic colour is not possible in this samples, as the range of tinges is very wide and not defined. The red-orange stripes do not coincide perfectly with bright/dark stripes visible in SEM-EDS images, indicating that the colour of the band is not necessarily linked to the average atomic number of the matrix.

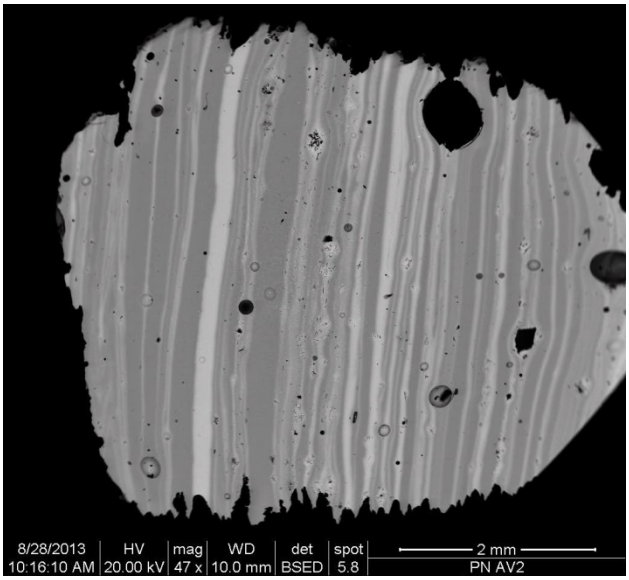

Fig. 5.30 *Pordenone samples is characterised by different atomic number in the glassy matrix, here evidenced by ifferent shades of grey. Voids and bubbles in black.*

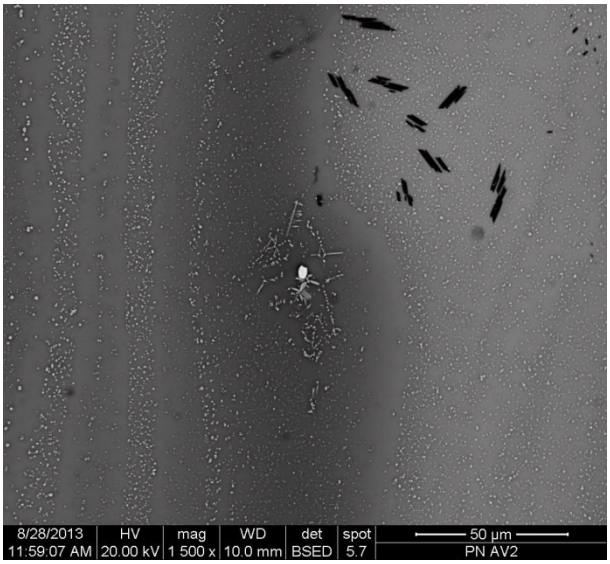

Fig. 5.30 *detailed image of sample PN AV2. The variabile atomic number in the glassy matrix is here evidenced by d ifference shades of grey. Bright dots are cuprite crystals, note the incipient dendrites at the center. The bright inclusion is constituted by cassiterite; black crystals are divitrification phases, probably combeite Na2Ca2,Si3O8*

Metallic copper was identified in the sealing-wax red (BF R1) and the brown samples (BF M1,2,3; PN M1,2 and TN M1,2,3) and in the olive red PN M3 and TN VOL1 and the dark amber TN NS1.

Olive red tesserae show an olive green, translucent glassy matrix with stripes of opaque red/brown glass where relatively abundant crystals of metallic copper are present. The dark amber TN NS1 is characterised by the presence of sporadic copper inclusions and abundant seeds and bubbles; brown samples from Pordenone show very small sporadic crystals of copper.

As evidenced in the SEM-BSE pictures (Fig. 5.32-33-34) metallic copper crystals tend to a cubic habitus, larger in the brown tesserae from Trento (up to 3-5 **µ**m), smaller in the Brown from Pordenone and Bestie Ferite samples (up to 1-2 **µ**m) and nanometric (≈100 nm) in the red sample from the Bestie Ferite mosaic (fig.32). The two brown tesserae from Pordenone (PN M1 and2), dark red striped in black, do not show any chemical or mineralogical difference in the darker bands with respect to the reddish areas.

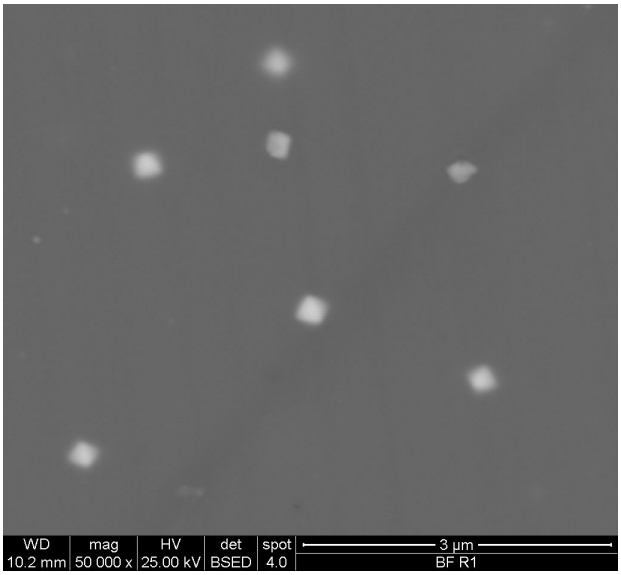

Fig.5.32 *: SEM BSE image of the single sealing-wax red sample of the Aquileia assemblage. Nanometric crystals of copper (XRD data) showing cubic habitus*

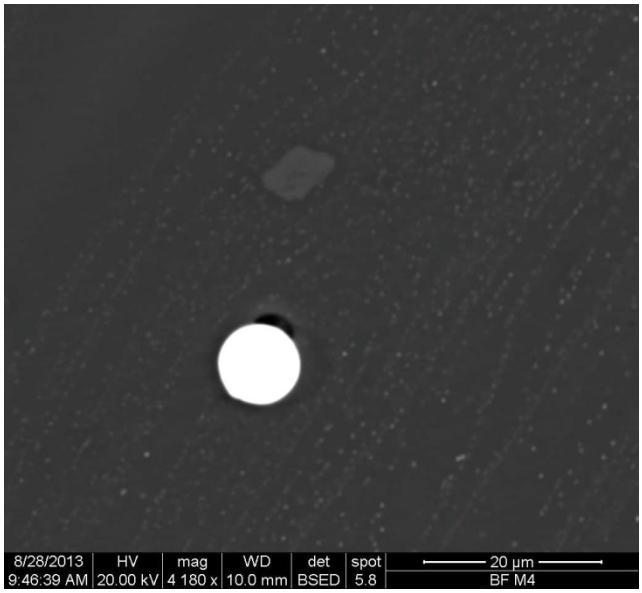

Fig, 5.33 *Brownish tesserae from Aquileia, note the presence of very abundant nanometric crystal of copper (XRD data). The large bright circular inclusion is a metallic copper drop*

Copper rich crystals such as cuprite and metallic copper nanoparticles are often associated to large metallic copper prills (see Fig 5.31-33-34) and in the case of brown tesserae from Aquileia and Trento, iron oxides (Fig. 5.34b).

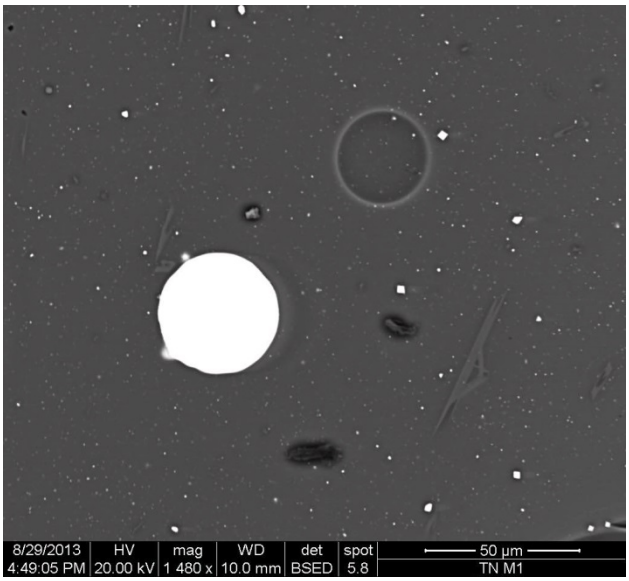

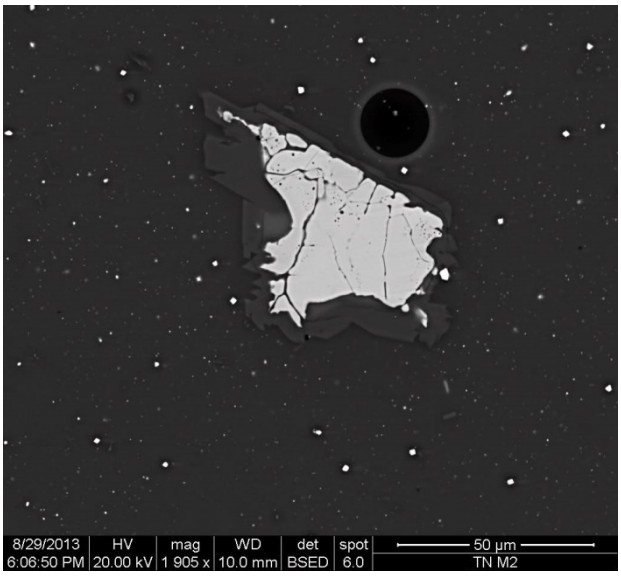

Fig. 5.34 *a Brown tesserae from Trento, note the presence of abundant micrometric- to nanometric crystals of copper showing cubic habitus. The large bright circular inclusion* ***(a)*** *is a metallic copper drop, the irregular grey inclusion* ***(b)*** *is an iron oxide of probably wustite surrounded by wollastonite (SEM-EDS data) while the grey acicular inclusion are wollastonite crystals.*

As in the case of copper coloured turquoise and green tesserae, relic phases of a copper ore were frequently identified and they will be discussed in the paragraph "Other inclusion".

In addition, three brown tesserae from Aquileia (BF M1,2,4) evidence the presence of abundant large black inclusions interpreted as metallurgical slags.

In SEM-BSE images these inclusions, seldom angular, are constituted by different grains characterised by different habitus and average atomic numbers (Fig 5.48-49). The surrounding glassy matrix is characterised by high atomic number that indicates that a partial dissolution of the inclusion has occurred.

Under higher magnification, the inclusion appear of two main kinds:

1) Large fayalitic inclusions (Fig.:5.50a-b) constituted by large irregular crystals of fayalite Fe_2SiO_4 (grey) associated to small dendrites of iron oxide and characterised by the presence of iron rich interstitial glass (dark grey);

2) Large aggregates of iron oxides (Fig.5.51), probably wustite (FeO), surrounded by wollastonite crystals (grey) and prills of metallic copper of various dimensions.It is to be noted that metallic copper, which is dispersed into the glassy matrix shows higher dimension around iron oxides inclusions (Fig. 5.51).

The presence of fayalite (fig. 5.50a-b), hypothesised on the basis of SEM-EDS data (see fig. AA) was confirmed by MicroRaman spectroscopy (FIG AB), while the probable wustite (fig. 5.51) was checked by means of SEM-EDS data only.

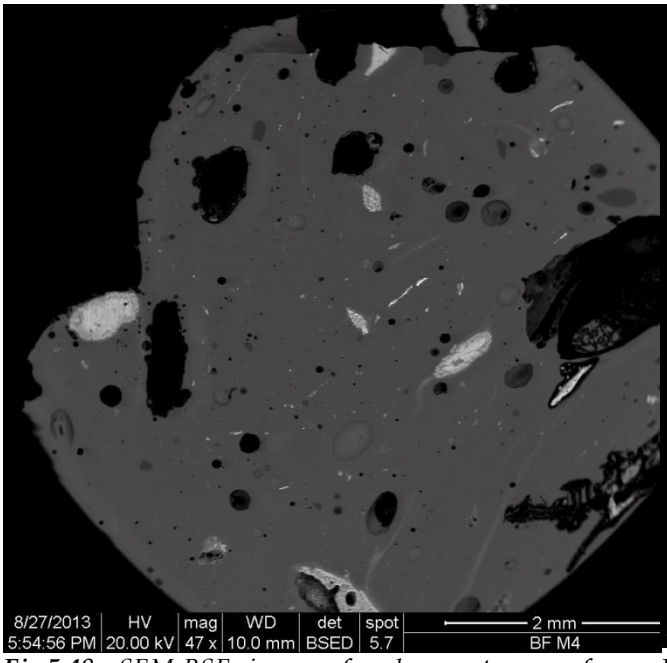

Fig.5.48: *SEM-BSE image of a brown tesserae from Aquileia: the very abundant and larg inclusion of high atomic number (i.e:bright) appear partly dissolved (bright stripes). Abundant gas bubbles and voids*

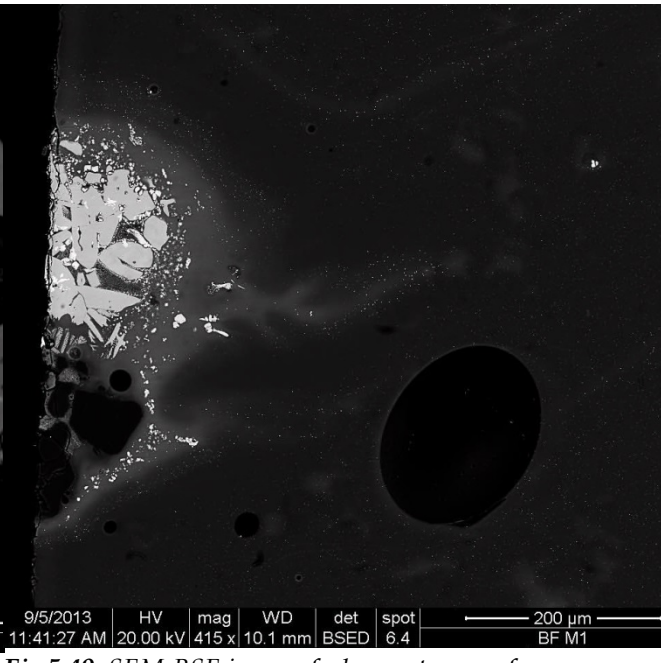

Fig.5.49: *SEM-BSE image of a brown tesserae from Aquileia showing the partial dissolution of the slag*

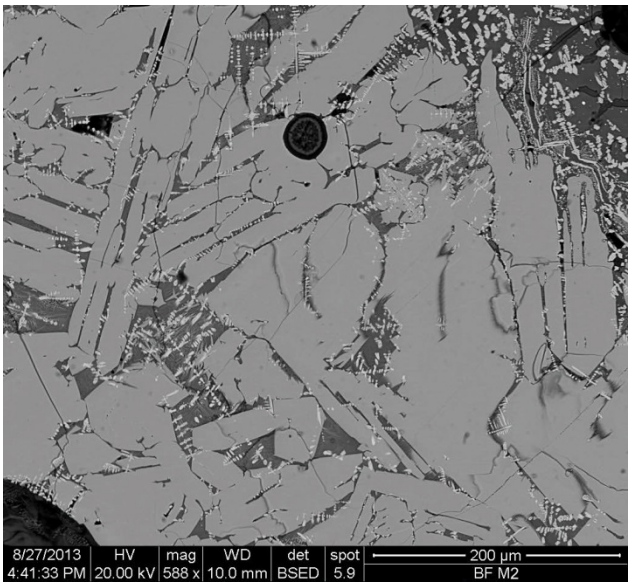

Fig.5.50(a): SEM BSE image of detailed of a fayalitic slag: large grain of fayalite (grey), interstitial glass (darker grey) and iron oxides (white dendrites)

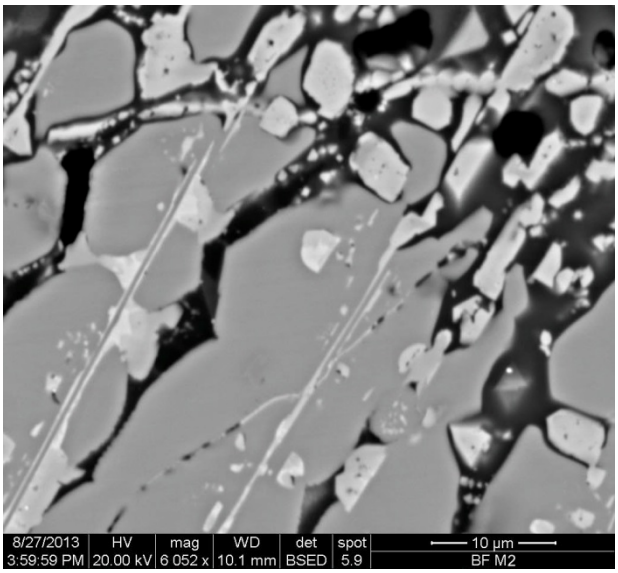

Fi g.5-50 b: SEM BSE image of detailed of a fayalitic slag: large grain of fayalite (grey) and iron oxides, probable wustite FeO, white) (p.a.1 is reported in fig, AA). Black corresponds to interstitial glass.

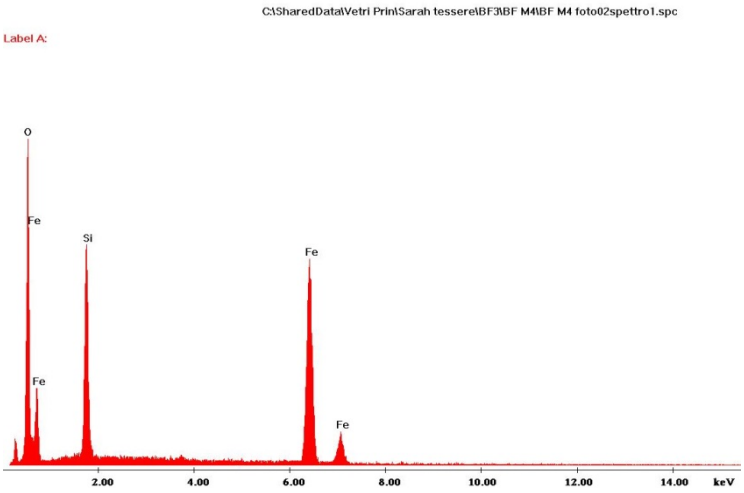

Fig.: SEM-EDS spectrum of the fayalite inclusion in fig. 5.50 point 1

	a.p. 1	***Ref. fayalite***
	Ox wt%	
SiO2	28.92	*29.49*
FeO	69.22	*70.51*
	At%	
Fe	53.57	*54.81*
Si	17.51	*13.78*
O	28.92	*31.41*

SEM-EDS analysis of fayalite (point 1) compared to reference data in italics for fayalite (www.webminerals.com)

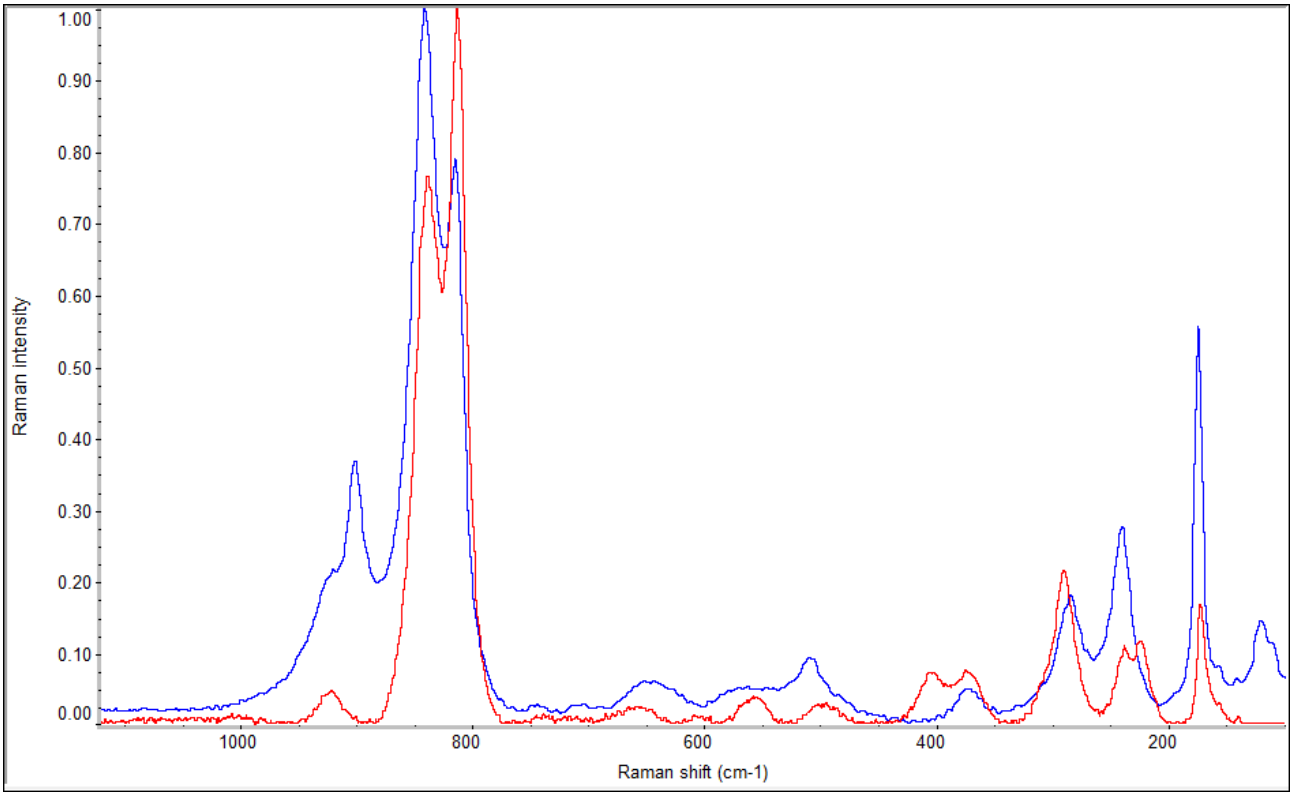

Fig.: Raman spectrum of the fayalite of fig. 5.50: the acquired spectrum (blue) is compared to the reference spectrum (red)

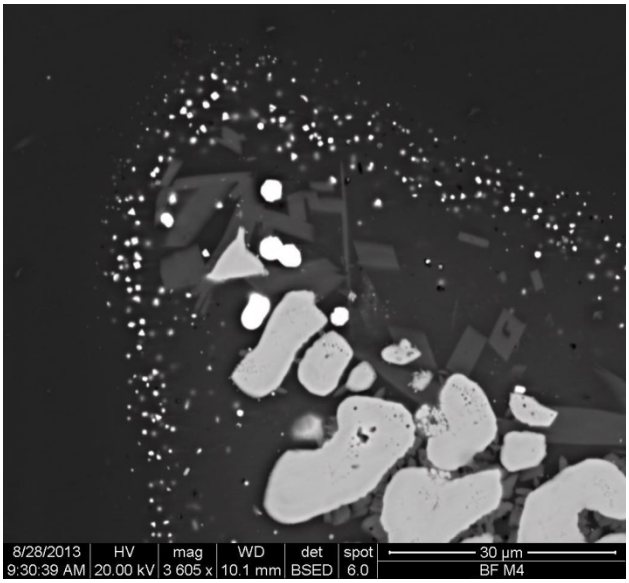

Fig. 5.51: SEM-BSE image of iron oxide, probable wustite FeO (grey globular inclusions) with metallic copper prills (white) and crystals of probable wollastonite CaSiO3 2 indicates the analytical point reported in fig AB



Fig.5.52 : SEM-BSE image: metallic copper nanoparticles (white) and crystals of probable wollastonite $CaSiO_3$ in (grey)

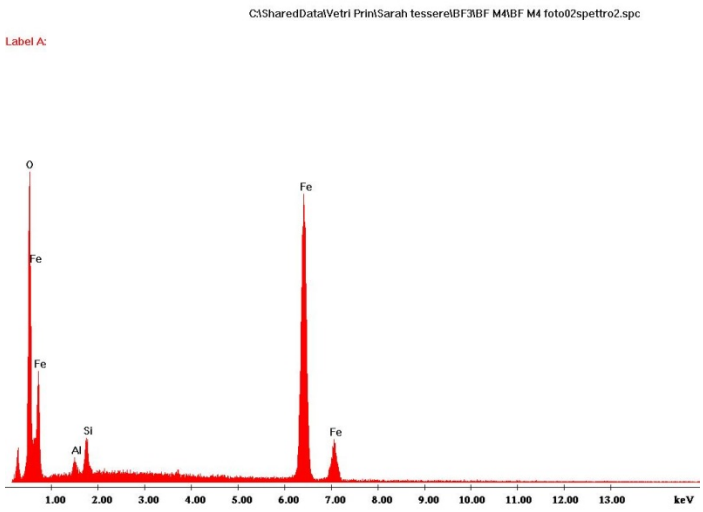

	a.p.2	***ref. Wustite***
O	24.09	*22.27*
Fe	71.8	*77.73*
Si	2.83	-
Al	1.28	-

Fig. AB (a) SEM-EDS spectrum of a.p.2 of fig 5.51, probable wustite inclusion. (b) qualitative analysis: results are reported wt% of the element compared to reference values for wustite (webminerals.com)

- **Discussion**

Red tesserae here analysed cover a wide range of chemical composition anf textural features, indicative of the multitude of possible techniques and raw materials involved in the production of this kind of glass.

Cuprite, in the form of small cubic crystals or large dendrites, is usually found in high lead-high copper glasses (Freestone 1987; Brill and Cahill 1988; Cable and Smedley 1992; Barber et al. 2003; Freestone and Stapleton 2003; Bayley 2005; Gliozzo et al. 2008; Silvestri et al. 2014a) suggesting that elevated copper is necessary for the nucleation of cuprite and elevated lead probably helps the formation of crystals. In the present assemblages cuprite was detected only in high-copper, high-lead orange tesserae, but TN-AV1 constitutes and exception: its relatively low lead (8%wt) suggests that probably an excess of copper is more important that an excess of lead in the formation of cuprite. Cuprite crystals are very abundant in the orange samples, but only in PN AV2 it occasionally shows dendritic habitus and larger dimensions; red bands and stripes in orange tesserae tend to correspond to larger crystals dimensions and the sporadic dendrites tend to red colour, as already demonstrated by previous works (Ahmed and Ashour 1981).

Copper crystals on the contrary are usually detected in low-copper, low-lead glasses (Freestone 1987; Freestone and Stapleton 2003; Barber et al. 2003; Peake and Freestone 2012; Silvestri et al. 2014a) the present assemblages confirm this evidence: excluding the

orange samples, all the red and brown tesserae are opacified with metallic copper and were e produced with variable-although low contents of copper and lead. The red and brown glasses are produced with low-copper, low lead glass.

While in sample TN AV1 different colour can be associated with different crystallite size and density, in the case of PN AV1 no clear explanation can be given of the difference in colour.

In the dark amber TN NS1, copper crystals are relatively rare and the sample also presents abundant seeds and bubbles. The unclear colour, the partial opacity, the low density of opacifying agents and the presence of large relics and gas bubbles suggest that this tessera may represent a failed attempt of a red tesserae, or the product of re-melting of different glasses.

Red olive/red striped tesserae (PN -M3 and TN VOL1) are olive green glasses where thin stripes of red glass are present, characterised by small copper-rich inclusions and larger drops. The development of the red and green colours in copper-rich glasses are due to opposite redox conditions, reducing in the case of red and oxidizing in the case of green; the olive/red tesserae, showing both colours, may be the result of a bad control on redox conditions that would have caused the development of reduced and oxidized area in the melt, developing different colours.

The precipitation of copper or cuprite crystals is aided by the addition of internal reducing agents. In the present assemblages iron is present in elevated concentration in tesserae BF M1,2,4 in absence of lead tin and antimony and it represents therefore the only measurable reducing agent;

Antimony tin and lead are present in all the other tesserae in variable concentrations, in association with relatively high iron content. A remarkable content of iron characterise also the dark brown tesserae TN M1,2 and it might be responsible for the dark colour.

The use of charcoal or plant ash as reducing agent was also often suggested. Charcoal was proved to be an effective internal reducing agent (Guido et al. 1984; Freestone 1987; Cable and Smedley 1992; Schibille et al. 2012). The use of vegetal ashes may result in a variation of the chemical composition of the base glass toward plant ash.
The addition of vegetal ash or charcoal is here hypothesise, that may also explain the

intermediated composition between natron and plant ash glass evidenced in red and orange glasses TN AV, PN AV1 and BFAV1

In the case of copper-red glass it is not possible to determinate whether copper was introduced through a copper mineral or a metallic alloy: the development of copper-rich crystals causes an elution of copper in the glassy matrix therefore the ratios between the different elements are not preserved; in this case, the presence of relics is of particular interest to determinate the raw materials employed.

In tesserae BF M1,2,3 a very uncommon kind of relic inclusion was identified: the presence of angular metallurgical slags, crushed and added to the glass. Establishing whether the slags derive from a copper or copper smelting or from iron smithing is not easy, because the presence of fayalite can occur in all the above processes; the evidenced presence of copper prills around the partly dissolved slags is not a proof of the presence of copper in the slag, as the prills could have been generated by the locally reducing environment produced by dissolving iron. The simultaneous presence of relic chalcocite in the same samples suggests that copper was introduced by a copper sulphide, and iron (the only internal reducing agent identified) was introduced by metallurgical slags. On the other hand, the presence of zinc in the glassy matrix may indicate also the use of metalworking scraps as a source of copper.

The existence of cross-craft interactions between metal and glass working has been extensively examined in the past years: the metallurgical origin of the copper, antimony and tin employed in ancient glassmaking has already been discussed in the previous paragraphs, but the evidence of slag addition in glassmaking are very rare: an examples of systematic use of this technology was identified in Anglo-Saxon red and black beads dated to the 5th-7th century AD (Peake and Freestone 2012), while sporadic examples were recovered in other Anglo-Saxon and Merovingian sites but any other evidence is known in Roman-late Roman glasses. The identification of slag inclusion in copper red glass dated to the Roman times seems to contradict the hypothesis formulated by Peake, that this technology originated in early medieval Europe (Peake and Freestone 2012).

Red tesserae from the "Bestie Ferite" cover a wide range of chemical composition and technological evidences, indicating that tesserae of comparable colour employed in the mosaic derived from different suppliers.

5.2.6 QUARZ+ BUBBLES

- Intro

Quarz and other sand relics as K-feldspars are very common in glass tesserae, opacification obtained by means of quartz and bubbles is very rare.

Late Byzantine glass tesserae from Hosios Loukas opacified by the addition of crushed quartz and Anglo Saxon glass beads opacified with solely bubbles are reported by Freestone and Peake, respectively (Freestone et al. 1990; Peake 2014) while later examples of bubbles as opacifier are reported for the pale green tessera of St. Marc Baptistery (Venice-Italy) dated to the 14th century AD Mosaic tessera (Verità 2000).

The presence of gas bubbles in combination with abundant seeds was reported in late Roman flesh-coloured and white sectilia of the "Thomas Panel", probably made in Egypt around the 375 AD (Brill and Whitehouse 1988) and in mosaic tesserae of the 10-14th century (Verità 2000).

At the moment it is not possible to speculate whether the rarity of this technique in the archaeological reports reflects a real scarcity, or it is related to the analytical approach employed in the study of glass: some scholars may have neglected the bubbles and/or considered quartz relics as unintentional; in addition, many glass tesserae assemblages were analysed by means of bulk chemical analysis, without a preliminary textural examination. It is possible that quartz-and-bubbles opacified glasses were more frequent and were probably employed in absence of other opacifiers and/or when opalescent tesserae were required.

- **Results**

Some tesserae tesserae from Aquileia (BF AZ1,2,3,5, BF VCH1,2,3, BF CE2, BF AQ1) Pordenone (PN AQ1) appear semi-opaque and their textural examination evidenced the presence of gas bubbles and sand relics in a large quantity in virtual absence of other opacyfiers (fig 5.15-5.16).

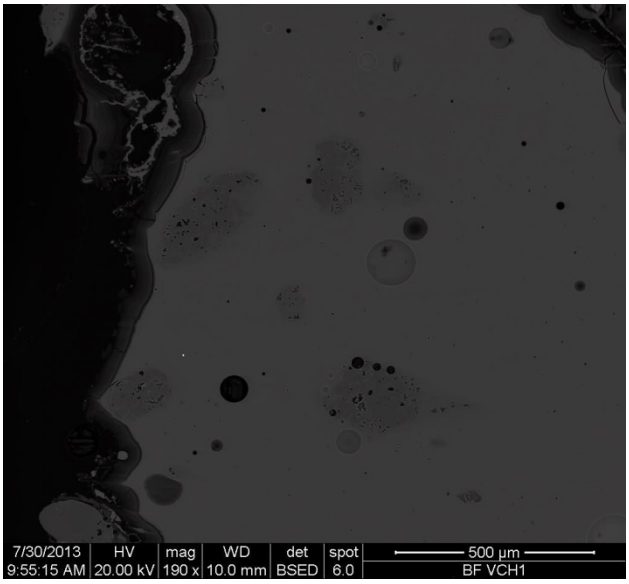

Fig.5.15 : SEM BSE image of a pale green sample from Aquileia (left). Parltly dissolved sand relics, mainly quartz and K-feldpsars (dark grey) and gas bubbles (black)

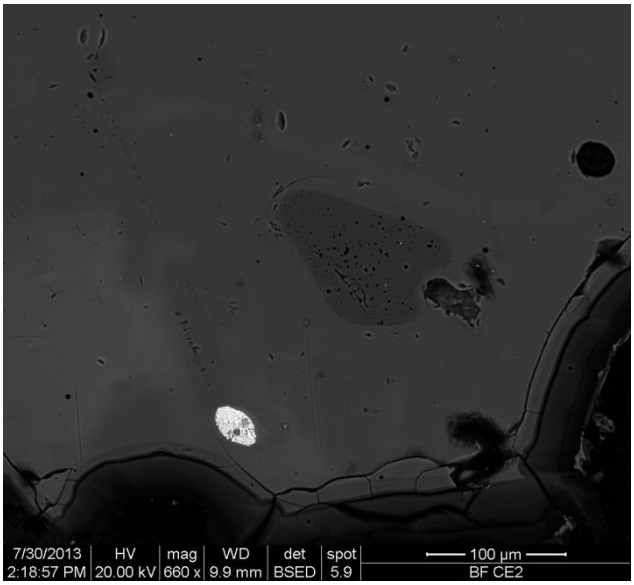

Fig.5.16 : SEM BSE image of a pale blue sample from Aquileia (left). Quarz relic (large grey inclusion) and a cassiterite relic (bright lump)

sample	**quartz**	**cristobalite**
BF AQ1	X	
BF AQ2	X	
BF AZ1	X	
BF CE2	X	
BF VCH1	X	X
BF VCH2	X	
BF VCH3	X	

Tab 5.9: XRPD of samples probably opacified with quartz and bubbles. Only samples giving some diffraction pattern are here reported.

Sand relics are represented by relatively large inclusions characterised by rounded-irregular shape and low average atomic number; SEM-EDS data suggest that in most o Such textural uncommon feature was mainly identified in tesserae of the chromatic groups aquamarine (AQ), pale green (VCH) pale blue (CE) from Aquileia and in an aquamarine sample from Pordenone; in addition relatively abundant relics of quartz and bubbles (although less abundant then in the previously described samples) were also identified in the azure sample BF AZ1,2,3 from Aquileia where quartz and bubbles relics are found in association with low quantity of other opacifiers as tin oxides.

XRPD performed on the whole tesserae allowed to identify quartz as the only mineralogical phase present in samples BF-AQ1 and BF-AQ 2 (aquamarine), BF-AZ1

(azure), BF-CE 2 (pale blue), BF-VCH 2, 3 (pale green) and in the aquamarine sample PN-AQ1, while sample BF VCH1 evidenced the presence of quartz and cristobalite.

- **Discussion**

Sporadic sand relic composed of quartz and K-feldspars and abundant gas bubbles are common textural features that were identified in almost all the tesserae here investigated.

Under the consideration that opacity is, together with colour, one of the main characteristic of a mosaic tessera, it is possible that sand relics and gas bubbles identified in large quantity are employed as intentional opacifiers.

All the tesserae here considered are semi-opaque, as the opacifying power of quartz and bubbles is less effective than that of antimony or tin based opacifiers; the majority of quartz+bubbles opacified glasses were found in the mosaic of Bestie Ferite in Aquileia. The presence of such abundant relics of sand is here considered as desired and probably deliberate on the basis of the consideration that Roman and Byzantine glassmakers were able to produce clear colourless glass; the presence of sporadic seed is common in mosaic tesserae, such abundance though is very uncommon; the contemporary presence of abundant gas bubbles also is unlikely to be unintentional

In the azure samples from Aquileia, some inclusion of tin oxide (in BF AZ1) and Ca-antimonates (BF-AZ 2,3,4) were also identified, but the density is too to act as opacifiers. while in the aquamarine samples BF AQ1,2, PN AQ1 and in the pale green and the pale blue BF-CE2 they represent the main opacifying agent, accompanied by sporadic inclusions of relic cassiterite

The addition of quartz in the form of sand is the more likely hypothesis for the tesserae here examined, as relics of K-feldspars and zircons were also identified (see next paragraph) and the shapes of the inclusion, that show sub-rounded rims, are not consistent with crushed materials.

The production technology of this opacification is unknown, in particular for what concerns bubbles production. The high quantity of gas bubbles indicates that they were produced at low temperature, when the melt was sufficiently viscous to trap gases; what caused the formation of abundant bubbles is not known; the presence of carbonatic

minerals in the sand is one of the possible explanations, although lime content of the samples is quite low and do not allow to take conclusions.

The large majority of quartz+ bubbles opacified glass was excavated in the mosaic of Aquileia, where truly opaque glass was also employed, therefore it is not possible to establish if the use of this uncommon technique was due to the need for opalescent tesserae for artistic purposes, or it was a consequence of the scarcity or cost of opaque glass. The mosaic is dated to the second half of the 4th century AD, and it is reasonable that antimony availability was decreasing, and its price probably increasing, therefore the presence of such uncommon and probably cheaper tesserae may be due also to economic reasons.

5.2.6 TEXTURAL FEATURES (OTHER INCLUSIONS)

- **INTRODUCTION**

Textural examination of the mosaic tesserae evidenced the presence of abundant relic and newly formed phases that do not act as opacifiers but can provide usefull information about the raw materials employed for primary glassmaking, colouring and opacification.

- **RESULTS AND DISCUSSIONS**

Sand relics

Sporadic inclusions of quartz and k-feldspars relics are common in mosaic tesserae here analysed: they are usually characterised by medium-large dimensions (up to several millimetres) irregular-rounded shape and are therefore interpreted as relic minerals.

Some tesserae show the presence of sporadic inclusion of relic crystals with very high atomic number and interpreted as zircons $ZrSiO_4$ (SEM-EDS data) (fig.5.37 -38)

Inclusions of zircons were identified pale green and pale blue tesserae BF VCH1,2,3, in the turquoise PN TU3 and in the dark amber TN NS1. It is to underline that, apart from the turquoise sample from Pordenone, the other tesserae showing zircon inclusion are characterised by the presence of very abundant sand relics such as quartz and k-feldspars, probably involved in the opacification of the glass (see paragraph "Quartz and bubbles")

and are consistent with the addition of sands in a secondary stage of production, to generate opacity in the glass.

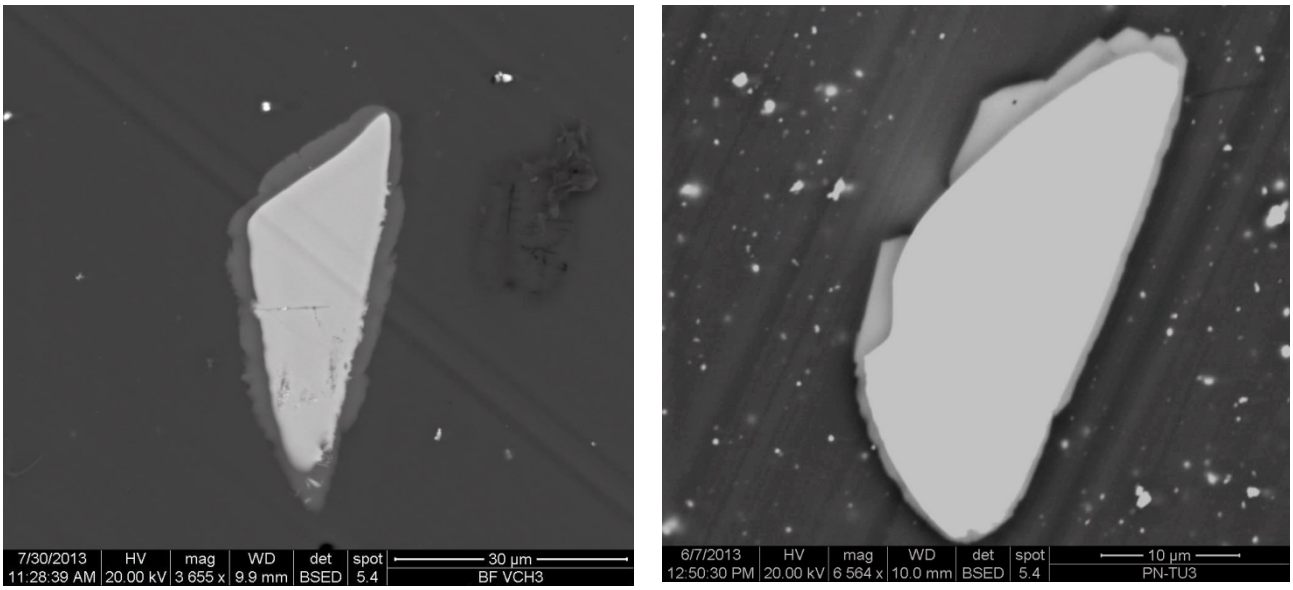

Fig.5.38:a-b: zircon crystal in a pale green tesserae from Aquileia (left) and in a turquoise tesserae from Pordenone (right). Note the partly reacted rim of the crystal wich shows the presence of sodium.

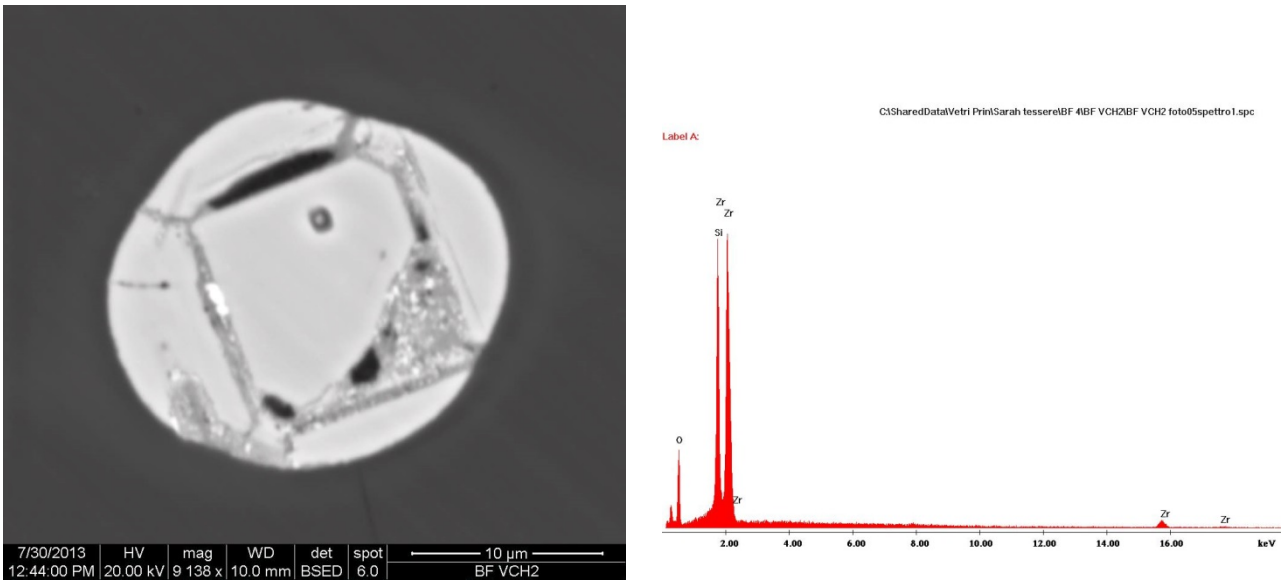

Fig.:5.37a-b: zircon crystal In a pale green tesserae from Aquileia and SEM EDS spectrum.

Very rare are Ca-phosphate relics (fig. 5.39): Ca-phosphate inclusions clustered with other sand relics were identified in BF GSO3 from Aquileia, TN GR1 and TN GR2, from Trento. The inclusion of sample presents an uncommon texture, characterised by an irregular

shape and a "spongy" structure, characterised by the presence of rounded-elongated regularly distributed on its surface and homogeneous in size. SEM-EDS data (fig 5.39 b) consistent with Ca-phosphate allow hypothesising that it is a bone relic, probably included with the sand (Fig.: 5.39) or a lime-bearing materials.

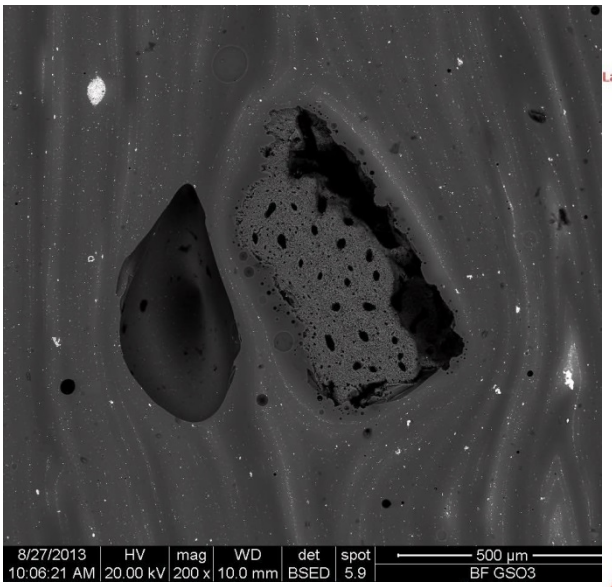

Fig.5.39: SEM-BSE image of a probable relic bone fragment in a yellow tesserae from Aquileia. Note the sponged structure and the low average atomic number.

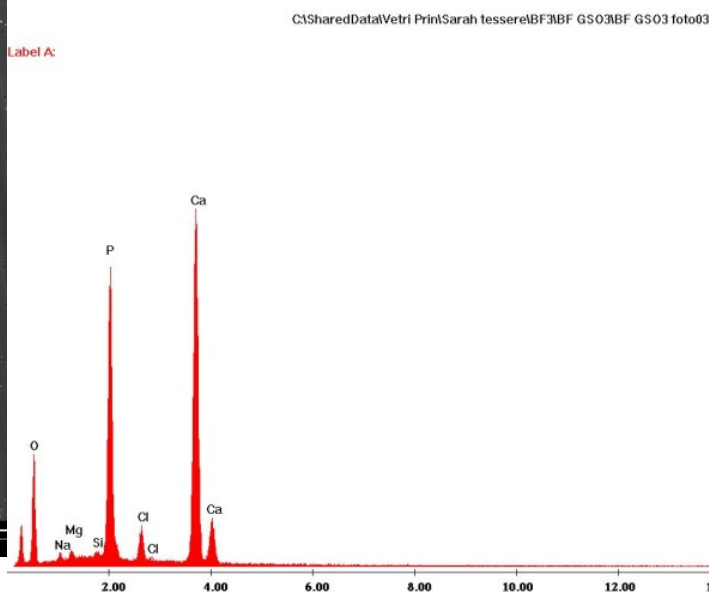

Fig5.39b : SEM-EDS spectrum acquired on the inclusion, consistent with a Ca-phosphate.

Metallic drops and copper-rich inclusions

Sporadic inclusion of gold, copper, silver, lead, and antimony in the form of various alloys were seldom detected in copper coloured tesserae (BF TU TR1, BF VS1, PN AV1,2; BF M3). Fig (5.40).

More frequent are drops of metallic copper or copper oxide in association with copper sulphide (probably chalcocite, Cu_2S according to SEM EDS data) (Fig 5.41-43), antimony and/or lead (Fig 5.41-5.45), reported in red, brown and orange tesserae from all the sites.

In particular relics of presumed chalcocite were identified in the brown tesserae (TN M1,2,3, BF M1,2,4, PN M1), in the olive/red (TN VOLl1) in the dark amber (TN NS1), yellow-green (TN VG2), dark green (BF VS2), pale green (BF VCH1,2) and pale blue (BF CE2) and suggests the use of copper minerals as a source of copper, although the use of different copper-rich materials at the same time must be taken into account.

In the brown BF M3 the presence of prills of copper,gold and silver suggests the use of metalworking scraps probably as copper bearing materials while in the dark green BF VS2 the addition of an alloy is testified by the presence of a relic of gold-silver copper alloy(Fig. 5.40)

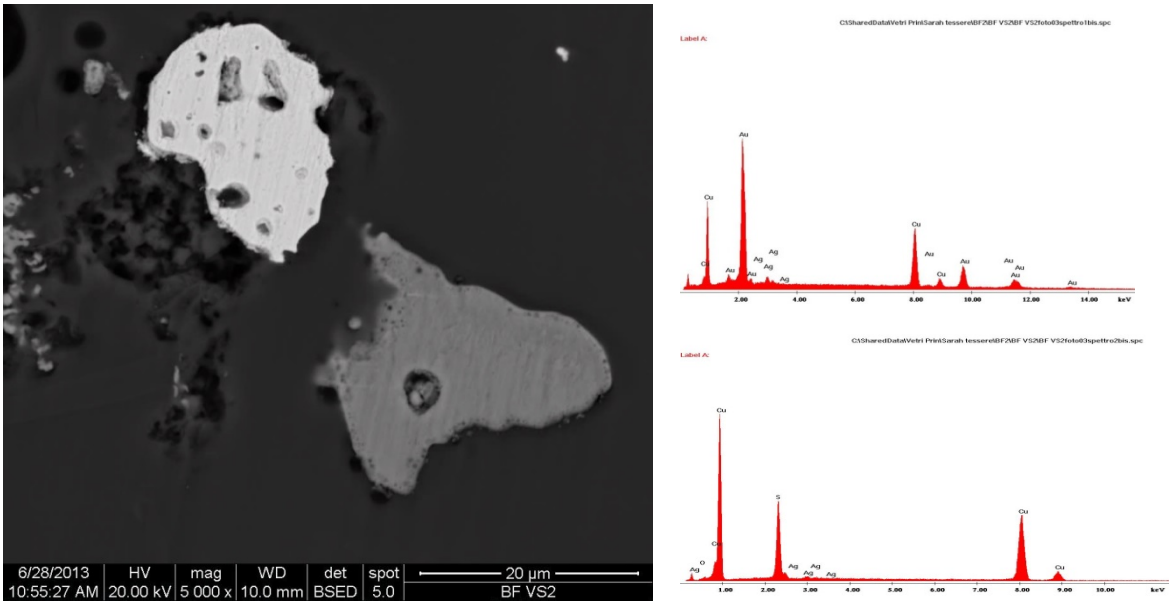

FIG:5.40 SEM BSE Image of a dark green tessera: the white inclusion is gold-silver copper alloy Au:Ag:Cu= 61:4:35, while the grey one is a probable chalcocite inclusion(SEM EDS data)

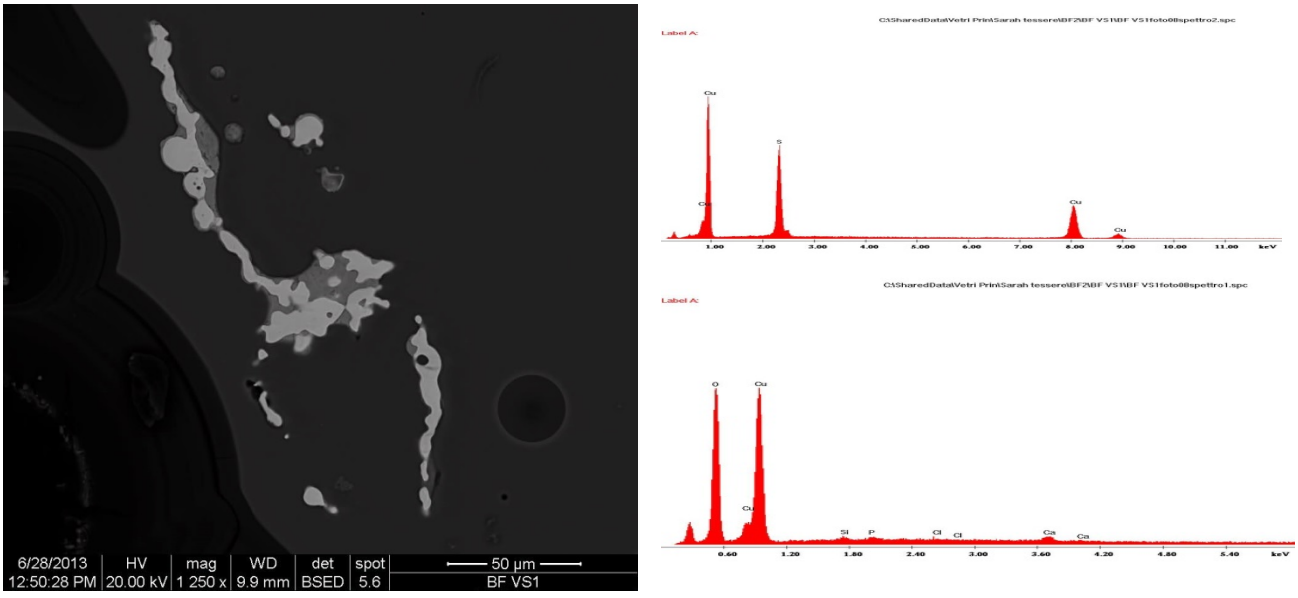

Fig. 5.41copper-rich inclusion in a dark green tesserae from Aquileia: relic of probable chalcocite (white) associated with copper oxide (grey) and SEM EDS spectra

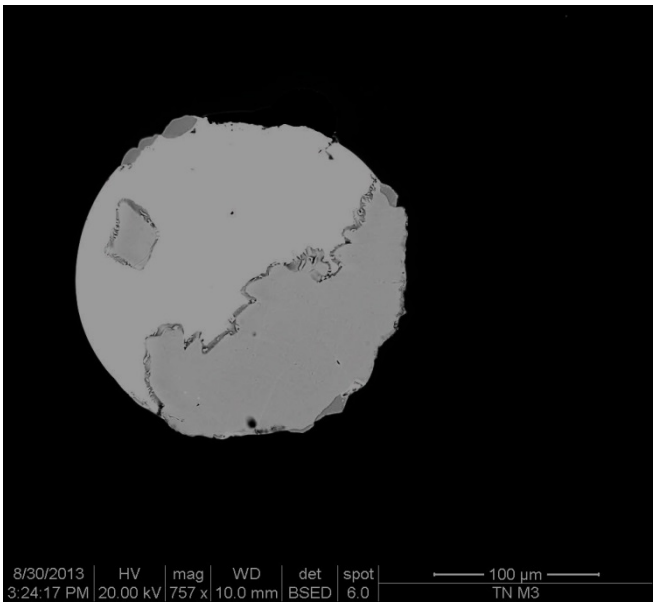

FIG.:5.42 *high-contrast image of a copper-rich segregated droplet in a brown tesserae from Trento: the grey zones (1) are made of metallic copper and the white zones (2) are made of lead.*

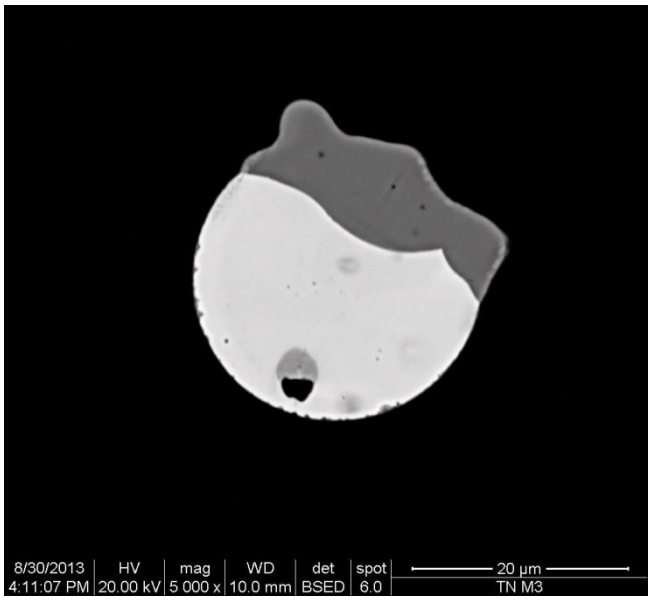

FIG.5.43*: high-contrast image of a copper-rich segregated droplet in a brown tesserae from Trento: the grey zone is probably chalcocite, the white zone a copper-antimony alloy (Cu:Sb= 90:10)*

Cassiterite and malayaite

Relics of tin oxide, probably interpreted as cassiterite SnO_2 (EDS data) are relatively frequent and were detected in almost all the copper coloured and in the tin-opacified tesserae: BF Ce1,2; BF VCH1,2,3; BF TU1, BF AQ1,BF VG1, BF VP2; Pn CE1, PN TU3, PN AQ1,PN AV1,2; TN BS1, TN AQ1, TN TU3, TN AV1, TN VG2, TN VOl1, TN VS1.

Inclusions of cassiterite are sporadic, generally constituted by small flakes and occasionally small clusters (Fig. 5.45). In the case of copper-coloured turquoise samples, cassiterite is probably introduced with the copper-bearing mineral while in the case of orange/red/brown samples, it might represent one of the tin-bearing materials employed to add tin as internal reducing agent. Sample BF AZ1, opacified with quartz and bubbles, contains abundant inclusions of tin oxide that, even though too rare to be considered as intentional opacifiers, are more frequent than usual, suggesting that the tessera is derived from the mixing of different glasses coloured/opacified with different techniques.

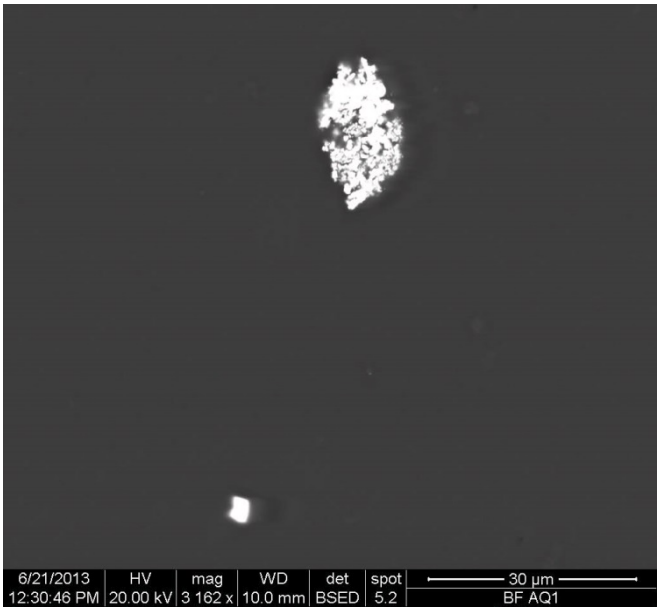

Fig.:5.44 probable relics of cassiterite in aquamarine tesserae BF AQ1 (white clusters)

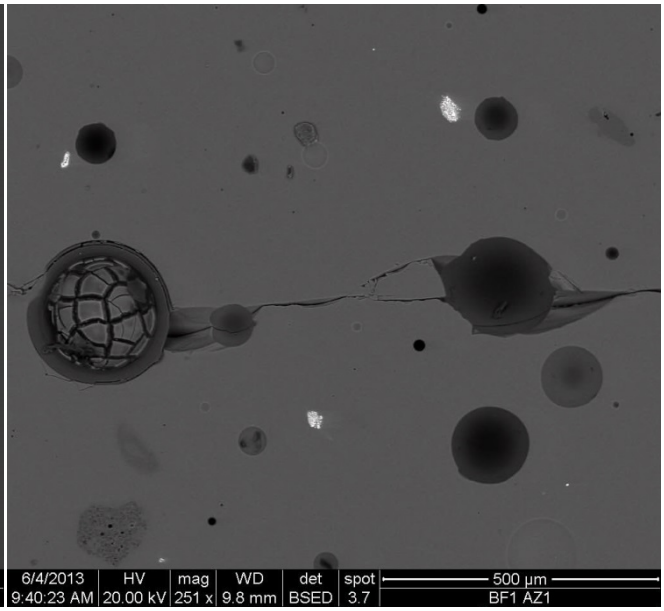

Fig.:5.45 probable relics of cassiterite in BF AZ1 (white clusters) and quartz (grey) and bubbles (rounded black)

In copper and tin-rich samples TN TU3, TN AV1, TN VOL1, TN VOL2; PN AV1, PN AV2 cassiterite was seldom detected in presence of euhedral crystals of relatively high atomic number, (see fig 5.46-47) and interpreted as newly-formed malayaite $CaSnSiO_5$ by means of SEM_EDS DATA and micro Raman spectroscopy (fig 5.48a-b)

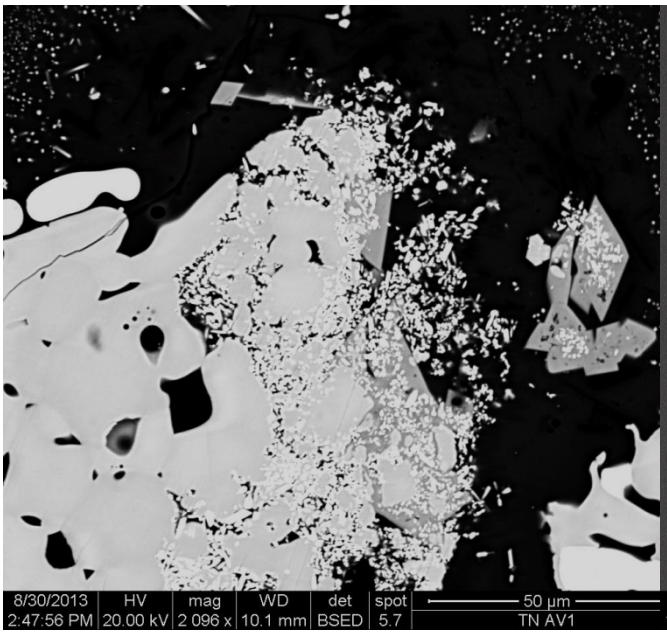

Fig::5.46 sem BSE image (high contrast) of an orange sample from Trento: large globular incusions of copper oxide (white) small crystals of tin oxide probably SnO2 (small bright flakes) and euhedral crystals of newly-formed malayaite CaSnSiO3 (grey). The glassy matrix is here black. The small bright dots at the border of the image are cuprite crystals

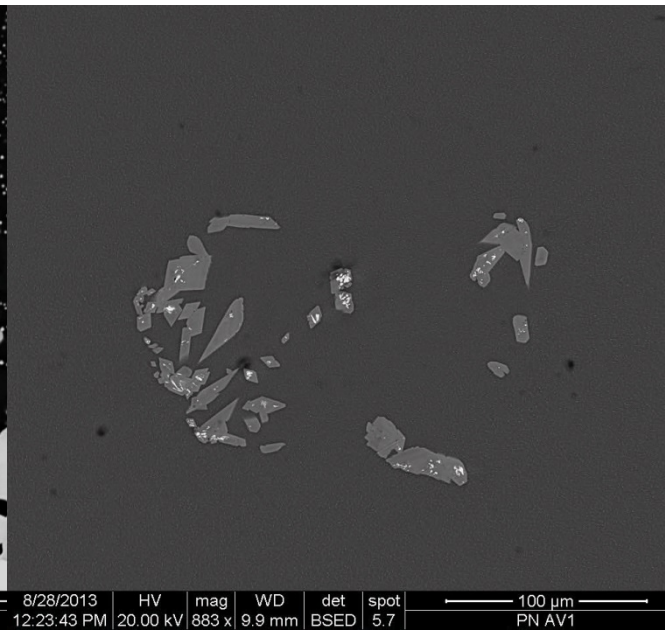

Fig5.47:: sem BSE image (high contrast) of an orange sample from Pordenone: small flakes of tin oxide (small bright flakes) and euhedral large crystals of newly-formed malayaite CaSnSiO5 (grey).

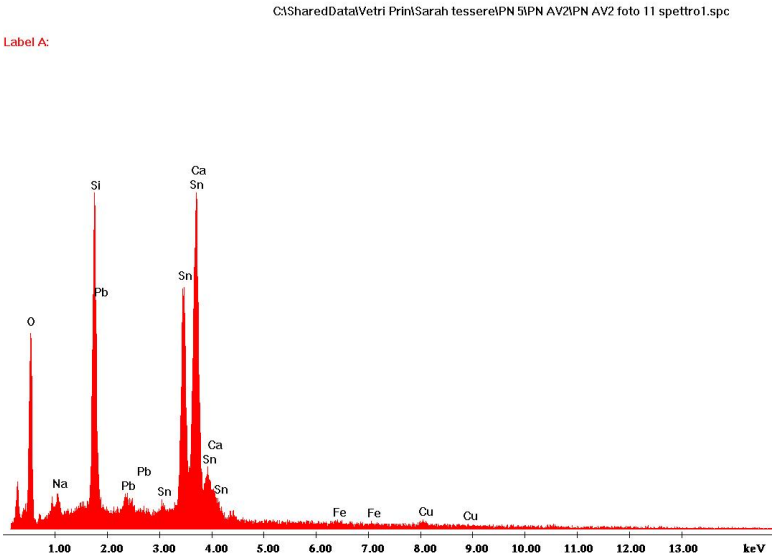

Fig.:5.48a (left) SEM-EDS spectrum of Malayaite (fig. 5.47)

Fig.:5.48b (below)Raman spectrum: of malayaite (fig. 5.47)in blue; reference spectrum of malayaite from RUFF mineralogical database in red.

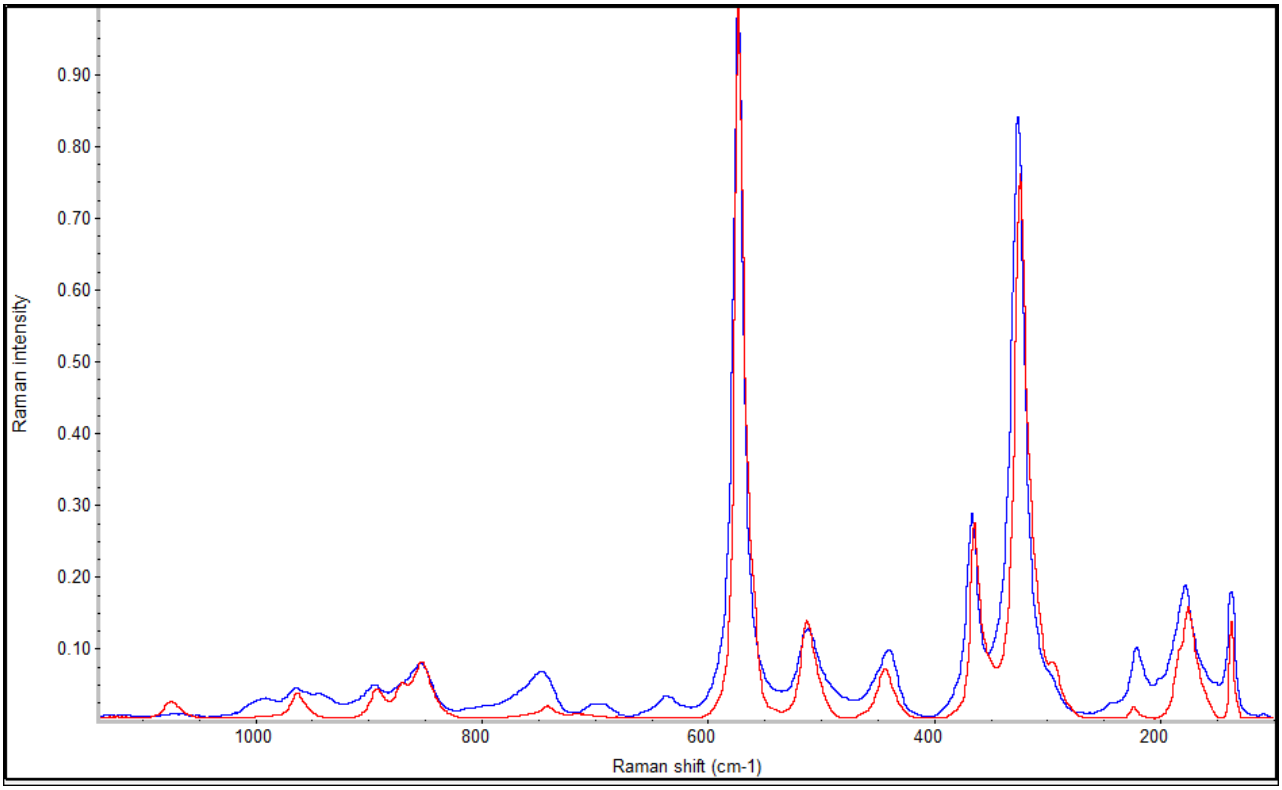

Chromatic group	Site	Label	n	Glassy matrix	Opacifier/ pigment	Colourant/ decolourizer
Dark blue	BF	BS	1	Soda-lime	*none*	copper
	TN		1			
	PN		1			
Opaque blue	BF	B	1	Soda-lime	Ca-antimonates	cobalt
	TN	BO	1			
	PN		1			
Translucent blue	*BF*	-	-	Soda-lime	-	-
	TN	B	1		*none*	cobalt
	PN	-	-		-	-
Azure	BF	AZ	3	Soda-lime	Quarz+bubbles	cobalt
			2		Ca-antimonates	
	TN		1			
	PN		2			
Pale blue	BF	CE	1	Soda-lime	Quarz+ bubbles	copper
			1		Ca-antimonates	
	TN		1			
	PN		1			
Turquoise opaque	BF	TU	1	Soda-lime	Ca-antimonates	copper
	TN		2			
	PN		1	Soda-lead		
			2	Soda-lime		
Turquoise translucent	BF	TU TR		Soda-lime	*none*	copper
	TN	-	-	-	-	-
	PN	-	-	-	-	-
Aquamarine	BF	AQ	2	Soda-lime	Quarz+bubbles	copper
	TN		1		Ca-antimonates	
	PN		1		Quarz+bubbles	
Dark green opaque	BF	VS	1	Soda-lime	Pb-stannate	copper
	TN		1			
	PN		1	Soda-lead	Pb- antimonate	
Dark green translucent	BF	VS1	1	Soda-lime	*none*	copper
	TN		1			
	PN	V TR	2	Soda-lead		iron
Green	BF	VP	2	Leaded	Pb-stannate	copper
			2	Soda-lead		
	TN		2		Pb-Sn-antimonate	
	PN		1		Pb-antimonate	
Pale green	BF	V CH	3	Soda-lime	Quartz+bubbles	copper
	TN		1			
	PN		1		Ca-antimonate	
Olive green	BF	-		-	-	-
	TN	VOL	1	Soda-lime	none	copper
	PN	-	-	-	-	-
Yellow-green	BF	VG		Soda-lead	Pb-stannate	iron
	TN			Soda-lead		iron+ copper
	PN		1	Soda-lead	Pb-antimonate	iron
	BF		3	Soda-lead	Pb- antimonate	-

Yellow		GSO	1	leaded	Pb- stannate	
	TN		2	Soda-lead		-
	PN		1	leaded	Pb-antimonate	
			1	Soda-lead	Pb-Sn antimonate	-
Pale amber	BF	-	*0*	-	-	-
	TN	-	*0*	-	-	-
	PN	NC	1	Soda-lead		iron
Orange	BF	AV	1	leaded	Cuprite	-
	TN		1	Soda-lead		
	PN		2	leaded		
Red	BF	R	1	Soda-lead	Metallic copper	-
	TN	-	-	-	-	
	PN	-	-	-	-	
Brown	BF	M	3	Soda-lime	Metallic copper	-
			1	Soda-lead		
	TN		3			
	PN		2			
Dark amber	BF	-	-		-	-
	TN	NS	1	Soda-lead	Metallic copper	-
	PN	-	-		-	-
Olive/red	BF	-			-	-
	TN	TN VOL1	1		Metallic copper	copper
	PN	PN M3	1	leaded		copper
Grey	BF	GR	1	Soda-lime	Ca-antimonates	-
	TN		2			
	PN		1			
White	BF	-	*0*		-	-
	TN	BI OP	1	Soda-lime	Ca-antimonates	-
	PN		1	Soda-lead		
Colourless	BF	TRINC	1	Soda-lime	none	Mn+Sb
	TN		1			none
			1			Sb
	PN	-	-		-	-
Gold	BF	AU	1	Soda-lime	none	Mn+Sb
	TN		1			-
	PN	AU,AG	3			Mn

A summary of the different chemical and textural features is reported in table 5. 7.

On the basis of the chemical and mineralogical evidences, direct comparisons among the three sites can be made.

A high degree of comparability was evidenced in the tesserae of chromatic groups dark blue (BS), Blue (BO) and grey (GR), that in the three site present comparable glassy matrices, chromoforic ions and opacifying phases.

A medium degree of comparability is highlighted in the chromatic groups azure (AZ), pale green (VCH), pale blue (CE), aquamarine (AQ) that differ mainly for their opacifying phase that in Aquileia is quartz and bubbles, while in the other sites is Ca-antimonate; the chromatic groups orange (AV), turquoise (TU), brown (M), olive red (PN M3 and TN VOL1) differ for their glassy matrices. A very low degree of comparability is highlighted in the chromatic groups dark green, green, yellow green and green, that present different opacifying phases and glassy matrices in the three site and seldom within a single site too.

5.2.7 GLASS TESSERAE- CONCLUSIONS

The study of three assemblages of glass tesserae excavated in north-eastern Italian sites provided a unique insight into glass-and glassmaking between the 2nd ad the 5th century AD.

As expected for Roman and late roman tesserae, most of the sample are a silica soda-lime base glass produced with natron as a flux. Sample from Pordenone and Trento seem to be made with Roman base-glass composition, while in a group from Aquileia some signs of Later glass compositions are visible, in most of the cases corresponding to uncommon or new opacifying techniques.

The most common chromophoric element identified is copper, responsible for the turquoise, aquamarine, pale blue, pale green, dark blue transulcent, green, and part o f the dark green and, when in the form of copper oxide or metallic copper, of the red, orange and brown tesserae. Cobalt is responsible for the blue and azure colour of the tesserae.

The copper or cobalt coloured blue-green tesserae are generally opacified with Ca-antimonate, with the exception of those from Aquileia where of some pale blue, azure, aquamarine and pale green samples are partly opacified with sand relics and gas bubbles and partly with other compounds, indicating a probable practise of glass recycling.

Lead-antimonate are responsible for the colouring and opacity of yellow tesserae from Aquileia and Pordenone, green tesserae from Pordenone; one yellow tessera and all the green and dark green from Aquileia are opacified with lead-stannate while in Trento samples and in one yellow from Pordenone, lead-tin antimony oxides are identified.

Cuprite is responsible for the orange and the red stripes in high lead, plant ash glasses, while in the low-lead glass metallic copper was identified as responsible for red and brown colours.

The presence of cross-craft interaction between metalworking and glassmaking was investigated: copper alloys were probably employed as colouring elements in some copper-coloured tesserae, and metallurgical slags were added in brown samples from Aquileia, probably with the intention of introducing iron and/or copper.

Each assemblage seems to have some specific compositional and technological traits: differently from those of Pordenone and Aquileia, copper coloured tesserae from Trento do not contain zinc in detectable levels (apart from a very high copper sample); yellow and green tesserae are coloured and opacified with different yellow pigments in each site and azure, pale green, aquamarine and pale blue tesserae from Aquileia show a specific and uncommon opacification technique, with sand relics and gas bubbles.

Among the three assemblages Aquileia shows the higher degree of internal variability in terms of glassy matrices and opacifiers and the prompt reception of technological innovations (as the tin-base opacifiers), that co-exist with the Roman tradition of calcium or lead antimonate and uncommon technological solutions, such as the addition of slags to copper red tesserae, and the opacification with quartz and bubbles.

REFERENCES

Ahmed, A. A., and Ashour, G. M., 1981, Effect of heat treatment on the crystallisation of cuprous oxide in glass, *Glass Technology*, **22**, 24–33.

Arletti, R., Fiori, C., and Vandini, M., 2010, A study of glass tesserae from mosaics in the monasteries of Daphni and Hosios Loukas (Greece), *Archaeometry*, **52**(5), 796–815.

Bamford, C. R., 1977, *Colour Generation and Control in Glass*, Vol. 3, Elsevier Scientific Publishing Company, Amsterdam-Oxford-NewYork.

Barber, D. J., Freestone, I. C., and Mpulding, K. M., 2003, Ancient copper red glasses: investigation and analysis by microbeam techniques, In *From mine to microscope. Advances in the study of ancient technology* (eds. A. J. Shortland, I. C. Freestone, and T. Rehren), 115–27.

Bayley, J., 2005, Roman enamel and enamelling: new finds from Castelford, Yorkshire, In *Annales du 16e Congrès de l'Association International pour l'Histoire du verre*, Vol. London, 72–5, Nottingham.

Brems, D., Degryse, P., Hasendocks, F., Gimeno, D., Silvestri, A., Vassilieva, E., Luypaers, S., and Honings, J., 2012, Western Mediterranean sand deposits as a raw material for Roman glass production, *Journal of Archaeological Science*, **39**, 2897–907.

Brill, R. H., and Cahill, N. D., 1988, A red opaque glass from Sardis and some thoughts on red opaques in general, *Journal of Glass Studies*, **30**, 16–27.

Brill, R. H., and Whitehouse, D., 1988, The Thomas Panel, *Journal of Glass Studies*, **30**, 34–50.

Brill, R. H., 1999, *Chemical analyses of Early Glasses*, Corning Museum of Glass, Corning, NY.

Cable, M., and Smedley, J. W., 1992, The replication of an opaque red glass from Nimrud, In *Early Vitreous materials* (eds. M. Bimson, and I. C. Freestone), 151–64, British Museum Occasional paper 56, London.

Cascales, C., Alonso, J. A., and Rasines, I., 1986, NEW PYROCHLORES Pb//2(MSb) O//6//. //5 (M equals Ti,Zr,Sn,Hf)., *Journal of Materials Science Letters*, **5**(6), 675–7.

Clark, R. J. H., Cridland, L., Kariuki, B. M., Harris, K. D. M., and Withnall, R., 1995, Synthesis, structural characterisation and Raman spectroscopy of the inorganic pigments lead tin yellow types I and II and lead antimonate yellow: Their identification on medieval paintings and manuscripts, *Journal of the Chemical Society, Dalton Transactions*(16), 2577–82.

Conventi, A., Neri, E., and Verità, M., 2012, SEM-EDS analysis of ancient gold leaf glass mosaic tesserae. A contribution to the dating of the materials, In *IOP Conference Series: Materials Science and Engineering*, Vol. 32.

Ferrer, P., Ruiz-Moreno, S., Lopez-Gil, A., Chillon, M. C., and Sandalinas, C., 2012, New results in the characterization by Raman spectroscopy of yellow pigments used in ceramic artworks of the 16th and 17th centuries, *Journal of Raman Spectroscopy*, **43**(11), 1805–10.

Fiori, C., Vandini, M., and Mazzotti, V., 2004, *I colori del vetro antico. Il vetro musivo bizantino*, Il prato, Padova.

Foster, H. E., and Jackson, C. M., 2009, The composition of "naturally coloured" late Roman vessel glass from Britain and the implications for models of glass production and supply, *Journal of Archaeological Science*, **36**(2), 189–204.

Foster, H. E., and Jackson, C. M., 2010, The composition of late Romano-British colourless vessel glass: glass production and consumption, *Journal of Archaeological Science*, **37**(12), 3068–80.

Freestone, I. C., 1987, Composition and microstructure of copper opaque red glass, In *Early vitreous material. British Museum Occasional Paper, 56* (eds. M. Bimson, and I. C. Freestone), 173–91, British Museum, London.

Freestone, I. C., Bimson, M., and Buckton, D., 1990, Compositional categories of Byzantine Glass tesserae, In *Annales du 11e Congrés de l'Association Internationale pour l'Histoire du Verre, Bâle, 29 aout-3 septembre 1988 (1990 Amsterdam)*, Vol. Basel- Swi, Amsterdam.

Freestone, I. C., Stapleton, C. P., and Rigby, V., 2003, The production of red glass and enamel in the late Iron Age, Roman and Byzantine periods, In *Trought a glass brightly: studies in Byzantine and Medieval art and archaeology presented to David Buckton* (ed. C. Entwistle), 142–55, Oxbow Books, Oxford.

Freestone, I. C., and Stapleton, C. P., 2003, The production of red glass and enamel in the Late Iron Age, Roman and Byzantine periods., In *Throught a glass brightly-studies in Byzantine and Medieval Art and Archaeology presented to David Buckton* (ed. C. Entwistle), Vol. Izmir, 142–54, Oxbow, Oxford.

Freestone, I. C., 2006, Glass production in Late Antiquity and the Early Islamic period: a geochemical perspective, *Geological Society, London, Special Publications*, **257**(1), 201–16.

Gliozzo, E., Santagostino Barbone, A., Dacapito, F., Turchiano, M., Memmi, I., and Volpe, G., 2008, The sectilia panels of Faragola (Ascoli Satriano, Italy): a multi-analytical study of the red, orange and yellow glass slabs, *Archaeometry*, **50**(3), 451–73.

Gliozzo, E., Santagostino Barbone, A., Turchiano, M., Memmi, I., and Volpe, G., 2012, The coloured tesserae decorating the vaults of the Faragola balneum (Ascoli Satriano, Foggia, southern Italy), *Archaeometry*, **54**(2), 311–31.

Gratuze, B., Soulier, I., Barrandon, J. N., and Foy, D., 1992, De l'origine du cobalt dans les verres, *Revue d'Archéométrie*, **16**, 97–108.

Guido, M., Henderson, J., Cable, M., Bayley, J., and Biek, L., 1984, A bronze age glass bead from Wilsford Whilshire, In *Proceeding of the Prehistoric Society* (eds. T. C. Champion, and E. J. G), 245–54, The Prehistoric Society.

Heck, M., and Hoffmann, P., 2000, Coloured opaque glass beads of the Merovingians, *Archaeometry*, **42**(2), 341–57.

Heck, M., Rehren, T., and Hoffmann, P., 2003, The production of lead-tin yellow at merovingian schleitheim (Switzerland), *Archaeometry*, **45**(1), 33–44.

Henderson, J., 2000, *The Science and Archaeology of Materials: An Investigation of Inorganic Materials*, Vol. 106, Routledge.

Hradil, D., Grygar, T., Hradilová, J., Bezdicka, P., Grunwaldová, V., Fogaš, I., and Miliani, C., 2007, Microanalytical identification of Pb-Sb-Sn yellow pigment in historical European paintings and its differentiation from lead tin and Naples yellows, *Journal of Cultural Heritage*, **8**(4), 377–86.

Jackson, C. M., 2005, Making colourless glass in the Roman period, *Archaeometry*, **47**(4), 763–80.

Jacson, C. M., 2005, Making colourless glass in the Roman period, *Archaeometry*, **47**(4), 763–80.

Lahlil, S., Biron, I., Galoisy, L., and Morin, G., 2008, Rediscovering ancient glass technologies through the examination of opacifier crystals, *Applied Physics A*, **92**(1), 109–16.

Lahlil, S., Biron, I., Cotte, M., Susini, J., and Menguy, N., 2009, Synthesis of calcium antimonate nano-crystals byÂ theÂ 18thÂ dynasty Egyptian glassmakers, *Applied Physics A*, **98**(1), 1–8.

Lahlil, S., Biron, I., Cotte, M., and Susini, J., 2010, New insight on the in situ crystallization of calcium antimonate opacified glass during the Roman period, *Applied Physics A*, **100**(3), 683–92.

Lahlil, S., Cotte, M., Biron, I., Szlachetko, J., Menguy, N., and Susini, J., 2011, Synthesizing lead antimonate in ancient and modern opaque glass, *Journal of Analytical Atomic Spectrometry*, **26**(5), 1040–50.

Lilyquist, C., and Brill, R. H., 1993, *Studies in Early Egyptian Glass*, Metropolitan Museum of Art, New York.

Mass, J. L., Stone, R. E., and Wypyski, M. T., 1998, The mineralogical and metallurgical origins of Roman opaque colored glasses, In *The prehistory and history of glassmaking technology, ceramics and civilazation* (eds. W. D. Kingery, and P. McCray), 121–44, The American Ceramic Society, Ohio.

Mass, J. L., Wypyski, M. T., and Stone, R. E., 2002, Malkata and Lisht glassmaking technologies: towards a specific link between second millenium BC metallurgists and glassmakers, *Archaeometry*, **44**(1), 67–82.

Mirti, P., Davit, P., and Gulmini, M., 2002, Colourants and opacifiers in seventh and eighth century glass investigated by spectroscopic techniques, *Analytical and bioanalytical chemistry*, **372**(1), 221–9.

Molina, G., Odin, G. P., Pradell, T., Shortland, A. J., and Tite, M. S., 2014, Production technology and replication of lead antimonate yellow glass from New Kingdom Egypt and the Roman Empire, *Journal of Archaeological Science*, **41**, 171–84.

Neri, E., and Verità, M., 2013, Glass and metal analyses of gold leaf tesserae from 1st to 9th century mosaics. A contribution to technological and chronological knowledge, *Journal of Archaeological Science*, **40**(12), 4596–606.

Nicholson, P. T., Jackson, C. M., and Trott, K. M., 1997, The Ulu Burun Glass Ingots, Cylindrical Vessels and Egyptian Glass, *The Journal of Egyptian Archaeology*, **83**, 143–53.

Peake, J. R. N., and Freestone, I. C., 2012, Cross-craft interactions between metal and glass working: slag additions to early Anglo-Saxon red glass, **8422**, 842204.

Peake, J. R. N., 2014, Early Anglo-Saxon glass beads: composition and origins based on the finds from RAF Lakenheat, Suffolk, , Cardiff University.

Rooksby, H. P., 1964, A yellow cubic lead tin oxide opacifier in ancient glasses, *The phisics and chemistry of glasses*, **5**, 20–5.

Ruffini, A., Fiori, C., and Vandini, M., 1999, Chemical characterisation of ancient mosaic glasses Caratterizzazione chimica di vetri musivi antichi. Parte 2: Elaborazione dei dati analitici], *Ceramurgia*, **29**(5-6), 361–8+i.

Sandalinas, C., and Ruiz-Moreno, S., 2004, Lead-tin-antimony yellow: Historical manufacture, molecular characterization and identification in seventeenth-century italian painting, *Studies in Conservation*, **49**(1), 41–52.

Sandalinas, C., Ruiz-Moreno, S., López-Gil, A., and Miralles, J., 2006, Experimental confirmation by Raman spectroscopy of a Pb-Sn-Sb triple oxide yellow pigment in sixteenth-century Italian pottery, *Journal of Raman Spectroscopy*, **37**(10), 1146–53.

Sayre, E. V, and Smith, R. W., 1961, Compositional categories of ancient glass, *Science*, **133**(3467), 1824–6.

Schibille, N., Degryse, P., Corremans, M., and Specht, C. G., 2012, Chemical characterisation of glass mosaic tesserae from sixth-century Sagalassos (south-west Turkey): Chronology and production techniques, *Journal of Archaeological Science*, **39**(5), 1480–92.

Shortland, A. J., 2002a, The use and origin of antimonate colorants in Early Egyptian glass, *Archaeometry*, **44**(4), 517–30.

Shortland, A. J., 2002b, The use and origin of antimonate colorants in early Egyptian glassâ€¢, *Archaeometry*, **44**(4), 517–30.

Shortland, A. J., Tite, M. S., and Ewart, I., 2006, ANCIENT EXPLOITATION AND USE OF COBALT ALUMS FROM THE WESTERN OASES OF EGYPTâ€¢, *Archaeometry*, **48**(1), 153–68.

Shortland, A. J., Rogers, N., and Eremin, K., 2007, Trace element discriminants between Egyptian and Mesopotamian Late Bronze Age glasses, *Journal of Archaeological Science*, **34**(5), 781–9.

SHUGAR, A. N., 2000, BYZANTINE OPAQUE RED GLASS TESSERAE FROM BEIT SHEAN, ISRAEL*, *Archaeometry*, **42**(2), 375–84.

Silvestri, A., Molin, G., and Salviulo, G., 2008, The colourless glass of Iulia Felix, *Journal of Archaeological Science*, **35**(2), 331–41.

Silvestri, A., Tonietto, S., and Molin, G., 2011, The palaeo-Christian glass mosaic of St. Prosdocimus (Padova, Italy): Archaeometric characterisation of "gold" tesserae, *Journal of Archaeological Science*, **38**(12), 3402–14.

Silvestri, A., Tonietto, S., Molin, G., and Guerriero, P., 2012a, The palaeo-Christian glass mosaic of St. Prosdocimus (Padova, Italy): Archaeometric characterisation of tesserae with antimony- or phosphorus-based opacifiers, *Journal of Archaeological Science*, **39**(7), 2177–90.

Silvestri, A., Tonietto, S., D'Acapito, F., and Molin, G., 2012b, The role of copper on colour of palaeo-Christian glass mosaic tesserae: An XAS study, *Journal of Cultural Heritage*, **13**(2), 137–44.

Silvestri, A., Tonietto, S., Molin, G., and Guerriero, P., 2014a, The palaeo-Christian glass mosaic of St. Prosdocimus (Padova, Italy): Archaeometric characterisation of tesserae with copper- or tin-based opacifiers, *Journal of Archaeological Science*, **42**(1), 51–67.

Silvestri, A., Tonietto, S., Molin, G., and Guerriero, P., 2014b, The palaeo-Christian glass mosaic of St. Prosdocimus (Padova, Italy): Archaeometric characterisation of tesserae with copper- or tin-based opacifiers, *Journal of Archaeological Science*, **42**(1), 51–67.

Tite, M. S., 2003, Production technology for copper-and cobalt-blue vitreous materials from the New Kingdom site of Amarna- a reappraisal., *Archaeometry*, **2**.

Tite, M. S., Pradell, T., and Shortland, A. J., 2008, Discovery, production and use of tin-based opacifiers in glasses, enamels and glazes from the late iron age onwards: A reassessment, *Archaeometry*, **50**, 67–84.

Turner, W. E. S., and Rooksby, H. P., 1959, A study of the opalising agents in ancient glasses throughout three thousand four hundred years, *Glastechnische Berichte*(8), 17–28.

Verità, M., and Vallotto, M., 1998, Analisi chimica di reperti vitrei del IV secolo dC rinvenuti a Sevegliano (Udine), *Quaderni Friulani di Archeologia*, **8**, 7–19.

Verità, M., 2000, Tecniche di fabbricazione dei materiali musivi vitrei. Indagini chimiche e mineralogiche., In *Medieval Mosaics. Light,color, materials* (eds. E. Borsook, F. Gioffredi Superbi, and G. Pagliarulo), Silvana Editoriale, Cinisello Balsamo (MIlano).

Verità, M., and Vallotto, M., 2003, Analisi delle tessere musive, In *Il mosaico di Santa Punziana a Roma. Il restauro* (ed. V. Tiberia), 178–99, Ediart, Todi.

Verità, M., 2006, Tessere vitree a foglia d'oro nei mosaici di Aquileia, *Quaderni Friulani di Archeologia*, **16**, 7–12.

Verità, M., Maggetti, M., Sagui, L., and Santopadre, P., 2013, Colors of roman glass: An investigation of the yellow sectilia in the gorga collection, *Journal of Glass Studies*, **55**, 39–52.

Vezzalini, G., Fiori, C., and Vandini, M., 2011, Mosaic Glass From St Peter'S, Rome: Manufacturing Techniques and Raw Materials Employed in Late 16Th-Century Italian Opaque Glass, *Archaeometry*, **53**(2), 364–86.

Welham, K., Jackson, C. M., and Smedley, J. M., 1998, Colour formation in sealing wax red glass, In *Annales du 14e Congrès de l'Association International pour l'Histoire du Verre*, Vol. Venezia-Mi, 11–5.

Wypyski, M. T., and Becker, L., 2005, Glassmaking technology at Antioch, In *The arts of Antioch* (eds. L. Becker, and C. Kondoleon), 116–75, Worchester Art Museum, Worchester.

CONCLUDING REMARKS

The present study, focused on north-eastern Italian glass between Roman times and late Antiquity, has shed light on the raw materials, production technologies and reception of the innovations in the area

Differently from the approach usually employed in archaeometric studies of ancient glass, vessels and mosaic tesserae were investigated in parallel with the aim of highlighting any common features or differences between the raw materials, and the production technologies employed in the two classes of materials.

The methodological approach employed involved an articulated set of analytical techniques that were selected in order to guarantee high standards of accuracy and precision of the measurements and an accurate and exhaustive characterisation of the samples.

The examination of vessels and glass-working indicators highlighted the great comparability of the two north Adriatic harbours of Classe and Aquileia in terms of glass composition and provenance of raw materials, indicating that the two cities in the Late Antiquity were supplied from the same eastern Mediterranean locations and their glass provisions were probably aimed for similar consumption markets. Poor evidences for glass recycling suggest that the two cities were regularly supplied with fresh glass, mostly of HIMT and Sèrie 3.2 composition; Levantine1 glass, is less present in both cities, though still available. The finding of vessels, glassworking wastes and chunks of similar composition supports the hypothesis of a local glassworking activity in both Classe and Aquileia.

Archaeological and analytical evidences suggest that, probably, HIMT primary furnaces also produced intentionally-coloured blue glass. This evidence, in contrast with what was usually reported for coloured glass, suggests that the addition of colouring elements did not take place in secondary workshops only, and that coloured blue glass was produced and commercialized in the form of chunks also in the Late Antiquity.

The glass tesserae assemblages here analysed show a strong link with the early Roman glass technology in terms of base glass and opacifying techniques. The tesserae from Aquileia, however, show a greater degree of internal variability that include some uncommon opacifying techniques, probably referable to the Late Antiquity, associated with a base glass composition not entirely consistent with the early Roman ones.

Deeply coloured and opaque glass employed in vessels and mosaic tesserae of comparable colour evidenced a substantial homogeneity of colouring/opacifying techniques and glass composition, in particular in the case of blue, yellow, red, green and white glass,

confirming the hypothesis that mosaic *tesserae* and vessels were produced with the same materials.

The gradual decrease of the use of antimony in the 4th century in both decolouring and opacifying, and the rise of new compositional groups of glass are well represented in the Aquileian assemblages, which highlights a prompt reception of the new glass composition and technological innovations and confirms the role of the city as a cultural outpost in the Mediterranean Late Antique world.

APPENDIX A1

Glass finds from the Domus of Tito Macro (Fondi Ex Cossar).

CHUNKS

IG: 545559 AQ-FC-PV_1

Site: “Fondi ex Cossar” - Aquileia (UD)	Year : 2010	US: 3061	
N fragments 1	N. objects: 1		
	green		
Dimensions: H 4,5; L 4,6 cm	Weight: 28,97 g	Dating of the type: N.I.	

IG: 560697 AQ-FC-PV_2

Site : “Fondi ex Cossar” - Aquileia (UD)	Year 2011	US: 3189	
N. fragments: 1	N. objects: 1		
	Blue		
Dimensions: H 3; L 8,5 cm	Weight : 44,68 g	Dating of the type: N.I.	

GLASSWORKING WASTES

IG: 544087 -FC-SL_1

Site: “Fondi ex Cossar” - Aquileia (UD)	Year: 2009	US: 1005	
N. frammenti: 1	n. objects		
	Note: Incolore		
Dimensions: H 0,4; L 4,3 cm	Weight: 1,36 g	Dating of the type: N.I.	

IG: 544106 AQ-FC-SL_2

Site “Fondi ex Cossar” - Aquileia (UD)	Year: 2009	US: 262	
N. fragments: 1	N. objects: 1		
	green		
Dimensioni: H 2; L 3,7 cm	Weight 4,04+0,41 g	Dating of the type: N.I.	

IG: 560527 AQ-FC-SL_3

Site “Fondi ex Cossar” - Aquileia (UD)	Year: 2011	US: 3211	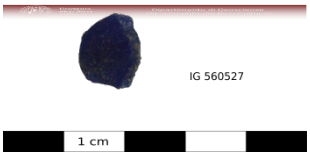
N. fragments: 1	N. objects: 1		
	Note: Blue opaque		
Dimensions: H 1,3; L 1 cm	Weight: 0,88 g	Dating of the type: N.I.	

IG: 561536 AQ-FC-SL_4

Scavo: “Fondi ex Cossar” - Aquileia (UD)	Anno di scavo: 2011	US: 4006	
N. fragments: 1	N. objects: 1		
	Note: turquoise opaque		
Dimensions: H 1; L 1,3 cm	Peso frammento: 0,78 g	Dating of the type: N.I.	

DISH - TYPE: ISINGS 118

IG: 545615 CAMPIONE:AQ-FC-118_1

Site: “Fondi ex Cossar” - Aquileia (UD)	Year: 2010	US: 3044	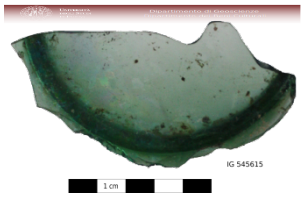
N. fragments: 1	N. objects: 1		
Bottom	Note: green		
Dimensions: Diametro 9 cm	Weight : 26,98 g	IV-inizio V sec.d.C.	

IG: 561260 CAMPIONE:AQ-FC-118_2

Site : “Fondi ex Cossar” - Aquileia (UD)	Year 2011	US: 5111	
N. fragments: 1	N. objects: 1		
Bottom	Note: green-brown		
Dimensions: Diametro 12 cm	Weight: 20,7 g	IV-inizio V sec.d.C.	

LAMP - CROWFOT-HARDEN A

IG: 561028 AQ-FC-C.H.A_1

Site “Fondi ex Cossar” - Aquileia (UD)	Year: 2011	**US**: 4128	
N. fragments: 1	N. objects: 1		
Bottom	**Note**: green		
Dimensions L. 2,3 cm	Weight: 14,07 g	IV-inizio V sec.d.C.	

BOWL ISINGS 1/18

IG: 545064 AQ-FC-1/18_1

Site “Fondi ex Cossar” - Aquileia (UD)	Year: 2009	**US**: 14	
N. fragments: 1	N. objects: 1		
Rim	**Note**: mosaic glass, green, opaque yellow, opaque red		
Dimensions: L 2,7; H 2,2 cm	Weight: 1,56 g	I metà I sec. d.C.	

BOWL ISINGS 1/18

IG: 546564 AQ-FC-1/18_2

Site “Fondi ex Cossar” - Aquileia (UD)	Year: 2010	**US**: 316	
N. fragments: 1	N. objects: 1		
Wall	**Note**: amber		
Dimensions: H. 3 cm	Weight 1,03 g	II metà I sec.a.C.-I metà I sec. d.C.	

IG: 546566 AQ-FC-1/18_3

Site: “Fondi ex Cossar” - Aquileia (UD)	**year**: 2010	**US**: 316	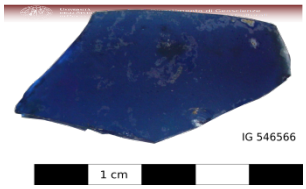
N. fragments: 1	N. objects: 1		
Rim	**Note**: Blue		
Dimensions: Diametro 13 cm	Weight 7,41 g	II metà I sec. a.C.-I metà I sec. d.C.	

BOWL ISINGS 116

IG: 533518 AQ-FC-116_1

Site: “Fondi ex Cossar” - Aquileia (UD)	**Year** : 2009	**US**: 33	
N. fragments: 1	N. objects: 1		
wall	**Light blue**		
Dimensions: L 5; H 6,8 cm	Weight 8,55 g	Dating of the type:: IV sec. d.C.	

ISINGS 116 LATE

IG: 560338 AQ-FC-116_2

Site “Fondi ex Cossar” - Aquileia (UD)	**Year:** 2011	**US**: 3132	
N. fragments: 2	N. objects: 1		
Rim + bottom	**Note**: colourless		
Dimensions D max 13; min. 7 cm	Weight 9,12 g	: inizio V sec. d.C.	

ISINGS 117

IG: 534703 CAMPIONE:AQ-FC-117_1

Site : “Fondi ex Cossar” - Aquileia (UD)	Year: 2009	US: 1005	
N. fragments: 1	N. objects: 1		
Rim	Note:green		
Dimensioni: Diametro 17 cm	Weight: 1,69 g	Dating of the type: IV sec. d.C.	

IG: 560701 CAMPIONE:AQ-FC-117_2

Site: “Fondi ex Cossar” - Aquileia (UD)	Year: 2011	US: 3189	

N. fragments: 1	N. objects: 1		
bottom	Note: green		
Dimensions: Diametro 4 cm	Weight 14,44 g	IV sec. d.C.	

IG: 560834 AQ-FC-117_3

Site: “Fondi ex Cossar” - Aquileia (UD)	Year: 2011	US: 3156	
N. fragments: 1	N. objects: 1		
wall	Note: yellow-green		
Dimensioni: L. 6,8; H. 3,3 cm	Weight 4,66 g	IV sec. d.C.	

IG: 561106 AQ-FC-117_4

Site: “Fondi ex Cossar” - Aquileia (UD)	Year:: 2011	US: 5104	
N. fragments: 1	N. objects: 1		
Bottom	Note: green		
Dimensioni: Diametro 5 cm	Weight: 22,31 g	IV sec. d.C.	

IG: 561259 AQ-FC-117_5

Site: “Fondi ex Cossar” - Aquileia (UD)	Year:: 2011	US: 5111	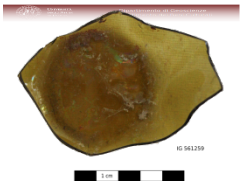
N. fragments: 1	N. objects: 1		
Bottom	Note: yellow green		
Dimensions: Diametro 5 cm	Weight: 21,37 g	IV sec. d.C.	

IG: 561280 AQ-FC-117_6

Site: “Fondi ex Cossar” - Aquileia (UD)	Year: 2011	US: 3306	
N. fragments: 3	N. objects: 1		
Bottom+ wall	Note: colourless		
Dimensioni: H 6; 4,5 cm	Weight: 5,67 g	IV sec. d.C.	

ISINGS 117 LATE

IG: n.a. :AQ-FC-117_7

Site: “Fondi ex Cossar” - Aquileia (UD)	Year: 2009	US: 246=225	
N. fragments: 1	N. objects: 1		
Parte conservata: orlo	Note: light blue		
Dimensions: Diametro 22 cm	Weight: 3,04 g	Dating of the type:: inizio V sec. d.C.	

ISINGS 3

IG: 533712 AQ-FC-3_1

Site: “Fondi ex Cossar” - Aquileia (UD)	Year:: 2009	US: 242	
N. fragments: 1	N. objects: 1		
Rim	Note: pale blue		
Dimensioni: Diametro 8,7 cm	Peso frammento: 4,19 g	Dating of the type: I sec. d.C.	

IG: 545700 AQ-FC-3_2

Site “Fondi ex Cossar” - Aquileia (UD)	Year: 2010	US: 219	
N. fragments: 1	N. objects: 1		
wall	Note: Blue		
Dimensioni: H. 2 cm	Peso frammento: 1,69 g	Dating of the type: I metà I sec. d.C.	

IG: 546440 AQ-FC-3_3

Site “Fondi ex Cossar” - Aquileia (UD)	Year:: 2010	US: 318	
N. fragments: 1	N. objects: 1		
wall	Note: mosaic glass, blue and white opaque		
Dimensions: H. 2,5 cm	weight: 3,61 g	I metà I sec. d.C.	

IG: 547390 :AQ-FC-3_4

Site “Fondi ex Cossar” - Aquileia (UD)	Year: 2010	US: 487	
N. fragments: 1	N. objects: 1		
Rim	Note: amber		
Dimensioni: Diametro 10,2 cm	weight: 15,02 g	I metà I sec. d.C.	

ISINGS 42

IG: 533516+534915 AQ-FC-42_1

Site “Fondi ex Cossar” - Aquileia (UD)	Year: 2009	US: 33+1013	
N. fragments: 2	N. objects: 1		
Bottom	Note: pale blue		
Dimensions: Diametro 7 cm	weight: 3,23 g	II metà I-II sec.d.C.	

IG: 544051 CAMPIONE:AQ-FC-42_2

Site “Fondi ex Cossar” - Aquileia (UD)	Year:: 2009	US: 124	
N. fragments: 1	N. objects: 1		
bottom	Note: green		

Dimensions: Diametro 11 cm	weight: 4,32 g	II metà I-II sec.d.C.	

IG: 546331 AQ-FC-42_3

Site: “Fondi ex Cossar” - Aquileia (UD)	Year: 2010	US: 2000	
N. fragments: 1	N. objects: 1		
Rim	Note: light blue		
Dimensionis: Diametro n.i.; H 1,1:L 2,1 cm	weight: 1,06 g	II metà I-II sec.d.C.	

ISINGS 42/LIMBURG

IG: 547779 AQ-FC-42L_1

site: “Fondi ex Cossar” - Aquileia (UD)	year: 2010	US: 687	
N. fragments: 1	N. objects: 1		
Rim	Note: colourless		
Dimensioni: Diametro 12 cm	weight: 3,8 g	II sec. d.C.	

IG: 547840 AQ-FC-42L_2

Site: “Fondi ex Cossar” - Aquileia (UD)	Year: 2010	US: 629	
N. fragments: 1	N. objects: 1		
Rim	Note: Azzurro		
Dimensions: Diametro 20 cm	weight: 2,21 g	II sec. d.C.	

TIPOLOGIA: ISINGS 85

IG: 534104 AQ-FC-85_1

Scavo: “Fondi ex Cossar” - Aquileia (UD)	Anno di scavo: 2009	US: 123	
N. fragments: 1	N. objects: 1		
Rim	Note: colourless		
Dimensions: Diametro 7 cm	weight: 5,51 g	II metà II-III sec. d.C.	

IG: 534799+534800 AQ-FC-85_2

Site: “Fondi ex Cossar” - Aquileia (UD)	Year: 2009	US: 98	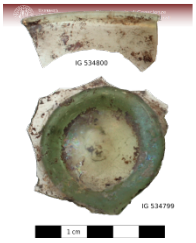
N. fragments: 2	N. objects: 1		
Rim + bottom	Note: green		
Dimensions: Diametro max 10; Diametro min. 4,5 cm	Weight: 4,08 g	II metà II-III sec. d.C.	

IG: 544052 AQ-FC-85_3

Site “Fondi ex Cossar” - Aquileia (UD)	Year: 2009	US: 124	
N. fragments: 1	N. objects: 1		
rim	Note: colourless		
Dimensions: Diametro 11 cm	weight 2,7 g	II metà II-III sec. d.C.	

IG: 544053 AQ-FC-85_4

Site: “Fondi ex Cossar” - Aquileia (UD)	Year : 2009	US: 124	
N. fragments: 2	N. objects: 1		
Parte conservata: orlo	Note: Azzurro		
Dimensioni: Diametro 12,2 cm	weight: 8,03 g	II metà II-III sec. d.C.	

IG: 544283+544435 AQ-FC-85_5

Site: “Fondi ex Cossar” - Aquileia (UD)	Year : 2009	US: 227+1050	
N. fragments: 2	N. objects: 1		
rim	Note: colourless		
Dimensioni: Diametro 11 cm	weight: 2,18 g	II metà II-III sec. d.C.	

IG: 544432 CAMPIONE:AQ-FC-85_6

Site : “Fondi ex Cossar” - Aquileia (UD)	Year : 2009	US: 227	
N. fragments: 1	N. objects: 1		
Parte conservata: orlo	Note: colourless		
Dimensioni: Diametro 9 cm	weight 1,96 g	III sec. d.C.	

IG: 544436 CAMPIONE:AQ-FC-85_7

Site : “Fondi ex Cossar” - Aquileia (UD)	Year : 2009	US: 227	
N. fragments: 2	N. objects: 1		
rim	Note: light blue		
Dimensions Diametro 12 cm	weight: 4,46 g	II metà II-III sec. d.C.	

IG: 545072 CAMPIONE:AQ-FC-85_8

Site : “Fondi ex Cossar” - Aquileia (UD)	Year : 2009	US: 14	
N. fragments: 2	N. objects: 1		
rim	Note: colourless		

Dimensions: Diametro 13 cm	weight 2,84 g	II metà II-III sec. d.C.	

IG: 545076 CAMPIONE:AQ-FC-85_9

Site “Fondi ex Cossar” - Aquileia (UD)	Year : 2009	US: 14	
N. fragments: 1	N. objects: 1		
rim	Note: colourless		
Dimensions: Diametro 6 cm	weight 2,48 g	II metà II-III sec. d.C.	

TIPOLOGIA: ISINGS 96

IG: 533027 CAMPIONE:AQ-FC-96_1

site: “Fondi ex Cossar” - Aquileia (UD)	year: 2009	US: 1037	
N. fragments: 1	N. objects: 1		
wall	Note: yellow- blue		
Dimensions H 2,4; L 3,5 cm	weight: 2,44 g	IV sec. d.C.	

IG: 546844

site: “Fondi ex Cossar” - Aquileia (UD)	year: 2010	US: 71	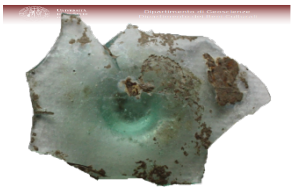
N. fragments: 1	N. objects: 1		
Botto,	Note: pale blue		
Dimensions: H 3,5; L 4,5 cm	weight N.I. g	IV-inizio V sec.d.C.	

IG: 546918 :AQ-FC-96_2

site “Fondi ex Cossar” - Aquileia (UD)	Anno di scavo: 2010	US: 2021	
N. fragments: 1	N. objects: 1		
wall	Yellow- blue		
Dimensions: H 4,5; L 3,5 cm	weight3,26 g	IV sec. d.C.	

IG: 547377 AQ-FC-96_3

Site “Fondi ex Cossar” - Aquileia (UD)	Year : 2010	US: 3158	
N. fragments: 1	N. objects: 1		
Wall with rim and bottom	Note: blue-green		
Dimensioni: Diametro 10,7; H. 6 cm	weight: 15,23 g	IV sec. d.C.	

BOTTLE ISINGS 104

IG: 533520 AQ-FC-104_1

site “Fondi ex Cossar” - Aquileia (UD)	Year : 2009	US: 33	
N. fragments: 1	N. objects: 1		
wall	Note: green		
Dimensions: H 4,8; L 4,3 cm	Weight : 6,87 g	IV-inizio V sec. d.C.	

IG: 534102 AQ-FC-104_2

Site : “Fondi ex Cossar” - Aquileia (UD)	Year : 2009	US: 123	
N. fragments: 1	N. objects: 1		
neck	Note: colourless with colourless wire applied		
Dimensions: H 3,8 cm	weight: 6,39 g	IV-V sec.d.C.	

IG: 560102 AQ-FC-104_3

Scavo: “Fondi ex Cossar” - Aquileia (UD)	Year : 2011	US: 5010	
N. fragments: 1	N. objects: 1		
Rim	Note: yellow		
Dimensions: Diametro 6 cm	weight: 3,2 g	IV-I metà V sec. d.C.	

IG: 560700 AQ-FC-104_4

Site “Fondi ex Cossar” - Aquileia (UD)	Year : 2011	US: 3189	
N. fragments: 1	N. objects: 1		
Parte conservata: collo e spalla	Note: light blue		
Dimensioni: Diametro max 8,5 cm	weight: 16,83 g	: IV-V sec. d.C.	

IG: 560709 AQ-FC-104_5

Site: “Fondi ex Cossar” - Aquileia (UD)	year: 2011	US: 3189	
N. fragments: 1	N. objects: 1		
wall	Note: Blue		
Dimensions: Diametro spalla 6 cm	weight: 2,07 g	IV-V sec.d.C.	

IG: 561452 AQ-FC-104_6

Scavo: “Fondi ex Cossar” - Aquileia (UD)	Year : 2011	US: 5147	

N. fragments: 1	N. objects: 1		
rim	Note: green, applied wire		
Dimensions: Diametro 7 cm	weight	IV-I metà V sec. d.C.	

BEAKER - ISINGS 106 LATE

IG: 534250 AQ-FC-106_1

Site : “Fondi ex Cossar” - Aquileia (UD)	year: 2009	US: 54	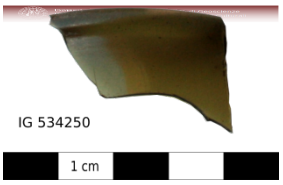
N. fragments: 1	N. objects: 1		
Rim	Note: brown		
Dimensions: Diametro n.i.; H 2,2; L 3 cm	weight: 2,05 g	inizio V sec. d.C.	

IG: 534317 AQ-FC-106_2

site “Fondi ex Cossar” - Aquileia (UD)	year: 2009	US: 135	
N. fragments: 1	N. objects: 1		
Parte conservata: fondo	Note: green		
Dimensions: H 3; L4,5 cm	weight: 7,17 g	inizio V sec. d.C.	

IG: 547984 AQ-FC-106_3

Site “Fondi ex Cossar” - Aquileia (UD)	year: 2011	US: 5008	
N. fragments: 1	N. objects: 1		
Parte conservata: orlo	Note: Azzurro-verde		
Dimensioni: Diametro 8 cm	Peso frammento: 2,04 g	inizio V sec. d.C.	

IG: 560218+560254 AQ-FC-106_4

Site : “Fondi ex Cossar” - Aquileia (UD)	year: 2011	US: 4046	
N. fragments: 2	N. objects: 1		
Parte conservata: fondo	Note: Bruno. Campionato solo 560218		
Dimensioni: Diametro 4 cm	Peso frammento: 7,18+0,44 g	: inizio V sec. d.C.	

IG: 560747 AQ-FC-106_5

Site “Fondi ex Cossar” - Aquileia (UD)	year: 2011	US: 4071	
N. fragments: 1	N. objects: 1		
bottoms	Note: Bruno-verde		
Dimensioni: Diametro 3,5 cm	weight: 6,52 g	: inizio V sec. d.C.	

IG: 561470 AQ-FC-106_6

Site: “Fondi ex Cossar” -	year	US: 3310	

Aquileia (UD)			
N. fragments: 1	N. objects: 1		
rim	Note: Verde		
Dimensioni: Diametro 10 cm	weight: 6 g	Datazione generale tipologia: inizio V sec. d.C.	

BEAKER ISINGS 106C

IG: 534769+534768+534764+534766 AQ-FC-106_7

Scavo: “Fondi ex Cossar” - Aquileia (UD)	year: 2009	US: 65	
N. fragments: 4	N. objects: 1		
Rim	Note: yellow green		
Dimensions: Diametro 8 cm	weight: 4,84 g	IV-inizio V sec. d.C.	

IG: 544449 AQ-FC-106_8

Site: “Fondi ex Cossar” - Aquileia (UD)	year: 2009	US: 78	
N. fragments: 4	N. objects: 1		
Rim	Note: yellow		
Dimensions: Diametro 11 cm	weight 5 g	IV-inizio V sec. d.C.	

IG: 546910 AQ-FC-106_9

site “Fondi ex Cossar” - Aquileia (UD)	Year 2010	US: 2021	
N. fragments: 4	N. objects: 1		
Rim+ wall	Note: Verde		
Dimensions: diametro n.i.; H 2,5; L 4,8 cm	weight: 6,54 g	IV-inizio V sec. d.C.	

IG: 547983 AQ-FC-106_10

Scavo: “Fondi ex Cossar” - Aquileia (UD)	Anno di scavo: 2011	US: 5008	
N. fragments: 1	N. objects: 1		
rim	Note: green		
Dimensioni: Diametro 11 cm	weight 2,58 g	IV-inizio V sec. d.C.	

IG: 560748 AQ-FC-106_11

Scavo: “Fondi ex Cossar” - Aquileia (UD)	Anno di scavo: 2011	US: 4071	
N. fragments: 1	N. objects: 1		
Parte conservata: orlo	Note: green		

Dimensioni: Diametro 8 cm	weight: 3,43 g	IV-inizio V sec. d.C.	

BEAKER ISINGS 109

IG: 533061 CAMPIONE: AQ-FC-109_1

Site : “Fondi ex Cossar” - Aquileia (UD)	Year : 2009	US: 1109	
N. fragments: 1	N. objects: 1		
bottom	Note:light blue		
Dimensions: L. 2,2 cm	weight: 1,77 g	IV sec. d.C.	

IG: 533596 AQ-FC-109_2

site: “Fondi ex Cossar” - Aquileia (UD)	Year : 2009	US: 24	
N. fragments: 1	N. objects: 1		
bottom	Note:colourless		
Dimensions: Diametro 4,5 cm	weight: 10,39 g	IV sec.d.C.	

IG: 533601 AQ-FC-109_3

site: “Fondi ex Cossar” - Aquileia (UD)	Year : 2009	US: 24	
N. fragments: 1	N. objects: 1		
bottom	Note: colourless		
Dimensions: Diametro 5 cm	weight 13,22 g	IV sec. d.C.	

IG: 534735+534740 AQ-FC-109_4

site: “Fondi ex Cossar” - Aquileia (UD)	Year 2009	US: 1043	
N. fragments: 2	N. objects: 1		
bottom	Note: green		
Dimensions: Diametro 4,5 cm	weight 4,31 g	IV sec. d.C.	

IG: 534908 AQ-FC-109_5

site: “Fondi ex Cossar” - Aquileia (UD)	Year : 2009	US: 1013	
N. fragments: 1	N. objects: 1		
bottom	Note: green		
Dimensioni: Diametro 4 cm	weight: 3,39 g	IV sec. d.C.	

IG: 544050 AQ-FC-109_6

site: “Fondi ex Cossar” - Aquileia (UD)	Year: 2009	US: 124	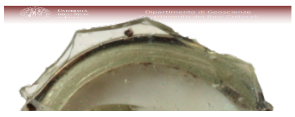
N. fragments: 1	N. objects: 1		

bottom	Note: green		
Dimensions: Diametro 5 cm	weight: 6,44 g	IV sec. d.C.	

BEAKER ISINGS 109B/111

IG: 534316 AQ-FC-111/109b_1

Scavo: “Fondi ex Cossar” - Aquileia (UD)	Anno di scavo: 2009	US: 135	
N. fragments: 1	N. objects: 1		
foot	Note: green		
Dimensions: Diametro 4 cm	weight: 4,48 g	I metà V sec. d.C.	

IG: 560084 AQ-FC-111/109b_2

Scavo: “Fondi ex Cossar” - Aquileia (UD)	Anno di scavo: 2011	US: 3075	
N. fragments: 1	N. objects: 1		
foot	Note: pale blue		
Dimensions Diametro 5 cm	weight: 3,01 g	I metà V sec. d.C.	

IG: 560202 AQ-FC-111/109b_3

Scavo: “Fondi ex Cossar” - Aquileia (UD)	Anno di scavo: 2011	US: 4046	
N. fragments: 1	N. objects: 1		
bottom	Note: green		
Dimensions Diametro 4,5 cm	weight: 10,07 g	I metà V sec. d.C.	

GOBLET - ISINGS 111

IG: 533517 AQ-FC-111-1

Site “Fondi ex Cossar” - Aquileia (UD)	Year : 2009	US: 33	
N. fragments: 1	N. objects: 1		
Rim	Note: colourless		
Dimensions Diametro 6 cm	weight: 3,7 g	II metà V-inizio VIII sec. d.C.	

IG: 534496 AQ-FC-111_2

Scavo: “Fondi ex Cossar” - Aquileia (UD)	Anno di scavo: 2009	US: 35	
N. fragments: 1	N. objects: 1		
Rim	Note: light blue		
Dimensions Diametro 8 cm	weight 4,32 g	II metà V-inizio VIII sec.d.C.	

IG: 534689 AQ-FC-111_3

site: “Fondi ex Cossar” - Aquileia (UD)	year: 2009	US: 1005	
N. fragments: 1	N. objects: 1		
foot	Note: yellow		
Dimensions: Diametro 3,2 cm	weight: 4,44 g	II metà V-inizio VIII sec.d.C.	

IG: 534692 AQ-FC-111_4

site: “Fondi ex Cossar” - Aquileia (UD)	year: 2009	US: 1005	
N. fragments: 1	N. objects: 1		
foot	Note: yellow		
Dimensions: Diametro 4 cm	weight: 1,9 g	II metà V-inizio VIII sec.d.C.	

IG: 544281 AQ-FC-111_5

site: “Fondi ex Cossar” - Aquileia (UD)	year: 2009	US: 1050	
N. fragments: 1	N. objects: 1		
rim	Note: colourless		
Dimensioni: Diametro 11,2 cm	weight: 1,87 g	II metà V-inizio VIII sec.d.C.	

IG: 544437 AQ-FC-111_6

site “Fondi ex Cossar” - Aquileia (UD)	year: 2009	US: 227	
N. fragments: 1	N. objects: 1		
rim	Note: pale blue		
Dimensioni: Diametro 9,2 cm	weight 4,28 g	II metà V-inizio VIII sec.d.C.	

IG: 560088 AQ-FC-111_7

site “Fondi ex Cossar” - Aquileia (UD)	year: 2011	US: 3192	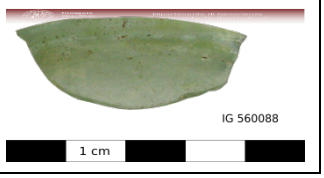
N. fragments: 1	N. objects: 1		
rim	Note: green		
Dimensioni: Diametro 9 cm	weight: 2,33 g	II metà V-inizio VIII sec.d.C.	

IG: 561465 CAMPIONE:AQ-FC-111_8

site: “Fondi ex Cossar” - Aquileia (UD)	year: 2011	US: 50000	
N. fragments: 1	N. objects: 1		
body	Note: Blue		

Dimensionis Diametro min. 1,5; Diametro max 7; H. 4,5 cm	weight: 14,36 g	Datazione generale tipologia: V-VI sec. d.C.	

ALABASTRON - GROSE II.2

IG: 544284 CAMPIONE: AQ-FC-ALAB_1

Site “Fondi ex Cossar” - Aquileia (UD)	year: 2009	US: 1050	
N. fragments: 1	N. objects: 1		
wall	Note: core-formed, blue with white and yellow opaque decorations		
Dimensions: Diametro 3,2 cm	weight 3 g	250-300 a. C.	

APPENDIX A2

Mosaic tesserae from the mosaic of the Domus delle Bestie Ferite", Aquileia, 2nd half of the 4th century AD.

Name	PROVENANCE	COLOUR	Note	Weight (g)	PICTURE
AQ-BF-BS 1	Dominus	Dark blue	Translucent	0.7155	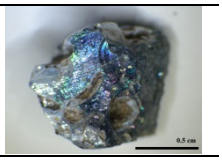
AQ-BF-B 1	Net	Blue	Micro sample	0.0489	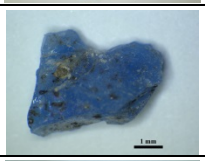
AQ-BF-AZ 1	motivo treccia ovest	Azure		0.3457	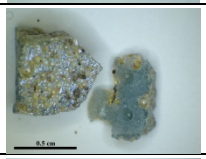
AQ-BF-AZ 2	Summer	Azure		0.5488	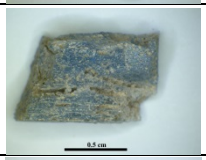
AQ-BF-AZ 3	Summer	Azure		0.5123	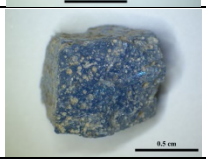
AQ-BF- AZ 4	Net	Azure	Micro sample	0.0124	
AQ-BF-AZ 5		Azure		1.8946	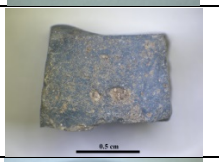
AQ-BF_CE 1	Geometric decoration (West)	Pale blue		0.5509	
AQ-BF-CE2	Dominus	Pale blue		0.7583	
AQ-BF-TU 1		Turquoise		0.5250	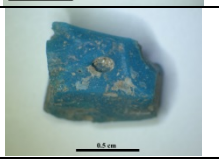

AQ-BF-TU TR 1	Lion	Turquoise	Translucent	0.0926	
AQ-BF-AQ 1	Net	Aquamarine		0.5889	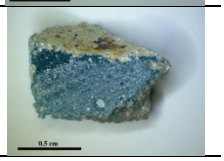
AQ-BF-AQ 2		Aquamarine		1.4653	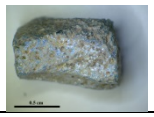
AQ-BF-VS 1		Dark green	Translucent	1.6010	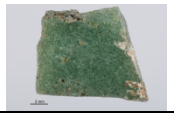
AQ-BF-VS2	Net	Dark green		0.1660	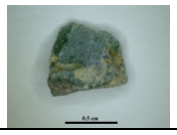
AQ-BF-VCH 1	*testa dominus*	*Pale green*		*1.7056*	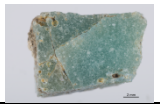
AQ-BF-VCH 2	*Lion*	*Pale green*		*0.4526*	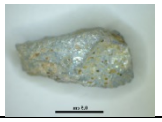
AQ-BF-R1	Estate	Red	Micro sample	0.0059	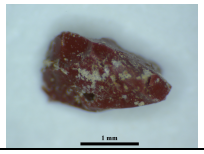
AQ-BF-M1	Geometric decoration (west)	Brown		0.9579	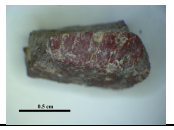
AQ-BF-M 2	Dominus	Brown		0.1774	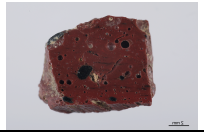
AQ-BF-M3	Summer	Brown	Micro sample	0.0065	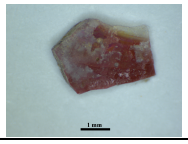
AQ-BF-M4		Brown		0.7986	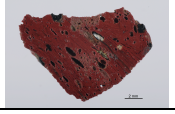

AQ-BF-GR 1		Grey		1.6262	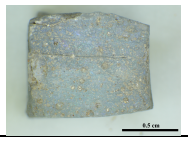
AQ-BF-TR INC 1	Lion	Colourless		0.3227	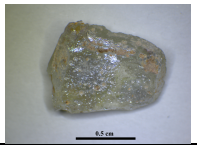
AQ-BF-TR INC 2	Lion	Colourless		0.2432	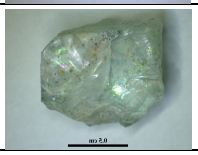
AQ-BF-TR INC 3		Colourless		1.0072	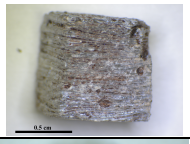
AQ-BF-AU1		Gold	Gold leaf	0.0521	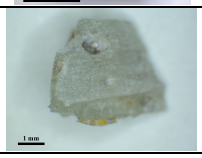

APPENDIX A3

Samples from Classe.

sample	type		dating	colour	picture
D1	beaker	Isings 96	4th-5th	green	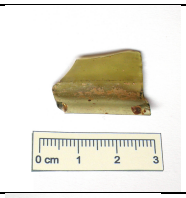
D2	beaker	Isings 96	4th-5th	green	
D3	beaker	Isings 96	4th-5th	green	
D5	beaker	Isings 96	4th-5th	green	
D7	beaker	Isings 109	4th-5th	Blue	
D8	beaker	Isings 96/106/109?	4th-5th	green	
D10	beaker	Isings 111	5th-8th	light blue	
D11	beaker	Isings 111	5th-8th	colourless	

D14	beaker	Isings 111	5th-8th	colourless	
D16	beaker	Isings 109	4th-5th	colourless	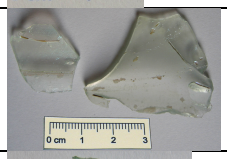
D18	Def. fragment	n.i	n.i.	blue-green	
D20	beaker	Isings 106	5th-6th	green	
D21	beaker	Isings 106	5th-6th	green	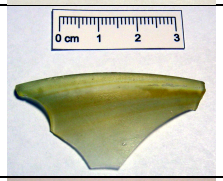
D23	beaker	Isings 109	4th-5th	light blue	
D24	beaker	Isings 109	4th-5th	green	
D25	beaker	Isings 96/106/109?	4th-5th	azzurro	
D26	beaker	Isings 107	4th-5th	blue	
D27	bottle	Isings 92		blue	
D28	bottle	Isings 126		green	

D29	bottle	Sternini 1995, p 279, Fig 11 n.131		Blue/green	
D30	bottle	Foy 2000,p 281, fig 29, n.13	data	Blue	
D32	bowl	Uboldi 1986, tav. 58	data	colourless	
D33	bowl with folded rim	n.i	n.i	light blue	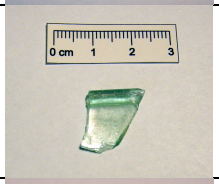
D34	bowl	n.i.	n.i	green	
D35	palm cup/lamp	n.i.	n.i	light blue	
D36	lamp	Uboldi 1999, p. 639, tav. 123, n. 9		colourless	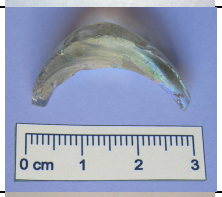
D37	lamp	Non identificata	n.i	colourless	
D38	Conical pushed-in bottom	Leciejewicz, Tabaczynska, Tabaczinski 1977, p. 173, fig. 130, n. 24		blue-green	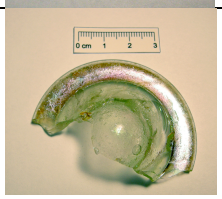
D39.1 D39.2	window pane	n.i	n.i	green	

A2	glassworking waste	n.i	n.i	green	
A3	glassworking waste	n.i	n.i	green	
BLC	glassworking waste	n.i	n.i	*light blue*	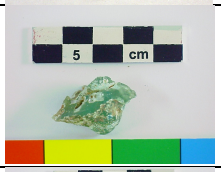
BLS	glassworking waste	n.i	n.i	*green*	
CVC	glassworking waste	n.i	n.i	*green*	
CVG	glassworking waste	n.i	n.i	*green*	
CVS	glassworking waste	n.i	n.i	*green*	
C4	glassworking waste	n.i	n.i	*green*	
G1	glassworking waste	n.i	n.i	*green*	
G3	glassworking waste	n.i	n.i	*green*	
G4	glassworking waste	n.i	n.i	*green*	

GRA	glassworking waste	n.i	n.i	*azzurro*	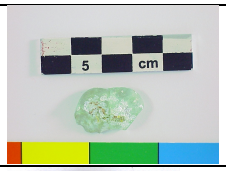
F-D	glassworking waste	n.i	n.i	*green*	
F-D-D12	glassworking waste	n.i	n.i	blue/green	
M1	glassworking waste	moil	n.i	*green*	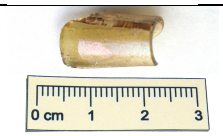
PF	glassworking waste	n.i.	n.i	green	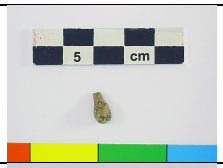
PV	glassworking waste	chunk	n.i	blue/green	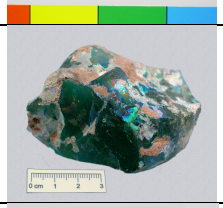
PVM	glassworking waste	chunk	n.i	*brown*	
PVA	glassworking waste	chunk	n.i	light blue	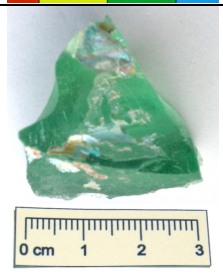
PVC	glassworking waste	chunk	n.i	light blue	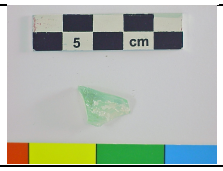

PVS	glassworking waste	chunk	n.i	green	
SCH	glassworking waste	*n.i*	n.i	green	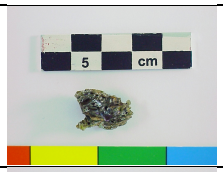
BL-SCH	glassworking waste	*n.i*	n.i	green	
T-A	glassworking waste	*n.i*	n.i	green	
TB	glassworking waste	*n.i*	n.i	green	
T-C	glassworking waste		n.i	green	
US T04	glassworking waste			light blue	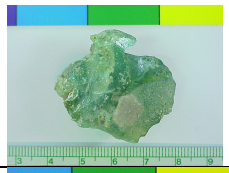
US T10	glassworking waste			green	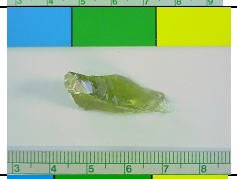
US T12	glassworking waste			blue/green	

US PV01	glassworking waste	chunk		green	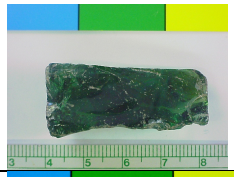
US G05	glassworking waste			green	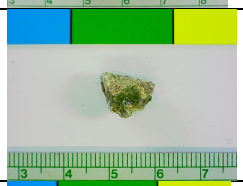
US G06	glassworking waste				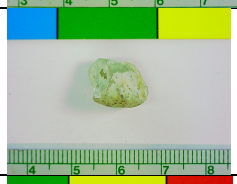
US D50	beaker	Is.106	5th-6th	Yellow green	
US D51	beaker	Is.106	5th-6th	green	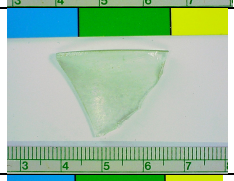
US D52	beaker	(Is 106) Sternini 1995	5th-6th	green	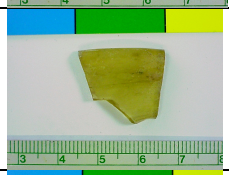
US D53	beaker	Is.111?	5th-8th	green	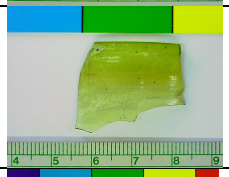
US D54	beaker	Is.96	4th-5th	green	
US D55	lamp	Y. Israeli 2008		light blue	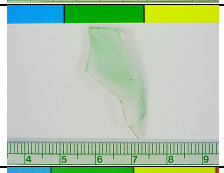
US D56	beaker	Is 106	5th-6th	green	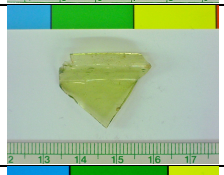
US D57	beaker	Is. 106 (sternini 1995)	5th-6th	Blue/green	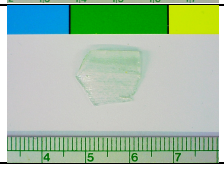

US D58	beaker	I. 106 (sternini 1995)	5th-6th	Blue/green	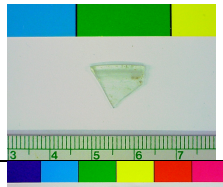
US D59	beaker	Is 96	4th-5th	green	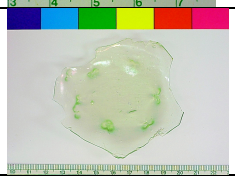

APPENDIX 4

Glass mosaic tesserae from Pordenone

colour	Name	notes	Wight (g)	picture
Dark blue	PN-T-BS 1	translucent	1.3492	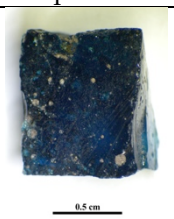
Blue	PN-T-BO 1		1.0536	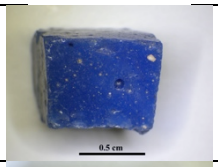
Azure	PN-T-AZ 1		1.1216	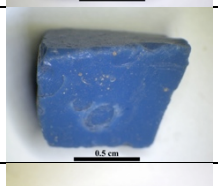
Azure	PN-T-AZ 2		1.4468	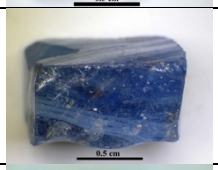
Turquoise	PN-T-TU 1		0.7255	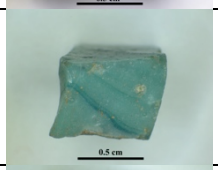
Turquoise	PN-T-TU 2		1.1628	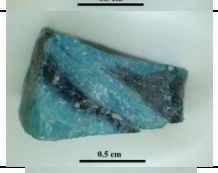
Turquoise	*PN-T-TU 3 (?)*		*0.5556*	
Pale blue	PN-T-CE 1		1.1248	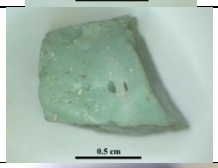
Aquamarine	PN-T-AQ 1		1.1871	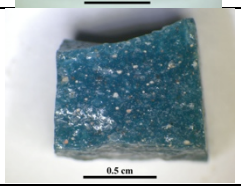

Dark green	PN-T-VS 1		1.3381	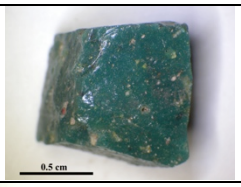
Dark green	PN-T-VTR 1	translucent	1.1287	
Dark green	PN-T-VTR 2	translucent	1.0372	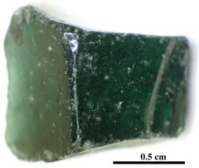
Green	PN-T-VP 1		1.4361	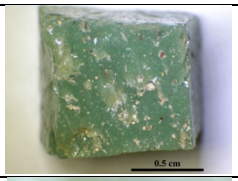
Pale green	PN-T-VCH 1		1.2139	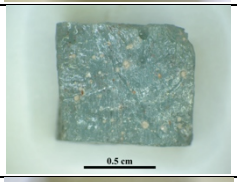
Yellow green	PN-T-VG 1		1.1708	
Yellow	PN-T-GSO 1		1.1291	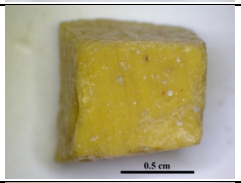
Yellow	PN-T-GSO 2	Semiopaque with opaque stripes	1.3050	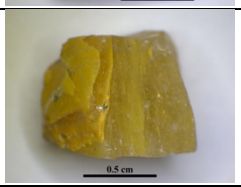
Orange	PN-T-AV 1		1.0958	
Orange	PN-T-AV 2	Orange with red stripes	0.5602	

brown	PN-T-M 1		1.2173	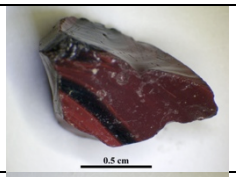
brown	PN-T-M 2		0.2706	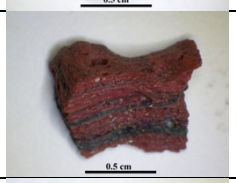
Olive /Red	PN-T-M 3	Translucent olive green tesserae with red stripes	0.8157	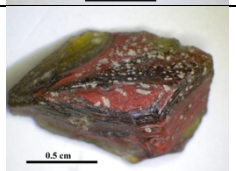
Light amber	PN-T-NC 1	semitranslucent	1.0837	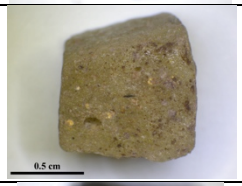
Grey	PN-T-GR 1		1.0285	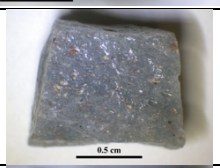
white	PN-T-BIOP 1		1.3602	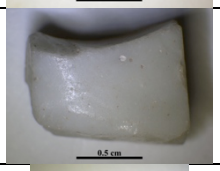
Gold	PN-T-AU 1	Tesserae with gold leaf and cartellina	2.5361	
Gold	PN-T-AU 2	Tessera with gold foil and cartellina	2.7561	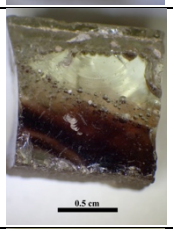
Gold	*PN-T-AG 1*	*Tesserae with cartellina, gold foil absent*	*2.7967*	

APPENDIX 5
Samples from Trento

colour	name	Notes	Provenance	Weight (g)	PICTURE
colourless	TN-SMM-TR INC 1		cassa 137- US 885 Fase 350	0.9274	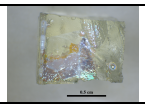
gold	TN-SMM-AU1	gold foil and *cartellina*	cassa 140- US 1024 fase 240- 2	1.7832	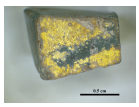
white	TN-SMM-BIOP 1		cassa 136 US 952 fase 370	0.2656	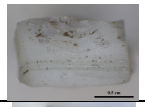
grey	TN-SMM-GR 1		cassa 136 US 952 fase 370-2	1.0929	
grey	TN-SMM-GR 2		cassa 153- US 1046 fase 240- 1	0.9002	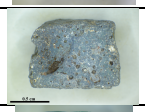
pale blue	TN-SMM-CE 1		cassa 106 tombe US 809 fase 470	0.9530	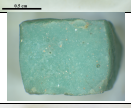
aquamarine	TN-SMM-AQ 1		cassa 127 US 871 fase 350-1	1.2577	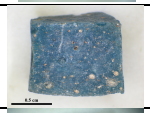
aquamarine	TN-SMM-AQ 2		cassa 106 tombe us 817 fase 470	1.4655	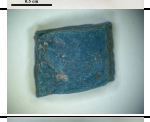
turquoise	TN-SMM-TU 1		cassa154- US 907 fase 240	1.0718	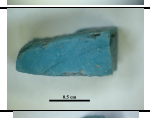
turquoise	TN-SMM-TU 2		cassa 106 tombe US 827fase 470	0.5839	
turquoise	TN-SMM-TU 3		cassa 136 US 952 fase 370	0.8292	
azure	TN-SMM-AZ 1		cassa 127- US 871 fase 350-1	1.0170	
azure	TN-SMM-AZ 2		cassa 137- US 885 fase 350	1.5762	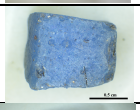
blue	TN-SMM-BO 1		cassa 136 US 952 fase 370-1	0.6016	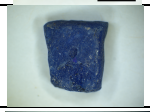
blue	TN-SMM-B 1	translucent	cassa 127- US 871 fase 350-1	0.8523	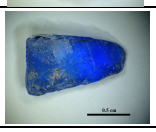

dark blue	TN-SMM-BS 1	translucent	cassa 153- US 1046 fase 240	1.7593	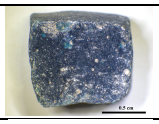
brown	TN-SMM-M1		cassa 127- US 871 fase 350	1.1957	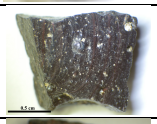
brown	TN-SMM-M 2		cassa 136 US 952 fase 370	1.3353	
brown/dark red	TN-SMM-M3		cassa 137- US 885 fase 350	1.5556	
bdarkamber	TN-SMM-NS 1	Brownish amber semiopaque	cassa 137- US 885 fase 350	0.8273	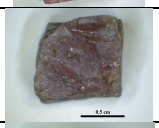
orange	TN-SMM-AV 1	Orange with red bands	cassa 216- US 798 fase 350	0.7195	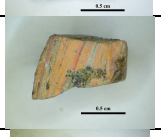
yellow	TN-SMM-GSO 1		cassa 127- US 871 fase 350-2	1.1559	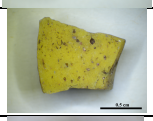
yellow	TN-SMM-GSO 2		cassa 127- US 871 fase 350-1	1.0520	
yellow-green	TN-SMM-VG 1		cassa 153- US 1046 fase 240	1.3674	
yellow-green	TN-SMM-VG 2	translucent	cassa 127- US 871 fase 350	1.3266	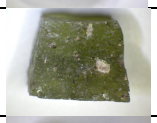
light green	TN-SMM-VCH 1		cassa 140- US 1024 fase 240		
green	TN-SMM-VP1		cassa 127- US 871 fase 350	1.6668	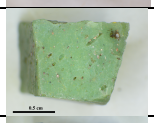
green	TN-SMM-VP 2		cassa 216- US 798 fase 350	1.0524	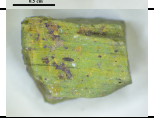
olive /red	TN-SMM-VOL 1	Olive green translucent with red bands	cassa 136 US 952 fase 370-1	0.8155	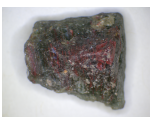
olive green	TN-SMM-VOL 2	translucent	cassa 136 US 952 fase 370-2	0.8423	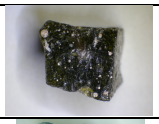
dark green	TN-SMM-VS 1		cassa 153- US 1046 fase 240	0.8225	
Dark green	TN-SMM- VS 2		cassa 117 US 858 fase 360	1.5787	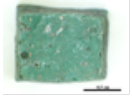

Table 4.1

sample	**SiO2**	**Na2O**	**CaO**	**Al2O3**	**Fe2O3**	**MnO**	**TiO2**	**MgO**	**K2O**	**P2O5**	**SO3**	**Cl**	**SnO2**	**Sb2O3**	**Co**	**Cu**	**Pb**	**Zn**	***tot***
AQ-FC-1/18_1 red	59.72	14.42	9.02	2.02	1.74	0.50	0.15	2.49	1.53	1.00	0.19	1.14	0.25	0.32	<200	13531	34923	734	*99.30*
AQ-FC 1/18_1 green	63.30	15.50	7.84	2.31	2.19	0.65	0.15	1.34	0.93	0.30	0.31	1.11	0.15	0.57	350	15778	3750	334	*98.66*
AQ-FC-1/18 yellow	65.82	13.74	5.79	1.75	0.85	0.05	0.07	0.49	0.73	0.02	0.28	1.37	<0.04	0.87	<200	9303	42194	<321	*97.01*
AQ-FC-3_3 blu	67.88	17.18	7.98	2.55	0.94	0.80	0.07	0.67	0.90	0.12	0.30	0.84	<0.04	0.03	530	639	<696	<321	*100.40*
AQ-FC-3_3 white	66.17	15.19	7.47	2.44	0.44	1.15	0.05	0.81	0.83	0.09	0.47	0.43	<0.04	4.41	<200	389	<696	<321	*100.05*
AQ-FC-ALAB1 blu	67.18	18.31	6.70	2.26	0.83	1.57	0.06	0.63	0.81	0.07	0.37	1.03	0.02	0.32	662	969	796	<321	*100.42*
AQ-FC ALAB1 white	64.98	13.67	6.59	2.34	0.57	1.56	0.03	0.62	1.26	0.13	0.57	0.58	0.00	4.21	289	243	5350	<321	*97.75*
AQ-FC-ALAB1_yellow	61.01	11.60	6.19	1.89	0.82	1.21	0.04	0.47	0.91	0.05	0.28	0.85	0.02	0.92	12	377	110961	<321	*97.39*
AQ-FC-SL4 mean (turquioise)	67.00	14.30	6.66	2.45	1.01	0.53	0.10	0.77	2.03	0.15	0.35	0.75	0.06	2.37	<200	12209	2772	<321	*100.07*
AQ-FC-SL3 mean (blu)	68.15	16.00	6.14	2.22	1.31	0.52	0.05	0.60	0.55	0.06	0.34	0.94	<0.04	2.27	953	1941	2638	<321	*99.74*

Table 4.2

sample	group	composition	SiO2	Na2O	CaO	Al2O3	Fe2O3	MnO	TiO2	MgO	K2O	P2O5	SO3	Cl	SnO2	Sb2O3	Co	Cu	Pb	V	Cr	Ni	Zn	Ga	Rb	Sr	Y	Zr	Nb	Ba	La	Ce	Nd	Th	U
AQ-FC 1/18-2	FC coloured	Amber	67.10	18.69	9.45	2.34	0.34	0.02	0.06	0.54	0.62	0.10	0.40	1.05	<0.04	<0.04	<3	29	23	7	6	5	20	<5	14	463	8	35	4	201	<10	21	15	3	<3
AQ-FC 1/18-3	FC coloured	Blue	67.62	16.65	8.81	2.25	1.28	0.34	0.05	0.53	0.66	0.11	0.47	0.57	<0.04	0.35	341	576	55	15	12	9	204	<5	16	466	7	35	15	180	<10	30	17	<3	<3
AQ-FC 109-6	FC coloured	Nat. Coloured	69.21	17.22	7.10	2.33	0.50	0.75	0.08	0.53	0.61	0.09	*0.28*	*1.25*	*<0.04*	*<0.04*	7	75	62	27	11	6	23	<5	14	438	6	47	<3	252	<10	<10	21	<3	<3
AQ-FC 3-1	FC coloured	Roman	70.02	16.35	7.38	2.45	0.42	0.34	0.06	0.46	0.64	0.15	0.15	1.06	<0.04	<0.04	22	54	79	11	13	6	18	<5	13	379	8	40	<3	248	<10	13	17	<3	7
AQ-FC 3-2	FC coloured	Blue	*69.07*	17.08	*7.60*	2.60	1.00	0.25	0.06	0.51	0.67	0.09	0.24	1.11	<0.04	<0.04	410	346	23	13	10	12	31	<5	15	398	6	36	20	225	<10	<10	17	5	<3
AQ-FC 3-4	FC coloured	Nat. Coloured	69.51	18.42	*7.39*	2.19	0.29	0.02	0.05	0.43	0.51	0.07	0.29	1.42	<0.04	<0.04	<3	8	13	6	8	<3	10	<5	13	373	5	38	5	205	23	22	18	5	<3
AQ-FC 42-1	FC coloured	Nat. Coloured	72.16	15.27	*7.03*	2.55	0.35	0.20	0.06	0.43	0.46	0.10	0.13	1.27	<0.04	<0.04	<3	11	17	14	10	3	14	<5	13	362	6	40	31	211	10	23	24	5	<3
AQ-FC 42-3	FC coloured	Nat. Coloured	71.76	15.37	*7.39*	2.28	0.39	0.36	0.07	0.48	0.65	0.17	0.09	1.11	<0.04	<0.04	8	43	42	11	8	10	21	<5	13	382	8	42	3	222	<10	25	15	<3	<3
AQ-FC 109-2	FC colourless1	Sb decoloured	68.79	19.40	6.35	1.85	0.51	0.03	0.09	0.64	0.35	0.03	0.36	1.34	<0.04	0.46	3	27	26	12	14	5	19	<5	11	411	7	50	17	108	<10	18	22	5	<3
AQ-FC 109-3	FC colourless1	Sb decoloured	68.11	19.30	6.23	2.57	0.50	0.03	0.09	*0.70*	0.38	0.04	*0.35*	*1.56*	*<0.04*	*0.70*	<3	22	25	12	14	<3	24	<5	11	457	7	49	24	91	<10	38	19	4	<3
AQ-FC 117-6	FC colourless1	Sb decoloured	70.61	18.19	5.52	2.63	0.37	0.01	0.07	0.38	0.35	0.03	0.26	1.43	<0.04	0.78	<3	24	37	7	14	5	19	<5	11	345	4	46	24	78	<10	24	24	4	<3
AQ-FC 85-1	FC colourless1	Sb decoloured	69.57	16.50	8.16	2.43	0.82	0.03	0.14	0.69	0.56	0.07	0.30	1.15	<0.04	0.53	3	32	83	16	18	7	35	<5	13	587	8	69	<3	129	<10	36	28	<3	3
AQ-FC 85-3	FC colourless1	Sb decoloured	73.17	17.48	5.05	1.79	0.35	0.02	0.06	0.34	0.41	0.03	0.21	1.37	<0.04	0.56	<3	38	44	10	8	4	26	<5	12	312	6	41	32	100	<10	43	24	<3	<3
AQ-FC 85-6	FC colourless1	Sb decoloured	72.54	17.62	5.52	1.75	0.36	0.01	0.07	0.35	0.36	0.03	0.26	1.48	<0.04	0.39	<3	14	19	9	13	4	20	<5	12	340	6	45	22	114	<10	24	19	6	<3
AQ-FC SL-1	FC colourless1	Sb decoloured	72.48	17.96	*4.67*	1.93	0.33	0.01	0.06	0.35	0.35	0.03	0.30	1.56	<0.04	0.69	<3	29	24	9	10	<3	20	<5	10	260	5	43	<3	108	<10	33	24	6	<3
AQ-FC 104-1	FC colourless2	Mn decoloured	66.19	17.57	6.22	2.54	1.93	1.81	0.05	1.18	0.30	0.05	0.25	1.37	<0.04	<0.04	11	55	61	61	70	21	36	<5	10	416	13	263	5	853	<10	25	<10	<3	4
AQ-FC 104-4	FC colourless2	Mn decoloured	68.59	15.73	8.24	2.82	0.54	1.93	0.08	0.68	0.36	0.07	0.17	1.31	<0.04	<0.04	10	32	9	38	14	15	23	<5	12	567	7	40	33	430	<10	11	11	6	<3
AQ-FC 109-4	FC colourless2	Mn decoloured	69.43	14.79	8.03	2.67	0.38	1.49	0.07	0.45	0.66	0.12	*0.22*	*1.00*	*<0.04*	*<0.04*	12	17	13	46	16	11	18	<5	13	490	7	39	<3	394	<10	21	16	4	4
AQ-FC-111_1	FC colourless2	Mn decoloured	*69.87*	*15.62*	*8.43*	*2.65*	*0.43*	*1.39*	*0.08*	*0.63*	*0.48*	*0.06*	*0.10*	*1.21*	*<0.04*	*<0.04*	<200	<265	<696	*n.a.*	*n.a.*	*n.a.*	*n.a.*	*n.a.*	*n.a.*	*n.a.*	*n.a.*	*n.a.*	*n.a.*	*n.a.*	*n.a.*	*n.a.*	*n.a.*	*n.a.*	*n.a.*
AQ-FC 111-6	FC colourless2	Mn decoloured	69.27	15.64	8.29	2.74	0.37	1.11	0.06	0.48	0.59	0.09	0.24	0.66	<0.04	0.00	10	15	21	36	13	8	13	<5	14	488	8	38	17	356	<10	28	18	3	<3
AQ-FC 42L-1	FC colourless2	Mn decoloured	70.01	15.73	7.40	2.29	0.39	1.33	0.06	0.50	0.44	0.14	0.16	1.22	<0.04	<0.04	10	20	15	29	13	15	24	<5	11	502	7	41	<3	286	10	23	14	3	4
AQ-FC 85-2	FC colourless2	Mn decoloured	68.21	14.88	8.86	3.04	0.53	2.17	0.08	0.63	0.52	0.10	0.10	1.18	<0.04	<0.04	12	39	8	38	15	10	18	<5	13	595	8	37	<3	627	<10	21	<10	4	<3
AQ-FC 85-4	FC colourless2	Mn decoloured	69.59	15.10	7.78	2.68	0.38	1.44	0.06	0.46	0.68	0.12	0.26	0.97	<0.04	<0.04	13	16	9	47	13	11	20	<5	15	477	7	37	<3	368	12	14	10	3	6
AQ-FC 85-5	FC colourless2	Mn decoloured	69.20	16.01	7.43	2.55	0.38	1.47	0.06	0.45	0.69	0.09	0.15	1.24	<0.04	<0.04	12	14	20	36	13	*7*	17	<5	17	459	7	39	27	374	<10	11	13	3	<3
85_7 media	FC colourless2	Mn decoloured	69.72	15.98	8.30	2.63	0.39	1.31	0.09	0.60	0.45	0.06	0.11	1.32	<0.04	<0.04	<200	<265	<696	n.a.	n.a.	<350	<321	n.a.	n.a.	n.a.	n.a.	n.a.	n.a.	n.a.	n.a.	n.a.	n.a.	n.a.	n.a.
AQ-FC 85-8	FC colourless2	Mn decoloured	69.98	15.08	8.18	2.67	0.38	1.28	0.06	0.46	0.60	0.10	0.19	1.10	<0.04	<0.04	10	17	12	28	16	*7*	19	<5	14	476	7	39	21	367	<10	23	10	6	<3
AQ-FC 111-5	FC colourless3	Mn+Sb decoloured	69.89	17.36	6.73	2.16	0.45	0.61	0.08	0.51	0.54	0.08	0.26	1.19	<0.04	0.34	5	25	72	22	13	5	21	<5	13	406	7	50	27	215	<10	20	25	<3	<3
AQ-FC 104-2	Fc colourless 3	Mn+Sb decoloured	70.09	17.43	6.84	2.25	0.45	0.65	0.08	0.51	0.55	0.08	0.27	1.18	<0.04	0.33	7	32	55	24	8	7	22	<5	14	422	7	48	26	231	<10	25	<10	<3	<3
AQ-FC 106-2	Fc colourless 3	Mn+Sb decoloured	69.97	18.21	6.20	2.14	0.50	0.44	0.09	0.55	0.53	0.10	0.28	1.23	<0.04	0.46	4	35	96	13	22	4	26	<5	13	371	6	56	28	174	<10	14	24	<3	<3
AQ-FC 42-2	Fc colourless 3	Mn+Sb decoloured	69.25	17.25	*7.09*	2.40	0.48	0.79	0.07	0.54	0.60	0.10	0.30	1.17	<0.04	0.28	12	94	66	25	10	28	22	<5	13	436	6	49	26	277	<10	22	25	<3	<3
AQ-FC 42L-2	Fc colourless 3	Mn+Sb decoloured	70.78	16.51	6.96	2.37	0.57	0.51	0.09	0.62	0.72	0.20	0.21	1.16	<0.04	<0.04	15	267	341	16	16	*7*	31	<5	15	396	12	56	34	220	<10	22	15	<3	<3
AQ-FC 85-9	Fc colourless 3	Mn+Sb decoloured	69.66	17.20	6.70	2.25	0.47	0.61	0.08	0.50	0.61	0.09	0.26	1.24	<0.04	0.33	5	24	*67*	24	16	*7*	24	<5	14	406	5	49	9	231	<10	18	15	<3	<3
AQ-FC 104-3	FC/1a	HIMT	63.07	18.01	*7.33*	2.86	3.57	2.21	0.47	1.46	0.41	0.13	0.33	1.15	<0.04	<0.04	14	74	42	112	59	34	50	<5	11	559	15	209	6	356	11	10	17	<3	<3
AQ-FC 106-1	FC/1a	HIMT	65.15	16.00	5.52	*2.97*	4.20	1.65	0.64	1.46	0.44	0.16	0.19	1.01	<0.04	<0.04	15	121	41	105	82	49	60	<5	12	454	19	295	14	292	15	11	20	<3	<3
AQ-FC 106-4	FC/1a	HIMT	65.06	16.94	6.03	3.01	3.90	1.75	0.57	1.41	0.42	0.14	0.20	0.98	<0.04	<0.04	14	119	42	116	96	105	51	<5	11	497	19	254	6	364	34	<10	23	<3	<3
AQ-FC 106-5	FC/1a	HIMT	65.89	17.35	4.83	3.16	3.46	1.96	0.60	1.17	0.48	0.11	0.30	0.95	<0.04	<0.04	15	96	25	99	78	39	52	<5	13	368	16	267	5	549	13	17	<10	3	3
AQ-FC 117-2	FC/1a	HIMT	67.53	15.02	4.94	3.12	3.11	2.09	0.69	1.29	0.45	0.10	0.13	1.05	<0.04	<0.04	16	95	39	89	94	47	50	<5	12	398	16	295	*7*	386	21	23	12	<3	<3
AQ-FC 117-5	FC/1a	HIMT	64.54	18.14	5.36	2.98	4.37	1.79	0.59	1.13	0.39	0.17	0.29	1.16	<0.04	<0.04	12	114	26	109	77	51	50	<5	11	425	18	266	6	353	18	29	19	<3	4
AQ-FC 118-2	FC/1a	HIMT	67.57	15.93	4.83	3.09	3.32	2.28	0.64	1.19	0.47	0.10	0.17	0.98	<0.04	<0.04	18	114	21	95	87	44	57	<5	13	382	15	267	6	373	<10	18	17	3	3
AQ-FC 104-6	FC/1a	HIMT	64.62	17.91	4.89	3.13	3.59	1.73	0.63	1.19	0.45	0.11	0.28	1.05	<0.04	<0.04	11	85	22	95	80	37	45	<5	12	368	16	269	*7*	491	13	13	<10	6	5
AQ-FC-104-5	FC/1b	HIT	*66.71*	*18.51*	*5.77*	*2.66*	*2.89*	*0.10*	*0.55*	*1.12*	*0.30*	*0.00*	*0.29*	*1.07*	*<0.04*	*<0.04*	*2406*	*3271*	*2828*	*n.a.*	*n.a.*	*<350*	*<321*	*n.a.*	*n.a.*	*n.a.*	*n.a.*	*n.a.*	*n.a.*	*n.a.*	*n.a.*	*n.a.*	*n.a.*	*n.a.*	*n.a.*
AQ-FC 106-10	FC/1b	HIMT	63.57	19.22	5.11	3.12	2.33	2.65	*0.83*	1.31	0.38	0.06	0.25	1.05	<0.04	<0.04	16	116	11	57	90	29	38	<5	11	396	12	355	6	531	15	23	<10	7	4
AQ-FC 106-11	FC/1b	HIMT	66.86	17.66	6.75	2.62	1.32	1.60	*0.38*	0.89	0.58	0.07	0.31	1.11	<0.04	<0.04	11	109	171	40	48	14	31	<5	13	453	12	168	*7*	694	11	28	<10	<3	<3
AQ-FC 106-6	FC/1b	HIMT	67.03	18.33	6.57	2.27	1.69	1.15	0.24	0.85	0.56	0.10	0.22	1.16	<0.04	<0.04	11	59	57	57	30	18	28	<5	15	469	10	111	29	279	28	19	21	<3	<3
AQ-FC 106-7	FC/1b	HIMT	64.91	19.46	5.50	2.72	1.95	2.47	0.74	1.33	0.33	0.04	0.36	1.13	<0.04	<0.04	11	92	20	60	91	27	46	<5	12	428	14	394	6	346	14	18	21	5	<3
AQ-FC 106-8	FC/1b	HIMT	65.62	18.72	6.40	2.46	1.50	2.01	0.32	0.91	0.46	*0.07*	0.38	1.11	<0.04	<0.04	8	66	*75*	38	46	58	31	<5	11	517	12	156	33	267	<10	<10	16	<3	<3
AQ-FC 106-9	FC/1b	HIMT	65.44	19.44	6.22	2.49	1.53	1.60	0.42	0.97	0.32	0.05	0.30	1.18	<0.04	<0.04	11	48	20	48	51	33	28	<5	10	463	10	191	5	547	<10	12	<10	4	<3
AQ-FC 111-3	FC/1b	HIMT	65.35	20.02	8.02	2.08	0.81	1.36	0.13	0.82	0.56	0.08	0.50	0.97	<0.04	<0.04	6	62	*73*	26	15	11	20	<5	11	606	10	74	<3	282	<10	<10	10	<3	7
AQ-FC 111-4	FC/1b	HIMT	65.80	17.50	7.93	2.54	1.09	1.79	0.18	1.11	0.61	0.09	0.46	0.86	<0.04	<0.04	8	85	68	30	26	17	24	<5	12	*697*	9	90	3	415	<10	17	11	<3	3
AQ-FC-111_8	FC/1b	HIT	*66.81*	*19.07*	*6.24*	*2.54*	*2.30*	*0.25*	*0.44*	*1.09*	*0.40*	*0.02*	*0.27*	*1.20*	*<0.04*	*<0.04*	*1879*	*3138*	*1595*	*n.a.*	*n.a.*	*<350*	*<321*	*n.a.*	*n.a.*	*n.a.*	*n.a.*	*n.a.*	*n.a.*	*n.a.*	*n.a.*	*n.a.*	*n.a.*	*n.a.*	*n.a.*
AQ-FC 117-1	FC/1b	HIMT	65.08	18.65	5.80	2.55	1.63	2.27	0.52	1.20	0.30	0.04	0.18	1.52	<0.04	<0.04	9	34	13	50	63	18	31	<5	9	449	11	239	5	329	13	15	14	5	<3
AQ-FC 117-3	FC/1b	HIMT	64.89	19.54	5.63	2.75	2.53	1.34	0.52	1.04	0.40	0.09	0.33	1.36	<0.04	<0.04	11	66	28	65	66	28	36	<5	13	406	13	233	35	246	21	16	19	<3	<3
AQ-FC 117-4	FC/1b	HIMT	65.36	17.69	6.32	2.86	2.43	1.82	0.46	1.04	0.69	0.12	0.29	1.02	<0.04	<0.04	14	88	96	66	62	25	45	<5	13	437	15	204	6	584	18	21	<10	<3	<3
AQ-FC 118-1	FC/1b	HIMT	66.12	18.39	7.13	2.32	1.68	1.13	0.32	0.90	0.53	0.12	0.36	0.98	<0.04	<0.04	22	93	244	49	44	19	38	<5	10	537	15	144	5	267	13	14	17	<3	5
AQ-FC-96_1	FC/1b	HIMT	*65.02*	*20.15*	*6.39*	*2.50*	*1.76*	*1.93*	*0.52*	*1.02*	*0.35*	*0.04*	*0.29*	*1.35*	*<0.04*	*<0.04*	*<350*	*<265*	*<696*	*n.a.*	*n.a.*	*<350*	*<321*	*n.a.*	*n.a.*	*n.a.*	*n.a.*	*n.a.*	*n.a.*	*n.a.*	*n.a.*	*n.a.*	*n.a.*	*n.a.*	*n.a.*
AQ-FC- 96_1blue	FC/1b	HIMT	*62.73*	*18.93*	*6.07*	*2.67*	*3.71*	*1.89*	*0.54*	*1.05*	*0.42*	*0.02*	*0.24*	*1.15*	*0.05*	*<0.04*	*2737*	*8245*	*8279*	*n.a.*	*n.a.*	*<350*	*612*	*n.a.*	*n.a.*	*n.a.*	*n.a.*	*n.a.*	*n.a.*	*n.a.*	*n.a.*	*n.a.*	*n.a.*	*n.a.*	*n.a.*
AQ-FC-96_2	FC/1b	HIMT	*65.79*	*19.62*	*6.06*	*2.43*	*1.55*	*2.20*	*0.54*	*1.44*	*0.33*	*0.02*	*0.27*	*1.30*	*<0.04*	*<0.04*	*<200*	*<265*	*<696*	*n.a.*	*n.a.*	*<350*	*<321*	*n.a.*	*n.a.*	*n.a.*	*n.a.*	*n.a.*	*n.a.*	*n.a.*	*n.a.*	*n.a.*	*n.a.*	*n.a.*	*n.a.*
AQ-FC-96_2blue	FC/1b	HIMT	*62.83*	*18.27*	*6.11*	*2.55*	*1.52*	*2.15*	*0.52*	*1.30*	*0.39*	*0.02*	*0.29*	*1.08*	*<0.04*	*<0.04*	*<200*	*49227*	*<696*	*n.a.*	*n.a.*	*<350*	*424*	*n.a.*	*n.a.*	*n.a.*	*n.a.*	*n.a.*	*n.a.*	*n.a.*	*n.a.*	*n.a.*	*n.a.*	*n.a.*	*n.a.*
AQ-FC CHA1	FC/1b	HIMT	66.62	17.59	6.94	2.63	1.45	1.68	0.39	0.92	0.58	0.09	0.26	1.02	<0.04	<0.04	14	178	575	46	50	13	74	<5	11	445	19	181	30	702	13	24	<10	<3	<3
AQ-FC-PV2	FC/1b	HIT	*62.99*	*19.66*	*6.54*	*2.63*	*3.48*	*0.43*	*0.38*	*1.37*	*0.47*	*0.02*	*0.32*	*1.28*	*<0.04*	*<0.04*	*6697*	*2405*	*6225*	*n.a.*	*n.a.*	*<350*	*473*	*n.a.*	*n.a.*	*n.a.*	*n.a.*	*n.a.*	*n.a.*	*n.a.*	*n.a.*	*n.a.*	*n.a.*	*n.a.*	*n.a.*
AQ-FC 106-3	FC/2	Levantine1	66.08	16.95	8.72	2.91	0.97	1.30	0.14	0.62	1.24	0.17	0.21	0.64	<0.04	<0.04	20	170	57	36	47	152	36	<5	21	506	9	72	<3	376	<10	17	11	<3	3
AQ-FC 109b/111-2	FC/2	Levantine1	70.41	15.21	9.09	2.40	0.34	0.02	0.06	0.57	0.63	0.04	0.24	1.14	<0.04	<0.04	<3	11	15	6	19	8	10	<5	16	488	9	39	29	203	<10	17	20	5	<3
AQ-FC 109b/111-3	FC/2	Levantine1	66.82	16.52	8.79	2.83	0.53	1.63	0.09	0.53	1.45	0.16	0.23	0.48	<0.04	<0.04	32	99	96	47	13	17	52	<5	21	471	9	50	<3	539	<10	<10	<10	<3	<3
AQ-FC- 109_1	FC/2	Levantine1	*65.67*	*18.17*	*9.48*	*2.59*	*0.45*	*1.91*	*0.06*	*0.76*	*0.46*	*0.09*	*0.20*	*1.17*	*<0.04*	*<0.04*	*<200*	*<265*	*<696*	*n.a.*	*n.a.*	*<350*	*<321*	*n.a.*	*n.a.*	*n.a.*	*n.a.*	*n.a.*	*n.a.*	*n.a.*	*n.a.*	*n.a.*	*n.a.*	*n.a.*	*n.a.*
AQ-FC 116-1	FC/2	Levantine1	67.70	15.84	9.43	3.03	0.44	0.33	0.08	0.51	1.49	0.21	0.24	1.29	<0.04	<0.04	9	31	447	11	12	10	17	<5	23	448	13	42	25	266	<10	26	19	<3	<3
AQ-FC 96-3	FC/2	Levantine1	67.73	*17.87*	7.60	2.51	0.46	1.16	0.07	0.46	1.12	0.11	0.25	0.81	<0.04	<0.04	4	68	70	19	21	5	26	<5	19	405	7	45	3	361	<10	12	<10	<3	<3
AQ-FC 109/111-1	FC/3	Série 3.2	69.21	17.98	6.50	1.97	1.07	0.65	0.12	0.61	0.41	0.06	0.28	1.03	<0.04	<0.04	6	51	14	26	22	16	24	<5	13	442	8	67	19	196	13	<10	19	5	<3
AQ-FC 109-5	FC/3	Série 3.2	67.09	19.78	6.90	1.92	0.60	0.41	0.10	0.79	0.47	0.05	*0.44*	*1.36*	*<0.04*	*0.27*	5	71	74	17	10	4	24	<5	9	550	9	56	<3	181	<10	12	20	<3	37
AQ-FC 111-2	FC/3	Série 3.2	69.39	18.90	5.71	1.91	0.54	0.76	0.10	0.50	0.40	0.04	0.35	1.14	<0.04	<0.04	5	24	25	25	11	5	17	<5	13	379	6	60	29	250	21	10	17	4	<3
AQ-FC 111-7	FC/3	Série 3.2	66.50	19.43	6.90	2.05	1.38	1.16	0.20	0.75	0.53	0.07	0.35	1.26	<0.04	<0.04	10	75	74	41	26	13	28	<5	13	478	9	103	29	243	12	12	17	<3	<3
AQ-FC 116-2	FC/3	Série 3.2	69.40	17.86	6.97	1.71	0.53	1.14	0.08	0.54	0.31	0.04	0.31	1.29	<0.04	<0.04	4	19	35	20	9	6	23	<5	12	488	6	53	33	246	<10	19	15	<3	<3
AQ-FC 117-7	FC/3	Série 3.2	68.34	20.04	6.32	1.65	0.47	0.81	0.08	0.51	0.40	0.04	0.40	1.24	<0.04	<0.04	6	22	15	35	8	5	14	<5	12	442	6	48	31	227	<10	<10	16	5	<3
AQ-FC PV-1	FC/3	Série 3.2	66.70	20.82	*7.20*	1.48	0.45	0.82	0.08	0.47	0.29	0.03	0.45	1.43	<0.04	<0.04	<3	20	9	21	12	4	12	<5	10	514	6	48	<3	203	10	13	16	5	4
AQ-FC SL-2	FC/3	Série 3.2	68.04	19.53	6.76	1.59	0.48	0.75	0.08	0.52	0.30	0.03	*0.27*	*1.42*	<0.04	<0.04	5	23	22	22	11	4	20	<5	11	443	6	49	10	211	13	28	18	4	<3

Table 4.3

group	composition	n		SiO2	Na2O	CaO	Al2O3	Fe2O3	MnO	TiO2	MgO	K2O	P2O5	SO3	Cl	SnO2	Sb2O3	Co	Cu	Pb
FC coloured amber	int. coloured amber	2	mean	68.31	18.56	8.42	2.27	0.32	0.02	0.06	0.49	0.57	0.09	0.35	1.24	<0.04	<0.04	<3	19	18
			dev.st	1.70	0.19	1.46	0.11	0.04	0.00	0.01	0.08	0.08	0.02	0.08	0.26				15	7
FC coloured blue	int. coloured blue	2	mean	68.35	16.87	8.21	2.43	1.14	0.30	0.06	0.52	0.67	0.10	0.35	0.84	<0.04	0.18	376	461	39
			dev.st	1.03	0.30	0.86	0.25	0.20	0.06	0.01	0.01	0.01	0.01	0.16	0.38		0.23	49	163	23
FC coloured- int. (tot)	Int.coloured	4	mean	68.33	17.71	8.31	2.35	0.73	0.16	0.06	0.50	0.62	0.09	0.35	1.04	*<0.04*	0.10	189	240	29
			dev.st	1.15	1.00	0.98	0.18	0.49	0.16	0.01	0.05	0.07	0.02	0.10	0.35		0.16	265	313	15
FC coloured	naturally coloured	4	mean	70.79	16.05	7.23	2.40	0.42	0.41	0.07	0.48	0.59	0.13	0.16	1.17	<0.04	<0.04	12	46	50
			dev.st	1.40	0.92	0.19	0.12	0.06	0.24	0.01	0.04	0.09	0.04	0.08	0.10			8	27	27
FC coloured (tot)		8	mean	69.56	16.88	7.77	2.37	0.57	0.29	0.06	0.49	0.60	0.11	0.26	1.11	*<0.04*	*<0.04*	158	143	39
			dev.st	1.77	1.25	0.88	0.15	0.36	0.23	0.01	0.05	0.08	0.03	0.13	0.25			200	207	24
FC colourless1 high Al	Sb decoloured	3	mean	69.43	18.00	6.64	2.54	0.56	0.02	0.10	0.59	0.43	0.05	0.30	1.38	<0.04	0.67	2	26	48
			dev.st	1.26	1.41	1.37	0.10	0.23	0.01	0.04	0.18	0.11	0.02	0.04	0.21		0.13	1	5	31
FC colourless1low alumina	Sb decoloured	4	mean	71.75	18.12	5.40	1.83	0.39	0.02	0.07	0.42	0.37	0.03	0.28	1.44	<0.04	0.52	3	27	28
			dev.st	1.99	0.88	0.72	0.08	0.08	0.01	0.01	0.15	0.03	0.00	0.06	0.10		0.13			
FC colourless1 tot	Sb decoloured	7	mean	71.08	17.84	5.86	2.18	0.46	0.02	0.08	0.47	0.40	0.04	0.28	1.43	<0.04	0.55	<3	24	37
			dev.st	2.01	1.03	1.15	0.39	0.17	0.01	0.03	0.17	0.08	0.01	0.05	0.14		0.20	1	10	20
FC colourless2	Mn decoloured	11	media	69.35	15.40	8.07	2.68	0.42	1.51	0.07	0.53	0.56	0.10	0.18	1.10	<0.04	<0.04	11	21	13
			dev.st	0.62	0.44	0.47	0.20	0.07	0.33	0.01	0.09	0.12	0.03	0.06	0.20			1	9	5
FCcolourless3	Sb+Mn decoloured	6	media	69.94	17.33	6.75	2.26	0.49	0.60	0.08	0.54	0.59	0.11	0.26	1.19	<0.04	0.31	8	80	116
			dev.st	0.51	0.54	0.31	0.11	0.05	0.12	0.01	0.04	0.07	0.05	0.03	0.03		0.12	4	96	111
FC/1 (tot)	HIMT	29	media	65.40	18.21	6.05	2.72	2.49	1.71	0.51	1.16	0.44	0.08	0.28	1.13	<0.04	0.16	443	2122	826
			dev.st	1.35	1.24	0.78	0.26	1.00	0.62	0.15	0.18	0.10	0.05	0.07	0.15		0.09	1173	7745	2057
FC/1a	HIMT	8	mean	65.77	16.76	5.20	3.07	3.71	1.89	0.62	1.26	0.44	0.13	0.22	1.03	<0.04	<0.04	14	106	31
			st dev	1.30	1.15	0.46	0.08	0.47	0.23	0.04	0.13	0.03	0.03	0.07	0.07			2	14	9
FC/1b	HIMT	20	media	65.48	18.66	6.38	2.60	1.85	1.84	0.44	1.09	0.44	0.07	0.30	1.17	<0.04	<0.04	12	81	100
			dev.st	1.04	0.89	0.70	0.21	0.59	0.43	0.14	0.20	0.13	0.03	0.07	0.17			4	36	146
FC/1b	HIMT blue	2	mean	62.96	18.78	6.10	2.62	2.65	2.03	0.53	1.18	0.40	0.02	0.27	1.12	0.04	0.15	2211	23083	4323
			st dev	0.08	0.45	0.01	0.08	1.57	0.16	0.01	0.17	0.01	0.01	0.04	0.04		0.18		23103	5621
FC/1b	HIT blue	3	mean	65.74	19.15	6.21	2.63	2.89	0.26	0.46	1.20	0.39	0.02	0.29	1.18	<0.04	<0.04	2864	2368	3548
			st dev	2.06	0.59	0.40	0.07	0.61	0.17	0.09	0.15	0.08	0.01	0.03	0.10			2052	337	2396
FC/2 (tot)	Lev.1	6	media	67.44	16.76	8.85	2.71	0.53	1.06	0.08	0.57	1.07	0.13	0.23	0.92	<0.04	<0.04	16	76	137
			dev.st	1.65	1.15	0.69	0.25	0.22	0.74	0.03	0.10	0.43	0.06	0.02	0.33			12	63	176
FC/2a	Lev.1	3	mean	66.88	17.11	8.37	2.75	0.65	1.36	0.10	0.54	1.27	0.15	0.23	0.64	<0.04	<0.04	19	112	74
			dev.st	0.83	0.69	0.67	0.21	0.28	0.24	0.04	0.08	0.17	0.03	0.02	0.17			11	43	16
FC/2b	Lev.1	3	media	69.06	15.53	9.26	2.72	0.39	0.18	0.07	0.54	1.06	0.13	0.24	1.22	<0.04	<0.04	5	21	231
			dev.st	1.36	0.32	0.17	0.32	0.05	0.16	0.01	0.03	0.43	0.09	0.00	0.07			5	14	305
FC/3	Série 3.2	8	media	67.78	19.37	6.81	1.82	0.70	0.87	0.11	0.61	0.41	0.05	0.37	1.24	<0.04	<0.04	6	41	38
			dev.st	1.45	0.97	0.63	0.22	0.32	0.29	0.04	0.14	0.10	0.02	0.08	0.16			2	24	28

group	composition	n		V	Cr	Ni	Zn	Ga	Rb	Sr	Y	Zr	Nb	Ba	La	Ce	Nd	Th	U
FC coloured amber	int. coloured amber	2	mean	7	7	<3	15	<5	14	418	7	37	5	203	<10	22	17	4	<3
			dev.st	1	1		7		1	64	2	2	1	3		1	2	1	
FC coloured blue	int. coloured blue	2	mean	14	11	11	118	<5	16	432	7	36	18	203	<10	<10	17	<3	<3
			dev.st	1	1	2	122		1	48	1	1	4	32			0		
FC coloured- int. (tot)	Int.coloured	4	mean	10	9	11	66	<5	15	425	7	36	11	203	<10	13	17	<3	<3
			dev.st	5	3		72		1	10	0	1	9	0		12	0		

Table 4.3

FC coloured	naturally coloured	4	mean	16	11	6	19	<5	13	390	7	42	17	233	<10	20	19	<3	<3
			dev.st	8	2	3	4		1	33	1	3	20	20		6	4		
FC coloured (tot)		8	mean	13	10	7	43	<5	14	408	7	39	13	218	<10	22	18	<3	<3
			dev.st	6	2	3	66		1	42	1	4	11	24	9	6	3		
FC colourless1 high Al	Sb decoloured	3	mean	12	15	5	26	<5	12	463	6	55	17	99	<10	33	24	3	<3
			dev.st	5	2	3	8		1	121	2	13	13	27		8	5	1	
FC colourless1low alumina	Sb decoloured	4	mean	10	11	4	21	<5	11	331	6	45	24	108	<10	30	22	6	<3
			dev.st																
FC colourless1 tot	Sb decoloured	7	mean	10	12	4	22	<5	10	366	6	46	19	95		28	21	4	3
			dev.st	3	5	2	7		4	134	2	15	9	29		11	7	2	
FC colourless2	Mn decoloured	11	media	37	14	11	19	<5	14	507	7	39	25	400	11	19	13	4	5
			dev.st	7	1	3	3		2	48	0	1	7	100	1	6	3	1	1
FCcolourless3	Sb+Mn decoloured	6	media	21	14	10	24	<5	14	406	7	51	25	225	<10	20	21	<3	<3
			dev.st	5	5	9	4		1	22	2	4	8	33		4	5		
FC/1 (tot)	HIMT	29	media	71	66	49	56	<5	12	455	14	231	11	439	17	19	17	5	<3
			dev.st	27	21	41	62		1	76	3	75	11	166	6	6	4	1	
FC/1a	HIMT	8	mean	101	85	53	52	<5	12	413	17	273	7	401	19	19	18	<3	<3
			st dev	9	8	23	5		1	49	2	16	3	88	8	7	4		
FC/1b	HIMT	20	media	55	56	27	38	<5	11	476	13	209	12	464	14	18	14	<3	<3
			dev.st	19	18	11	13		2	77	3	82	12	189	6	5	6		
FC/1b	HIMT blue	2	mean			<350	<321												
			st dev																
FC/1b	HIT blue	3	mean			<350	<321												
			st dev																
FC/2 (tot)	Lev.1	6	media	24	22	38	50	<5	20	464	9	50	12	349	<10	15	12	<3	<3
			dev.st	17	14	57	56		3	39	2	13	14	128		8	7		
FC/2a	Lev.1	3	mean	34	27	58	38	<5	20	461	8	56	2	425	<10	11	7	<3	<3
			dev.st	12	15	67	11		1	42	1	12	1	81		6	3		
FC/2b	Lev.1	3	media	9	16	9	14	<5	20	468	11	41	27	235	<10	22	20	<3	<3
			dev.st	4	5	1	5		5	28	3	2	3	45		6	1		
FC/3	Série 3.2	8	media	26	14	8	20	<5	12	482	7	62	25	227	14	16	16	5	<3
			dev.st	8	6	5	5		1	67	2	18	9	32	4	7	3	1	

Table 4.4

Sample	group	compositio	macro	type	SiO2	Na2O	CaO	Al2O3	Fe2O3	MnO	TiO2	MgO	K2O	P2O5	SO3	Cl	SnO2	Sb2O5	Co	Cu	Pb	Sc	V	Cr	Ni	Zn	Ga	Rb	Sr	Y	Zr	Nb	Ba	La	Ce	Nd	Th	U
D1	CL1a	HIMT	beaker	Is 96	63.71	18.45	6.22	3.07	3.17	1.87	0.60	1.53	0.54	0.10	0.26	1.07	<0.04	<0.04	<200	900	6500					<321												
D3	CL1a	HIMT	beaker	Is 96	65.63	18.66	5.86	2.42	3.12	2.12	0.31	0.97	0.43	0.06	0.06	1.30	<0.04	<0.04	<200	<265	<696					<321												
D5	CL1a	HIMT	beaker	Is 96	64.30	17.76	5.59	2.97	3.52	1.85	0.62	1.20	0.45	0.14	0.25	1.20	<0.04	<0.04	7	98	35	<5	99	83	*44*	67	<5	11	413	16	289	4	257	11	18	30	<3	4
BLS	CL1a	HIMT	waste		64.56	16.54	6.05	3.08	3.84	2.08	0.62	1.35	0.50	0.16	0.25	1.09	<0.04	<0.04	18	133	125	<5	107	83	*54*	55	8	14	474	18	273	6	299	17	10	26	<3	5
A2	CL1a	HIMT	waste		64.73	17.71	6.11	3.1	3.4	1.17	0.54	1.37	0.53	0.13	0.21	1.30	<0.04	<0.04	9	79	31	<5	110	74	*36*	42	<5	14	419	15	226	5	266	34	15	36	<3	6
PVM	CL1a	HIMT	waste	chunk	64.83	16.82	6.03	2.94	3.6	1.66	0.55	1.35	0.39	0.13	0.19	1.25	<0.04	<0.04	17	104	57	<5	118	76	*68*	48	8	12	457	15	212	6	376	<10	15	16	<3	6
CVG	CL1a	HIMT	waste		64.09	16.45	6.15	2.98	4.12	1.83	0.54	1.36	1.08	0.13	0.19	1.26	<0.04	<0.04	17	125	145	<5	128	73	*44*	54	8	29	493	20	231	8	378	<10	<10	14	<3	4
PVS	CL1a	HIMT	waste		64.12	18.34	5.99	3.04	3.19	1.57	0.54	1.54	0.40	0.11	0.29	1.58	<0.04	<0.04	11	96	169	<5	84	70	*34*	81	<5	10	451	17	240	8	288	25	21	26	<3	<3
TB	CL1a	HIMT	waste		64.89	16.80	6.18	3.02	3.56	1.64	0.54	1.36	0.95	0.12	0.17	1.41	<0.04	<0.04	15	119	48	<5	118	68	*34*	50	<5	28	505	15	236	7	380	<10	14	18	<3	<3
PF	*CL1b*	HIMT	*waste*		*62.31*	*18.97*	*5.86*	*2.94*	*2.24*	*2.32*	*0.62*	*1.82*	*1.09*	*0.11*	*0.51*	*1.49*	*<0.04*	*<0.04*	*<200*	*<265*	*<696*					*<321*												
SCH	CL1b	HIMT	waste		63.44	18.70	5.87	2.86	2.11	2.54	0.58	2.13	0.85	0.09	0.25	1.23	<0.04	<0.04	<200	<265	<696					<321												
BL SCH	CL1b	HIMT	waste		63.94	18.07	6.16	3.01	2.68	1.86	0.45	1.77	0.85	0.13	0.19	1.38	<0.04	<0.04	<200	<265	<696					<321												
D2	CL1b	HIMT	beaker	Is 96	66.18	17.77	6.79	2.84	2.46	1.73	0.44	1.36	0.55	0.05	0.25	0.89	<0.04	<0.04	<200	<265	<696					<321												
D20	CL1b	HIMT	beaker	Is 106	65.66	17.77	6.08	2.82	2.27	1.54	0.48	1.24	0.54	0.04	0.22	1.02	<0.04	<0.04	<200	<265	<696					<321												
D28	CL1b	HIMT	bottle	Is. 126	67.25	16.92	5.47	2.88	2.07	2.24	0.56	0.95	0.43	0.05	0.16	1.27	<0.04	<0.04	27	121	74	<5	62	69	*38*	40	<5	14	415	13	252	38	805	<10	17	<10	<3	<3
D 39.1	CL1b	HIMT	window pane		66.72	17.65	6.21	2.62	1.65	2.31	0.58	1.04	0.27	0.02	0.17	1.06	<0.04	<0.04	<200	<265	<696					400												
D39.2	CL1b	HIMT	window pane		66.79	17.66	6.19	2.58	1.92	2.07	0.57	0.95	0.35	0.04	0.18	1.32	<0.04	<0.04	11	63	20	<5	67	65	*16*	37	<5	11	457	13	271	5	1004	<10	34	<10	3	3
CVS	CL1b	HIMT	waste		66.04	17.67	4.78	3.07	2.09	2.44	0.69	1.48	0.63	0.05	0.19	1.29	<0.04	<0.04	20	43	111	<5	107	91	*34*	42	8	15	527	16	295	7	739	<10	22	<10	<3	5
F-D	CL1b	HIMT	waste		67.53	16.08	6.22	3.03	2.40	1.22	0.60	1.47	0.48	0.06	0.13	1.40	<0.04	<0.04	11	54	24	<5	82	73	*21*	34	<5	12	443	14	268	30	267	<10	26	25	4	<3
US D53	CL1b	HIMT	beaker	Is. 111	64.77	18.67	5.50	3.08	1.98	2.55	0.58	1.49	0.44	0.01	0.20	1.27	<0.04	<0.04	<200	<265	<696					<321												
US D56	CL1b	HIMT	beaker	Is. 106	67.95	17.90	6.01	2.38	1.50	2.25	0.26	0.94	0.40	0.06	0.20	1.25	<0.04	<0.04	<200	<265	<696					<321												
US-D54	CL1b	HIMT	beaker	Is.96	68.63	17.24	5.81	2.42	1.38	2.28	0.25	0.87	0.38	0.03	0.21	1.10	<0.04	<0.04	<200	<265	<696					<321												
D8	CL1b	HIMT	beaker	Is 96/106/109?	64.56	16.87	7.33	2.86	2.89	1.50	0.45	1.21	0.64	0.16	0.26	0.89	<0.04	<0.04	22	119	181	<5	87	61	*31*	51	<5	12	601	17	201	25	374	<10	13	21	<3	<3
US D52	CL1b	HIMT	beaker	Is.106 late	65.47	16.97	8.17	2.62	1.51	2.06	0.19	1.53	0.73	0.21	0.25	0.95	<0.04	<0.04	<200	0	<696					<321												
D24	CL1b	HIMT	beaker	Is 109	63.08	21.17	5.15	2.80	1.83	2.51	0.60	0.93	0.34	0.04	*0.16*	*1.44*	<0.04	<0.04	12	65	17	<5	66	79	*65*	30	<5	10	380	12	261	5	1181	<10	27	<10	7	<3
D34	CL1b	HIMT	cup	n.i.	63.64	21.02	5.68	2.73	2.05	1.49	0.49	0.96	0.37	0.08	0.31	1.62	<0.04	<0.04	9	52	17	<5	61	62	*18*	32	<5	12	442	11	240	8	321	<10	17	21	5	<3
D29	CL1b	HIMT	bottle	Sternini 1995	65.34	20.31	6.00	2.47	1.26	1.45	0.30	1.24	0.42	0.05	0.22	1.83	<0.04	<0.04	35	87	39	<5	38	34	*21*	30	<5	12	536	9	144	10	420	<10	21	<10	<3	<3
US PV01	CL1b	HIMT	waste	chunck	65.13	20.64	5.92	2.25	1.37	1.98	0.30	1.31	0.32	0.04	0.20	1.67	<0.04	<0.04	<200	<265	<696					<321												
D30	CL1b	HIMT	bottle	Foy 2000	67.42	19.70	5.36	2.82	2.05	0.11	0.77	1.08	0.36	0.01	0.25	1.41	<0.04	<0.04	600	840	1490					<321												
D26	CL1b	HIMT	beaker	Is 106	66.47	18.11	5.79	2.97	1.84	0.13	0.43	1.10	0.40	0.01	0.27	1.48	<0.04	<0.04	1212	1795	1377					<321												
D27	CL1b	HIMT	bottle	Is.92	64.53	20.41	6.44	2.65	2.18	0.30	0.34	0.92	0.49	0.02	0.36	1.18	<0.04	<0.04	1630	2840	<696					<321												
US D50	CL1c	HIMT	beaker	Is. 106	65.34	19.35	7.69	2.23	0.81	1.78	0.14	1.00	0.53	0.12	0.33	1.13	<0.04	<0.04	<200	<265	<696					<321												
US-T12	CL1c	HIMT	waste		65.44	18.47	7.59	2.55	1.05	1.13	0.14	1.31	0.66	0.11	0.22	1.14	<0.04	<0.04	<200	<265	<696					<321												
D18	CL2/a	Lev.1	n.i	n.i.	71.27	14.96	8.40	3.04	0.35	0.04	0.07	0.60	0.96	0.04	0.09	1.01	<0.04	<0.04	<200	<265	<696					<321												
D21	CL2/a	Lev.1	beaker	Is 106	68.01	16.52	9.92	2.81	0.30	0.03	0.07	0.67	0.86	0.03	0.14	1.08	<0.04	<0.04	<200	<265	<696					<321												
US T04	CL2/a	Lev.1	waste		70.34	16.01	7.87	2.86	0.43	0.03	0.08	0.62	0.82	0.08	0.15	1.03	<0.04	<0.04	<200	<265	<696					<321												
US T04	CL2/a	Lev.1	waste		70.34	16.01	7.87	2.86	0.43	0.03	0.08	0.62	0.82	0.08	0.15	1.03	<0.04	<0.04	<200	<265	<696					<321												
US G05	CL2/a	Lev.1	waste		69.25	15.21	7.91	2.81	0.46	0.03	0.09	0.61	2.46	0.15	0.11	1.17	<0.04	<0.04	<200	<265	<696					<321												
D33	CL2 /b?	Lev.1	cup	n.i.	69.67	17.10	7.26	2.46	0.45	0.56	0.10	0.69	0.75	0.10	0.13	1.10	<0.04	<0.04	<200	430	<696					<321												
US D58	CL2 /b	Lev.1	beaker	Is. 106 late	68.02	16.39	8.19	2.86	0.33	0.90	0.05	0.54	1.00	0.16	0.18	1.06	<0.04	<0.04	<200	0.0211	<696					<321												
C4	CL2 /b	Lev.1	waste		68.21	14.87	9.63	2.94	0.64	0.66	0.09	0.65	1.40	0.20	0.09	1.06	<0.04	<0.04	5	44	119	<5	21	17	8	77	<5	20	504	10	49	3	327	<10	11	23	<3	<3
US-T10	CL2 /b	Lev.1	waste		65.91	15.21	10.57	2.91	0.62	0.89	0.10	0.64	2.03	0.31	0.15	0.50	<0.04	<0.04	<200	<265	<696					<321												
US D55	CL2 /b	Lev.1	lamp	Y. Israeli 2008	65.84	15.47	10.60	2.82	0.60	0.91	0.09	0.61	2.07	0.34	0.14	0.49	<0.04	<0.04	<200	<265	<696					<321												
D7	CL3	Sèrie 3.2	beaker	Is 109	68.76	19.02	5.70	1.96	2.14	0.34	0.12	0.51	0.55	0.02	0.27	0.90	<0.04	<0.04	2060	4110	4180					<321												
D10	CL3	Sèrie 3.2	goblet	Is 111	68.07	21.10	6.26	1.97	0.65	0.82	0.13	0.77	0.40	0.01	0.29	1.26	<0.04	<0.04	<200	<265	<696					<321												
D11	CL3	Sèrie 3.2	goblet	Is 111	68.29	18.17	6.93	2.04	0.98	0.77	0.12	0.71	0.43	0.01	0.22	1.07	<0.04	<0.04	<200	<265	<696					<321												
D14	CL3	Sèrie 3.2	goblet	Is 111	69.05	20.02	6.99	1.56	0.38	0.72	0.09	0.62	0.37	0.00	0.31	1.29	<0.04	<0.04	<200	<265	<696					<321												
CVC	CL3	Sèrie 3.2	waste		68.30	18.97	6.14	1.83	0.82	0.61	0.12	0.61	0.72	0.05	0.33	1.24	<0.04	<0.04	6	38	88	<5	25	24	19	20	<5	23	424	8	64	<3	207	<10	14	20	<3	3
GRA	CL3	Sèrie 3.2	waste		68.97	19.31	5.89	1.75	0.56	0.83	0.09	0.58	0.84	0.03	0.29	1.32	<0.04	<0.04	8	25	34	<5	37	12	8	14	6	20	430	7	52	<3	222	10	22	14	<3	8
PVC	CL3	Sèrie 3.2	waste	chunk	69.04	19.38	6.11	1.77	0.65	0.51	0.10	0.56	0.44	0.04	0.35	1.23	<0.04	<0.04	4	29	16	<5	22	16	12	17	6	12	413	7	55	<3	203	<10	<10	26	6	<3
T-C	CL3	Sèrie 3.2	waste		67.82	19.76	6.50	1.78	0.58	0.52	0.11	0.64	0.44	0.02	0.32	1.19	<0.04	<0.04	<200	<265	<696					<321	n.d.												
A3	CL3	Sèrie 3.2	waste		68.15	19.41	6.28	1.84	0.78	0.58	0.12	0.59	0.57	0.04	0.27	1.45	<0.04	<0.04	3	33	38	<5	24	17	11	21	<5	16	438	8	63	12	208	<10	22	22	<3	<3
PV	CL3	Sèrie 3.2	waste	chunk	66.51	19.80	5.87	2.12	1.41	0.85	0.23	0.81	0.43	0.06	0.24	1.38	<0.04	<0.04	5	53	66	<5	36	31	16	38	<5	12	420	10	107	23	234	<10	23	25	<3	<3
F-D D12	CL3	Sèrie 3.2	waste		67.12	19.74	7.59	1.85	0.67	0.59	0.11	0.60	0.48	0.04	0.17	1.70	<0.04	<0.04	4	41	28	<5	32	72	18	22	<5	13	609	8	58	22	205	<10	<10	17	<3	<3
G3	CL3	Sèrie 3.2	waste		68.08	17.85	6.92	2.38	0.26	0.76	0.07	0.40	1.50	0.01	0.36	1.22	<0.04	<0.04	<200	<265	<696					<321												
G4	CL3	Sèrie 3.2	waste	pontil wad	67.11	17.63	6.50	2.38	1.25	1.35	0.27	1.00	0.88	0.01	0.36	1.14	<0.04	<0.04	<200	<265	<696					<321												
M1	CL3	Sèrie 3.2	waste	moil	69.18	18.66	6.80	2.12	0.77	0.98	0.21	0.73	0.42	0.04	0.21	1.28	<0.04	<0.04	<200	<265	<696					<321												
D16	CL3	Sèrie 3.2	beaker	Is 109	69.91	19.06	6.16	1.58	0.30	0.50	0.06	0.30	0.41	0.04	0.17	1.73	<0.04	<0.04	3	12	22	<5	16	17	52	14	<5	12	419	5	38	<3	197	<10	<10	11	3	3
D23	CL3	Sèrie 3.2	beaker	Is 109	71.96	17.39	4.95	1.94	0.61	0.74	0.18	0.49	0.47	0.03	0.12	1.52	<0.04	<0.04	7	13	9	<5	35	24	7	15	<5	12	366	7	93	12	226	12	18	21	6	<3
D25	CL3	Sèrie 3.2	beaker	Is 96/106/109	71.09	17.89	5.55	1.76	0.45	0.75	0.08	0.48	0.36	0.03	0.11	1.59	<0.04	<0.04	6	11	19	<5	34	14	8	20	<5	11	410	6	43	5	210	26	13	21	4	<3
D36	CL3	Sèrie 3.2	lamp	Uboldi 1999	71.42	17.64	5.82	1.86	0.58	1.10	0.10	0.52	0.34	0.03	0.14	1.42	<0.04	<0.04	<3	19	25	<5	19	10	3	22	<5	11	381	5	54	<3	272	<10	25	16	<3	<3
D37	CL3	Sèrie 3.2	lamp	n.i.	66.26	20.27	8.07	1.54	0.63	1.02	0.09	0.69	0.30	0.01	0.31	1.24	<0.04	<0.04	<200	<265	<696					<321												
D38	CL3	Sèrie 3.2	*conical pushed-in*	Leciejewicz 1977	70.92	18.02	6.24	1.59	0.34	0.62	0.06	0.31	0.39	0.03	0.15	1.61	<0.04	<0.04	3	11	12	<5	19	12	3	11	<5	12	437	5	38	15	210	14	20	21	4	<3
T-A	CL3	Sèrie 3.2	waste		66.52	19.34	8.01	1.99	0.71	0.13	0.15	0.81	0.62	0.04	0.31	1.38	<0.04	<0.04	<3	18	20	<5	16	15	3	17	<5	12	552	9	80	8	169	10	<10	18	4	<3
G1	CL3	Sèrie 3.2	waste		66.78	18.57	8.17	1.94	0.65	0.36	0.13	0.84	0.63	0.01	0.36	1.13	<0.04	<0.04	<200	<265	<696					<321												
BLC	CL3	Sèrie 3.2	waste		67.06	17.42	8.14	2.23	0.96	0.29	0.18	0.94	0.86	0.06	0.35	1.03	<0.04	<0.04	3	23	64	<5	23	26	21	21	6	17	546	10	92	<3	193	<10	14	23	<3	7
PVA	CL3?	Sèrie 3.2	waste	chunk	66.92	17.98	8.16	2.15	0.88	0.29	0.17	0.89	0.65	0.05	0.32	1.34	<0.04	<0.04	4	19	21	<5	20	83	41	18	<5	13	584	8	88	22	192	<10	26	21	4	<3
US D59	CL3	Sèrie 3.2	beaker	Is. 96	67.86	19.18	7.45	1.73	0.61	0.74	0.10	0.65	0.35	0.08	0.29	1.22	<0.04	<0.04	<200	<265	<696					<321												
US D57	CL3	Sèrie 3.2	beaker	Is.106	69.06	18.08	6.79	1.77	0.61	0.62	0.11	0.58	0.47	0.08	0.27	1.25	<0.04	<0.04	<200	<265	<696					<321												
US D51	CL3	Sèrie 3.2	beaker	Is. 106	67.93	18.16	7.90	1.94	0.86	0.77	0.12	0.71	0.55	0.09	0.24	1.30	<0.04	<0.04	<200	<265	0.067					<321												
US-G06	CL3	Sèrie 3.2	waste		66.60	21.85	5.75	1.80	0.52	0.96	0.11	0.62	0.30	0.02	0.44	1.23	<0.04	<0.04	<200	<265	<696					<321												
D32	**outlier**	Roman?	cup	Uboldi 1986	68.43	19.27	6.25	1.99	0.47	0.53	0.08	0.59	0.48	0.07	0.20	1.58	<0.04	0.50	4	20	66	28	18	10	<3	<321	<5	12	409	6	50	29	187	<10	21	16	<3	<3
D35	**outlier**	Roman?	palm cup/lamp	n.i.	71.44	18.92	5.41	1.77	0.32	0.01	0.08	0.45	0.36	0.01	0.22	1.28	<0.04	0.59	<200	<265	<696					<321												

Table 4.5

group	composition		SiO2	Na2O	CaO	Al2O3	Fe2O3	MnO	TiO2	MgO	K2O	P2O5	SO3	Cl	SnO2	Sb2O5	Co	Cu	Pb
CL1 tot	HIMT	mean	65.29	18.23	6.13	2.79	2.34	1.75	0.48	1.28	0.54	0.08	0.23	1.28	<0.04	<0.04	205	387	581
		st dev	8.93	2.78	1.06	0.45	0.89	0.65	0.16	0.31	0.19	0.05	0.06	0.27			447	694	1460
CL1a	HIMT	mean	64.54	17.50	6.02	2.96	3.50	1.76	0.54	1.34	0.58	0.12	0.21	1.27	<0.04	<0.04	13	207	889
		st dev	0.56	0.87	0.19	0.21	0.33	0.29	0.09	0.17	0.25	0.03	0.07	0.16			4	281	2268
CL1b mean	HIMT	mean	65.50	18.32	6.06	2.75	1.98	2.02	0.47	1.30	0.53	0.07	0.22	1.28	<0.04	<0.04	18	67	60
		st dev	1.74	1.48	0.75	0.25	0.46	0.42	0.15	0.35	0.22	0.05	0.08	0.26			9	77	689
CL1b blue	HIT	mean	66.14	19.40	5.87	2.82	2.02	0.18	0.51	1.03	0.42	0.02	0.29	1.36	<0.04	<0.04	1147	1825	1433
		st dev	1.47	1.18	0.54	0.16	0.17	0.10	0.22	0.10	0.07	0.01	0.06	0.16			518	1000	80
CL1c	HIMT weak	mean	65.39	18.91	7.64	2.39	0.93	1.46	0.14	1.16	0.60	0.11	0.27	1.14	<0.04	<0.04	<200	<265	<696
		st dev	0.07	0.63	0.07	0.23	0.17	0.46	0.00	0.22	0.10	0.01	0.08	0.01					
CL2/a	Lev1	mean	69.84	15.74	8.40	2.87	0.39	0.03	0.08	0.62	1.18	0.07	0.13	1.06	<0.04	<0.04	<200	<265	<696
		st dev	1.25	0.64	0.88	0.09	0.07	0.00	0.01	0.03	0.72	0.05	0.03	0.07					
CL/2b	Le1	mean	67.53	15.81	9.25	2.80	0.53	0.78	0.09	0.63	1.45	0.22	0.14	0.84	<0.04	<0.04	<200	<265	<696
		st dev	1.64	0.92	1.48	0.19	0.13	0.16	0.02	0.06	0.60	0.10	0.03	0.32					
CL/3	Sèrie 3.2	mean	68.38	18.92	6.70	1.90	0.68	0.68	0.13	0.64	0.54	0.03	0.27	1.31	<0.04	<0.04	163	297	290
		st dev	1.56	1.11	0.92	0.22	0.26	0.27	0.05	0.17	0.25	0.02	0.08	0.19			570	1055	1038

group	composition		V	Cr	Ni	Zn	Ga	Rb	Sr	Y	Zr	Nb	Ba	La	Ce	Nd	Th	U
CL1 tot	HIMT	mean	89	71	37	68	<5	14	468	15	243	11	490	<10	19	23	<3	<3
		st dev	28	17	16	85		6	94	4	54	10	278		7	8		
CL1a	HIMT	mean	109	75	45	57	<5	17	459	17	244	6	321	22	16	24	<3	5
		st dev	14	6	12	13		8	35	2	27	1	55	10	4	8		1
CL1b mean	HIMT	mean	71	67	31	77	<5	12	475	13	242	16	639	<10	19	19	<3	<3
		st dev	21	17	16	121		5	147	4	76	12	348		8	6		
CL1b blue	HIT	mean				<321												
		st dev																
CL1c	HIMT weak	mean				<321												
		st dev																
CL2/a	Lev1	mean				<321												
		st dev																
CL/2b	Le1	mean				<321												
		st dev																
CL/3	Sèrie 3.2	mean	26	27	16	19	<5	14	459	7	66	15	211	14	20	20	4	5.25
		st dev	8	22	14	6	0	4	78	2	22	7	24	7	5	4	1	2.62996

Label	Na2O	MgO	Al2O3	SiO2	P2O5	SO3	Cl	K2O	CaO	TiO2	MnO	Fe2O3	CoO	CuO	ZnO	SnO	Sb2O3	PbO	tot
BF AQ1	19.99	1.02	2.38	65.26	0.07	0.32	1.65	0.38	6.16	0.14	0.41	0.74	<0.03	1.36	<0.04	0.07	<0.04	0.34	100.29
BF AQ2	19.98	1.02	2.32	65.74	0.07	0.29	1.64	0.36	6.17	0.15	0.42	0.75	<0.03	1.35	<0.04	0.06	<0.04	0.37	100.68
BF AV1	7.14	1.31	3.87	37.27	0.35	0.16	0.38	0.87	7.30	0.37	0.15	2.73	<0.03	5.97	**0.19**	0.99	0.45	31.33	100.83
BF AZ1	20.23	1.02	2.31	65.06	0.09	0.32	1.73	0.40	6.39	0.15	0.69	**0.95**	<0.03	0.15	<0.04	0.32	<0.04	0.73	100.54
BF AZ2	18.41	0.85	2.10	66.72	0.12	0.31	1.30	0.58	6.96	0.09	0.63	0.83	0.03	0.38	<0.04	<0.04	1.06	0.25	100.61
BF AZ3	18.63	0.79	2.09	66.84	0.12	0.33	1.36	0.48	6.80	0.10	0.63	0.85	0.05	0.14	<0.04	<0.04	0.96	0.30	100.47
BF AZ4	15.82	0.69	2.53	67.72	0.14	0.34	0.91	0.70	6.16	0.09	0.61	0.91	0.08	0.17	<0.04	<0.04	3.02	0.23	100.12
BF AZ5	16.49	0.76	2.29	66.89	0.18	0.36	0.99	0.59	7.03	0.08	0.61	1.08	<0.03	0.09	<0.04	<0.04	2.38	0.24	100.04
BF B1	16.42	0.65	2.32	67.62	0.16	0.35	0.85	0.67	5.94	0.10	0.61	0.95	0.08	0.16	<0.04	<0.04	3.03	0.23	100.13
BF BS1	20.02	1.00	1.96	66.08	0.07	0.35	1.52	0.29	7.30	0.11	0.85	0.64	<0.03	0.55	<0.04	<0.04	0.05	<0.08	100.79
BF CE1	14.64	0.75	2.85	65.97	0.11	0.38	0.62	0.74	7.43	0.11	1.12	0.88	<0.03	1.41	<0.04	0.13	3.17	0.10	100.40
BF GR1	17.72	0.89	2.14	67.28	0.11	0.36	1.16	0.57	6.62	0.09	0.42	0.71	<0.03	0.08	<0.04	<0.04	1.83	0.14	100.12
BF GSO1	17.50	0.52	1.90	65.63	<0.05	0.27	1.25	0.47	5.88	0.07	0.31	0.45	<0.03	0.03	<0.04	<0.04	0.55	5.16	99.99
BF GSO2	16.60	0.58	1.96	63.69	0.06	0.37	0.87	0.60	4.56	0.13	0.42	1.28	<0.03	<0.03	<0.04	0.04	1.24	7.34	99.74
BF GSO3	17.66	0.70	2.12	66.03	0.07	0.32	1.04	0.57	4.49	0.16	0.59	1.38	<0.03	<0.03	<0.04	0.08	1.00	3.62	99.83
BF M1	19.42	0.90	2.01	64.37	<0.05	0.27	1.40	0.46	6.30	0.13	1.28	4.21	<0.03	0.46	**0.07**	<0.04	<0.04	0.08	101.35
BF M2	18.57	0.88	2.12	64.22	0.04	0.24	1.27	0.75	6.54	0.14	1.27	4.69	<0.03	0.62	**0.07**	<0.04	<0.04	<0.08	101.41
BF M3	14.17	2.21	1.93	60.66	0.91	0.34	0.77	2.47	9.32	0.13	0.50	3.19	<0.03	1.95	**0.06**	0.22	0.42	1.33	100.58
BF M4	18.91	0.90	2.14	64.72	<0.05	0.26	1.30	0.81	6.62	0.14	1.34	3.24	<0.03	0.75	**0.13**	<0.04	<0.04	0.09	101.35
BF TR INC1	15.73	0.45	2.37	72.42	0.11	0.12	1.15	0.52	7.07	0.05	0.14	0.35	<0.03	<0.03	<0.04	<0.04	<0.04	<0.08	100.48
BF TR INC2	19.09	0.93	1.96	67.20	<0.05	0.36	1.28	0.53	7.09	0.12	0.68	0.73	<0.03	<0.03	<0.04	<0.04	0.15	<0.08	100.12
BF TR INC3	19.41	0.76	2.07	67.90	0.07	0.28	1.59	0.38	6.36	0.10	0.96	0.52	<0.03	<0.03	<0.04	<0.04	0.05	<0.08	100.44
BF TU TR1	16.50	0.63	2.68	68.45	0.07	0.25	1.01	0.60	7.86	0.07	1.05	0.51	<0.03	1.01	<0.04	<0.04	<0.04	<0.08	100.69
BF TU1	17.95	0.64	2.13	66.35	<0.05	0.36	1.15	0.44	3.89	0.15	<0.05	1.09	<0.03	4.13	**0.07**	0.27	1.62	0.09	100.34
BF VCH3	18.13	0.87	2.19	66.87	<0.05	0.32	1.26	0.50	6.68	0.10	0.46	0.72	<0.03	0.78	<0.04	0.06	0.60	0.35	99.90
BF VG1	18.84	0.96	2.06	63.84	<0.05	0.27	1.30	0.50	5.82	0.13	1.09	1.93	<0.03	0.04	<0.04	0.23	<0.04	2.84	99.84
BF VP1	16.50	0.99	1.96	59.23	0.05	0.21	1.36	0.39	6.00	0.13	0.56	1.16	<0.03	1.80	<0.04	0.65	<0.04	8.81	99.81
BF VP2	18.00	0.99	1.94	61.55	0.05	0.21	1.59	0.36	6.44	0.15	0.24	1.04	<0.03	1.58	<0.04	0.45	0.13	5.50	100.20
BF VP3	17.05	0.97	2.07	60.38	0.09	0.20	1.44	0.49	5.83	0.16	0.67	1.35	<0.03	1.43	<0.04	0.37	0.09	6.90	99.48
BF VP4	17.15	0.90	1.99	58.67	0.05	0.22	1.34	0.38	5.80	0.12	0.96	0.97	<0.03	2.99	<0.04	0.60	<0.04	8.32	100.47
BF VS1	18.58	0.88	2.23	65.72	0.16	0.25	1.45	0.58	7.27	0.11	1.28	1.42	<0.03	0.90	**0.16**	<0.04	<0.04	<0.08	100.99
BF VS2	18.10	0.93	2.05	62.83	0.08	0.23	1.49	0.49	6.38	0.14	0.67	1.24	<0.03	2.16	<0.04	0.33	<0.04	3.61	100.73
BF- AU1	18.60	1.00	2.10	67.63	0.05	0.31	1.29	0.49	7.28	0.11	0.63	0.69	<0.03	<0.03	<0.04	<0.04	0.15	<0.08	100.33
BF-AU1cart	18.44	1.07	1.98	67.98	<0.05	0.30	1.25	0.57	7.42	0.12	0.69	0.74	<0.03	<0.03	<0.04	<0.04	0.15	<0.08	100.71
BF-CE2	18.69	0.90	3.22	67.83	<0.05	0.37	1.44	0.40	5.68	0.12	0.13	0.59	<0.03	0.86	<0.04	0.10	<0.04	0.13	100.47
BF-GSO4	15.56	0.59	1.93	54.93	<0.05	0.18	1.10	0.45	5.22	0.17	0.95	0.74	<0.03	<0.03	<0.04	1.73	<0.04	16.33	99.87
BF-R1	14.94	0.64	2.40	61.70	0.11	0.22	1.10	0.57	6.98	0.09	0.86	2.87	<0.03	1.19	<0.04	0.25	0.28	5.68	99.87
BF-VCH1	19.07	0.97	2.89	66.57	0.04	0.28	1.51	0.40	6.07	0.14	0.35	0.78	<0.03	0.42	<0.04	0.09	<0.04	0.38	99.95
BF-VCH2	18.92	0.92	2.97	68.03	<0.05	0.28	1.46	0.41	5.84	0.12	0.16	0.59	<0.03	0.45	<0.04	0.05	<0.04	0.04	100.26
PN AU2 Cart	16.29	0.65	2.31	69.45	0.09	0.12	1.21	0.53	7.99	0.06	1.87	0.37	<0.03	<0.03	<0.04	<0.04	<0.04	<0.08	*100.96*
PN AG1	16.29	0.65	2.25	69.26	0.09	0.13	1.29	0.54	8.01	0.06	1.77	0.38	<0.03	<0.03	<0.04	<0.04	<0.04	<0.08	*100.72*
PN AQ1	17.70	0.74	2.42	66.04	0.17	0.29	1.29	0.68	6.51	0.12	0.40	0.74	<0.03	2.30	<0.04	0.11	0.79	0.20	*100.50*
PN AU1	16.22	0.64	2.26	69.35	0.09	0.12	1.24	0.55	7.97	0.05	1.90	0.37	<0.03	<0.03	<0.04	<0.04	<0.04	<0.08	*100.76*
PN AU1 Cart	16.20	0.66	2.24	69.49	0.09	0.11	1.30	0.50	8.00	0.06	1.73	0.41	<0.03	<0.03	<0.04	<0.04	<0.04	<0.08	*100.79*
PN AU2	16.26	0.67	2.30	68.91	0.09	0.13	1.26	0.55	7.99	0.08	1.80	0.36	<0.03	<0.03	<0.04	<0.04	<0.04	<0.08	*100.40*
PN AV1	10.03	1.35	2.65	41.67	0.43	0.33	0.74	0.85	6.29	0.24	0.26	1.99	<0.03	8.34	<0.04	1.36	0.56	23.88	*100.98*
PN AV2 orange band	9.71	0.71	2.52	43.25	0.16	0.38	0.56	0.64	6.19	0.14	0.28	1.20	<0.03	8.94	**0.15**	1.00	1.40	23.41	*100.65*
PN AV2 red band	9.86	0.69	2.43	42.57	0.14	0.36	0.56	0.64	6.00	0.12	0.27	1.16	<0.03	7.71	**0.13**	0.97	1.38	25.48	*100.48*
PN AZ1	15.96	0.64	2.33	61.01	0.21	0.57	0.69	0.58	7.68	0.03	1.16	1.89	0.19	0.57	<0.04	<0.04	6.39	<0.08	*99.71*
PN AZ2	15.13	0.63	2.47	68.47	0.22	0.32	0.95	0.53	8.69	0.06	0.87	0.68	0.03	0.04	<0.04	<0.04	1.37	<0.08	*100.48*
PN BIOP1	14.89	0.46	1.99	67.82	0.18	0.36	0.63	0.54	5.85	0.04	0.66	0.39	<0.03	<0.03	<0.04	<0.04	4.67	1.29	*99.78*
PN BO1	15.06	0.80	2.49	66.11	0.24	0.42	0.68	0.74	6.70	0.09	0.63	1.12	0.17	0.26	<0.04	<0.04	4.40	0.11	*100.03*
PN BS1	19.32	0.65	2.16	66.89	0.11	0.31	1.39	0.61	5.85	0.11	0.57	0.63	<0.03	1.81	<0.04	0.14	0.62	0.09	101.30
PN CE1	15.58	0.74	2.75	65.36	0.18	0.41	0.73	0.68	6.37	0.11	0.43	0.98	<0.03	2.21	<0.04	0.10	3.74	0.13	*100.50*
PN GR1	17.91	0.73	2.46	67.48	0.20	0.29	1.14	0.69	6.73	0.11	0.59	0.74	<0.03	0.04	<0.04	<0.04	1.29	<0.08	*100.39*
Pn GSO1	17.28	0.66	2.10	66.22	0.08	0.28	0.99	0.62	4.99	0.14	0.67	0.88	<0.03	<0.03	<0.04	<0.04	0.85	3.76	*99.51*
PN GSO2 op band	13.76	0.49	2.23	61.23	0.06	0.17	0.90	0.49	6.76	0.07	0.44	0.95	<0.03	<0.03	<0.04	0.09	0.25	11.52	*99.39*
PN GSO2 transp	15.88	0.48	2.16	65.67	0.11	0.22	1.00	0.54	7.04	0.06	0.54	0.58	<0.03	<0.03	<0.04	0.10	0.52	5.11	*99.98*
PN M1	15.37	0.82	2.84	61.57	0.15	0.11	0.88	0.77	7.13	0.15	0.44	1.24	<0.03	1.27	**0.19**	0.34	0.40	6.27	*99.95*
PN M2	15.83	3.05	2.06	61.59	1.21	0.52	1.20	2.14	7.85	0.19	0.65	1.61	<0.03	1.62	**0.04**	0.19	0.85	0.83	*101.44*
PN M3 (V oliva)	12.76	0.92	2.79	51.78	0.16	0.18	0.98	0.78	7.58	0.16	0.34	1.42	<0.03	2.48	**0.06**	0.39	0.78	15.66	*99.20*
Pn NC1	16.76	0.59	2.41	68.67	0.09	0.19	1.21	0.56	6.88	0.09	0.35	0.51	<0.03	<0.03	<0.04	<0.04	0.26	1.82	*100.38*
PN TU2	17.71	0.67	2.21	64.86	0.11	0.41	1.10	0.56	5.32	0.11	0.14	0.74	<0.03	3.08	**0.06**	0.09	2.56	0.89	*100.63*
PN TU2 trasp band	17.83	0.87	2.52	62.86	0.31	0.37	1.15	0.69	5.54	0.13	0.22	0.88	<0.03	4.49	**0.11**	0.14	1.45	1.21	*100.77*
PN TU3	17.53	0.39	2.02	68.09	<0.05	0.21	1.38	0.50	4.52	0.07	<0.05	0.52	<0.03	2.83	**0.10**	0.21	1.89	0.31	*100.60*
PN V TR1	16.20	0.54	2.07	62.59	0.10	0.20	1.13	0.55	6.19	0.07	0.77	1.92	<0.03	<0.03	<0.04	0.13	0.38	7.25	*100.09*
PN V TR2	15.94	0.56	2.18	63.14	0.09	0.20	1.12	0.54	6.35	0.09	0.92	3.06	<0.03	<0.03	<0.04	0.11	0.31	5.40	*100.02*
PN VCH1	18.29	0.68	2.26	68.21	0.10	0.26	1.24	0.54	6.67	0.08	0.58	0.44	<0.03	0.68	<0.04	<0.04	0.88	<0.08	*100.91*
PN VG1	16.04	0.76	2.30	67.12	0.21	0.19	0.95	0.78	6.34	0.13	0.72	0.93	<0.03	0.04	<0.04	0.11	0.34	3.59	*100.54*
PN VP1	17.30	0.67	2.48	66.11	0.11	0.24	1.21	0.69	6.46	0.11	0.50	0.60	<0.03	1.06	<0.04	0.06	0.38	2.50	*100.48*
PN VS1	17.54	0.72	2.43	66.04	0.13	0.24	1.23	0.73	6.36	0.12	0.44	0.64	<0.03	2.52	<0.04	0.10	0.41	1.26	*100.92*
Pn-Tu1	15.72	0.93	2.39	65.27	0.30	0.38	0.81	0.84	6.75	0.09	0.63	0.69	<0.03	2.89	<0.04	0.29	2.52	0.40	*100.90*
TN AQ2	16.87	0.69	2.41	66.28	0.17	0.30	1.07	0.68	7.06	0.10	0.85	0.58	<0.03	2.17	<0.04	0.16	0.69	0.28	*100.36*
TN AU1	15.09	0.53	2.43	72.10	0.10	0.16	1.11	0.42	8.01	0.07	0.38	0.31	<0.03	<0.03	<0.04	<0.04	<0.04	<0.08	*100.72*
TN AU1 cart	15.14	0.53	2.39	71.99	0.08	0.15	1.11	0.42	7.84	0.07	0.35	0.33	<0.03	<0.03	<0.04	<0.04	<0.04	<0.08	*100.38*
TN AV1 orange band	11.67	1.92	2.05	50.62	0.65	0.54	0.80	1.47	7.03	0.18	0.27	1.28	<0.03	14.14	**0.07**	1.01	0.96	6.07	*100.76*
TN AV1 red band	12.94	1.94	2.11	52.13	0.62	0.49	0.85	1.45	7.26	0.17	0.28	1.36	<0.03	10.94	**0.06**	1.01	0.91	6.33	*100.87*
TN AZ1	16.12	0.67	2.49	67.52	0.17	0.40	0.85	0.68	7.24	0.07	0.81	0.63	<0.03	0.15	<0.04	<0.04	2.49	0.19	*100.48*
TN AZ2	16.24	0.69	2.37	67.47	0.19	0.42	0.94	0.60	6.76	0.10	0.57	0.82	0.03	0.12	<0.04	<0.04	2.88	0.29	*100.50*
TN B1	18.18	0.53	1.93	69.42	0.17	0.17	1.63	0.43	6.61	0.05	1.54	0.48	0.06	0.06	<0.04	<0.04	<0.04	<0.08	*101.24*
TN BI OP1	15.64	0.66	2.63	67.39	0.08	0.39	0.83	0.74	7.28	0.08	0.80	0.64	<0.03	0.07	<0.04	<0.04	2.88	0.23	*100.32*
TN BO1	16.40	0.63	2.32	68.95	0.19	0.24	1.15	0.59	7.06	0.07	0.78	0.84	0.10	0.17	<0.04	0.04	0.76	<0.08	*100.28*
TN BS1	17.55	0.70	2.36	64.50	0.22	0.28	1.34	0.68	5.95	0.14	0.53	0.81	<0.03	5.07	<0.04	0.13	0.56	0.26	*101.07*
TN CE1	16.76	0.79	2.66	63.88	0.18	0.47	0.87	0.67	6.62	0.11	0.23	0.98	<0.03	2.70	<0.04	0.14	3.02	0.09	*100.17*
TN GR1	17.14	0.76	2.32	67.80	0.06	0.34	0.95	0.71	6.57	0.09	0.31	0.70	<0.03	<0.03	<0.04	<0.04	2.60	<0.08	*100.35*
TN GR2	16.35	0.73	2.39	69.12	0.11	0.25	1.05	0.58	6.86	0.10	0.55	0.69	<0.03	0.06	<0.04	<0.04	1.49	0.19	*100.50*
TN GSO1	17.55	0.57	2.13	68.88	<0.05	0.29	1.20	0.53	6.67	0.08	1.09	0.26	<0.03	<0.03	<0.04	<0.04	0.45	0.51	*100.22*
TN NS1	16.77	0.73	2.31	66.04	0.10	0.28	1.08	0.74	6.35	0.10	0.64	1.59	<0.03	0.66	<0.04	0.06	0.66	2.38	*100.50*
TN TR INC 1	18.87	0.68	2.11	68.04	<0.05	0.31	1.36	0.57	7.20	0.09	<0.05	0.56	<0.03	<0.03	<0.04	<0.04	0.66	<0.08	*100.47*
TN TU1	16.11	0.70	2.50	65.13	0.20	0.39	0.89	0.72	7.22	0.09	0.73	0.67	<0.03	2.32	<0.04	0.22	1.64	0.40	*99.92*
TN TU3	16.03	0.71	2.44	64.95	0.18	0.39	0.89	0.70	7.25	0.09	0.74	0.66	<0.03	2.34	<0.04	0.21	1.78	0.41	*99.78*
TN V OL2	12.89	0.69	2.94	59.35	0.12	0.31	0.80	0.83	6.89	0.11	1.28	2.46	<0.03	2.07	<0.04	0.40	0.77	8.45	*100.34*

TN VCH1	17.23	0.77	2.51	64.06	0.14	0.40	1.01	0.62	6.53	0.12	0.20	0.91	<0.03	2.84	<0.04	0.16	3.22	0.12	*100.85*
TN VG1	16.38	0.84	2.26	66.25	0.15	0.29	1.22	0.72	6.94	0.09	0.43	1.36	<0.03	0.59	<0.04	0.09	0.64	2.27	*100.52*
TN VG2	15.89	0.77	2.82	67.10	0.12	0.28	1.05	0.86	7.52	0.10	0.97	1.59	<0.03	0.89	<0.04	0.04	0.44	0.50	*100.94*
TN VOL 1	16.11	0.90	2.78	66.44	0.17	0.27	1.11	0.81	6.81	0.16	0.58	1.91	<0.03	1.37	<0.04	0.15	0.57	0.87	*101.00*
TN VP1	16.47	0.67	2.38	64.83	0.12	0.23	1.18	0.65	6.63	0.10	0.62	0.74	<0.03	1.13	<0.04	0.13	0.56	3.58	*100.00*
TN VP2	16.35	0.62	2.30	64.91	0.12	0.24	1.18	0.65	6.54	0.11	0.61	0.69	<0.03	0.97	<0.04	0.16	0.66	3.99	*100.09*
TN VS1	17.51	0.71	2.44	66.32	0.14	0.28	1.24	0.71	7.10	0.11	0.34	0.98	<0.03	1.84	<0.04	0.10	0.72	0.49	*101.04*
TN VS2	16.67	0.66	2.42	66.42	0.13	0.23	1.21	0.62	6.97	0.10	0.76	0.76	<0.03	1.70	<0.04	0.11	0.50	1.07	*100.35*
TN- M3	15.31	0.75	2.60	60.61	0.11	0.27	0.96	0.79	6.27	0.11	0.34	2.62	<0.03	0.61	<0.04	0.31	0.68	8.09	*100.42*
TN-GSO2	16.56	0.53	2.28	66.86	0.05	0.26	1.13	0.57	6.45	0.11	0.78	0.45	<0.03	0.03	<0.04	0.09	0.49	3.63	*100.26*
TN-M1	14.51	0.81	2.73	62.84	0.18	0.28	0.98	0.85	7.01	0.10	0.84	4.10	<0.03	0.74	<0.04	0.24	0.64	3.61	*100.47*
TN-M2 dark band	14.36	0.81	2.84	62.82	0.16	0.27	0.94	0.80	6.97	0.11	0.86	3.89	<0.03	0.47	<0.04	0.21	0.75	4.65	100.94
TN-M2 paleband	14.01	0.81	2.75	62.76	0.15	0.29	0.93	0.87	7.10	0.10	0.87	2.71	<0.03	0.58	<0.04	0.17	0.85	5.40	100.37

gruppo	Label	Na2O	MgO	Al2O3	SiO2	P2O5	SO3	Cl	K2O	CaO	TiO2	MnO	Fe2O3	CoO	CuO	ZnO	SnO	Sb2O3	PbO	tot	*PbO/ (SiO2+Na2O+CaO)*
lead-glass	**TN V OL2**	12.89	0.69	2.94	59.35	0.12	0.31	0.80	0.83	6.89	0.11	1.28	2.46	<0.03	2.07	<0.04	0.40	0.77	8.45	*100.34*	*0.11*
lead-glass	**PN M3 (olive)**	12.76	0.92	2.79	51.78	0.16	0.18	0.98	0.78	7.58	0.16	0.34	1.42	<0.03	2.48	0.06	0.39	0.78	15.66	*99.20*	*0.22*
lead-glass	**PN GSO2 op band**	13.76	0.49	2.23	61.23	0.06	0.17	0.90	0.49	6.76	0.07	0.44	0.95	<0.03	<0.03	<0.04	0.09	0.25	11.52	*99.39*	*0.14*
lead-glass	**PN AV1**	10.03	1.35	2.65	41.67	0.43	0.33	0.74	0.85	6.29	0.24	0.26	1.99	<0.03	8.34	<0.04	1.36	0.56	23.88	*101.02*	*0.41*
lead-glass	**PN AV2 red band**	9.86	0.69	2.43	42.57	0.14	0.36	0.56	0.64	6.00	0.12	0.27	1.16	<0.03	7.71	0.06	0.97	1.38	25.48	*100.48*	*0.44*
lead-glass	**PN AV2 orange band**	9.71	0.71	2.52	43.25	0.16	0.38	0.56	0.64	6.19	0.14	0.28	1.20	<0.03	8.94	0.06	1.00	1.40	23.41	*100.65*	*0.40*
lead-glass	**BF VP1**	16.50	0.99	1.96	59.23	0.05	0.21	1.36	0.39	6.00	0.13	0.56	1.16	<0.03	1.80	0.06	0.65	<0.04	8.81	99.85	*0.11*
lead-glass	**BF VP4**	17.15	0.90	1.99	58.67	0.05	0.22	1.34	0.38	5.80	0.12	0.96	0.97	<0.03	2.99	<0.04	0.60	<0.04	8.32	100.47	*0.10*
lead-glass	**BF-GSO4**	15.56	0.59	1.93	54.93	0.01	0.18	1.10	0.45	5.22	0.17	0.95	0.74	<0.03	0.03	<0.04	1.73	<0.04	16.33	99.91	*0.22*
lead-glass	**BF AV1**	7.14	1.31	3.87	37.27	0.35	0.16	0.38	0.87	7.30	0.37	0.15	2.73	<0.03	5.97	0.06	0.99	0.45	31.33	100.83	*0.61*
silica-soda-lead	**TN NS1**	16.77	0.73	2.31	66.04	0.10	0.28	1.08	0.74	6.35	0.10	0.64	1.59	<0.03	0.66	<0.04	0.06	0.66	2.38	*100.50*	*0.03*
silica-soda-lead	**TN-GSO2**	16.56	0.53	2.28	66.86	0.05	0.26	1.13	0.57	6.45	0.11	0.78	0.45	<0.03	0.03	<0.04	0.09	0.49	3.63	*100.26*	*0.04*
silica-soda-lead	**TN- M3**	15.31	0.75	2.60	60.61	0.11	0.27	0.96	0.79	6.27	0.11	0.34	2.62	<0.03	0.61	<0.04	0.31	0.68	8.09	*100.42*	*0.10*
silica-soda-lead	**TN AV1 red band**	12.94	1.94	2.11	52.13	0.62	0.49	0.85	1.45	7.26	0.17	0.28	1.36	<0.03	10.94	0.06	1.01	0.91	6.33	*100.87*	*0.09*
silica-soda-lead	**TN AV1 orange band**	11.67	1.92	2.05	50.62	0.65	0.54	0.80	1.47	7.03	0.18	0.27	1.28	<0.03	14.14	0.07	1.01	0.96	6.07	*100.76*	*0.09*
silica-soda-lead	**TN VG1**	16.38	0.84	2.26	66.25	0.15	0.29	1.22	0.72	6.94	0.09	0.43	1.36	<0.03	0.59	<0.04	0.09	0.64	2.27	*100.52*	*0.03*
silica-soda-lead	**TN-M1**	14.51	0.81	2.73	62.84	0.18	0.28	0.98	0.85	7.01	0.10	0.84	4.10	n.d.	0.74	<0.04	0.24	0.64	3.61	*100.47*	*0.04*
silica-soda-lead	**TN-M2 paleband**	14.01	0.81	2.75	62.76	0.15	0.29	0.93	0.87	7.10	0.10	0.87	2.71	<0.03	0.58	<0.04	0.17	0.85	5.40	100.37	*0.06*
silica-soda-lead	**TN-M2 dark band**	14.36	0.81	2.84	62.82	0.16	0.27	0.94	0.80	6.97	0.11	0.86	3.89	<0.03	0.47	<0.04	0.21	0.75	4.65	100.94	*0.06*
silica-soda-lead	**TN VP1**	16.47	0.67	2.38	64.83	0.12	0.23	1.18	0.65	6.63	0.10	0.62	0.74	<0.03	1.13	<0.04	0.13	0.56	3.58	*100.00*	*0.04*
silica-soda-lead	**TN VP2**	16.35	0.62	2.30	64.91	0.12	0.24	1.18	0.65	6.54	0.11	0.61	0.69	<0.03	0.97	<0.04	0.16	0.66	3.99	*100.09*	*0.05*
silica-soda-lead	**TN VS2**	16.67	0.66	2.42	66.42	0.13	0.23	1.21	0.62	6.97	0.10	0.76	0.76	<0.03	1.70	<0.04	0.11	0.50	1.07	*100.35*	*0.01*
silica-soda-lead	**PN M1**	15.37	0.82	2.84	61.57	0.15	0.11	0.88	0.77	7.13	0.15	0.44	1.24	<0.03	1.27	<0.04	0.34	0.40	6.27	*99.95*	*0.07*
silica-soda-lead	**Pn NC1**	16.76	0.59	2.41	68.67	0.09	0.19	1.21	0.56	6.88	0.09	0.35	0.51	<0.03	<0.03	<0.04	<0.04	0.26	1.82	*100.38*	*0.02*
silica-soda-lead	**PN VG1**	16.04	0.76	2.30	67.12	0.21	0.19	0.95	0.78	6.34	0.13	0.72	0.93	<0.03	0.04	<0.04	0.11	0.34	3.59	*100.54*	*0.04*
silica-soda-lead	**Pn GSO1**	17.28	0.66	2.10	66.22	0.08	0.28	0.99	0.62	4.99	0.14	0.67	0.88	<0.03	<0.03	<0.04	<0.04	0.85	3.76	*99.53*	*0.04*
silica-soda-lead	**PN GSO2 transp**	15.88	0.48	2.16	65.67	0.11	0.22	1.00	0.54	7.04	0.06	0.54	0.58	<0.03	<0.03	<0.04	0.10	0.52	5.11	*99.98*	*0.06*
silica-soda-lead	**PN VP1**	17.30	0.67	2.48	66.11	0.11	0.24	1.21	0.69	6.46	0.11	0.50	0.60	<0.03	1.06	<0.04	0.06	0.38	2.50	*100.48*	*0.03*
silica-soda-lead	**PN VS1**	17.54	0.72	2.43	66.04	0.13	0.24	1.23	0.73	6.36	0.12	0.44	0.64	<0.03	2.52	<0.04	0.10	0.41	1.26	*100.92*	*0.01*
silica-soda-lead	**PN V TR1**	16.20	0.54	2.07	62.59	0.10	0.20	1.13	0.55	6.19	0.07	0.77	1.92	<0.03	0.03	<0.04	0.13	0.38	7.25	*100.12*	*0.09*
silica-soda-lead	**PN VTr2**	16.00	0.57	2.19	63.50	0.09	0.20	1.13	0.56	6.34	0.09	0.92	2.79	<0.03	0.02	<0.04	0.11	0.31	5.37	*100.07*	*0.06*
silica-soda-lead	**PN TU2**	17.71	0.67	2.21	64.86	0.11	0.41	1.10	0.56	5.32	0.11	0.14	0.74	<0.03	3.08	0.06	0.09	2.56	0.89	*100.63*	*0.01*
silica-soda-lead	**PN TU2 trasp band**	17.83	0.87	2.52	62.86	0.31	0.37	1.15	0.69	5.54	0.13	0.22	0.88	<0.03	4.49	0.11	0.14	1.45	1.21	*100.77*	*0.01*
silica-soda-lead	**PN BIOP1**	14.89	0.46	1.99	67.82	0.18	0.36	0.63	0.54	5.85	0.04	0.66	0.39	<0.3	<0.3	<0.04	<0.4	4.67	1.29	*99.78*	*0.01*
silica-soda-lead	**BF VP2**	18.00	0.99	1.94	61.55	0.05	0.21	1.59	0.36	6.44	0.15	0.24	1.04	<0.03	1.58	<0.04	0.45	0.13	5.50	100.20	*0.06*
silica-soda-lead	**BF VP3**	17.05	0.97	2.07	60.38	0.09	0.20	1.44	0.49	5.83	0.16	0.67	1.35	<0.03	1.43	<0.04	0.37	0.09	6.90	99.48	*0.08*
silica-soda-lead	**BF VS2**	18.10	0.93	2.05	62.83	0.08	0.23	1.49	0.49	6.38	0.14	0.67	1.24	<0.03	2.16	<0.04	0.33	<0.04	3.61	100.73	*0.04*
silica-soda-lead	**BF GSO3**	17.66	0.70	2.12	66.03	0.07	0.32	1.04	0.57	4.49	0.16	0.59	1.38	<0.03	<0.03	<0.04	0.08	1.00	3.62	99.83	*0.04*
silica-soda-lead	**BF GSO1**	17.50	0.52	1.90	65.63	0.02	0.27	1.25	0.47	5.88	0.07	0.31	0.45	<0.03	0.03	<0.04	<0.04	0.55	5.16	100.01	*0.06*
silica-soda-lead	**BF VG1**	18.84	0.96	2.06	63.84	0.02	0.27	1.30	0.50	5.82	0.13	1.09	1.93	<0.03	0.04	<0.04	0.23	<0.04	2.84	99.87	*0.03*
silica-soda-lead	**BF GSO2**	16.60	0.58	1.96	63.69	0.06	0.37	0.87	0.60	4.56	0.13	0.42	1.28	<0.03	<0.03	<0.04	0.04	1.24	7.34	99.74	*0.09*
silica-soda-lead	**BF M3**	14.17	2.21	1.93	60.66	0.91	0.34	0.77	2.47	9.32	0.13	0.50	3.19	<0.03	1.95	0.06	0.22	0.42	1.33	100.58	*0.02*
silica-soda-lead	**BF-R1**	14.94	0.64	2.40	61.70	0.11	0.22	1.10	0.57	6.98	0.09	0.86	2.87	<0.03	1.19	<0.04	0.25	0.28	5.68	99.87	*0.07*
silica-soda-lime	**TN GSO1**	17.55	0.57	2.13	68.88	0.04	0.29	1.20	0.53	6.67	0.08	1.09	0.26	<0.03	<0.03	<0.04	<0.04	0.45	0.51	*100.26*	*<0.01*
silica-soda-lime	**TN VG2**	15.89	0.77	2.82	67.10	0.12	0.28	1.05	0.86	7.52	0.10	0.97	1.59	<0.03	0.89	<0.04	0.04	0.44	0.50	*100.94*	*<0.01*
silica-soda-lime	**TN VOL 1**	16.11	0.90	2.78	66.44	0.17	0.27	1.11	0.81	6.81	0.16	0.58	1.91	<0.03	1.37	<0.04	0.15	0.57	0.87	*101.00*	*<0.01*
silica-soda-lime	**TN VCH1**	17.23	0.77	2.51	64.06	0.14	0.40	1.01	0.62	6.53	0.12	0.20	0.91	<0.03	2.84	<0.04	0.16	3.22	0.12	*100.85*	*<0.01*
silica-soda-lime	**TN VS1**	17.51	0.71	2.44	66.32	0.14	0.28	1.24	0.71	7.10	0.11	0.34	0.98	<0.03	1.84	<0.04	0.10	0.72	0.49	*101.04*	*<0.01*
silica-soda-lime	**TN CE1**	16.76	0.79	2.66	63.88	0.18	0.47	0.87	0.67	6.62	0.11	0.23	0.98	<0.03	2.70	<0.04	0.14	3.02	0.09	*100.17*	*<0.01*
silica-soda-lime	**TN TU1**	16.11	0.70	2.50	65.13	0.20	0.39	0.89	0.72	7.22	0.09	0.73	0.67	<0.03	2.32	<0.04	0.22	1.64	0.40	*99.92*	*<0.01*
silica-soda-lime	**TN TU3**	16.03	0.71	2.44	64.95	0.18	0.39	0.89	0.70	7.25	0.09	0.74	0.66	<0.03	2.34	<0.04	0.21	1.78	0.41	*99.78*	*<0.01*
silica-soda-lime	**TN AQ2**	16.87	0.69	2.41	66.28	0.17	0.30	1.07	0.68	7.06	0.10	0.85	0.58	<0.03	2.17	<0.04	0.16	0.69	0.28	*100.36*	*<0.01*
silica-soda-lime	**TN AZ1**	16.12	0.67	2.49	67.52	0.17	0.40	0.85	0.68	7.24	0.07	0.81	0.63	<0.03	0.15	<0.04	<0.04	2.49	0.19	*100.48*	*<0.01*

silica-soda-lime	**TN AZ2**	16.24	0.69	2.37	67.47	0.19	0.42	0.94	0.60	6.76	0.10	0.57	0.82	0.03	0.12	<0.04	<0.04	2.88	0.29	*100.50*	*<0.01*
silica-soda-lime	**TN BO1**	16.40	0.63	2.32	68.95	0.19	0.24	1.15	0.59	7.06	0.07	0.78	0.84	0.10	0.17	<0.04	0.04	0.76	<0.08	*100.28*	*<0.01*
silica-soda-lime	**TN B1**	18.18	0.53	1.93	69.42	0.17	0.17	1.63	0.43	6.61	0.05	1.54	0.48	0.06	0.06	<0.04	<0.04	<0.04	<0.08	*101.24*	*<0.01*
silica-soda-lime	**TN BS1**	17.55	0.70	2.36	64.50	0.22	0.28	1.34	0.68	5.95	0.14	0.53	0.81	<0.03	5.07	<0.04	0.13	0.56	0.26	*101.07*	*<0.01*
silica-soda-lime	**TN GR1**	17.14	0.76	2.32	67.80	0.06	0.34	0.95	0.71	6.57	0.09	0.31	0.70	<0.03	0.03	<0.04	<0.04	2.60	<0.08	*100.38*	*<0.01*
silica-soda-lime	**TN GR2**	16.35	0.73	2.39	69.12	0.11	0.25	1.05	0.58	6.86	0.10	0.55	0.69	<0.03	0.06	<0.04	<0.04	1.49	0.19	*100.50*	*<0.01*
silica-soda-lime	**TN TR INC 1**	18.87	0.68	2.11	68.04	0.03	0.31	1.36	0.57	7.20	0.09	0.01	0.56	<0.03	<0.03	<0.04	<0.04	0.66	<0.08	*100.50*	*<0.01*
silica-soda-lime	**TN AU1 cart**	15.14	0.53	2.39	71.99	0.08	0.15	1.11	0.42	7.84	0.07	0.35	0.33	<0.03	<0.03	<0.04	<0.04	<0.04	<0.08	*100.38*	*<0.01*
silica-soda-lime	**TN AU1**	15.09	0.53	2.43	72.10	0.10	0.16	1.11	0.42	8.01	0.07	0.38	0.31	<0.03	<0.03	<0.04	<0.04	<0.04	<0.08	*100.72*	*<0.01*
silica-soda-lime	**TN BI OP1**	15.64	0.66	2.63	67.39	0.08	0.39	0.83	0.74	7.28	0.08	0.80	0.64	<0.03	0.07	<0.04	<0.04	2.88	0.23	*100.32*	*<0.01*
silica-soda-lime	**PN M2**	15.83	3.05	2.06	61.59	1.21	0.52	1.20	2.14	7.85	0.19	0.65	1.61	<0.03	1.62	0.04	0.19	0.85	0.83	*101.44*	*<0.01*
silica-soda-lime	**PN VCH1**	18.29	0.68	2.26	68.21	0.10	0.26	1.24	0.54	6.67	0.08	0.58	0.44	<0.03	0.68	<0.04	<0.04	0.88	<0.08	*100.91*	*<0.01*
silica-soda-lime	**PN AG1**	16.29	0.65	2.25	69.26	0.09	0.13	1.29	0.54	8.01	0.06	1.77	0.38	<0.03	<0.03	<0.04	<0.04	<0.04	<0.08	*100.72*	*<0.01*
silica-soda-lime	**PN AU1 Cart**	16.20	0.66	2.24	69.49	0.09	0.11	1.30	0.50	8.00	0.06	1.73	0.41	<0.03	<0.03	<0.04	<0.04	<0.04	<0.08	*100.79*	*<0.01*
silica-soda-lime	**PN AU1**	16.22	0.64	2.26	69.35	0.09	0.12	1.24	0.55	7.97	0.05	1.90	0.37	<0.03	<0.03	<0.04	<0.04	<0.04	<0.08	*100.76*	*<0.01*
silica-soda-lime	**PN AU2 Cart**	16.29	0.65	2.31	69.45	0.09	0.12	1.21	0.53	7.99	0.06	1.87	0.37	<0.03	<0.03	<0.04	<0.04	<0.04	<0.08	*100.96*	*<0.01*
silica-soda-lime	**PN AU2**	16.26	0.67	2.30	68.91	0.09	0.13	1.26	0.55	7.99	0.08	1.80	0.36	<0.03	<0.03	<0.04	<0.04	<0.04	<0.08	*100.40*	*<0.01*
silica-soda-lime	**PN AZ1**	15.96	0.64	2.33	61.01	0.21	0.57	0.69	0.58	7.68	0.03	1.16	1.89	0.19	0.57	<0.04	<0.04	6.39	<0.08	*99.90*	*<0.01*
silica-soda-lime	**PN AZ2**	15.13	0.63	2.47	68.47	0.22	0.32	0.95	0.53	8.69	0.06	0.87	0.68	0.03	0.04	<0.04	<0.04	1.37	<0.08	*100.48*	*<0.01*
silica-soda-lime	**PN BO1**	15.06	0.80	2.49	66.11	0.24	0.42	0.68	0.74	6.70	0.09	0.63	1.12	0.17	0.26	<0.04	<0.04	4.40	0.11	*100.03*	*<0.01*
silica-soda-lime	**PN BS1**	19.28	0.64	2.15	66.70	0.09	0.27	1.40	0.63	5.87	0.13	0.58	0.62	<0.03	1.67	<0.04	0.17	0.63	0.12	*100.94*	*<0.01*
silica-soda-lime	**PN GR1**	17.91	0.73	2.46	67.48	0.20	0.29	1.14	0.69	6.73	0.11	0.59	0.74	<0.03	0.04	<0.04	<0.04	1.29	0.07	*100.46*	*<0.01*
silica-soda-lime	**Pn-Tu1**	15.72	0.93	2.39	65.27	0.30	0.38	0.81	0.84	6.75	0.09	0.63	0.69	<0.03	2.89	<0.04	0.29	2.52	0.40	*100.90*	*<0.01*
silica-soda-lime	**PN TU3**	17.53	0.39	2.02	68.09	0.01	0.21	1.38	0.50	4.52	0.07	<0.05	0.52	<0.03	2.83	0.10	0.21	1.89	0.31	*100.60*	*<0.01*
silica-soda-lime	**PN AQ1**	17.70	0.74	2.42	66.04	0.17	0.29	1.29	0.68	6.51	0.12	0.40	0.74	<0.03	2.30	<0.04	0.11	0.79	0.20	*100.50*	*<0.01*
silica-soda-lime	**PN CE1**	15.58	0.74	2.75	65.36	0.18	0.41	0.73	0.68	6.37	0.11	0.43	0.98	<0.03	2.21	<0.04	0.10	3.74	0.13	*100.50*	*<0.01*
silica-soda-lime	**BF AZ1**	20.23	1.02	2.31	65.06	0.09	0.32	1.73	0.40	6.39	0.15	0.69	0.95	<0.03	0.15	<0.04	0.32	<0.04	0.73	100.54	*<0.01*
silica-soda-lime	**BF AZ2**	18.41	0.85	2.10	66.72	0.12	0.31	1.30	0.58	6.96	0.09	0.63	0.83	0.03	0.38	<0.04	<0.04	1.06	0.25	100.61	*<0.01*
silica-soda-lime	**BF AZ3**	18.63	0.79	2.09	66.84	0.12	0.33	1.36	0.48	6.80	0.10	0.63	0.85	0.05	0.14	<0.04	<0.04	0.96	0.30	100.47	*<0.01*
silica-soda-lime	**BF AZ4**	15.82	0.69	2.53	67.72	0.14	0.34	0.91	0.70	6.16	0.09	0.61	0.91	0.08	0.17	<0.04	<0.04	3.02	0.23	100.04	*<0.01*
silica-soda-lime	**BF AZ5**	16.49	0.76	2.29	66.89	0.18	0.36	0.99	0.59	7.03	0.08	0.61	1.08	<0.03	0.09	<0.04	<0.04	2.38	0.24	100.04	*<0.01*
silica-soda-lime	**BF BS1**	20.02	1.00	1.96	66.08	0.07	0.35	1.52	0.29	7.30	0.11	0.85	0.64	<0.03	0.55	<0.04	<0.04	0.05	<0.08	100.79	*<0.01*
silica-soda-lime	**BF GR1**	17.72	0.89	2.14	67.28	0.11	0.36	1.16	0.57	6.62	0.09	0.42	0.71	<0.03	0.08	<0.04	<0.04	1.83	0.14	100.12	*<0.01*
silica-soda-lime	**BF VS1**	18.58	0.88	2.23	65.72	0.16	0.25	1.45	0.58	7.27	0.11	1.28	1.42	<0.03	0.90	0.16	<0.04	<0.04	<0.08	100.99	*<0.01*
silica-soda-lime	**BF AQ1**	19.99	1.02	2.38	65.26	0.07	0.32	1.65	0.38	6.16	0.14	0.41	0.74	<0.03	1.36	<0.04	0.07	<0.04	0.34	100.29	*<0.01*
silica-soda-lime	**BF AQ2**	19.98	1.02	2.32	65.74	0.07	0.29	1.64	0.36	6.17	0.15	0.42	0.75	0.00	1.35	0.04	0.06	<0.02	0.37	100.72	*<0.01*
silica-soda-lime	**BF TU1**	17.95	0.64	2.13	66.35	0.03	0.36	1.15	0.44	3.89	0.15	<0.05	1.09	<0.03	4.13	0.07	0.27	1.62	0.09	100.36	*<0.01*
silica-soda-lime	**BF TR INC3**	19.41	0.76	2.07	67.90	0.07	0.28	1.59	0.38	6.36	0.10	0.96	0.52	<0.03	<0.03	<0.04	<0.04	0.05	<0.08	100.44	*<0.01*
silica-soda-lime	**BF M4**	18.91	0.90	2.14	64.72	0.04	0.26	1.30	0.81	6.62	0.14	1.34	3.24	<0.03	0.75	0.13	<0.04	<0.04	0.09	101.39	*<0.01*
silica-soda-lime	**BF M2**	18.57	0.88	2.12	64.22	0.04	0.24	1.27	0.75	6.54	0.14	1.27	4.69	<0.03	0.62	0.07	<0.04	<0.04	0.07	101.49	*<0.01*
silica-soda-lime	**BF CE1**	14.64	0.75	2.85	65.97	0.11	0.38	0.62	0.74	7.43	0.11	1.12	0.88	<0.03	1.41	<0.04	0.13	3.17	0.10	100.40	*<0.01*
silica-soda-lime	**BF-VCH1**	19.07	0.97	2.89	66.57	0.04	0.28	1.51	0.40	6.07	0.14	0.35	0.78	<0.03	0.42	<0.04	0.09	<0.04	0.38	99.95	*<0.01*
silica-soda-lime	**BF VCH3**	18.13	0.87	2.19	66.87	0.04	0.32	1.26	0.50	6.68	0.10	0.46	0.72	<0.03	0.78	<0.04	0.06	0.60	0.35	99.94	*<0.01*
silica-soda-lime	**BF-VCH2**	18.92	0.92	2.97	68.03	0.00	0.28	1.46	0.41	5.84	0.12	0.16	0.59	<0.03	0.45	<0.04	0.05	<0.04	0.04	100.27	*<0.01*
silica-soda-lime	**BF-CE2**	18.69	0.90	3.22	67.83	0.01	0.37	1.44	0.40	5.68	0.12	0.13	0.59	<0.03	0.86	<0.04	0.10	<0.04	0.13	100.48	*<0.01*
silica-soda-lime	**BF B1**	16.42	0.65	2.32	67.62	0.16	0.35	0.85	0.67	5.94	0.10	0.61	0.95	0.08	0.16	<0.04	<0.04	3.03	0.23	100.13	*<0.01*
silica-soda-lime	**BF TU TR1**	16.50	0.63	2.68	68.45	0.07	0.25	1.01	0.60	7.86	0.07	1.05	0.51	<0.03	1.01	<0.04	<0.04	<0.04	<0.08	100.69	*<0.01*
silica-soda-lime	**BF TR INC1**	15.73	0.45	2.37	72.42	0.11	0.12	1.15	0.52	7.07	0.05	0.14	0.35	<0.03	<0.03	<0.04	<0.04	<0.04	<0.08	100.48	*<0.01*
silica-soda-lime	**BF TR INC2**	19.09	0.93	1.96	67.20	0.01	0.36	1.28	0.53	7.09	0.12	0.68	0.73	<0.03	<0.03	<0.04	<0.04	0.15	<0.08	100.12	*<0.01*
silica-soda-lime	**BF M1**	19.42	0.90	2.01	64.37	0.02	0.27	1.40	0.46	6.30	0.13	1.28	4.21	<0.03	0.46	0.07	<0.04	<0.04	0.08	101.37	*<0.01*
silica-soda-lime	**BF AZ4**	15.82	0.69	2.53	67.72	0.14	0.34	0.91	0.70	6.16	0.09	0.61	0.91	0.08	0.17	<0.04	<0.04	3.02	0.23	100.12	*<0.01*
silica-soda-lime	**BF- AU1**	18.60	1.00	2.10	67.63	0.05	0.31	1.29	0.49	7.28	0.11	0.63	0.69	<0.03	<0.03	<0.04	<0.04	0.15	0.04	100.37	*<0.01*
silica-soda-lime	**BF-AU1cart**	18.44	1.07	1.98	67.98	0.04	0.30	1.25	0.57	7.42	0.12	0.69	0.74	<0.03	<0.03	<0.04	<0.04	0.15	0.06	100.81	*<0.01*

Label	SiO2	Na2O	CaO	Al2O3	K2O	MgO	Fe2O3	TiO2	P2O5	SO3	Cl	*TiO2 * or*	*Fe2O3* or*
BF AQ1	66.71	20.43	6.28	2.43	0.38	1.05	0.75	0.14	0.07	0.32	1.68	*0.14*	*0.75*
BF AQ2	67.24	20.43	6.26	2.37	0.37	1.05	0.76	0.15	0.08	0.29	1.67	*0.15*	*0.76*
BF AV1	*60.84*	*11.65*	*11.82*	*6.32*	*1.41*	*2.14*	***1.40***	***0.12***	*0.58*	*0.26*	*0.62*	*0.61*	*4.42*
BF AZ1	66.31	20.62	6.47	2.36	0.40	1.04	0.96	0.15	0.09	0.32	1.75	*0.15*	*0.96*
BF AZ2	68.31	18.85	7.08	2.15	0.59	0.87	0.84	0.09	0.13	0.32	1.33	*0.09*	*0.84*
BF AZ3	68.25	19.02	6.91	2.14	0.49	0.81	0.87	0.10	0.13	0.33	1.38	*0.10*	*0.87*
BF AZ4	70.87	16.55	6.42	2.65	0.73	0.73	0.95	0.09	0.14	0.36	0.94	*0.09*	*0.95*
BF AZ4	70.62	16.50	6.42	2.64	0.73	0.72	0.95	0.09	0.14	0.36	0.94	*0.09*	*0.95*
BF AZ5	69.19	17.05	7.26	2.37	0.61	0.78	1.12	0.08	0.18	0.37	1.02	*0.08*	*1.12*
BF B1	70.51	17.12	6.19	2.42	0.70	0.67	0.99	0.11	0.17	0.36	0.89	*0.11*	*0.99*
BF BS1	67.04	20.31	7.35	1.99	0.29	1.02	0.65	0.11	0.08	0.35	1.53	*0.11*	*0.65*
BF CE1	70.10	15.55	7.87	3.02	0.79	0.80	0.94	0.11	0.12	0.41	0.66	*0.11*	*0.94*
BF GR1	68.98	18.17	6.78	2.20	0.58	0.92	0.73	0.09	0.11	0.37	1.19	*0.09*	*0.73*
BF GSO1	69.86	18.62	6.26	2.03	0.50	0.55	0.48	0.07	0.02	0.28	1.33	*0.07*	*0.48*
BF GSO2	70.05	18.26	5.02	2.15	0.67	0.64	1.41	0.14	0.07	0.41	0.96	*0.14*	*1.41*
BF GSO3	69.73	18.65	4.75	2.24	0.60	0.74	1.46	0.17	0.07	0.34	1.10	*0.17*	*1.46*
BF M1	65.59	19.79	6.33	2.05	0.46	0.92	**1.40**	**0.12**	0.02	0.27	1.40	*0.13*	*4.23*
BF M2	65.53	18.95	6.57	2.16	0.75	0.90	**1.40**	**0.12**	0.04	0.24	1.28	*0.14*	*4.71*
BF M3	*63.49*	*14.83*	*9.70*	*2.02*	*2.57*	*2.32*	***1.40***	***0.12***	*0.95*	*0.35*	*0.80*	*0.14*	*3.31*
BF M4	66.23	19.35	6.68	2.19	0.82	0.92	**1.40**	**0.12**	0.04	0.26	1.31	*0.14*	*3.27*
BF TU1	70.71	19.13	4.13	2.27	0.47	0.69	1.15	0.16	0.03	0.38	1.22	*0.16*	*1.15*
BF VCH3	68.41	18.55	6.84	2.24	0.51	0.89	0.74	0.10	0.04	0.33	1.29	*0.10*	*0.74*
BF VG1	66.64	19.66	6.08	2.15	0.52	1.00	2.02	0.14	0.02	0.29	1.36	*0.14*	*2.02*
BF VP1	67.21	18.73	6.82	2.23	0.45	1.12	1.32	0.15	0.06	0.24	1.54	*0.15*	*1.32*
BF VP2	66.81	19.54	6.97	2.11	0.39	1.08	1.12	0.16	0.06	0.22	1.72	*0.16*	*1.12*
BF VP3	66.72	18.84	6.48	2.29	0.54	1.08	1.50	0.17	0.10	0.23	1.60	*0.17*	*1.50*
BF VP4	67.29	19.67	6.62	2.28	0.44	1.04	1.10	0.14	0.06	0.26	1.52	*0.14*	*1.10*
BF VS1	67.28	19.02	7.37	2.28	0.58	0.90	1.44	0.11	0.16	0.25	1.47	*0.11*	*1.44*
BF VS2	67.37	19.41	6.79	2.20	0.52	1.00	1.32	0.15	0.08	0.24	1.58	*0.15*	*1.32*
BF- AU1	68.19	18.76	7.31	2.12	0.49	1.01	0.70	0.11	0.05	0.31	1.30	*0.11*	*0.70*
BF-CE2	68.66	18.91	5.73	3.26	0.40	0.91	0.60	0.12	0.01	0.37	1.45	*0.12*	*0.60*
BF-GSO4	67.86	19.22	6.46	2.38	0.55	0.72	0.92	0.22	0.02	0.22	1.36	*0.22*	*0.92*
BF-R1	67.25	16.29	7.62	2.61	0.62	0.70	**1.40**	0.10	0.12	0.24	1.20	*0.10*	*3.14*
BF-VCH1	67.41	19.31	6.15	2.93	0.40	0.98	0.79	0.14	0.04	0.29	1.53	*0.14*	*0.79*
BF-VCH2	68.52	19.06	5.87	2.99	0.41	0.93	0.59	0.12	0.00	0.28	1.47	*0.12*	*0.59*
PN AQ1	68.63	18.40	6.73	2.51	0.71	0.77	0.76	0.12	0.18	0.30	1.33	*0.12*	*0.76*
PN AV1	*63.24*	*15.23*	*9.45*	*4.02*	*1.27*	*2.05*	***1.40***	***0.12***	*0.66*	*0.49*	*1.12*	*0.35*	*2.99*
PN AV2 orange band	66.49	14.93	9.46	3.88	0.97	1.10	**1.40**	**0.12**	0.24	0.59	0.85	*0.21*	*1.84*
PN AV2 red band	66.28	15.36	9.30	3.78	0.99	1.08	**1.40**	**0.12**	0.22	0.56	0.86	*0.18*	*1.80*
PN AZ1	66.55	17.41	8.38	2.54	0.63	0.70	2.06	0.04	0.22	0.62	0.75	*0.04*	*2.06*
PN AZ2	70.09	15.49	8.86	2.53	0.54	0.64	0.70	0.06	0.23	0.33	0.96	*0.06*	*0.70*
PN BIOP1	72.64	15.95	6.28	2.13	0.58	0.49	0.42	0.04	0.19	0.39	0.68	*0.04*	*0.42*
PN BO1	70.00	15.95	7.09	2.64	0.78	0.85	1.19	0.10	0.26	0.44	0.72	*0.10*	*1.19*
PN BS1	68.86	19.91	6.00	2.22	0.64	0.66	0.63	0.13	0.10	0.28	1.43	*0.13*	*0.63*
PN CE1	69.96	16.68	6.78	2.94	0.72	0.79	1.05	0.12	0.19	0.44	0.78	*0.12*	*1.05*
PN GR1	68.83	18.27	6.84	2.51	0.70	0.75	0.75	0.11	0.20	0.29	1.16	*0.11*	*0.75*
Pn GSO1	69.95	18.25	5.30	2.22	0.66	0.69	0.93	0.15	0.08	0.29	1.05	*0.15*	*0.93*
PN GSO2 op band	69.87	15.70	7.76	2.54	0.56	0.56	1.09	0.08	0.06	0.19	1.03	*0.08*	*1.09*
PN GSO2 transp	70.06	16.94	7.51	2.30	0.58	0.51	0.62	0.06	0.11	0.23	1.06	*0.06*	*0.62*
PN M1	67.59	16.88	7.83	3.12	0.84	0.90	**1.40**	**0.12**	0.17	0.12	0.97	*0.16*	*1.37*
PN M2	*64.24*	*16.51*	*8.07*	*2.15*	*2.20*	*3.18*	***1.40***	***0.12***	*1.26*	*0.54*	*1.23*	*0.20*	*1.66*
PN M3	64.61	15.92	9.53	3.48	0.99	1.15	**1.40**	**0.12**	0.20	0.22	1.23	*0.20*	*1.79*
Pn NC1	70.37	17.18	7.03	2.47	0.57	0.61	0.52	0.09	0.09	0.19	1.23	*0.09*	*0.52*
PN TU2	69.58	19.00	5.67	2.37	0.60	0.71	0.79	0.12	0.12	0.43	1.17	*0.12*	*0.79*
PN TU2 trasp band	68.00	19.29	5.95	2.73	0.74	0.94	0.95	0.14	0.34	0.40	1.24	*0.14*	*0.95*
PN TU3	71.91	18.51	4.75	2.13	0.53	0.42	0.55	0.07	0.02	0.23	1.45	*0.07*	*0.55*
PN V TR1	68.44	17.72	6.76	2.27	0.60	0.60	2.10	0.08	0.11	0.21	1.23	*0.08*	*2.10*
PN V TR2	68.00	17.13	6.78	2.35	0.60	0.61	2.99	0.09	0.10	0.21	1.21	*0.09*	*2.99*
PN VCH1	69.68	18.69	6.75	2.31	0.55	0.69	0.45	0.08	0.10	0.26	1.26	*0.08*	*0.45*
PN VG1	70.48	16.84	6.62	2.41	0.81	0.80	0.98	0.13	0.22	0.20	0.99	*0.13*	*0.98*
PN VP1	69.22	18.11	6.73	2.59	0.72	0.70	0.62	0.12	0.11	0.25	1.26	*0.12*	*0.62*
PN VS1	69.29	18.40	6.61	2.55	0.75	0.76	0.67	0.13	0.14	0.25	1.28	*0.13*	*0.67*
Pn-Tu1	69.93	16.85	7.16	2.56	0.89	0.99	0.74	0.10	0.32	0.40	0.86	*0.10*	*0.74*
TN AQ2	69.14	17.59	7.34	2.52	0.71	0.72	0.60	0.10	0.17	0.31	1.11	*0.10*	*0.60*
TN AU1	72.38	15.14	7.99	2.44	0.42	0.53	0.31	0.07	0.10	0.16	1.10	*0.07*	*0.31*
TN AU1 cart	72.24	15.19	7.84	2.40	0.42	0.54	0.33	0.07	0.08	0.15	1.11	*0.07*	*0.33*
TN AV1 orange band	*65.21*	*15.03*	*8.99*	*2.64*	*1.88*	*2.48*	***1.40***	***0.12***	*0.84*	*0.69*	*1.02*	*0.23*	*1.64*
TN AV1 red band	*64.65*	*16.05*	*8.93*	*2.62*	*1.78*	*2.41*	***1.40***	***0.12***	*0.77*	*0.60*	*1.05*	*0.21*	*1.67*
TN AZ1	70.05	16.73	7.48	2.58	0.70	0.69	0.65	0.08	0.18	0.41	0.88	*0.08*	*0.65*
TN AZ2	70.19	16.89	6.99	2.47	0.62	0.72	0.85	0.10	0.19	0.44	0.97	*0.10*	*0.85*
TN B1	70.57	18.48	6.64	1.96	0.43	0.54	0.48	0.05	0.17	0.18	1.63	*0.05*	*0.48*
TN BI OP1	70.17	16.29	7.55	2.74	0.76	0.69	0.66	0.08	0.08	0.40	0.87	*0.08*	*0.66*
TN BO1	70.24	16.70	7.17	2.37	0.60	0.64	0.86	0.07	0.19	0.24	1.16	*0.07*	*0.86*
TN BS1	68.96	18.77	6.30	2.52	0.72	0.74	0.86	0.14	0.23	0.30	1.42	*0.14*	*0.86*
TN CE1	68.07	17.86	7.05	2.84	0.71	0.84	1.05	0.12	0.19	0.50	0.93	*0.12*	*1.05*
TN GR1	69.84	17.66	6.74	2.39	0.72	0.78	0.72	0.09	0.06	0.35	0.98	*0.09*	*0.72*
TN GR2	70.73	16.73	6.98	2.44	0.59	0.74	0.70	0.10	0.11	0.26	1.07	*0.10*	*0.70*
TN GSO1	70.32	17.92	6.79	2.17	0.54	0.58	0.27	0.08	0.04	0.30	1.22	*0.08*	*0.27*
TN GSO2	70.38	17.43	6.77	2.40	0.60	0.56	0.47	0.11	0.05	0.27	1.18	*0.11*	*0.47*
TN M1	66.88	15.45	7.42	2.91	0.90	0.86	**1.40**	0.11	0.19	0.30	1.03	*0.11*	*4.34*
TN M2 dark band	67.47	15.42	7.42	3.05	0.85	0.87	**1.40**	0.12	0.18	0.29	1.00	*0.12*	*4.13*
TN M2 paleband	68.11	15.21	7.68	2.98	0.94	0.88	**1.40**	0.11	0.16	0.32	1.00	*0.11*	*2.93*
TN NS1	69.06	17.53	6.65	2.41	0.77	0.77	**1.40**	0.11	0.11	0.30	1.13	*0.11*	*1.67*
TN TR INC 1	68.49	19.00	7.22	2.12	0.57	0.68	0.57	0.09	0.03	0.31	1.37	*0.09*	*0.57*
TN TU1	68.79	17.01	7.63	2.64	0.76	0.74	0.70	0.09	0.21	0.42	0.94	*0.09*	*0.70*
TN TU3	68.73	16.96	7.69	2.58	0.74	0.75	0.70	0.09	0.19	0.42	0.95	*0.09*	*0.70*
TN V OL2	68.16	14.80	7.89	3.38	0.95	0.79	**1.40**	**0.12**	0.14	0.35	0.91	*0.13*	*2.81*
TN VCH1	68.52	18.43	6.93	2.68	0.65	0.82	0.96	0.12	0.15	0.43	1.07	*0.12*	*0.96*
TN VG1	69.02	17.06	7.19	2.35	0.74	0.88	1.41	0.09	0.15	0.30	1.26	*0.09*	*1.41*
TN VG2	69.04	16.35	7.67	2.90	0.88	0.79	1.62	0.11	0.13	0.28	1.07	*0.11*	*1.62*
TN VOL 1	68.85	16.69	6.99	2.88	0.83	0.93	**1.40**	**0.12**	0.18	0.27	1.14	*0.16*	*1.96*
TN VP1	68.98	17.52	7.05	2.53	0.69	0.71	0.79	0.10	0.13	0.25	1.25	*0.10*	*0.79*
TN VP2	69.33	17.46	6.98	2.46	0.69	0.66	0.73	0.11	0.13	0.25	1.26	*0.11*	*0.73*
TN VS1	68.70	18.13	7.28	2.53	0.73	0.73	1.01	0.12	0.15	0.29	1.27	*0.12*	*1.01*
TN VS2	69.29	17.38	7.24	2.53	0.65	0.69	0.79	0.10	0.14	0.24	1.26	*0.10*	*0.79*
TN- M3	67.34	17.01	6.93	2.89	0.88	0.83	**1.40**	0.12	0.12	0.29	1.06	*0.12*	*2.90*

sample	O	Sn	Sb	Pb	Si	Fe	Cu	Zn	As	Ti	Cr	Mn	Co	S	Ni	*tot*
BF VP2-1	11.01	23.33	3.40	47.22	0.00	0.16	0.31	0.00	0.83	0.00	0.00	0.00	0.00	0.00	0.03	*86.31*
BF VP2-2	15.11	27.03	2.86	45.94	2.91	0.09	0.37	0.04	0.77	0.00	0.00	0.07	0.02	0.00	0.00	*95.21*
BF VP2-3	14.06	24.18	0.00	52.60	2.84	0.19	0.58	0.07	0.00	0.03	0.00	0.00	0.02	0.00	0.00	*94.57*
BF VP2-4	16.11	25.93	0.00	49.82	4.36	0.28	0.69	0.06	0.00	0.04	0.00	0.03	0.00	0.00	0.00	*97.31*
BF VP2-5	15.00	23.41	0.00	52.39	3.86	0.21	0.55	0.00	0.00	0.03	0.00	0.04	0.00	0.00	0.02	*95.51*
BF VP2-6	14.81	22.56	0.52	50.22	3.37	0.19	0.61	0.03	2.06	0.00	0.03	0.07	0.00	0.00	0.00	*94.47*
BF VP2-7	14.70	22.84	0.70	52.14	3.09	0.18	0.60	0.00	2.02	0.00	0.00	0.05	0.00	0.00	0.00	*96.32*
BF VP2-8	15.12	23.70	0.23	51.44	3.46	0.13	0.53	0.07	1.75	0.00	0.00	0.02	0.01	0.00	0.06	*96.52*
BF VP1-1	16.57	20.36	1.18	45.70	5.78	0.24	0.74	0.03	1.31	0.01	0.00	0.04	0.00	0.02	0.00	*91.99*
BF VP1-2	19.30	20.62	0.99	45.82	8.51	0.29	0.69	0.01	0.00	0.03	0.03	0.04	0.01	0.00	0.00	*96.36*
BF VP1-3	15.14	23.36	1.01	54.83	3.67	0.16	0.49	0.02	0.00	0.04	0.02	0.08	0.00	0.00	0.00	*98.81*
BF VP1-4	17.29	20.08	0.98	47.57	6.81	0.21	0.56	0.03	0.00	0.01	0.00	0.05	0.02	0.01	0.00	*93.61*
BF VP1-5	13.02	22.58	1.89	55.65	1.53	0.12	0.46	0.00	1.04	0.01	0.03	0.04	0.04	0.00	0.01	*96.40*
BF VP1-6	13.61	22.35	1.76	55.23	2.29	0.10	0.52	0.02	0.61	0.01	0.00	0.01	0.02	0.00	0.00	*96.52*
BF VP4-1	16.24	20.84	3.93	45.60	5.17	0.29	1.00	0.00	0.16	0.00	0.02	0.13	0.01	0.00	0.00	*93.37*
BF VP4-2	16.98	20.73	3.88	44.71	5.88	0.25	1.07	0.00	0.18	0.02	0.03	0.13	0.01	0.00	0.00	*93.88*
BF VP4-3	16.46	24.49	0.37	48.05	5.01	0.20	0.90	0.10	0.00	0.01	0.01	0.11	0.00	0.00	0.04	*95.75*
BF VP4-4	19.12	21.71	0.47	38.82	8.49	0.40	1.07	0.00	0.06	0.03	0.00	0.23	0.01	0.00	0.00	*90.43*
BF VP4-5	26.07	13.51	0.49	31.02	16.88	0.42	1.51	0.00	0.00	0.03	0.02	0.33	0.03	0.05	0.00	*90.34*
BF VP4-6	17.45	22.20	1.02	47.38	6.34	0.21	0.98	0.00	0.00	0.02	0.01	0.09	0.02	0.01	0.00	*95.73*
BF VP4-7	19.61	20.28	0.87	40.07	9.14	0.33	1.15	0.00	0.00	0.03	0.00	0.16	0.00	0.01	0.00	*91.64*
BF VS2-1	18.36	21.66	0.22	49.25	7.34	0.23	0.74	0.02	0.00	0.05	0.00	0.07	0.01	0.00	0.01	*97.97*
BF VS2-2	17.86	20.40	0.21	49.20	7.16	0.29	0.78	0.07	0.00	0.03	0.00	0.09	0.05	0.00	0.00	*96.15*
BF VS2-3	17.60	21.56	0.32	52.15	6.43	0.26	0.84	0.00	0.00	0.06	0.03	0.11	0.00	0.00	0.02	*99.37*
BF VS2-4	16.15	22.57	0.20	53.58	4.88	0.27	0.57	0.03	0.00	0.10	0.00	0.10	0.00	0.00	0.00	*98.46*
BF VS2-5	16.24	22.45	0.12	53.73	4.97	0.25	0.75	0.00	0.00	0.11	0.00	0.06	0.00	0.00	0.00	*98.69*
BF VS2-6	19.29	17.69	0.14	37.51	9.74	0.37	0.92	0.00	0.00	0.08	0.01	0.20	0.02	0.03	0.00	*86.00*
BF VS2-7	18.33	21.57	0.23	47.95	7.39	0.27	0.85	0.00	0.00	0.03	0.00	0.12	0.01	0.00	0.03	*96.77*
BF VS2-8	17.06	20.38	0.39	42.47	6.81	0.46	0.92	0.00	0.00	0.03	0.02	0.18	0.00	0.00	0.00	*88.72*
BF VS2-9	18.37	20.01	0.45	43.00	7.94	0.49	1.06	0.00	0.00	0.07	0.03	0.18	0.00	0.00	0.00	*91.60*

Ca-antimonate

BF-GR1

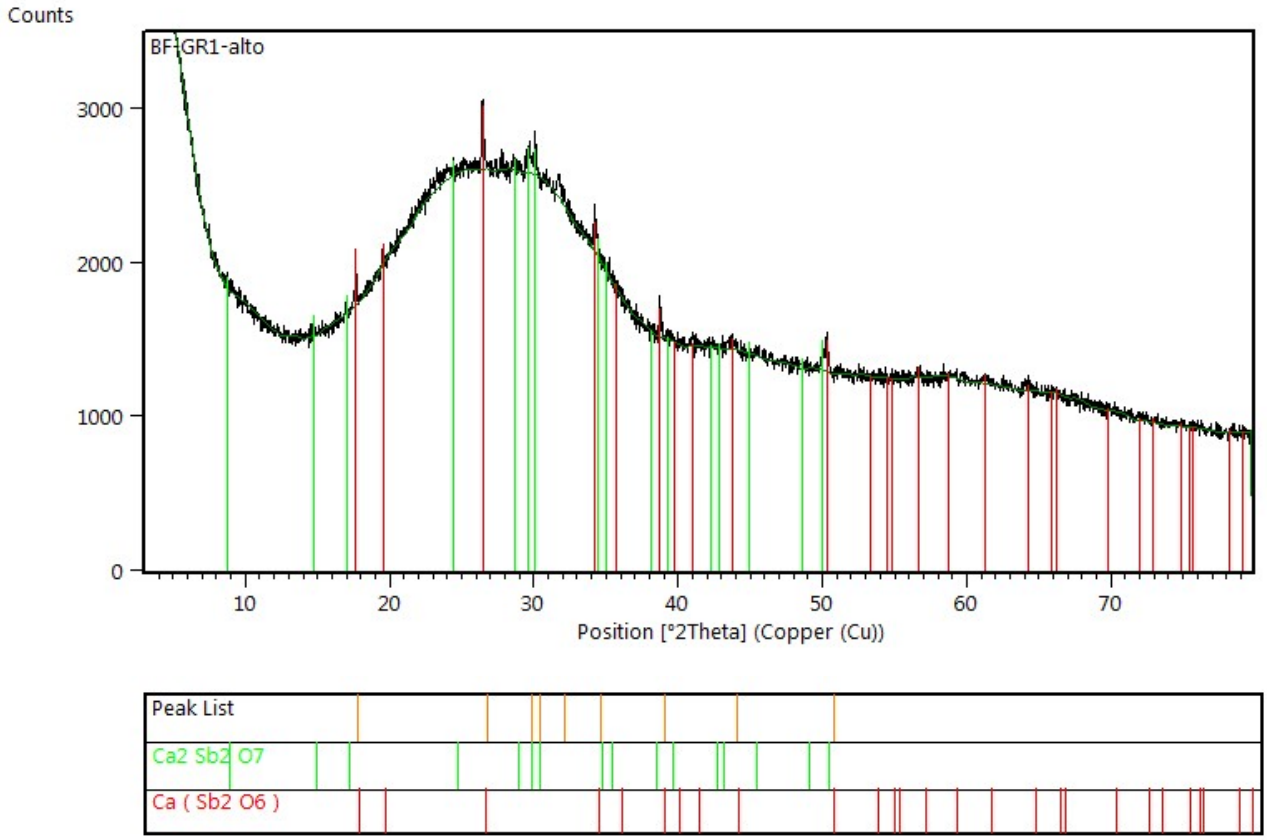

Name and formula

Reference code:	01-082-0518
Compound name:	Calcium Antimony Oxide
ICSD name:	Calcium Antimony Oxide
Empirical formula:	CaO_6Sb_2
Chemical formula:	Ca (Sb_2O_6)

Crystallographic parameters

Crystal system:	Hexagonal
Space group:	P-31m
Space group number:	162
a (Å):	5.2405
b (Å):	5.2405
c (Å):	5.0221
Alpha (°):	90.0000
Beta (°):	90.0000
Gamma (°):	120.0000
Calculated density (g/cm^3):	5.28
Volume of cell (10^6 pm^3):	119.44
Z:	1.00
RIR:	6.67

Subfiles and quality

Subfiles:	Inorganic
	Modelled additional pattern
Quality:	Calculated (C)

Comments

ICSD collection code:	074539
Creation Date:	01/01/1970
Modification Date:	01/01/1970
ICSD Collection Code:	074539
Calculated Pattern Original Remarks:	REM TEM 294
Calculated Pattern Original Remarks:	REM RVP
Temperature Factor:	ITF
Additional Patterns:	See PDF 46-1496.

References

Primary reference:	*Calculated from ICSD using POWD-12++*, (1997)
Structure:	DeBoer, B.G., Young, R.A., Sakthivel, A., *Acta Crystallogr., Sec. C,*, **50**, 476, (1994)

Peak list

No.	h	k	l	d [A]	2Theta[deg]	I [%]
1	0	0	1	5.02210	17.646	88.6
2	1	0	0	4.53841	19.544	33.1
3	1	0	1	3.36719	26.449	100.0
4	1	1	0	2.62025	34.193	47.9
5	0	0	2	2.51105	35.729	10.1
6	-1	-1	1	2.32307	38.730	47.1
7	2	0	0	2.26920	39.688	1.5
8	1	0	2	2.19716	41.047	4.5
9	2	0	1	2.06791	43.740	19.3
10	-1	-1	2	1.81296	50.287	50.1
11	2	1	0	1.71536	53.367	2.6
12	2	0	2	1.68360	54.456	3.9
13	0	0	3	1.67403	54.793	1.5
14	-2	-1	1	1.62328	56.658	17.6
15	1	0	3	1.57059	58.741	7.0
16	3	0	0	1.51280	61.220	14.5
17	3	0	1	1.44851	64.253	9.9
18	-2	-1	2	1.41641	65.891	2.8
19	-1	-1	3	1.41071	66.191	10.0
20	2	0	3	1.34713	69.753	4.8
21	2	2	0	1.31012	72.025	4.8
22	3	0	2	1.29581	72.948	7.8
23	-2	-2	1	1.26770	74.838	5.1
24	3	1	0	1.25873	75.464	1.3
25	0	0	4	1.25553	75.690	2.6
26	-3	-1	1	1.22096	78.233	5.9
27	1	0	4	1.21007	79.074	0.8
28	-2	-1	3	1.19806	80.025	5.1
29	-2	-2	2	1.16153	83.085	7.8
30	4	0	0	1.13460	85.518	0.7
31	-1	-1	4	1.13225	85.738	6.0

32	-3	-1	2	1.12527	86.400	0.9
33	3	0	3	1.12240	86.675	2.8
34	4	0	1	1.10671	88.218	2.0
35	2	0	4	1.09858	89.043	0.4

Structure

No.	Name	Elem.	X	Y	Z	Biso	sof	Wyck.
1	O1	O	0.37300	0.00000	0.28990	1.6700	1.0000	6k
2	SB1	Sb	0.33333	0.66667	0.50000	0.3160	1.0000	2d
3	CA1	Ca	0.00000	0.00000	0.00000	0.4400	1.0000	1a

Stick Pattern

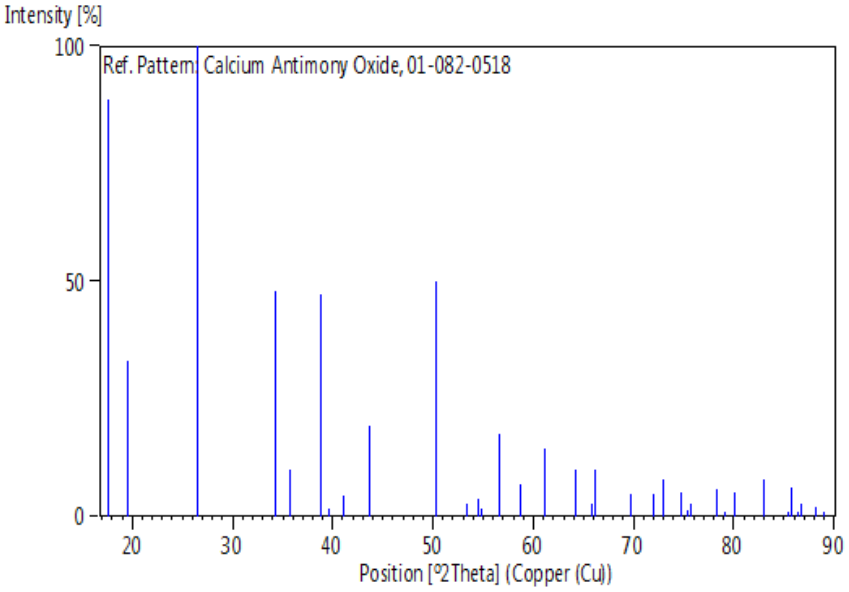

Name and formula

Reference code:	00-026-0293
Compound name:	Calcium Antimony Oxide
PDF index name:	Calcium Antimony Oxide
Empirical formula:	$Ca_2O_7Sb_2$
Chemical formula:	$Ca_2Sb_2O_7$

Crystallographic parameters

Crystal system:	Orthorhombic
a (Å):	7.2900
b (Å):	7.4500
c (Å):	10.2000
Alpha (°):	90.0000
Beta (°):	90.0000
Gamma (°):	90.0000
Volume of cell (10^6 pm^3):	553.97
Z:	4.00
RIR:	-

Subfiles and quality

Subfiles:	Inorganic
Quality:	Blank (B)

Comments

Color:	Yellowish white
Creation Date:	01/01/1970
Modification Date:	01/01/1970
Color:	Yellowish white
Additional Patterns:	To replace 2-1384.

References

Primary reference:	Butler et al., *J. Electrochem. Soc.*, **97**, 117, (1950)

Peak list

No.	h	k	l	d [A]	2Theta[deg]	I [%]
1	0	0	1	10.10000	8.748	40.0
2	0	1	1	5.98000	14.802	70.0
3	1	1	0	5.20000	17.038	60.0
4	1	1	2	3.64000	24.435	50.0
5	2	1	1	3.11000	28.681	40.0
6	0	2	2	3.02000	29.555	90.0
7	2	0	2	2.96600	30.106	90.0
8	2	2	0	2.60600	34.385	60.0
9	0	0	4	2.55700	35.066	40.0
10	2	1	3	2.35600	38.168	10.0
11	1	3	1	2.29500	39.223	10.0
12	1	3	2	2.13700	42.257	10.0
13	3	1	2	2.11100	42.803	20.0
14	2	3	1	2.01400	44.974	40.0
15	0	4	0	1.87200	48.596	40.0
16	4	0	0	1.82400	49.961	100.0

Stick Pattern

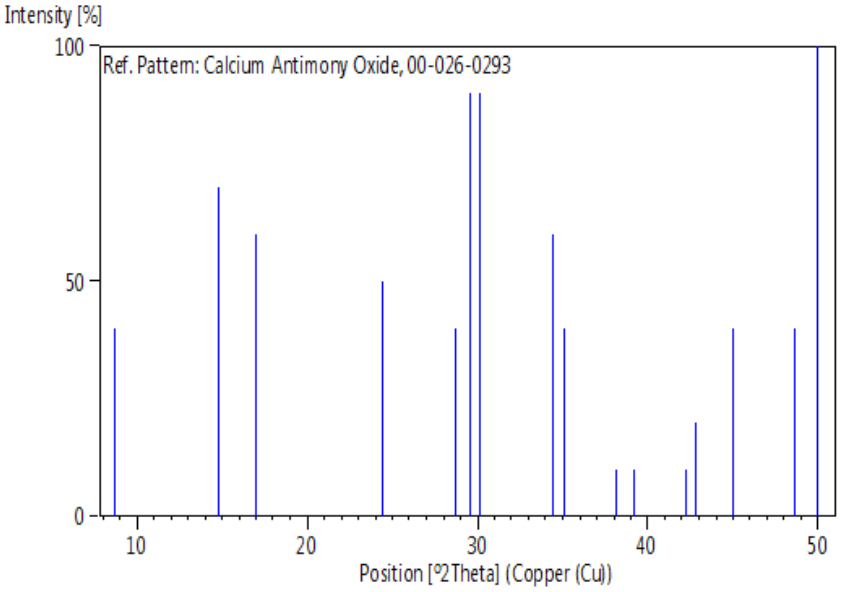

Pb- antimonate (Bindheimite)

PN-VG1

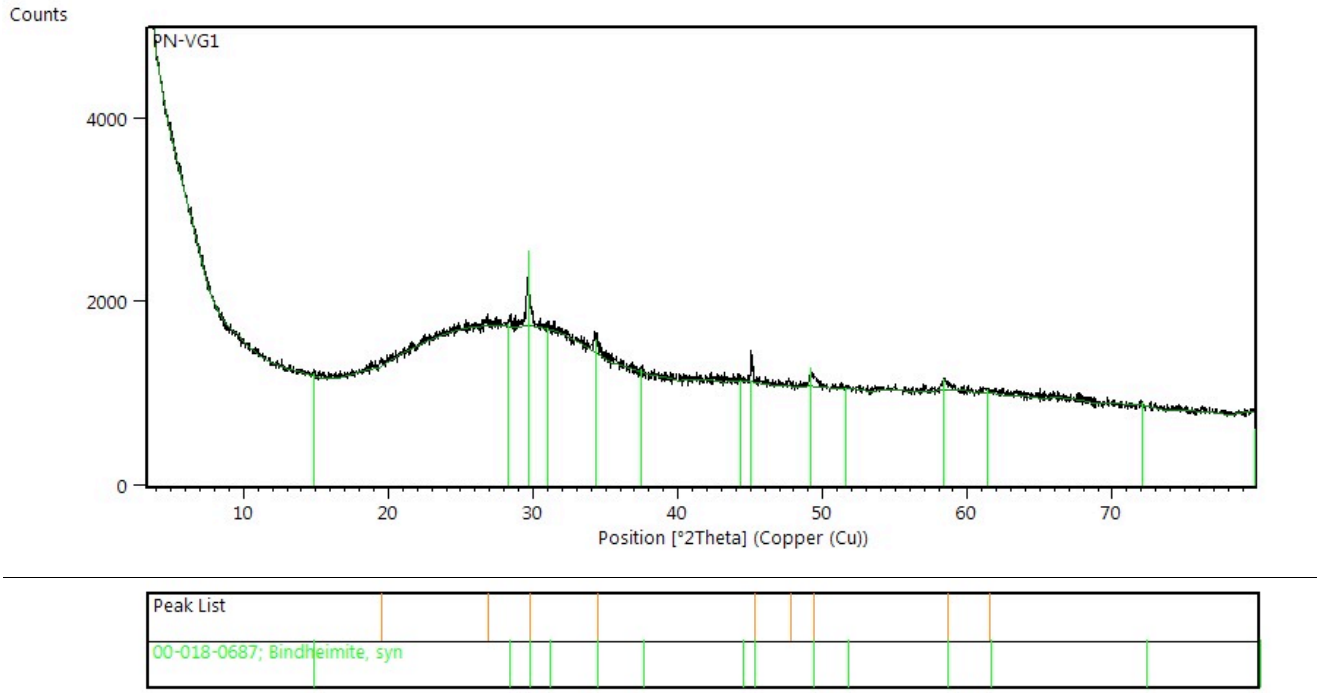

Name and formula

Reference code:	00-018-0687
Mineral name:	Bindheimite, syn
Compound name:	Lead Antimony Oxide
PDF index name:	Lead Antimony Oxide
Empirical formula:	$O_7Pb_2Sb_2$
Chemical formula:	$Pb_2Sb_2O_6$ (O , OH)

Crystallographic parameters

Crystal system:	Cubic
Space group:	Fd3m
Space group number:	227
a (Å):	10.4700
b (Å):	10.4700
c (Å):	10.4700
Alpha (°):	90.0000
Beta (°):	90.0000
Gamma (°):	90.0000
Calculated density (g/cm^3):	7.50
Measured density (g/cm^3):	7.32
Volume of cell (10^6 pm^3):	1147.73
Z:	8.00
RIR:	-

Status, subfiles and quality

Status:	Marked as deleted by ICDD
Subfiles:	Inorganic Mineral
Quality:	Blank (B)

Comments

Creation Date:	01/01/1970
Modification Date:	01/01/1970
Synthetic. Analysis:	Chemical analysis (wt.%): Sb_2O_5 34.5, As_2O_5 1.4, PbO 62.8, FeO 0.9, MgO 0.3. $Pb_{2.33}Sb_{1.77}A_{0.10}O_7$. Optical Data: B=184. Additional Patterns: To replace 2-1375 and 7-321. Deleted Or Rejected By: Deleted by 42-1355, lower Fn, PB 4/91.

References

Primary reference: Friedrich, Marse., *Z. Erzbergbau Metallhuettenwes.*, **15**, 72, (1962)

Peak list

No.	h	k	l	d [A]	2Theta[deg]	I [%]
1	1	1	1	5.97000	14.827	6.0
2	3	1	1	3.15000	28.309	4.0
3	2	2	2	3.01000	29.655	100.0
4				2.88000	31.027	2.0
5	4	0	0	2.61000	34.331	18.0
6	3	3	1	2.40000	37.442	6.0
7				2.04000	44.370	2.0
8	5	1	1	2.01000	45.068	2.0
9	4	4	0	1.85000	49.212	25.0
10	5	3	1	1.77000	51.596	2.0
11	6	2	2	1.58000	58.357	14.0
12	4	4	4	1.51000	61.345	6.0
13	8	0	0	1.31000	72.033	4.0
14	6	6	2	1.20000	79.870	4.0
15	8	4	0	1.17000	82.352	4.0
16	8	4	4	1.07000	92.094	2.0
17	10	2	2	1.00800	99.669	2.0
18	8	8	0	0.92600	112.580	2.0
19	10	6	2	0.88500	121.009	2.0
20	12	0	0	0.87300	123.857	4.0
21	12	4	0	0.82800	136.968	4.0
22	10	6	6	0.79900	149.193	2.0

23	12	4	4	0.78900	155.002	2.0

Stick Pattern

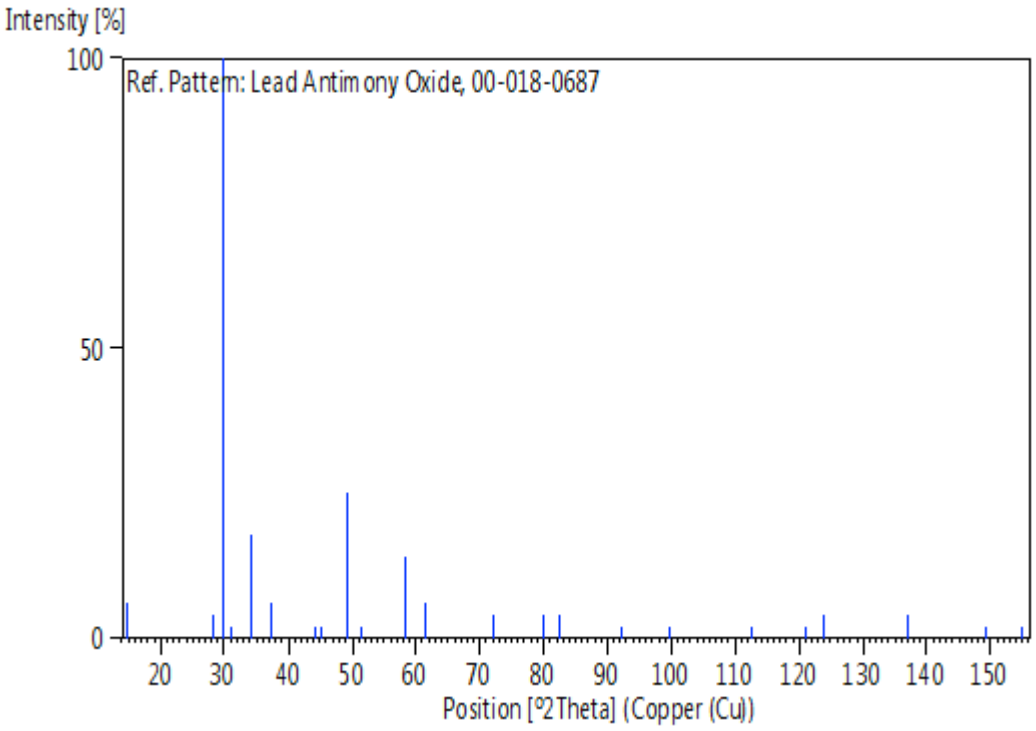

Pyrochlore (Pb,Sn,Sb-bearing)

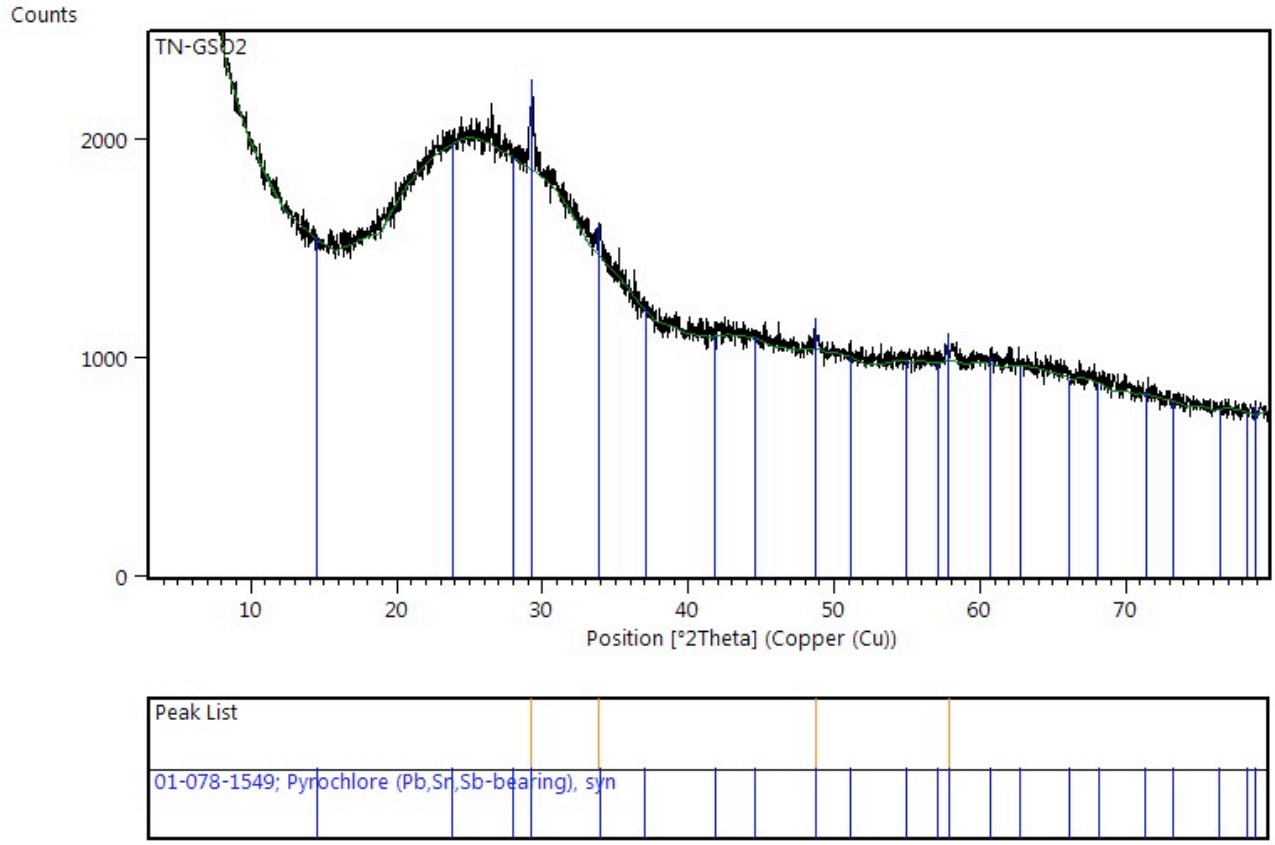

Name and formula

Reference code:	01-078-1549
Mineral name:	Pyrochlore (Pb,Sn,Sb-bearing), syn
Compound name:	Lead Tin Antimony Oxide
ICSD name:	Lead Tin Antimony Oxide
Empirical formula:	$O_{6.5}Pb_2SbSn$
Chemical formula:	Pb_2 (SnSb) $O_{6.5}$

Crystallographic parameters

Crystal system:	Cubic
Space group:	Fd-3m
Space group number:	227
a (Å):	10.5645
b (Å):	10.5645
c (Å):	10.5645
Alpha (°):	90.0000
Beta (°):	90.0000
Gamma (°):	90.0000
Calculated density (g/cm^3):	8.55
Measured density (g/cm^3):	8.55
Volume of cell (10^6 pm^3):	1179.09
Z:	8.00

RIR: 18.20

Subfiles and quality

Subfiles: Corrosion
Inorganic
Mineral
Modelled additional pattern
Quality: Calculated (C)

Comments

ICSD collection code: 062722
Creation Date: 01/01/1970
Modification Date: 01/01/1970
ICSD Collection Code: 062722
Test from ICSD: At least one TF missing
Sample Preparation: Prepared from oxides at 1273 K
Additional Patterns: See PDF 39-928.

References

Primary reference: *Calculated from ICSD using POWD-12++*, (1997)
Structure: Cascales, C., Alonso, J.A., Rasines, I., *J. Mater. Sci. Lett.*, **5**, 675, (1986)

Peak list

No.	h	k	l	d [A]	2Theta[deg]	I [%]
1	1	1	1	6.09942	14.511	3.8
2	2	2	0	3.73511	23.803	0.1
3	3	1	1	3.18532	27.989	3.2
4	2	2	2	3.04971	29.261	100.0
5	4	0	0	2.64112	33.914	36.3
6	3	3	1	2.42366	37.063	4.6
7	4	2	2	2.15647	41.857	0.3
8	5	1	1	2.03314	44.528	2.3
9	4	4	0	1.86756	48.719	35.1
10	5	3	1	1.78573	51.108	1.3
11	6	2	0	1.67039	54.923	0.1
12	5	3	3	1.61107	57.127	0.4
13	6	2	2	1.59266	57.849	32.8
14	4	4	4	1.52485	60.685	8.5
15	7	1	1	1.47933	62.760	0.5
16	6	4	2	1.41174	66.137	0.1
17	5	5	3	1.37538	68.120	0.6
18	8	0	0	1.32056	71.368	4.1
19	7	3	3	1.29066	73.286	0.5
20	8	2	2	1.24504	76.442	0.1
21	7	5	1	1.21988	78.315	0.6
22	6	6	2	1.21183	78.936	10.2
23	8	4	0	1.18115	81.409	8.9
24	9	1	1	1.15960	83.254	0.5
25	6	6	4	1.12618	86.313	0.1
26	9	3	1	1.10746	88.143	0.2

Structure

No.	Name	Elem.	X	Y	Z	Biso	sof	Wyck.
1	O1	O	0.37500	0.37500	0.37500	0.5000	0.5000	8b
2	O2	O	0.32000	0.12500	0.12500	0.5000	1.0000	48f
3	SB1	Sb	0.00000	0.00000	0.00000	0.5000	0.5000	16c
4	SN1	Sn	0.00000	0.00000	0.00000	0.5000	0.5000	16c
5	PB1	Pb	0.50000	0.50000	0.50000	0.5000	1.0000	16d

Stick Pattern

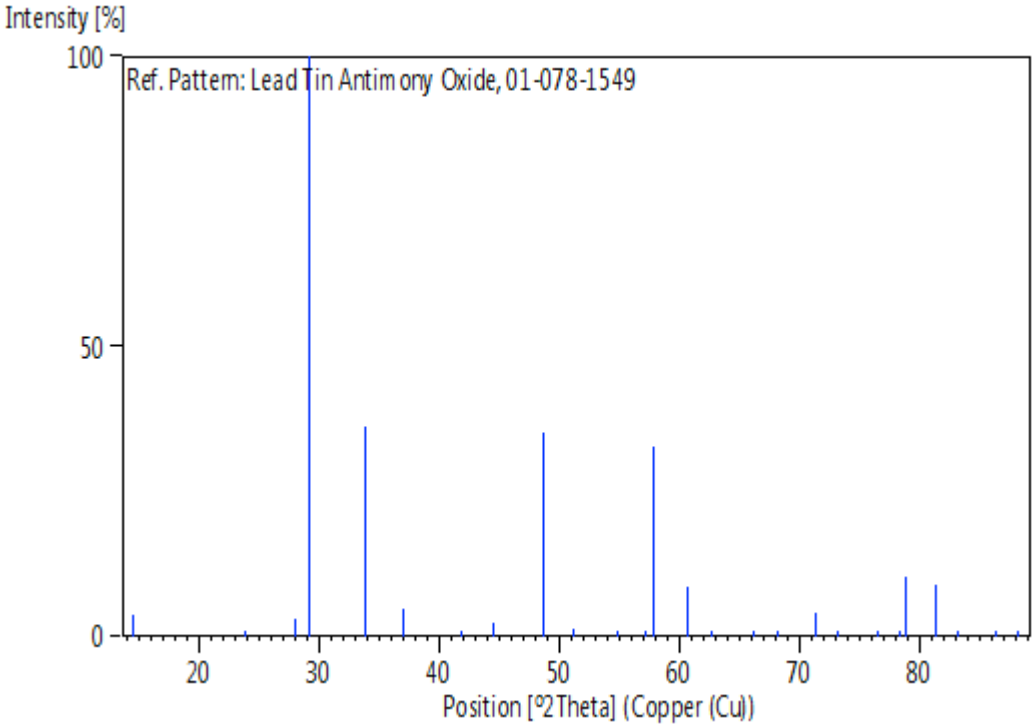

Copper

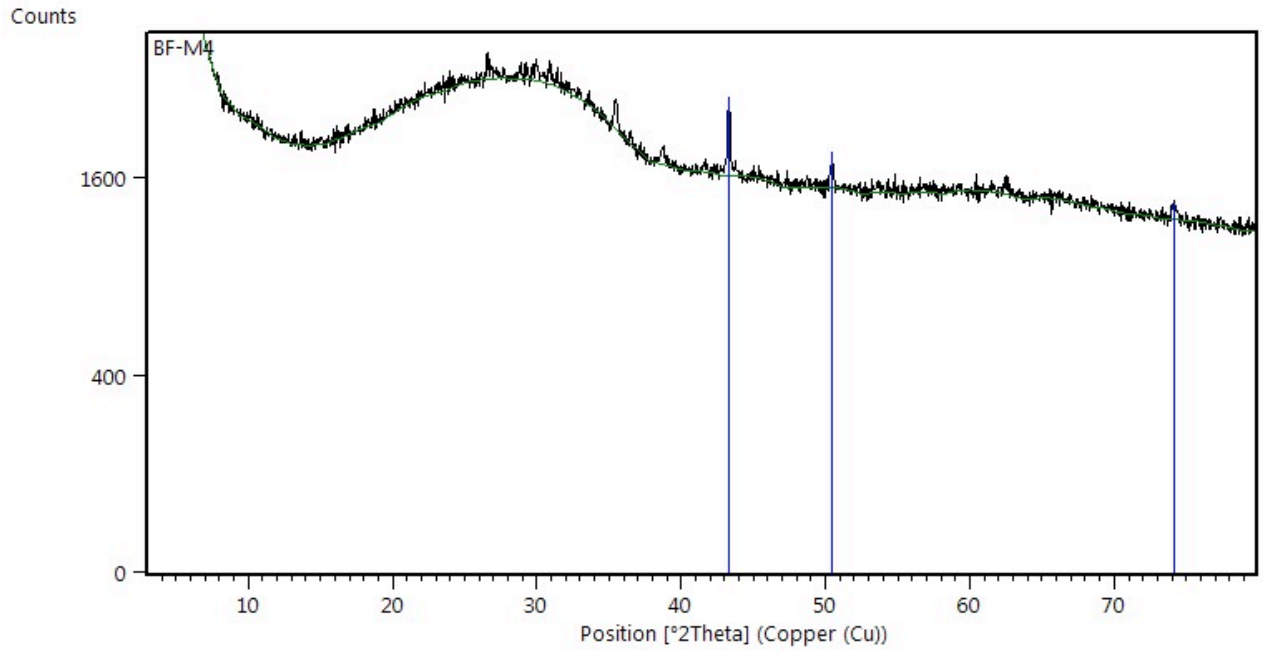

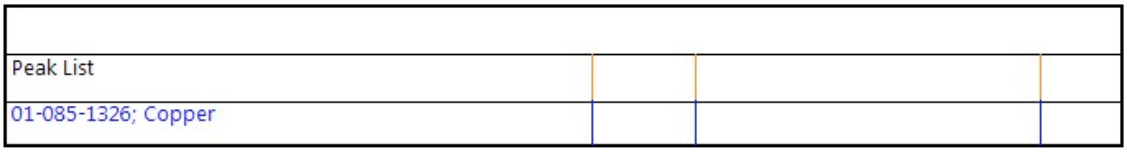

Name and formula

Reference code:	01-085-1326
Mineral name:	Copper
Compound name:	Copper
ICSD name:	Copper
Empirical formula:	Cu
Chemical formula:	Cu

Crystallographic parameters

Crystal system:	Cubic
Space group:	Fm-3m
Space group number:	225
a (Å):	3.6150
b (Å):	3.6150
c (Å):	3.6150
Alpha (°):	90.0000
Beta (°):	90.0000
Gamma (°):	90.0000
Calculated density (g/cm^3):	8.93
Measured density (g/cm^3):	8.96
Volume of cell (10^6 pm^3):	47.24
Z:	4.00

RIR: 8.86

Subfiles and quality

Subfiles: Alloy, metal or intermetalic
Corrosion
Inorganic
Mineral
Modelled additional pattern

Quality: Calculated (C)

Comments

ICSD collection code: 064699
Creation Date: 01/01/1970
Modification Date: 01/01/1970
ICSD Collection Code: 064699
Calculated Pattern Original Remarks: REM M PDF 4-836
Test from ICSD: No R value given
Test from ICSD: At least one TF missing
Additional Patterns: See PDF 4-836.

References

Primary reference: *Calculated from ICSD using POWD-12++*, (1997)
Structure: Swanson, H.E., Tatge, E., *Natl. Bur. Stand. (U.S.), Circ. 539*, **359**, 1, (1953)

Peak list

No.	h	k	l	d [A]	2Theta[deg]	I [%]
1	1	1	1	2.08712	43.317	100.0
2	2	0	0	1.80750	50.449	42.7
3	2	2	0	1.27810	74.126	17.1
4	3	1	1	1.08996	89.938	15.6

Structure

No.	Name	Elem.	X	Y	Z	Biso	sof	Wyck.
1	CU1	Cu	0.00000	0.00000	0.00000	0.5000	1.0000	4a

Stick Pattern

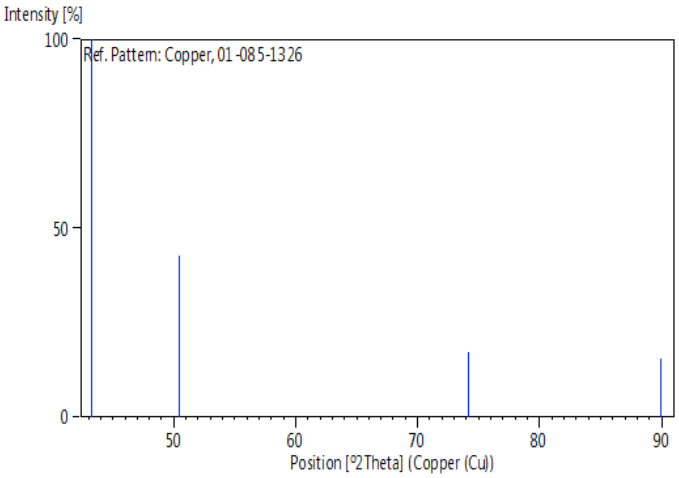

Cuprite

PN-AV1

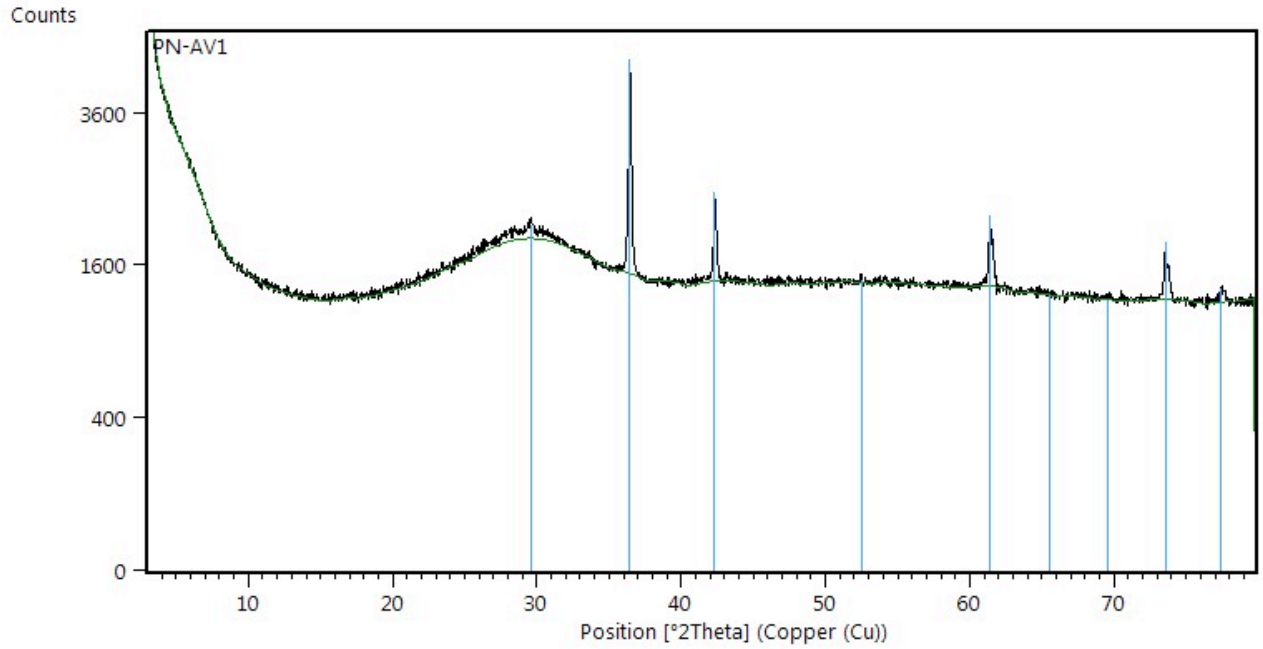



Name and formula

Reference code:	01-078-2076
Mineral name:	Cuprite
Compound name:	Copper Oxide
ICSD name:	Copper Oxide
Empirical formula:	Cu_2O
Chemical formula:	Cu_2O

Crystallographic parameters

Crystal system:	Cubic
Space group:	Pn-3m
Space group number:	224
a (Å):	4.2670
b (Å):	4.2670
c (Å):	4.2670
Alpha (°):	90.0000
Beta (°):	90.0000
Gamma (°):	90.0000
Calculated density (g/cm^3):	6.12
Volume of cell (10^6 pm^3):	77.69
Z:	2.00
RIR:	8.28

Subfiles and quality

Subfiles:	Alloy, metal or intermetalic
	Corrosion
	Inorganic
	Mineral
	Modelled additional pattern
Quality:	Calculated (C)

Comments

ICSD collection code:	063281
Creation Date:	01/01/1970
Modification Date:	01/01/1970
ICSD Collection Code:	063281
Calculated Pattern Original Remarks:	REM TEM 100
Calculated Pattern Original Remarks:	REM DEN
Calculated Pattern Original Remarks:	REM F Temperature factors have been deposited with the Briti
Calculated Pattern Original Remarks:	REM Library Lending Division, SUP. No. 42674
Sample Source or Locality:	Specimen from USA
Additional Patterns:	See PDF 5-667.

References

Primary reference:	*Calculated from ICSD using POWD-12++*, (1997)
Structure:	Restori, R., Schwarzenbach, D., *Acta Crystallogr., Sec. B: Structural Science*, **42**, 201, (1986)

Peak list

No.	h	k	l	d [A]	2Theta[deg]	I [%]
1	1	1	0	3.01723	29.583	5.3
2	1	1	1	2.46355	36.441	100.0
3	2	0	0	2.13350	42.329	34.7
4	2	1	1	1.74200	52.488	1.1
5	2	2	0	1.50861	61.408	26.5
6	2	2	1	1.42233	65.582	0.1
7	3	1	0	1.34934	69.622	0.3
8	3	1	1	1.28655	73.558	19.8
9	2	2	2	1.23178	77.417	4.3
10	3	2	1	1.14040	84.980	0.2

Structure

No.	Name	Elem.	X	Y	Z	Biso	sof	Wyck.
1	O1	O	0.25000	0.25000	0.25000	0.7738	1.0000	2a
2	CU1	Cu	0.00000	0.00000	0.00000	0.5000	1.0000	4b

Stick Pattern

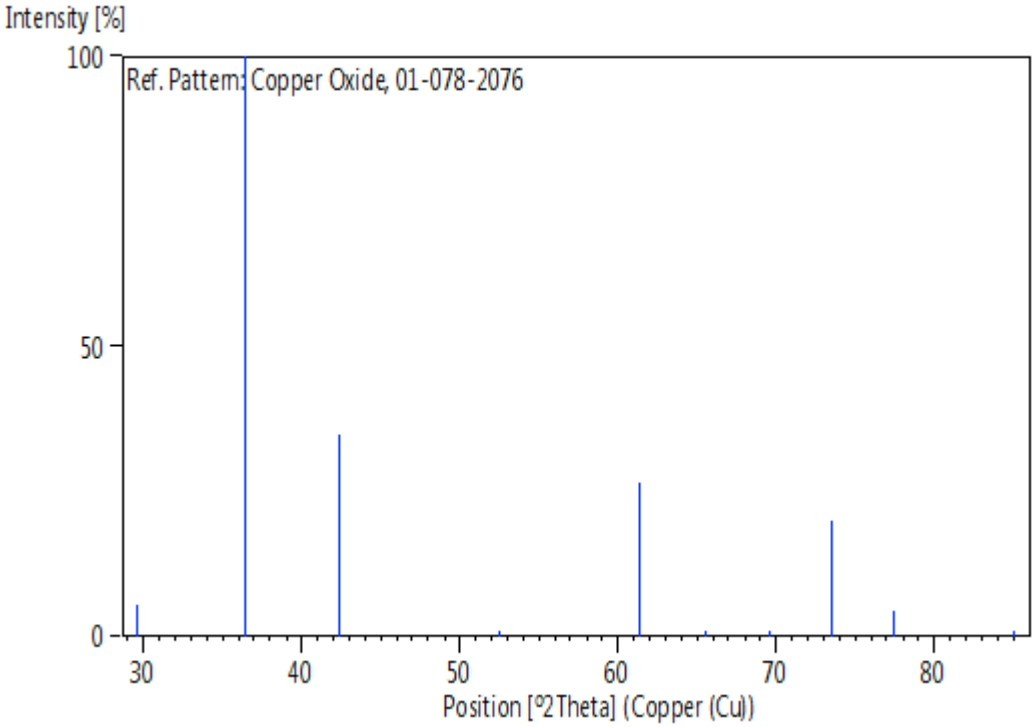

XRPD patterns of micro samples obtained by means of micro-XRPD

BF AV1 (orange): cuprite

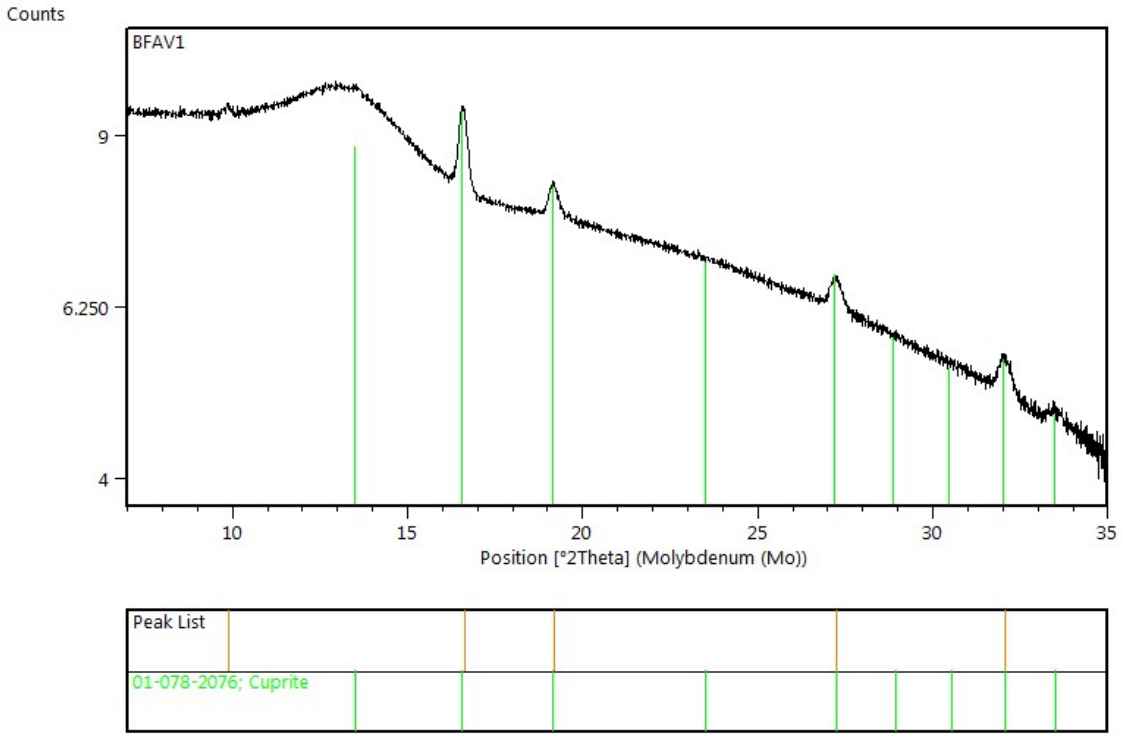

BF R1 (red): metallic copper

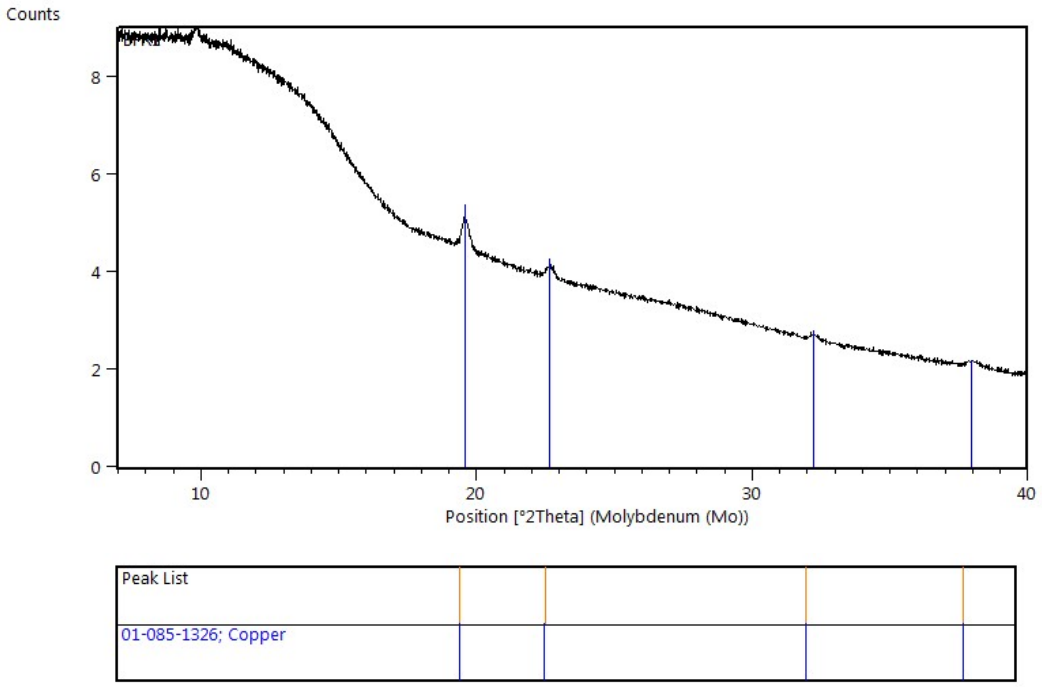

TN AV1 (orange and red striped)
Orange band: cuprite

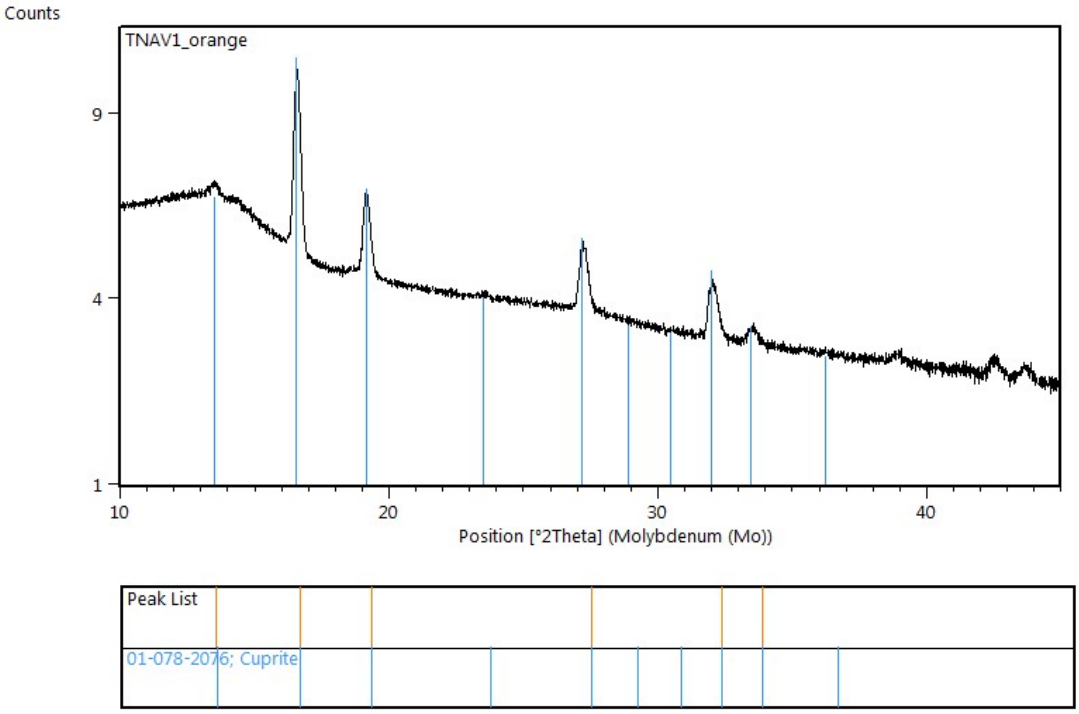

Red band: cuprite

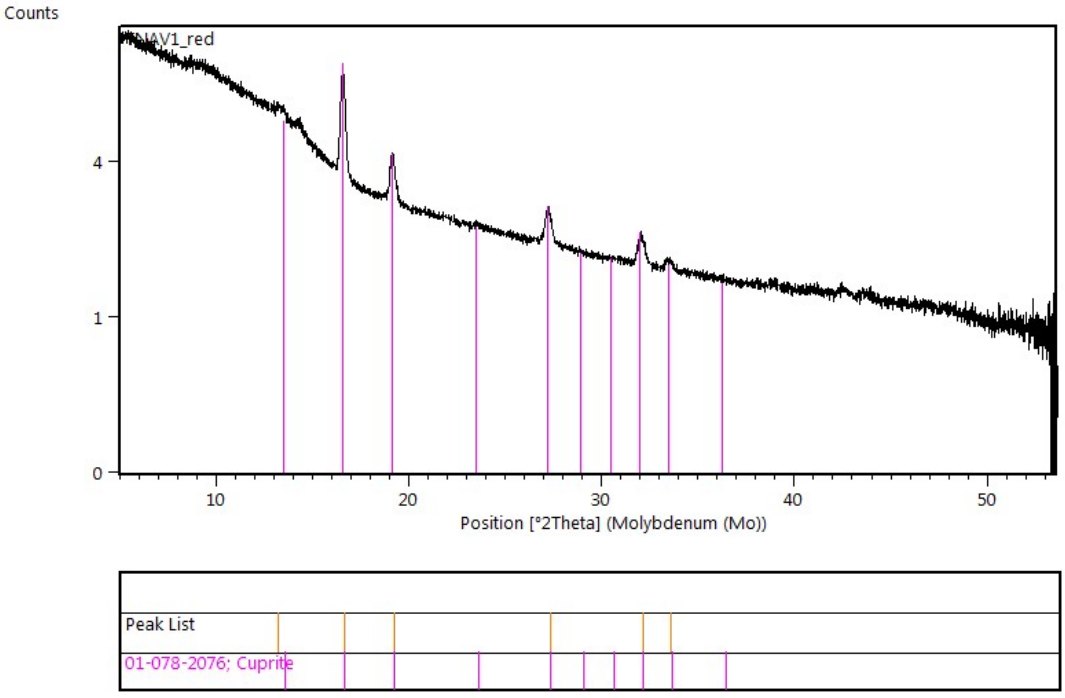

PN AV2 (orange and red striped): cuprite

